European Commission

JRC SCIENCE FOR POLICY REPORT

Atlas of the Human Planet 2018

A World of Cities

2018

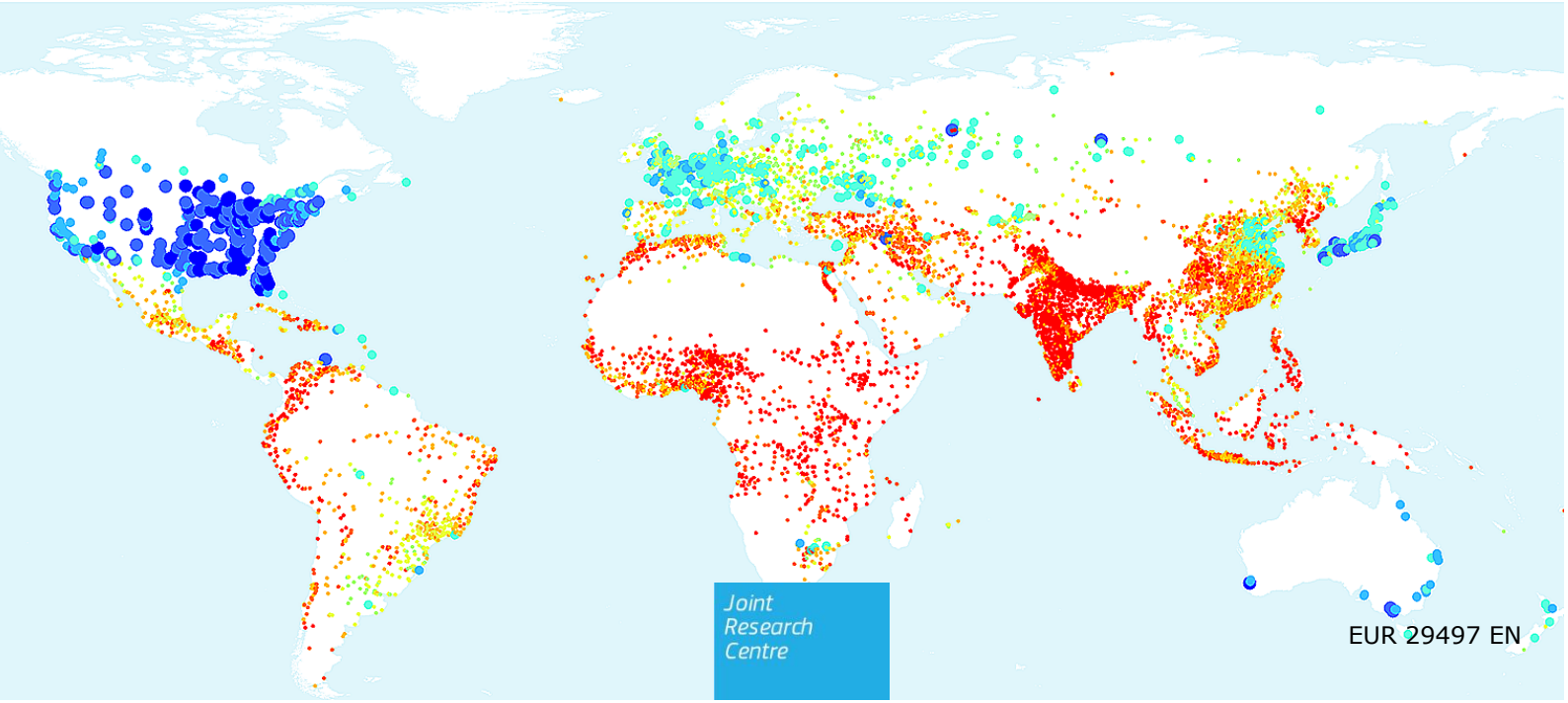

Joint Research Centre

EUR 29497 EN

Contact information
Name: Thomas Kemper
Address: Via Fermi, 2749 21027 ISPRA (VA) - Italy - TP 267
European Commission - DG Joint Research Centre
Space, Security and Migration Directorate
Disaster Risk Management Unit E.1
Email: thomas.kemper@jrc.ec.europa.eu
Tel.: +39 0332 78 55 76

EU Science Hub
https://ec.europa.eu/jrc

JRC114316

EUR 29497 EN

PDF ISBN 978-92-79-98185-2 ISSN 1831-9424 doi:10.2760/124503

Luxembourg: Publications Office of the European Union, 2018

Cover Image: The map classifies the Urban Centres included in the GHS-UCDB 2018 by the built-up space per inhabitant in the year 2015. The values are mapped in a colour range from red (low) to blue (high). The map illustrates the strong contrast between the densely populated cities of India, SE-Asia and Africa on the one hand, and the sprawling North American cities on the other hand.

How to cite this report: European Commission, Joint Research Centre, *Atlas of the Human Planet 2018 – A World of Cities*, EUR 29497 EN, European Commission, Luxembourg, 2018, ISBN 978-92-79-98185-2, doi:10.2760/124503, JRC114316.

Atlas of the Human Planet 2018

A World of Cities

2018

Contents

Abstract

The Atlas of the Human Planet 2018 describes the Urban Centre Database, produced in the framework of the Global Human Settlement Layer (GHSL) project, by applying a global definition of cities and settlements to the GHSL data.

The Atlas presents the key findings of the analysis of geographic, environmental and socio-economic variables that were gathered from free and open sources for each urban centre in the world.

Acknowledgements

This Atlas is the product of collaboration between the whole Global Human Settlement Layer (GHSL) team of the European Commission's Joint Research Centre, Directorate E "Space, Security and Migration", Disaster Risk Management Unit (JRC.E.1) and experts from other groups in the E1 unit, in other JRC directorates, in the European Commission as well as from other institutions.

This is the third edition of the Atlas and we would like to acknowledge not only the work of the main contributing authors, but also of the supporting team that with their extraordinary dedication and motivation made this Atlas happen, and in particular:

- Michele Melchiorri, for the general coordination support and editorship of the present Atlas, the generation of high quality figures and the contribution to the GHSL Urban Sustainable Development Goals (SDG) section;
- Aneta J. Florczyk, for the GHSL External Data Integration, the GHSL Data Quality Assessment and the GHSL Data Publication Coordination
- Christina Corbane, for the GHSL Earth Observation Data Processing Methodological Development and Coordination
- Sergio Freire, for the GHSL Census Spatial Data Analytics and Population Modelling Methodological Development and Coordination
- Daniele Ehrlich, for the GHSL Disaster Risk Reduction (DRR) Thematic Coordination
- Luigi Zanchetta, for the GHSL IT Infrastructure Development and Coordination
- Marcello Schiavina, for the GHSL Population Modelling Development
- Panagiotis Politis, Luca Maffenini, and Filip Sabo, for the GHSL Data Processing Tools Development
- Donato Airaghi, for the GHSL IT Infrastructure Support
- Pierpaolo Tommasi, for the GHSL Web Platform Development
- Martino Pesaresi, for the GHSL Scientific Catalysis, and
- Thomas Kemper, for the GHSL Scientific Leadership and the GHSL Team Management;

Moreover, we are grateful to our colleagues that were essential for the successful completion of the Atlas, and in particular:

- Lewis Dijkstra, Head of the Economic Analysis Sector at Directorate General for Regional and Urban Policy, European Commission, for his unexhausted capacity to provide stimulating challenges to the GHSL methodological development and to the GHSL data processing system
- Pierre Soille, Vasileios Syrris, and Pieter Kempeneers of the EC JRC Earth Observation Data and Processing Platform (JEODPP) team in the EC JRC Directorate I "Competences", Text and Data Mining Unit (JRC.I.3), for their extreme availability and patience in addressing the everlasting, always urging and unbelievable processing requests from the GHSL team
- Elisabetta Vignati, Monica Crippa, and Diego Guizzardi, of the EC JRC Directorate C "Energy, Transport and Climate", Air and Climate Unit (JRC.C.5), for their extremely valuable help in integrating and understanding the data from the JRC Emissions Database for Global Atmospheric Research (EDGAR)
- Luca Montanarella and Panos Panagos of the EC JRC Directorate D "Sustainable Resources", Land Resource Unit (JRC.D.3), for their timely and prodigious support in interpreting the data collected from the Harmonized World Soil Database

— Peter Salomon and the JRC Global Flood Awareness System team (GloFAS) of the EC JRC Directorate E "Space, Security and Migration", Disaster Risk Management Unit (JRC.E.1), for their precious help provided in integrating the hydrological data included in this Atlas

— Alessandro Dosio, of the EC JRC Directorate E "Space, Security and Migration", Disaster Risk Management Unit (JRC.E.1) for the valuable help provided for apprehending the secrets of the Heatwave Magnitude Index data integrated in this Atlas

— Gustavo Naumann of the EC JRC Directorate E "Space, Security and Migration", Disaster Risk Management Unit (JRC.E.1) for the great help provided in integrating the data on annual precipitation and temperature from the CRU TS v. 4.02 gridded time-series dataset

— Luca Vernaccini, supporting the Disaster Risk Management Knowledge Centre of the EC JRC, for the help provided in integrating the data from the UN Global Assessment report (GAR).

— Alexander Mackie and Ivan Hascic, of the Environmental Performance Information Division, in the Environmental Directorate of the Organisation for Economic Co-operation and Development (OECD), for their help in integrating the PM2.5 concentration data used in this Atlas

— John Schneider and Marc Pagani of the Global Earthquake Model (GEM) Initiative for the support in the accessing the new Global Seismic map integrated in this Atlas

— The Center for International Earth Science Information Network (CIESIN) in the Earth Institute of the Columbia University for their extremely valuable and continuous partnership in the production of the GHSL population grids, in the frame of the inter-ministerial Group on Earth Observation (GEO), Human Planet Initiative

Finally, we would like to thank the reviewers for their fast and constructive response:

— Alice Siragusa,

— Harm Greidanus,

— Tom De Groeve

Authors (in alphabetical order)

Christina Corbane, Daniele Ehrlich, Aneta Jadwiga Florczyck, Sergio Freire, Thomas Kemper, Michele Melchiorri, Martino Pesaresi, Marcello Schiavina

Executive summary

The 2018 edition of the *Atlas of the Human Planet* is dedicated to the *World of Cities*. The urban areas are today home to more than half of the world's seven billion people and their share will increase rapidly for years to come. However, there is a gap in the global monitoring of the urbanization process and all its dimensions. Until today, there is no globally harmonised definition of cities and settlements, which would be important for international comparability of cities. This Atlas uses a globally harmonised definition and presents the first globally consistent *Urban Centre Database (UCDB)*[1]. The database combines the city location (name) with the city extent (surface, shape), and describes each city with a set of geographical, socio-economic and environmental attributes, many of them going back 25 or even 40 years in time.

Policy context

The *Atlas of the Human Planet 2018* contributes directly to the voluntary commitment to develop a global, people-based definition of cities and settlements[2]. The definition is essential for monitoring of progress in achieving the goals of the 2030 Agenda for Sustainable Development[3]; several of the indicators linked to this goal are highly sensitive to where the boundary is drawn around a city. This Atlas is based on the UCDB, which provides harmonised city-level information for city networks like the Covenant of Mayors[4], and as such supports also the implementation of the New Urban Agenda[5].

For the Sendai Framework for Disaster Risk Reduction 2015-2030 (DRR)[6], the findings related to the exposure of cities to disasters will be included in the UN Global Assessment Report on Disaster Risk Reduction (GAR)[7], which is the flagship report of the United Nations on worldwide efforts to reduce disaster risk.

The *Atlas of the Human Planet 2018* is also a deliverable to the GEO (Group on Earth Observations) Human Planet Initiative[8]. The initiative maximises the use of (big) open data through artificial intelligence (AI) to bring EO data in the socio-economic and other domains. By developing a new generation of measurements and information products, the initiative provides new scientific evidence and a comprehensive understanding of the human presence on the planet that can support global policy processes with agreed, actionable and goal-driven metrics.

Key conclusions

The focus on the urban centres used in this edition of the *Atlas* was possible thanks to the voluntary commitment of the EU, OECD, World Bank, FAO, and UN-HABITAT to develop a global harmonised definition of cities and settlements. Applying this definition globally changes our perception on urbanisation, and therefore the partner of the commitment believe this definition is essential for a number of policy areas beyond this Atlas. In particular, the Sustainable Development Goals will profit from the better comparability of indicators.

The *Urban Centre Database (UCDB)* is a prime example of open, coordinated and sustained data sharing, as proposed by the Group on Earth Observations (GEO). The *Atlas* and the UCDB demonstrate that the combination of open data sets can generate new information. The new technology used for generating the Global Human Settlement Layer (GHSL) products allows producing global, yet locally consistent data for local action at the city level. However, the uptake of the data by decision makers for local, national or global reporting requires a regular update of the information, which could be achieved

[1] https://ghsl.jrc.ec.europa.eu/ucdb2018Overview.php
[2] https://ec.europa.eu/eurostat/cros/content/about_en
[3] https://sustainabledevelopment.un.org/post2015/transformingourworld
[4] https://www.covenantofmayors.eu/en/
[5] http://habitat3.org/the-new-urban-agenda/
[6] https://www.unisdr.org/we/coordinate/sendai-framework
[7] https://www.unisdr.org/we/inform/gar
[8] https://www.earthobservations.org/activity.php?id=119

for example through integration of products in the portfolio of the EU's Copernicus space programme.

Main findings

Although the discussions on the final definition of cities and settlements are ongoing, it is clear that the degree of urbanisation will change our view on urbanisation. With the current implementation of the Definition, the global degree of urbanisation reaches 81%, of which 48% of the population live in urban centres. The analysis derived from the UCDB highlights very diverse spatial development patterns across cities, regions of the world and income groups. Large population growth produces moderate increases in built-up surfaces for urban centres located in low-income countries, while moderate population growth produces large increases in built-up surfaces for UC located in high-income countries. Most of the urban centres expand over soils with a high agricultural suitability, posing important challenges and responsibilities to careful use of soil resources. Urban centres in Asia, Africa and Oceania have more than half of their urban population living below the global average night-time illumination value, threatening access to opportunities, decent housing and adequate standards of living. Urban centres concentrate more than 40% of the global population, in many of them people and assets are exposed to natural hazards. Especially in Asia and Africa, the increase in people exposure is due to natural population increase. Some continents are more exposed than others to certain hazards. For example, the number of urban centres exposed to storm surge in Asia is higher than the total number of urban centres in all the other continents combined. The GHS-UCDB can be of direct relevance to support policy as it offers baseline information for Sustainable Development Goals indicators to quantify the efficiency in the use of land and the generalised access to green areas.

Related and future JRC work

At the centre of the GHSL framework is the understanding of the planet aligned with the JRC space strategy. The project supports several Knowledge Centres[9] (Disaster Risk, Territorial Policies, Migration and Demography). The GHSL project is one key test cases of the Joint Research Centre Earth Observation Data and Processing Platform (JEODPP). The processing power and storage of JEODPP are essential for the success of GHSL, which relies on artificial intelligence approaches applied to global fine scale data sets.

The UN Statistical Commission is expected to vote on the global definition in 2020. In the run-up to the vote, the GHSL project supports the partners of the commitment (OECD, World Bank, FAO, and UN-HABITAT) with the promotion of the definition in the UN member states through workshops and pilot applications.

Following the successful test of the fitness for purpose the JRC, together with the Directorate-General for Regional and Urban Policy (DG REGIO) and Directorate-General (DG) for Internal Market, Industry, Entrepreneurship and SMEs (DG GROW), are working towards an integration of GHSL products based on Sentinel-1 and Sentinel-2 in the Land Service of the Copernicus programme.

Quick guide

The *Atlas of the Human Planet* 2018 is based on the UCDB, which relies on the GHSL data. GHSL combines satellite and socio-economic data to produce high resolution, global open information on built-up area and population. In the current release, it covers the epochs 1975, 1990, 2000 and 2015. The data sets are used in combination with socio-economic data sets to understand, where and in which built environment people live, and how the settlements and the population change over time. This knowledge is used in policy areas including environmental impact assessment, disaster risk assessment, transport, health care services, education, natural disasters and hazards and urban planning.

[9] https://ec.europa.eu/knowledge4policy/

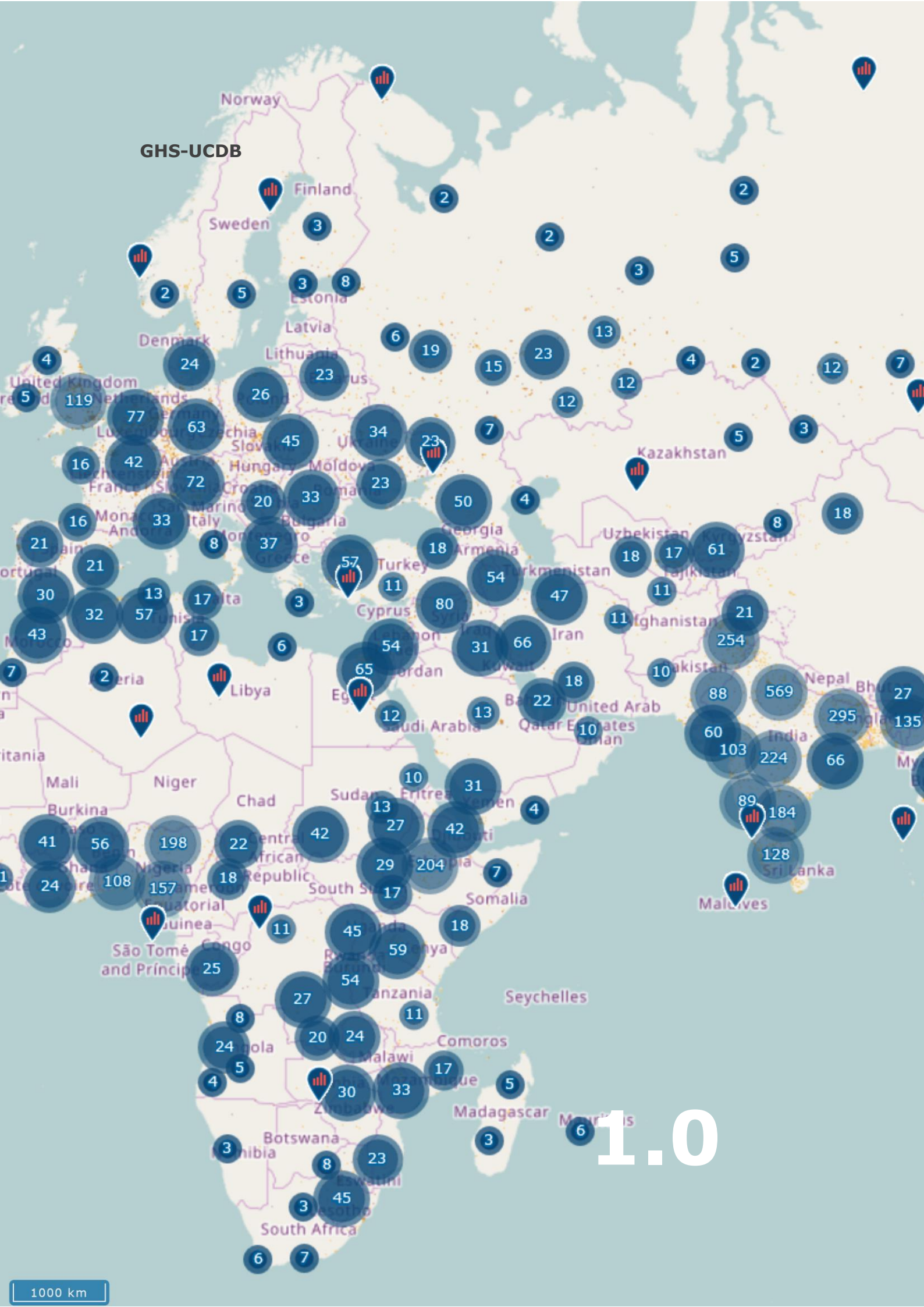
GHS-UCDB
1.0
Norway
Finland
Sweden
Estonia
Latvia
Lithuania
Denmark
United Kingdom
Netherlands
Germany
Poland
Belarus
Ukraine
Slovakia
Hungary
Moldova
Romania
Bulgaria
Serbia
Greece
Turkey
Cyprus
Georgia
Armenia
Kazakhstan
Uzbekistan
Kyrgyzstan
Tajikistan
Turkmenistan
Afghanistan
Iran
Iraq
Syria
Lebanon
Jordan
Kuwait
Saudi Arabia
United Arab Emirates
Qatar
Oman
Pakistan
India
Nepal
Sri Lanka
Maldives
Libya
Egypt
Sudan
Eritrea
Yemen
Somalia
Ethiopia
Kenya
Uganda
Rwanda
Burundi
Tanzania
Seychelles
Comoros
Madagascar
Mauritius
Malawi
Zambia
Zimbabwe
Mozambique
Botswana
Namibia
Eswatini
Lesotho
South Africa
Mali
Niger
Chad
Burkina
Nigeria
Cameroon
Central African Republic
South Sudan
Equatorial Guinea
São Tomé and Príncipe
Congo
Angola
Libya
Algeria
Tunisia
Morocco
Portugal
Spain
France
Italy
Malta
Andorra
Monaco
San Marino
Switzerland
Austria
Croatia
Slovenia
Czechia
Luxembourg
Belgium
1000 km

1 Introduction

The Atlas of the Human Planet 2018 is dedicated to the cities. Cities and urban areas are today home to more than half of the world's seven billion people. The latest urbanization trends indicate that an additional three billion people will be living in urban areas by 2050 (United Nations, Department of Economic and Social Affairs, Population Division, 2018), increasing the urban share of the world's population even more. However, the current era of rapid urbanization has been marred with inadequacy of capacity and sometimes resources to match urban development needs. Moreover, there is a gap in the global monitoring of the urbanization process in all its dimensions. Until today, there is no globally harmonised definition of cities and settlements, defining their size and boundaries.

This report uses the Degree of Urbanisation (Dijkstra and Poelman, 2014), a definition used to outlinr the spatial extent of cities and settlements, to create the first global, harmonized, consistent database of urban centres, the Urban Centre Database (UCDB). The database combines the city location (name) with the city extent (surface, shape), and describes each city with a number of geographic, socio-economic and environmental attributes, many of them going back 25 or even 40 years in time.

The (UCDB) is based on the Global Human Settlement Layer (GHSL) data. The GHSL project produces new, global, spatial information, evidence-based analytics and knowledge describing the human presence on the planet based mainly on two quantitative factors: i) the spatial distribution (density) of built-up structures, and ii) the spatial distribution (density) of resident population. Both factors are observed in the long-term temporal domain and per uniform surface units in order to support trends and indicators for monitoring the implementation of international framework agreements. The GHSL uses various input data including global, multi-temporal archives of fine-scale satellite imagery, census data, and volunteered geographic information. The satellite archives and available census data allow generating information layers for four epochs: 1975, 1990, 2000, and 2015.

The GHSL addresses the urbanization globally in a consistent fine-scale way. The pace at which urbanization occurs in different parts of the world, poses a number of challenges such as providing a safe, liveable urban environment with green spaces, efficient transport, protection against natural hazard risks and economic opportunities. In fact, the growth of urban area changes also the economic conditions and the demands for energy and resources (Zhou et al. 2015). The GHSL addresses the lack of essential global information on settlements focussing on the spatial extent of the built-environment and the population that lives within.

The GHSL uses satellite remote sensing as a primary source of information to delineate and size the physical extent of human settlements from large megacities to villages and towns. In the GHSL framework, the physical extent of the human settlement as collected by the satellite sensor is called "built-up area". This GHSL built-up area variable – referred to as GHS-BU – is produced by application of automatic supervised classification data processing methods to global streams of open decametric-resolution satellite imagery collected by the Landsat and Sentinel missions.

The GHSL project produces also global population density grids, called GHS-POP, by combining the GHS-BU with census data through spatial modelling techniques. The data integration process foresees the downscaling of the information from the national census district level to a regular, finer-scaled, gridded built up density information layer. The result is a population density information layer available at a 250x250 m^2 and 1x1 km^2 grid scale.

This document takes the analysis further by using the GHS-BU and GHS-POP layers as input for an urban-rural settlement classification model, producing a third GHSL information layer called GHS-SMOD. The GHS-SMOD builds on the "Degree of Urbanization" concept (Dijkstra and Poelman, 2014) applied to the GHSL data. The GHS-

SMOD is implemented at the 1x1 km^2 grid scale and, in the version used here, distinguishes between three main typologies of human settlements, based on population density cut-off values: "Urban Centres", "Urban Clusters" and "Rural Settlements".

The urban centres, which represent the most densely inhabited part of human settlements, are analysed in more detail in this atlas. They are extracted from the GHS-SMOD of the epoch 2015 and include more than 10,000 individual cities. Each urban centre is characterised by a number of variables describing the geography and the environment of the place as well as socio-economic parameters and the potential exposure of an urban centre to natural disasters. The high-level process of information extraction and aggregation of the information in the Urban Centre Database (GHS-UCDB) is schematised in Figure 1.

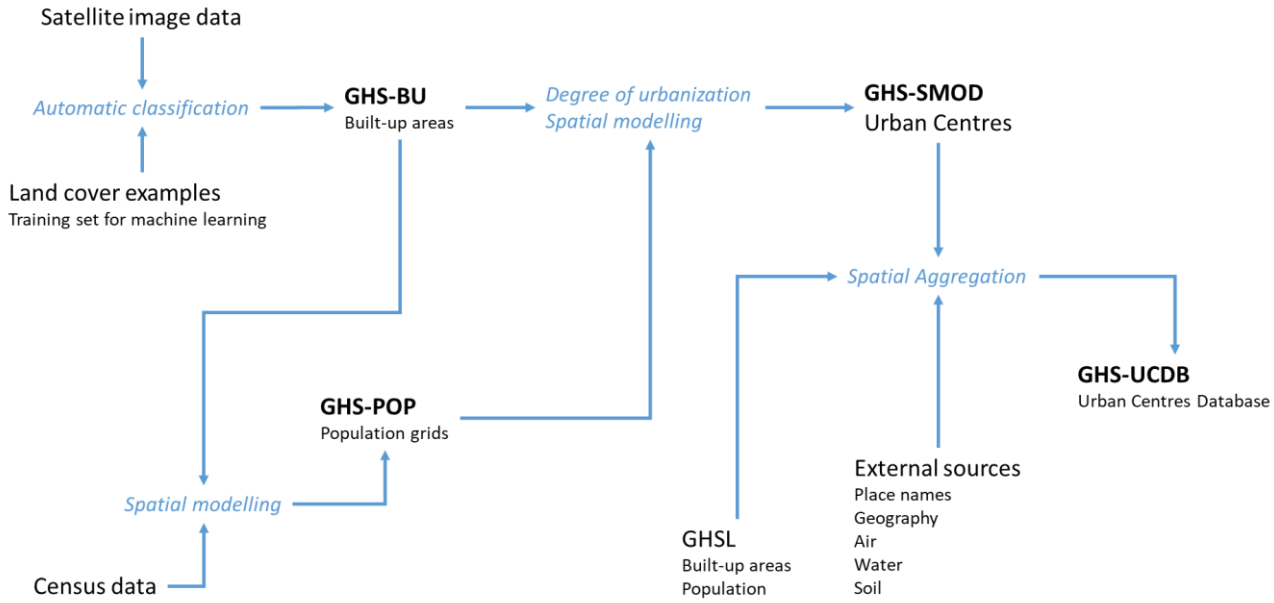

Figure 1 - conceptual schema of the GHSL input data, processing and products

This Atlas provides thus a global overview of over 10,000 cities and their characteristics collected in a systematic way using state-of-the-art global information sources available in the open (scientific) domain. The information is used to generate indicators for use by policymaking and/or for prioritizing funding allocation. The information are also used to generate indicators to monitor targets and goals set by the 2030 Agenda for Sustainable Development and the linked international framework including the Sendai Framework for DRR, the Paris Climate Agreements and the New Urban Agenda.

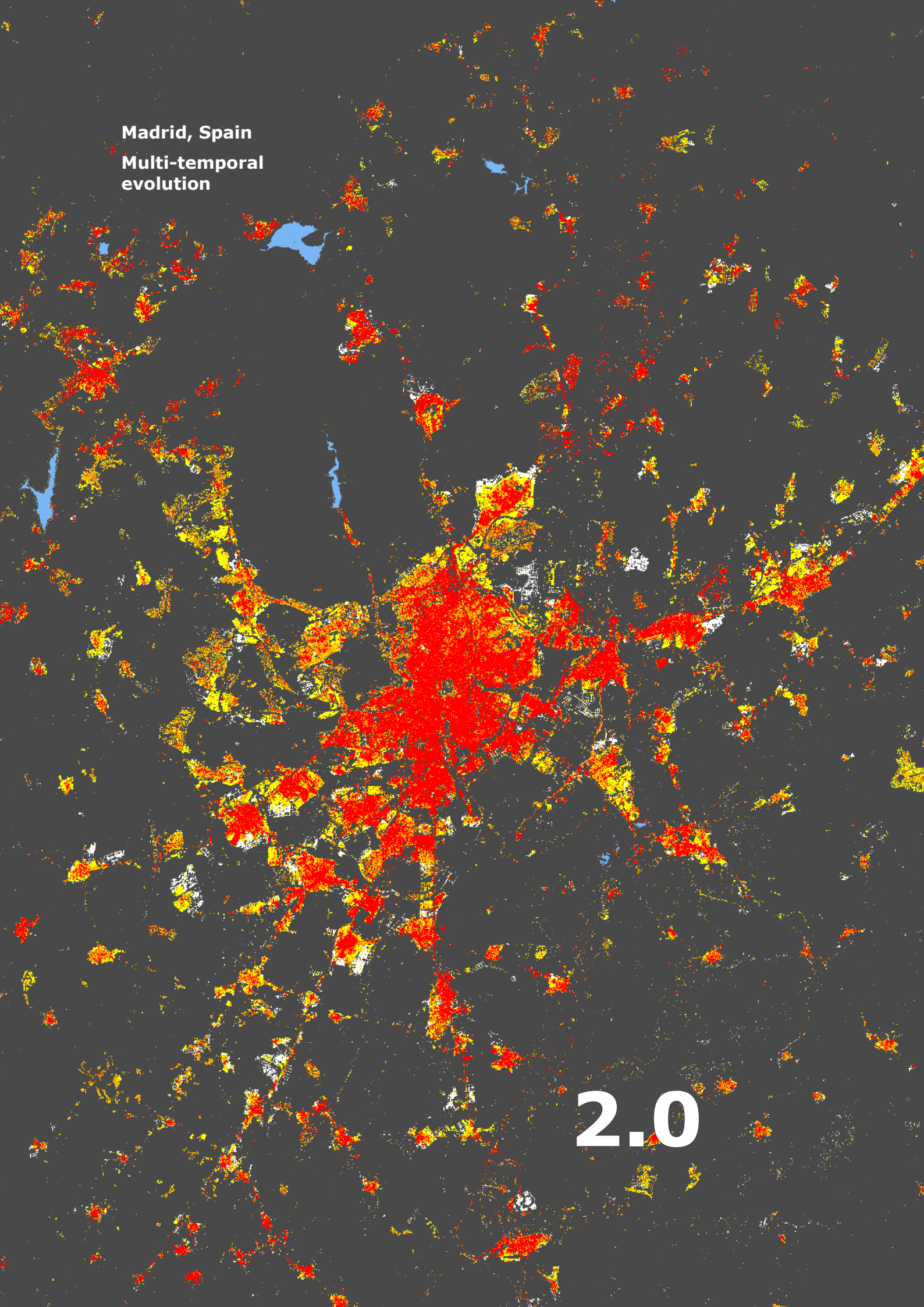
Madrid, Spain
Multi-temporal evolution
2.0

2 The GHSL conceptual framework

2.1 Background

The GHSL concept was introduced by the European Commission (EC), Joint Research Centre (JRC) during the years 2008-2011, in the frame of the former program named "Information Support for Effective and Rapid External Action" (ISFEREA), developing new image information mining technologies in support to geo-spatial information analysis for global security and stability (Halkia et al., 2007). The notion of the basic categories and information abstractions used by the GHSL were introduced after a critical revision of the available satellite-derived information products (land-use/land-cover) when applied to the quantification of the presence of built-up structures in support to spatial modelling and assessment activities (Pesaresi and Ehrlich, 2009), (Pesaresi et al., 2013). In particular, the first application areas in post-disaster/post-conflict damage, needs and reconstruction assessment (including refugee camps and temporary or rapidly changing settlement monitoring (Jasani et al., 2009), (Pesaresi et al., 2013), (Pesaresi et al., 2015a)) set the requirements for the GHSL's automatic image-data mining methods:

- robustness against real-world, big earth data scenarios, involving large-volume, largely heterogeneous/unstructured data sources (incl. remote sensing and other data) and rapidly changing data specifications,
- robustness against multi-stakeholder scenarios with diverging analytical requests,
- effectiveness in providing output analytics under conditions of time constraints and limited computational resources such as during crisis management operations.

On 21 February 2011, the JRC announced the successful completion of the first large-scale experiment of the global human settlement layer (GHSL) using European medium resolution ENVISAT ASAR satellite data and automatic image pattern recognition algorithms[10] for delineation of built-up surfaces. Later in 2012, an initial prototype of the GHSL system was successfully tested in a large-scale exercise. The test included the automatic recognition of built-up areas over more than 50 millions km² of land surface, using a heterogeneous set of data collected from optical sensors ranging from 0.5 to 10 meters spatial resolution, with a large variety of sensor spectral characteristics. The test demonstrated the technical feasibility of the GHSL concept, including the satellite-sensor-agnostic nature of the GHSL remote sensing data processing paradigm (Pesaresi et al., 2013).

In 2013, the GHSL data processing system was successfully tasked to produce the first seamless pan-European settlement layer at 2.5 m spatial resolution in support to European cohesion policies (Ferri et al., 2014), (Florczyk et al., 2015).

In support to the discussions of the post-2015 international frameworks, the initial set of requirements was extended to the monitoring of the implementation of these the frameworks: the Sendai Framework for Disaster Risk Reduction (DRR) 2015-2030, the 2030 Agenda for Sustainable Development, the Paris Climate Agreement, and the New Urban Agenda (Martino Pesaresi et al., 2016b), (Pesaresi et al., 2017).

These frameworks are accompanied by targets and further elaborated through indicators that focus on measurable outcomes. Indicators are action oriented, global in nature and universally applicable well-fitting with the synoptic and globally systematic characteristics of remote sensing data.

[10] EUScience Hub: Mapping Human Settlements Globally (https://ec.europa.eu/jrc/en/news/mapping-human-settlements-globally-8276)

2.2 Principles

One of the aims of the GHSL project was to provide a public platform prototype to support alternative implementations of indicators for the monitoring of international frameworks. Consequently, the GHSL data sets were designed with a modular, hierarchical abstraction schema. This schema facilitates the knowledge sharing and the conceptual convergence even in complex, international, multi-stakeholder discussions. In addition, the GHSL information production system is fully open and free, is in line with the strategy of the Group of Earth Observation (GEO) and the Global Earth Observation System of Systems (GEOSS) (Doldirina, 2015), (Anderson et al., 2017), and the European Commission's Open Data Policy[11].

The GHSL concept it is currently framed around three general goals or requirements:

i) operating in an open and free data and methods access policy (open input, open method, open output),

ii) enabling reproducible, scientifically defendable, fine-scale, synoptic, complete, planetary-size, and cost-effective information production, and

iii) facilitating information sharing and multilateral democratization of the information production, and collective knowledge building.

The first and second requirements call for public, scientific control of the data and the information production methods generating the GHSL information and derived findings. The second and third general requirements call for automatic information production methods being able to process systematically the large mass of baseline data lowering down the cost of the information production. Consequently, various independent entities may produce the information. This moves the human efforts from the information extraction to the discussion of the observed facts and ultimately to derive decisions. In the frame of the above, there are three main principles applied in the design of the GHSL automatic information production system. They are shortly recalled here: i) test and apply real-word (big) data scenarios, ii) produce evidence-based output analytics, and iii) facilitate repeatability of the results.

2.2.1 Real-word (Big) Data Scenarios

The real world data scenario is calling for a pragmatic, adaptive approach in complex data-information-stakeholder scenarios. On the one hand, the planetary-size, multi-temporal, fine-scale data generate large volumes of information. On the other hand, international, multi-stakeholder scenarios coupled with fast technological development generate rapidly changing data specifications and even contradictory semantics and assumptions. An old-fashioned layering of not centrally harmonized data generates gaps and inconsistencies in both spatial and thematic components of the data. In such scenarios, the adoption of a strict normative approach would easily lead to the system irrelevance and failure with respect to the reality check.

The GHSL takes instead a pragmatic adaptive perspective. Artificial intelligence (AI) is used to find relevant association between different data streams at different levels of abstraction/semantics and different scales with a minimal set of possible assumptions. In this perspective, the whole universe of data shall be used for testing of hypothesis. Efficient computational machine learning methods allow discovering association between any given data and information at any collected sensor/data parameters conditions, with no necessity of model transfer (Pesaresi et al., 2013), (Martino Pesaresi et al., 2016a), (Pesaresi, 2014), (M. Pesaresi et al., 2016c).

The GHSL information production workflow is supported by the definition of a new AI approach for the satellite data classification process named "Symbolic Machine Learning"

[11] Communication on open data (COM (2011) 882)

(SML), and working with the similar principles used in genomics for the DNA sequences characterization (M. Pesaresi et al., 2016b). The SML approach allows machines to learn efficiently new association rules between satellite data instances and target abstraction classes in the case of GHSL for instance the "built-up areas". The SML is robust against the presence of high levels of noise in the training set or "examples" used by the machine learning process. The noise may include large temporal, scale, and thematic/semantic differences among the input "examples" used by the machine learning process, and the satellite data records to be classified or the target class abstractions to be recognized (Pesaresi et al., 2015b). The SML algorithm allows designing a robust supervised data classification process using available global data as training examples, just approximating the scale and thematic requirements of the information retrieval tasks. This fact drastically reduces the human labour traditionally needed for the training set collection.

2.2.2 Evidence-based output analytics

International framework agreements such as the New Urban Agenda, the SDGs, and the Sendai Framework for DRR are linked to national and multi-national (as in the case of the European Union) policy processes driven by decision makers operating at various levels of governance. Data and evidences may (shall) contribute to policy processes by providing indicators that focus on measurable outcomes and allow evaluating, comparing and benchmarking alternatives of action. In order to be suitable for supporting policy decisions, the data and the AI-driven analytics must be defendable from the accusation to be affected by prejudice supporting specific political and/or economical interest. In order to mitigate that risk, the GHSL implements two explicit design solutions:

i) The output categories or abstractions delivered by the AI processes applied to the data generating the GHSL information are designed with a modular abstraction schema allowing multi-stakeholder and multi-disciplinary communication flows, and improving semantic interoperability of the GHSL information. This approach it is innovative compared to common practices in remote sensing derived products, e.g. the classical land cover products (Pesaresi and Ehrlich, 2009).

ii) The data processing rules generated by the AI machine learning processes are accessible by human inspection and understanding allowing the collective discussion of the whole information production process, without introducing processing segments acting as black boxes.

A corollary of the "evidence-based output analytics" principle, also linked to the next "full repeatability" principle, is that some common practices applied to remote sensing data products are not allowed in the GHSL information production. For instance, no expert-driven post-processing and masking operations are applied to the output of the GHSL that is considered as integrally automatic (then formally explicit and controllable), data-driven information production system. If main anomalies are reported in a given GHSL output release, they are summarized in the data disclaimer and in the data quality description layers, and they are used to benchmark the improvements of next GHSL data and method releases.

2.2.3 Full Repeatability

Repeatability of measurements refers to the ability to repeat measurements made on the same subject under identical conditions (National Institute for Standards and Technology, 2007). Variability in measurements made on the same subject under identical conditions can be attributed to errors originated by the measurement process itself. The measurements generated by the GHSL system are fully repeatable. The same input data and the same information extraction method produces identical numerical result or measure until the last significant digit. This is a requirement needed to maintain full control of data, methods and results lineages in the "Real-word (Big) Data Scenarios" as described in the first principle above. It is also a requirement for measurements

implicating legal consequences as in the case of international frameworks monitoring. Moreover, full repeatability increases trust in the new data and analytics generated by new technologies, especially if non-experts are involved in the evaluation of the results. A corollary of this principle is that GHSL avoids the use of AI methods based on random iterative optimization processes not allowing full repeatability of the same results under the same initial conditions.

2.3 The GHSL data releases

2.3.1 Past data releases

The first public release of the GHSL data including built-up surface grids, resident population grids, and urban/rural classification schema for the epochs 1975, 1990, 2000, and 2015 was announced at the third United Nations Conference on Housing and Sustainable Urban Development (Habitat III) in October 2016. The data is freely accessible through the JRC Open Data Portal (https://data.jrc.ec.europa.eu/) and the GEOSS portal (http://www.geoportal.org/).

Since 2017, the GHSL data and tools contribute to the GEO Human Planet Initiative, which is one of the initiatives in the GEO work program[12]. The free and open access to data is one of the core principles of GHSL and GEO Human Planet Initiative, in order to favour an open forum for discussion for academy, international stakeholders, governmental bodies and private firms. To support such discussion, a prelease of GHSL data is shared first within the GEO Human Planet community. In 2018, such a data package was shared with the community (Florczyk et al., 2018).

The public release of the new data sets is accompanied with a new edition of the Atlas of the Human Planet that describes the core findings linked to the new data release (Martino Pesaresi et al., 2016b; Pesaresi et al., 2017). Accordingly, this Atlas of the Human Planet 2018 supports the latest GHSL data package, which is described in the following.

2.3.2 Improvements in the GHSL 2018 release

Since its public release in October 2016, the GHSL data were used by a large number of users from different thematic domains as well as from all regions of the world. Many provided valuable feedback on the quality of the data. In addition, new technical developments in terms of data availability and refinement of methodology allowed for a significant improvement of the data. With respect to the previous release in 2016, the current GHSL release 2018 implements two main improvements:

i) Improved GHS-BU and GHS-POP baseline information production

ii) Introduction of the new Urban Centres Database (UCDB)

The new GHS-BU data were produced during 2017 and 2018 by reprocessing the global Landsat image data collections with an improved classification method mainly due to the introduction of better global, fine-scale training sets that were made available recently. The improved GHSL workflow integrated, amongst others, new Sentinel-1 (radar) data collected during 2016, and implemented a new global information optimization processes aiming to improve the reliability and stability of the automatic information extraction from satellite images through automated selection of the best from a number of alternative processing options (Corbane et al., 2017a).

Consequently, the new GHS-POP grids were also reprocessed using the improved GHS-BU input grids, and including improvements in the spatial harmonization and gap-filling processes applied to the input census data (Freire et al., 2018).

Both new data sets were subsequently used to derive an updated settlement model based on the degree of urbanisation. From the 2015 grid of GHS-SMOD, the new Urban

[12] http://earthobservations.org/documents/work_programme/geo_2017_19_Work_Programme.pdf

Centres Database (GHS-UCDB) was derived. The GHS-UCDB was generated by spatial integration of the urban centres with the GHSL grid data (built-up areas, resident population) and with other sources supporting the characterization of the urban centres (see chapters 5 for details).

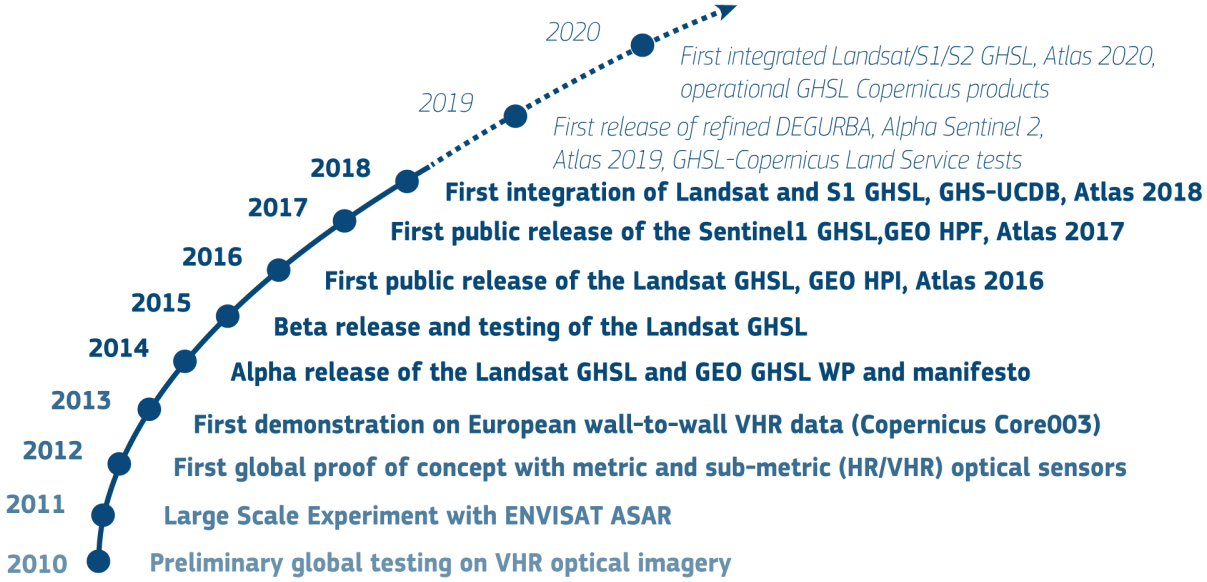

Figure 2 Evolution of the GHSL framework and key science for policy deliverables

The urban centres database proof of concept (developed in the first trimester of 2018) supported the JRC contribution to the World Urban Forum 9 convened by UN-Habitat in February 2018 with the goal to improve the collective knowledge of sustainable urban development. The preliminary version of the urban centres database characterised the circa 10,000 urban centres with attributes including built-up areas and population (and built-up areas per capita) in the four GHSL epochs (1975, 1990, 2000, and 2015), night-time lights (also multi-temporal). In addition to these variables, the database included environmental metrics (greenness index, PM2.5 concentration, imperviousness index and proximity to natural protected areas), and other proxy information useful to exposure analysis (i.e. people and built-up areas in the urban centre located at the sea level or below or located in slopes greater than 15°). This information was made available through the GHSL website and supported training activities and policy talks (especially by DG-REGIO).

2.4 Fundamentals

The GHSL consists of three main information components hierarchically placed at three different levels of abstraction: Global Human Settlement built-up areas (GHS-BU), the GHS population grids (GHS-POP) and the GHS urban/rural classification model (GHS-SMOD).

At the base of the hierarchy - including the most spatially accurate and the least abstract information level - we have a layer collecting concrete evidences about the human presence on the planetary surface as seen from global Earth Observation systems. In the GHSL paradigm, the fundamental link between Earth Observation sensor data and the human presence is the observable presence of built-up structures or buildings. From the GHSL perspective, the "building" makes the physical part of the human settlement fabric or spatial extension that is observable and measurable using the available global sensors. At this basic level the GHSL reports about *built-up areas (GHS-BU)*, as *areas (spatial units) where buildings can be found* (Pesaresi, 2016). The concept of "buildings" formalized by the GHSL are *enclosed constructions above ground which are intended or used for the shelter of humans, animals, things or for the production of economic goods*

and that refer to any structure constructed or erected on its site (Pesaresi et al., 2013). This abstraction is very similar to the standard topographic definition of the "building" class as compiled in the INSPIRE directive[13], except that the condition of the *permanency of the structure* it is not in the GHSL definition. The GHSL definition of built-up also to includes refugee camps, informal settlements, slums and other temporary settlements and shelters.

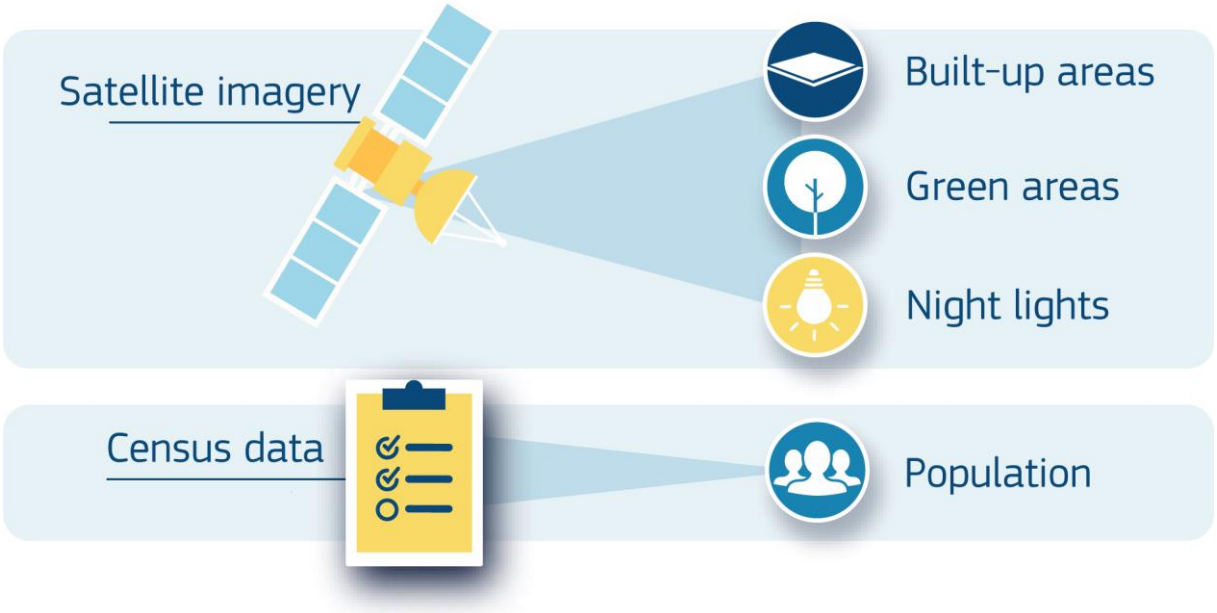

Figure 3 GHSL input data and main output information

The intermediate abstraction information layer of the GHSL is the population grid or GHS-POP that is produced in an in-between spatial resolution. This information layer is derived from the combination of global collections of national population census data and global built-up areas as extracted from Earth Observation data analytics (GHS-BU). In the approach taken by the GHSL, the population data collected by national censuses with heterogeneous criteria and heterogeneous update time are harmonized in the space and time domains in to the GHS-POP grids, by systematic and consistent application of the same set of data interpolation and spatial disaggregation methods to the best available global spatial baseline data {Freire_al_2016}.

The top abstraction information layer of the GHSL it is the urban/rural classification model (GHS-SMOD). It is provided with the least spatial detail (1 km) by combining the two less-abstract and more-spatially-detailed built-up and population grids, GHS-BU and GHS-POP, respectively. The GHS-SMOD model implemented by the GHSL it is consistent with the "Degree of urbanisation" (DEGURBA) model adopted by EUROSTAT[14]. It discriminates 3 settlement class abstractions: 1) Cities, 2) Towns and suburbs and 3) Rural areas. The discrimination is based on the population density in the square kilometre grid[15], total settlement population and other spatial generalization parameters.

In the GHSL paradigm, the base layer GHS-BU it is designed to be the most stable against different visions and approaches, while GHS-SMOD is the most abstract and as such exposed to conceptual changes and alternative problem settings proposed by the different stakeholders involved in the post-2015 international framework processes. The modular hierarchical abstraction schema used in the GHSL design allows to protect the investment made in the global, fine-scale information gathering from perturbations on

[13] INSPIRE Infrastructure for Spatial Information in Europe D2.8.III.2 Data Specification on Buildings – Draft Technical Guidelines http://inspire.ec.europa.eu/documents/Data_Specifications/INSPIRE_DataSpecification_BU_v3.0rc3.pdf

[14] http://ec.europa.eu/eurostat/web/degree-of-urbanisation/overview

[15] densely, intermediate density and thinly populated areas

the abstract classification schema that may be introduced by different decision-makers involved in the process and potentially producing different problem setting and abstractions. On the other side, the modular hierarchical abstraction schema facilitates the test of alternative abstract models on the same agreed information baseline, facilitating the discussion and the comparison of the results also between international stakeholders not necessary sharing the same high abstraction definitions.

The following sections help the reader to understand fundamental concepts of GHSL and its data. The first subparagraph deals with extraction of information from satellite imagery (2.4.1) and built-up definition.

The second paragraph explore the process allows to combine built-up grids with census data to produce the population grids (2.4.2).

The third paragraph (2.4.3) illustrates the key elements and rules of the settlement model, derived from the New Degree of Urbanization (Lewis Dijkstra and Hugo Poelman 2014): specifically, the rules for defining *Urban Centres*, *Urban Clusters* and rural settlements are illustrated.

The forth paragraphs show with simple images, and example of three GHSL datasets (GHS Built-up, GHS POP and S-MOD) for the city of Madrid, Spain (2.4.4).

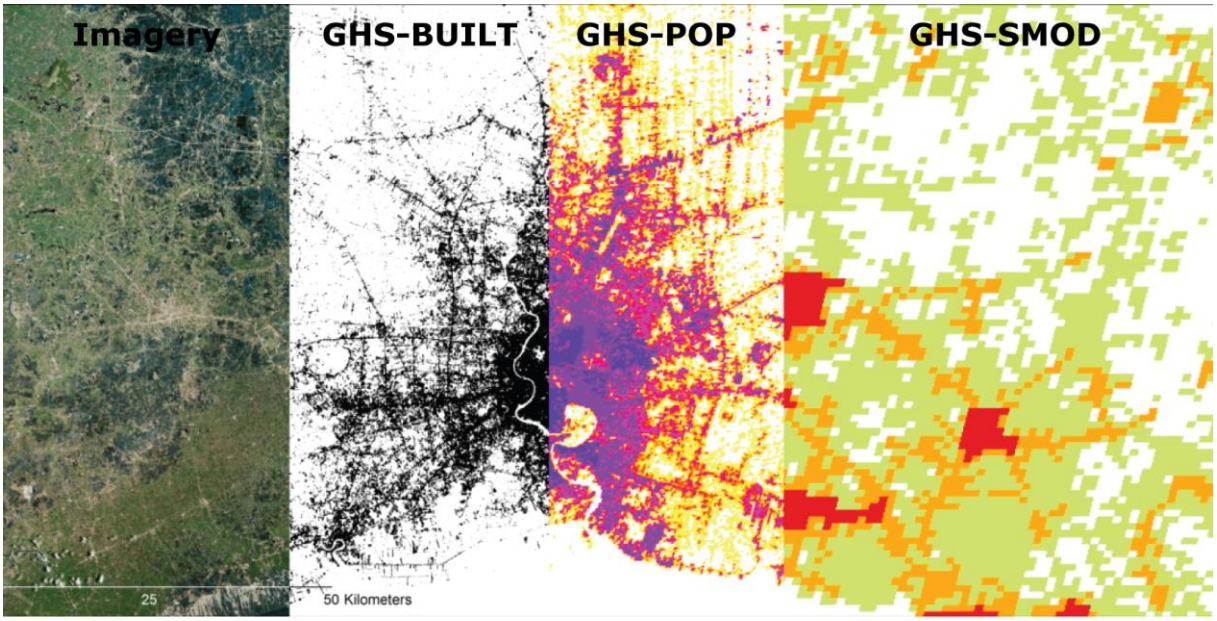

Figure 4 Transition from imagery to built-up areas extraction (GHS-BU), population modelling (GHS-POP), and settlements classification (GHS-SMOD), examples in the area of Bangkok (Thailand).

2.4.1 From Earth's surface to built-up area

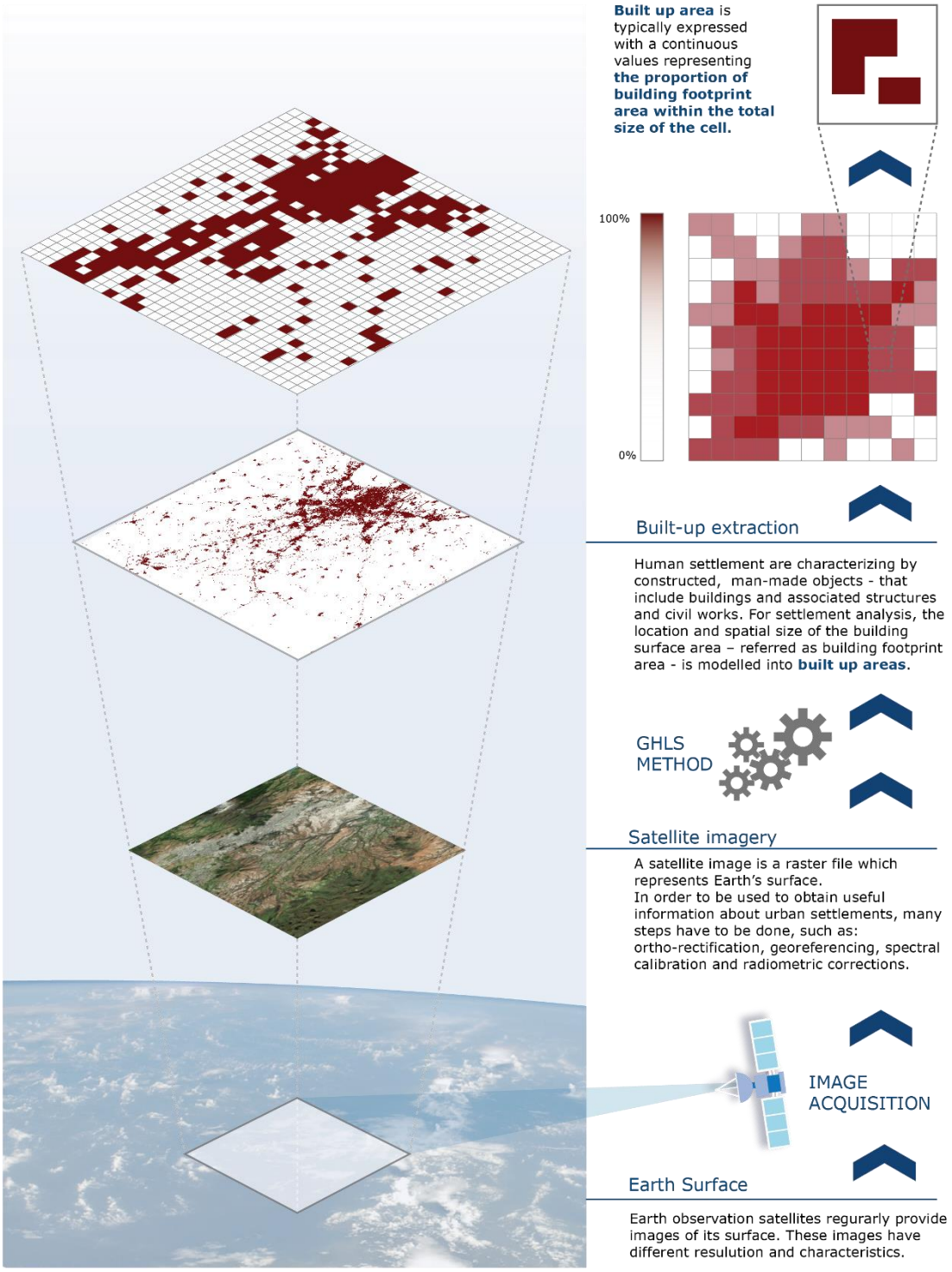

Figure 5 The figure describes the information extraction process from the satellite images of the earth surface (bottom) to the built-up area extraction (middle) to the aggregated built-up area density (top).

2.4.2 From Built-up area to population grid

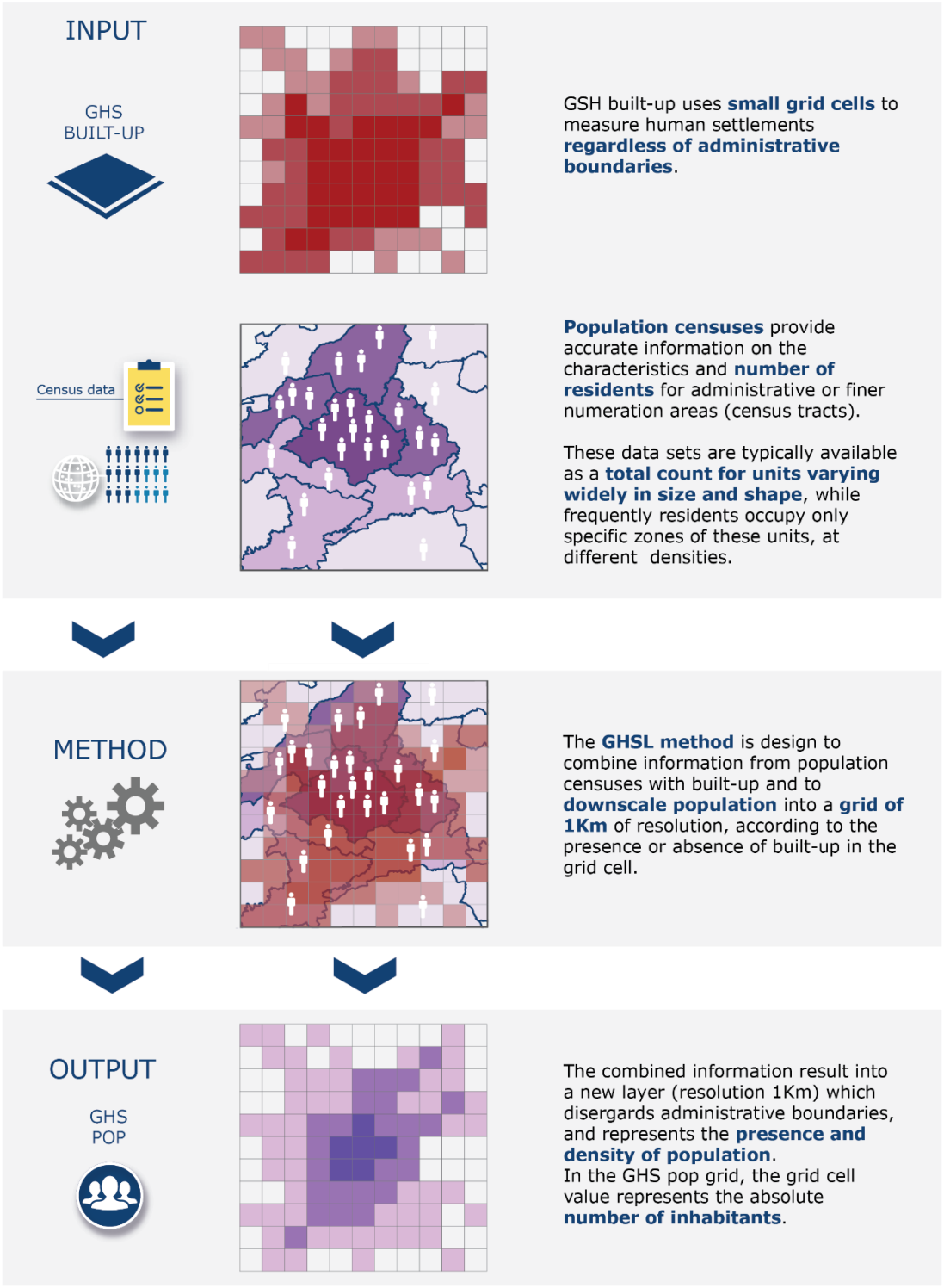

Figure 6 The figure illustrates the combination of GHS-BU with the census data to produce a regular fine scale grid of population density.

2.4.3 An example from the city of Madrid, Spain

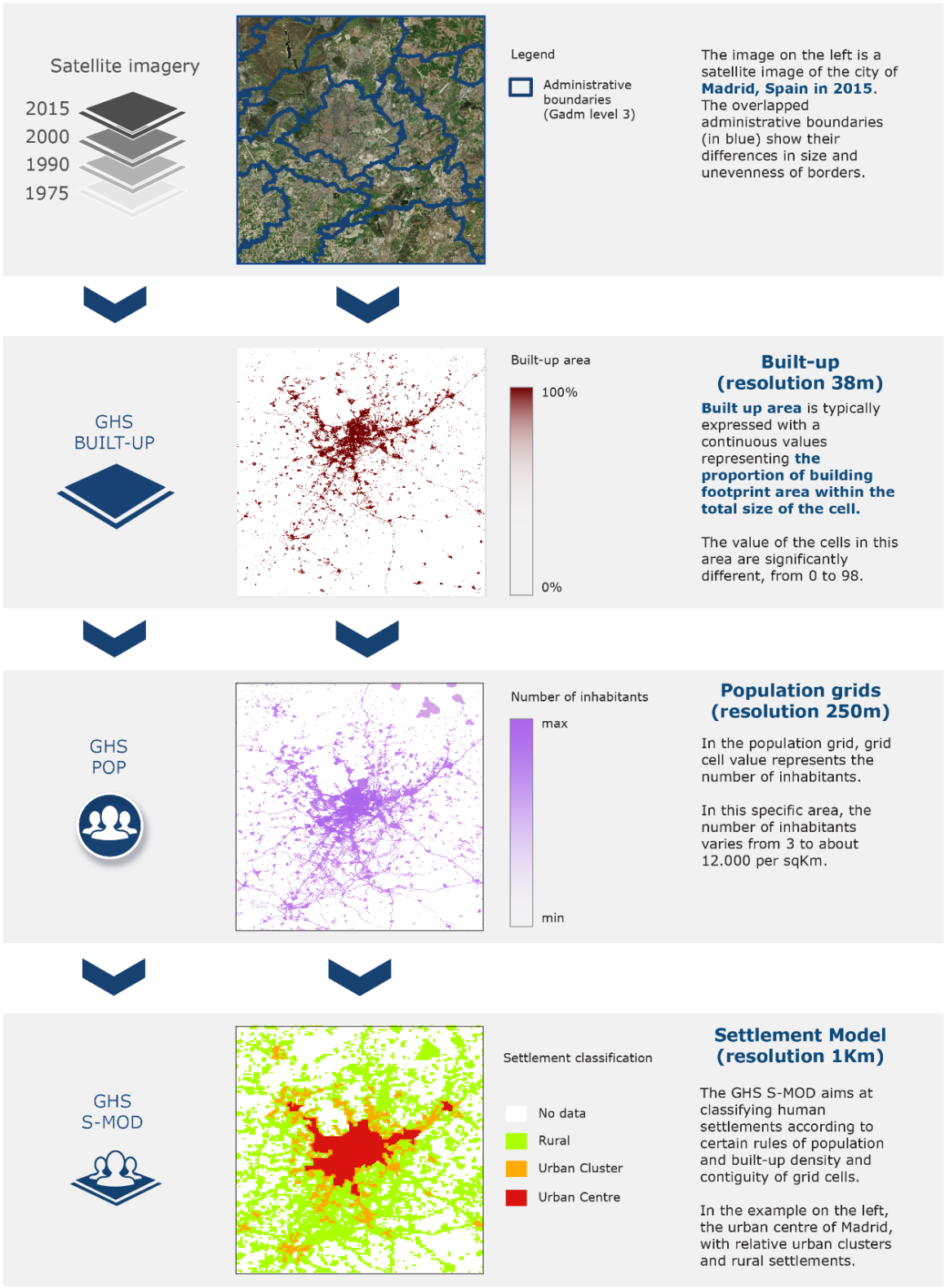

Figure 7 The GHS-BU and GHS-POP are combined to classify the gird cells into rural and urban areas. See chapter 3 for details on the model.

2.5 The GHSL institutional context

In 2018, the GHSL activities are supported by the JRC scientific working plan 2018-2019 in the frame of the JRC Directorate E "Space, Security & Migration". At the centre of the GHSL framework is the understanding of the planet, fully aligned with the JRC space strategy. At the JRC, the GHSL framework of data and tools supports several Knowledge Centres (KC): the KC for Disaster Risk Management, the KC for Sustainable Development, the KC for Territorial Modelling, and the KC for Security & Migration. Moreover, the GHSL is one key use cases for processing and analysis of big earth data of the JRC Earth Observation Data and Processing Platform (JEODPP) (Soille et al., 2017). The GHSL project is testing in the JEODPP the use of AI for automated information extraction from large data cubes such as those provided by the Sentinel satellites of the European Copernicus program. In fact, the next GHSL releases will integrate Copernicus Sentinel data (Corbane et al., 2017a). Following the successful test of the fitness for purpose of GHSL, the JRC is working, together with the Directorate-General for Regional and Urban Policy (DG REGIO) and DG for Internal Market, Industry, Entrepreneurship and SMEs (DG GROW) towards a regular and operational monitoring of global built-up area and population densities based on the processing of Sentinel data. The experiences made with the JEODPP will facilitate the implementation of the approaches on the new Data and Information Access Services (DIAS)[16] of the Copernicus Programme.

GHSL information are particularly salient in the disciplinary contexts of disaster risk reduction, urbanization and human settlements dynamics, where fine scale information on the presence of people and built-up areas are of high importance (Chmutina and Bosher, 2017). GHSL data served to quantify the process of urbanization (Melchiorri et al., 2018), observe population density (Smith, 2017), and inform policy making on 40 years of human settlements development (Martino Pesaresi et al., 2016b) and exposure to natural hazards (Pesaresi et al., 2017).

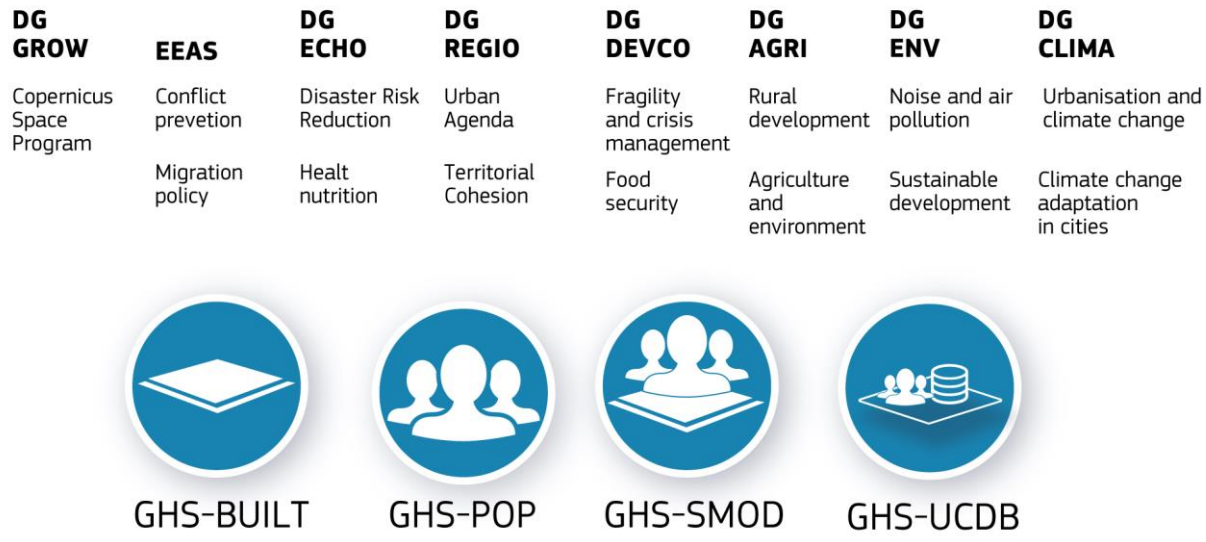

Figure 8 GHSL products supporting specific sectors of DGs

[16] https://www.copernicus.eu/en/access-data/dias

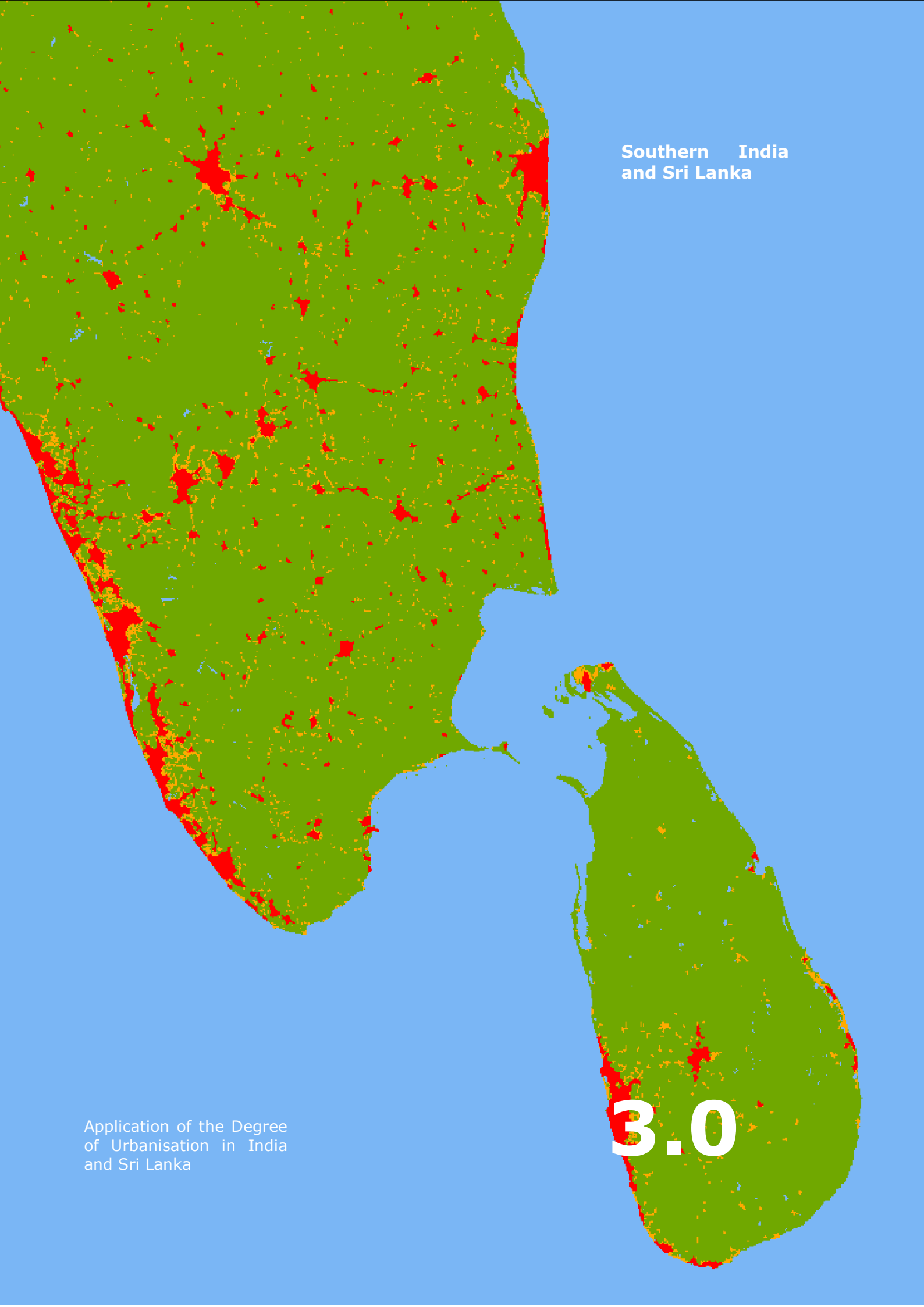

Application of the Degree of Urbanisation in India and Sri Lanka

3 Global Definition of cities and settlements

The Department of Economic and Social Affairs of the United Nations reports in the 2018 Revision of the World Urbanisation Prospect: "globally, more people live in urban areas than in rural areas, with 55 % of the world's population residing in urban areas in 2018." However, the UN acknowledges that the analysis relies on the data produced by national sources, which reflect the definitions and criteria established by national authorities. Therefore, the criteria used to identify urban areas vary from country to country and may not be consistent even between different data sources within a given country. About half of the definitions described in the report's methodological annex, include a minimum population size, either exclusively or in combination with other indicators or criteria. A specific size threshold is mentioned for 100 countries. Of these, the vast majority (85%) use a threshold of 5,000 or less. The most popular thresholds are 5,000 with 27 countries and 2,000 with 24 countries. Japan and China are outliers with thresholds that are ten to twenty times higher, respectively 50,000 and 100,000.

To address this issue, the European Union, the OECD and the World Bank launched a voluntary commitment to develop a global, people-based definition of cities and settlements during the third United Nations Conference on Housing and Sustainable Urban Development (Habitat III) in October 2016. Since then Food and Agriculture Organisation (FAO) and UN-Habitat have also joined this commitment. FAO is the 'custodian' UN agency for 21 SDG indicators for which a harmonised definition of rural areas is needed. UN-Habitat is the 'custodian' UN agency for 8 SDG indicators, for which a harmonised of city definition is needed.

These definitions are designed to support the New Urban Agenda[17], the global strategy to improve agricultural and rural statistics (GSARS)[18] and the monitoring of Sustainable Development Goals (SDG). Agreeing the first global consistent definition of cities and rural areas can also help many other policies and research areas.

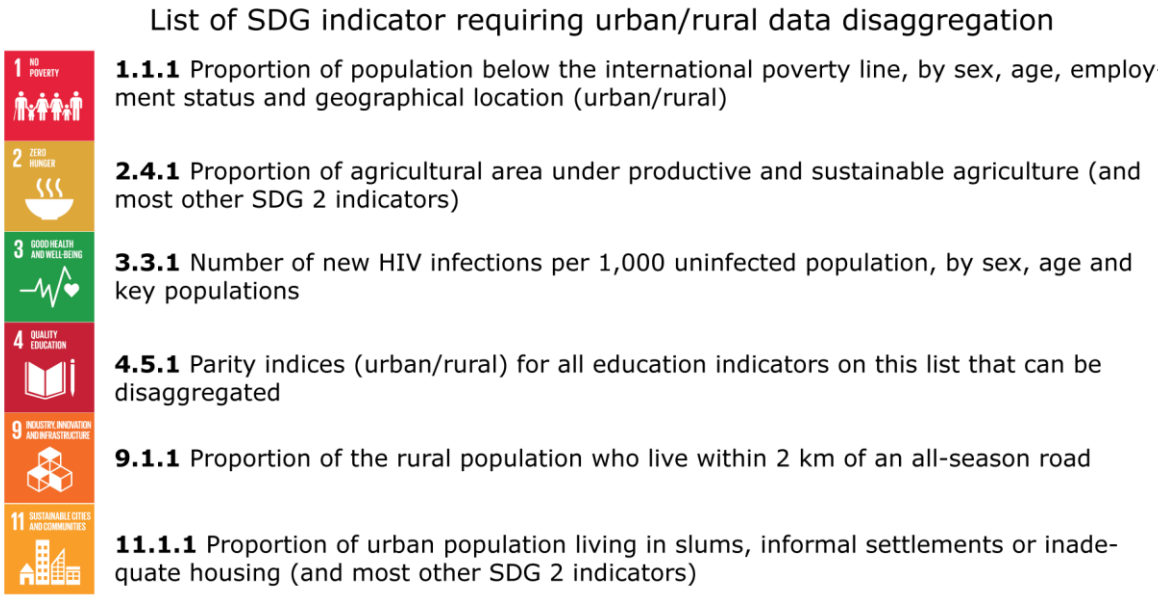

Figure 9 List of SDG indicators requiring urban/rural data disaggregation

3.1 Policy Context

With the adoption of the Sustainable Development Goals and its monitoring framework, the need to harmonise data collection and indicators monitoring is a cornerstone of the

[17] http://nua.unhabitat.org/
[18] http://gsars.org/en/

implementation process of the 2030 Development Agenda. Several of the indicators linked to goals require disaggregation in urban and rural classes, and are highly sensitive to where the boundary is drawn around a city (Figure 10).

List of urban SDG indicators sensitive to the city boundaries

11.2.1 Proportion of population that has convenient access to public transport

11.3.1 Ratio of land consumption rate to population growth rate

11.6.2 Annual mean levels of fine particulate matter (e.g. PM2.5 and PM10) in cities

11.7.1 Average share of the built-up area of cities that is open space for public use for all

Figure 10 List of urban SDG indicators sensitive to city boundaries

Figure 11 presents the examples of the fictive cities of Broadville and Narrowtown. In the former an expansive boundary is used to define a city, in the latter instead, a more restrictive one. It sheds light on indicators that are substantially sensitive to density of people and to the settings of the urban realm that can be drastically affected by the city definition being used. While the city centre tends to have convenient access to public transport, the outskirts of a city are often less well endowed. Accordingly, if a restrictive boundary is drawn the SDG performance could be better off. Similar considerations apply to air pollution, and share of open spaces (Table 1). An additional remark is proposed for demographic accounting. In Figure 11 the total population of the area between 1990 and 2015 is constant. While it declines in the central portion of the city. When a narrow city definition is adopted this area would report about demographic decline while from a functional standpoint the area of interest maintains its population and need for resources.

The goal of the voluntary commitment is to propose a definition to the UN Statistical Commission in 2020 that will complement national definitions and facilitate international comparisons. A harmonised definition of cities can support SDG monitoring by making data collection and reporting homogeneous across the globe. National definitions, and consequently the reporting of the United Nations Department for Economic and Social Affairs (UNDESA) through the World Urbanization Prospects, are considerably heterogeneous across territories (Buettner 2015; Forstall and Chan 2015). In particular, half the national definitions are based on an administrative designation which cannot be replicated in other countries. Even when national definitions rely on population size and/or density, the thresholds vary substantially. The variation in national definitions will have a direct effect on the collection of data, statistics, and SDG reporting.

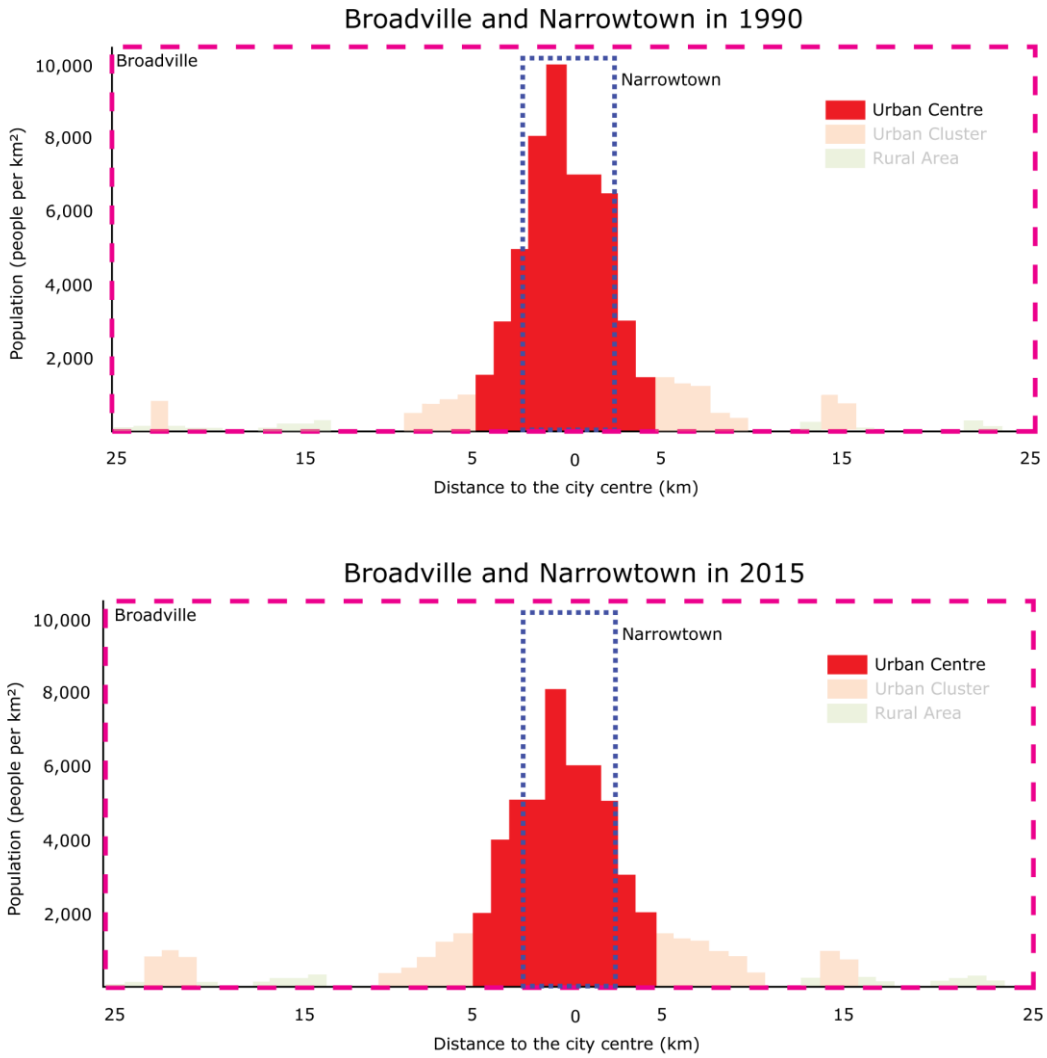

Figure 11 Examples of Broadville and Narrowtown to display an expansive and restrictive definition of a city. While between 1990 and 2015 population increases in Broadville, it declines in Narrowtown. Not just SDG indicators reporting depends on the boundaries, but also demographic information such as city size and population change.

Table 1 Effects of narrow or broad drawing of city boundaries

	Population	**Density**	**Air pollution**	**Access to transport**	**Share of open space**	**Land use growth**
Broadville	600,000	Low	Low	Poor	High	Rapid
Narrowtown	150,000	High	High	Excellent	Low	No growth

3.2 Model Description

The "Urban Centres" (UC) using the Degree of Urbanisation are defined as: "high-density clusters of contiguous grid cells of 1 km^2 with a density of at least 1500 inhabitants per km^2 and a minimum population of 50000"[19]. The UC as implemented in the current GHSL settlement model (SMOD) formulation is defined as: "the spatially-generalized high-density clusters of contiguous grid cells of 1 km^2 with a density of at least 1,500 inhabitants per km2 of land surface or at least 50% built-up surface share per km2 of land surface, and a minimum population of 50,000."

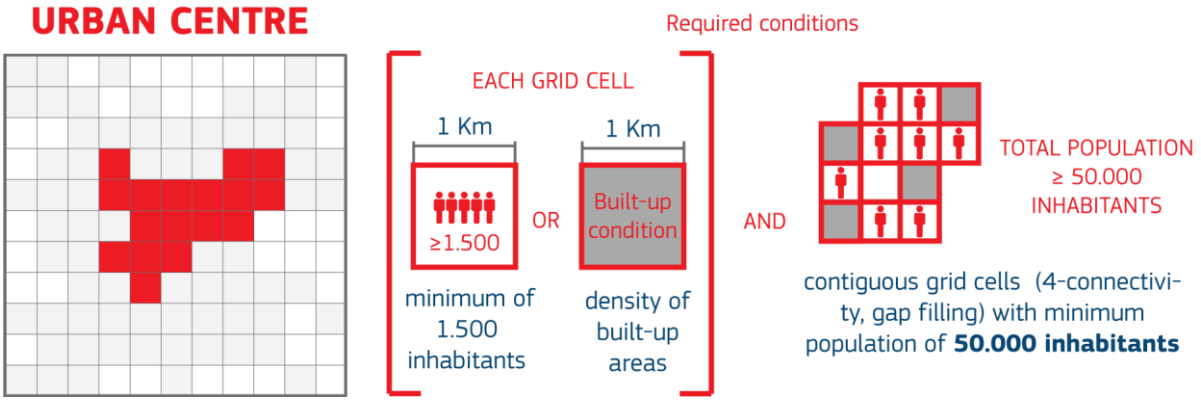

Figure 12 Schema representing an abstract urban centre, grid cell criteria, and population size threshold

The original degree of urbanisation was based on the population size, density and contiguity of local administrative units level 2 (LAU2). However, this method is based on LAU2s, which vary considerably in area size; hence the results are distorted and reduce the comparability between countries with large LAU2s and small LAU2s. This well-known problem, known as Modifiable Area unit problem (Gehlke and Biehl, 1934), is solved by using the GHSL population grid (or any other high-resolution population grid).

This is illustrated for the city of Cork, Ireland (Figure 13). Cork lies at the mouth of river lee into Lough Mahon. The land use is characterised by a typical mix of residential areas and some patches of industrial/commercial units. According to the land use map the city is well confined and is surrounded by agricultural areas and semi-natural vegetation (top left). The highest population densities are in the urban centre and the residential areas, dropping significantly in the agricultural areas (top right). The Degree of Urbanisation grid (bottom right) clearly reflects this. It maps very well the dense urban centre of Cork and classifies the less dense suburbs as urban clusters connected with the urban centre or as individual town. When comparing this with the Degree of Urbanisation applied to the LAU2 (bottom-left), the urban centres match well. However, the surrounding LAU2s are all classified as towns and suburbs, despite the fact that only a small part of the LAU2 is occupied by settlements. This problem aggravates, when working at a global scale, where administrative layers are often available only at district level or worse.

[19] European Commission, Regional Working Paper 2014, A harmonised definition of cities and rural areas: the new degree of urbanisation, Lewis Dijkstra and Hugo Poelman http://ec.europa.eu/regional_policy/sources/docgener/work/2014_01_new_urban.pdf

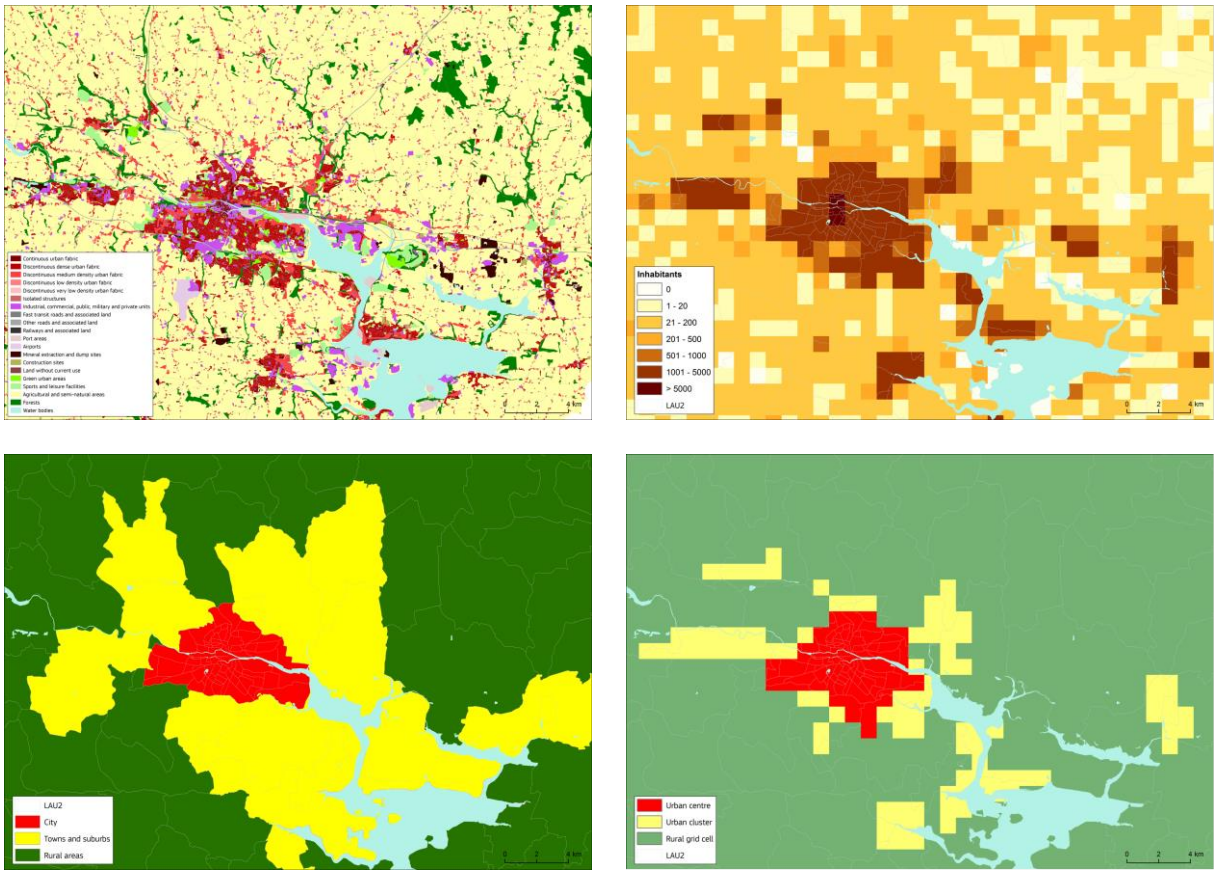

Figure 13 City of Cork (Ireland). Land use map based on Urban Atlas[20] (top left); GEOSTAT population grid[21] (top right); Degree of Urbanisation applied to the GEOSTAT grid (bottom right); Degree of Urbanisation applied to the LAU2 (bottom left).

3.3 Examples of urban centres across the globe

As the Global Definition of Cities and Settlements is applied to the Global Human Settlement Layer grids (built-up areas and population grids) that possess global coverage, it is possible to identify more than 10,000 urban centres across the entire planet Earth (Figure 14).

In order to illustrate morphological diversity, the series of figures below present selected examples of 1 km^2 urban centre cells with similar population density of different geographical areas. Examples are sourced in the urban centres of: Dakar (Senegal, Africa), Chandigarh (India, Asia), Busto Arsizio (Italy, Europe), and Havana (Cuba, Caribbean). While the population density estimate in GHS-POP within the 1 km^2 in the area within the red box is constant (5,000 people ± 5%), the samples below display the degree of heterogeneity of morphological characteristics (i.e. the physical morphology of the urban setting and landscape –built-up areas density, or vegetation patterns – greenness).

[20] https://land.copernicus.eu/local/urban-atlas
[21] https://ec.europa.eu/eurostat/web/gisco/geodata/reference-data/population-distribution-demography/

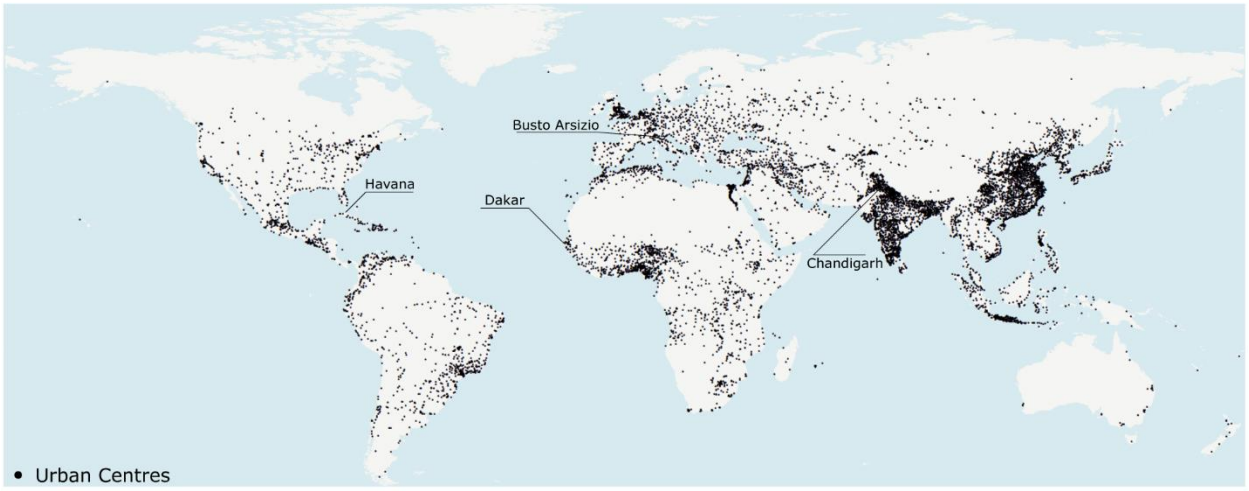

Figure 14 Global representation of urban centres location

Many of the characteristics that can be observed in the list of urban centres samples below, are also computed and provided as attributes of the 10,000 urban centres in the Urban Centred Database. Examples include: population density, share of open spaces, and greenness. The examples below provide physical and morphological evidences to reinforce the perception of diversity of cities (*World Cities Report 2016 Urbanization and Development: Emerging Futures* 2016).

The first example (Figure 15) shows the urban centre of Dakar and it displays a VHR satellite imagery, through which the human eye can perceive the building footprints. Figure 16 displays the very same location and extent using Landsat (30m resolution) imagery, which is used in the GHSL workflow to map built-up areas (GHS-BU). While this examples show the substantial difference between VHR and decametric resolution imagery, some consideration should be devoted to the availability of the two different information types. Although for some parts of the planet Earth VHR image has been collected, this information is oftentimes produced for commercial purposes, subject access costs (i.e. licensing, prices), moreover it rarely results in global coverage, and frequently information over long periods is unavailable. In contrast, Landsat resources were made open and free by USGS in 2009, contain records since 1975 yet, their resolution is not as detailed as the former typology of information.

Figure 15 Example of Urban Centre in Africa, in the area of Dakar (Senegal)

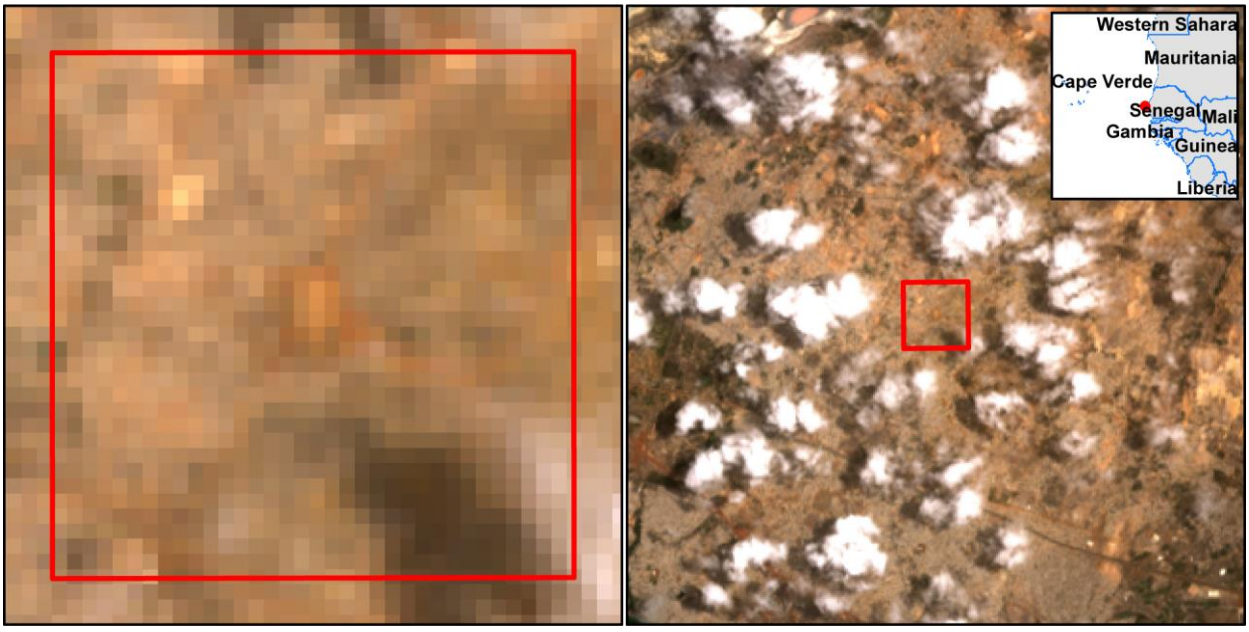

Figure 16 Landsat satellite imagery in the area of Dakar (same location as in Figure 15) showing the 30m resolution of the sensor from which GHS-BU is produced.

Figure 17 Example of Urban Centre in Asia, in the area of Chandigarh (India)

Figure 18 Example of Urban Centre in Europe, in the area of Busto Arsizio (Italy)

Figure 19 Example of Urban Centre in the Caribbean, in the area of Havana (Cuba)

Figure 20 © Adobe Stock, 2018

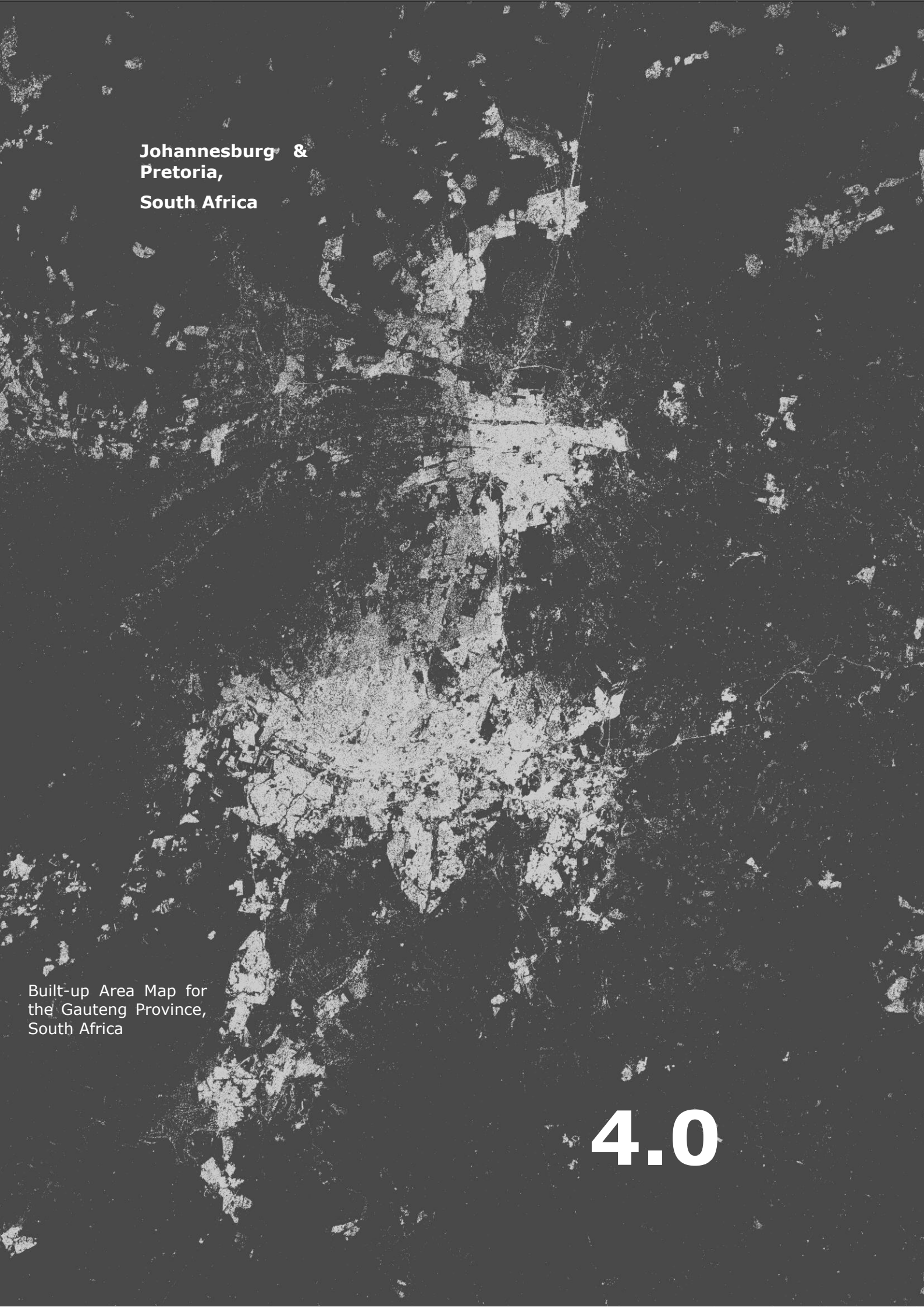

Built-up Area Map for the Gauteng Province, South Africa

4.0

4 Data

4.1 Multi-temporal built-up grids (GHS-BU)

The built-up grids used in this Atlas are based on the global, multi-temporal evolution of built-up surfaces derived from Landsat data collections organized in four epochs 1975, 1990, 2000 and 2014 (referred to as GHS_LDSMT_2017). It is the result of the re-processing 33,202 Landsat images organized in four data collections, centred at 1975, 1990, 2000 and 2014, as follows:

- 7,597 scenes acquired by the Multispectral Scanner (MS) (collection 1975);
- 7,375 scenes acquired by the Landsat 4-5 Thematic Mapper (TM) (collection 1990);
- 8,788 scenes acquired by the Landsat 7 Enhanced Thematic Mapper Plus (ETM+) (collection 2000); and
- 9,442 scenes acquired by Landsat 8 (collection 2014).

The first version of this data set was released in 2016 (GHS_LDSMT_2015) and is now significantly improved as described in the following. The GHSL method for built-up surface recognition from satellite data is fully automatic and reproducible. The procedure is based on the Symbolic Machine Learning (SML, Pesaresi et al. 2016b) and uses existing global land cover products as training sets. For each pixel, it provides a probability (confidence) that it is built-up or not.

The resulting multi-temporal product encodes the presence of built-up surfaces according to the earliest epoch for which the built-up surface presence was detected (i.e. 1975, 1990, 2000, or 2014 epoch) at approximately 38 m resolution.

The characteristics of the SML classifier allow incremental learning and improvement of the classification outputs as soon as new data depicting built-up areas become available. In other words, the outputs of the SML classifier in one experiment can be used as a training set in the subsequent experiments.

The approach based on incremental learning in the frame of the SML allows incorporating new, updated learning sets and adjusting what has been learned according to previous examples. This learning method has the advantage of achieving superior efficiency for training minimizing the impact on accuracy. Another beneficial point is that the performance can slightly improve. The results can only get better after each iteration since the level of noise is progressively decreasing with each run of the GHSL workflow. Having this in mind, the four Landsat data collections were reprocessed on the JEODPP with a revised workflow for built-up area extraction and for the fusion of the four epochs into one multi-temporal product. The global built-up layer derived from Sentinel-1 data (GHS_S1) provides a more detailed learning set of built-up areas. The Sentinel-1 (GHS_S1) data set was in turn derived from the GHS_LDSMT_2015, leading to a successive refinement and improvement of the results (see Corbane et al., under review for details). According to the results of a global validation exercise using detailed building footprints (Corbane et al., under review) for 277 areas of interest spread across different continents, the new GHS-LDMST_2017 provides the best balanced accuracy (BA), yielding BA=0.86.

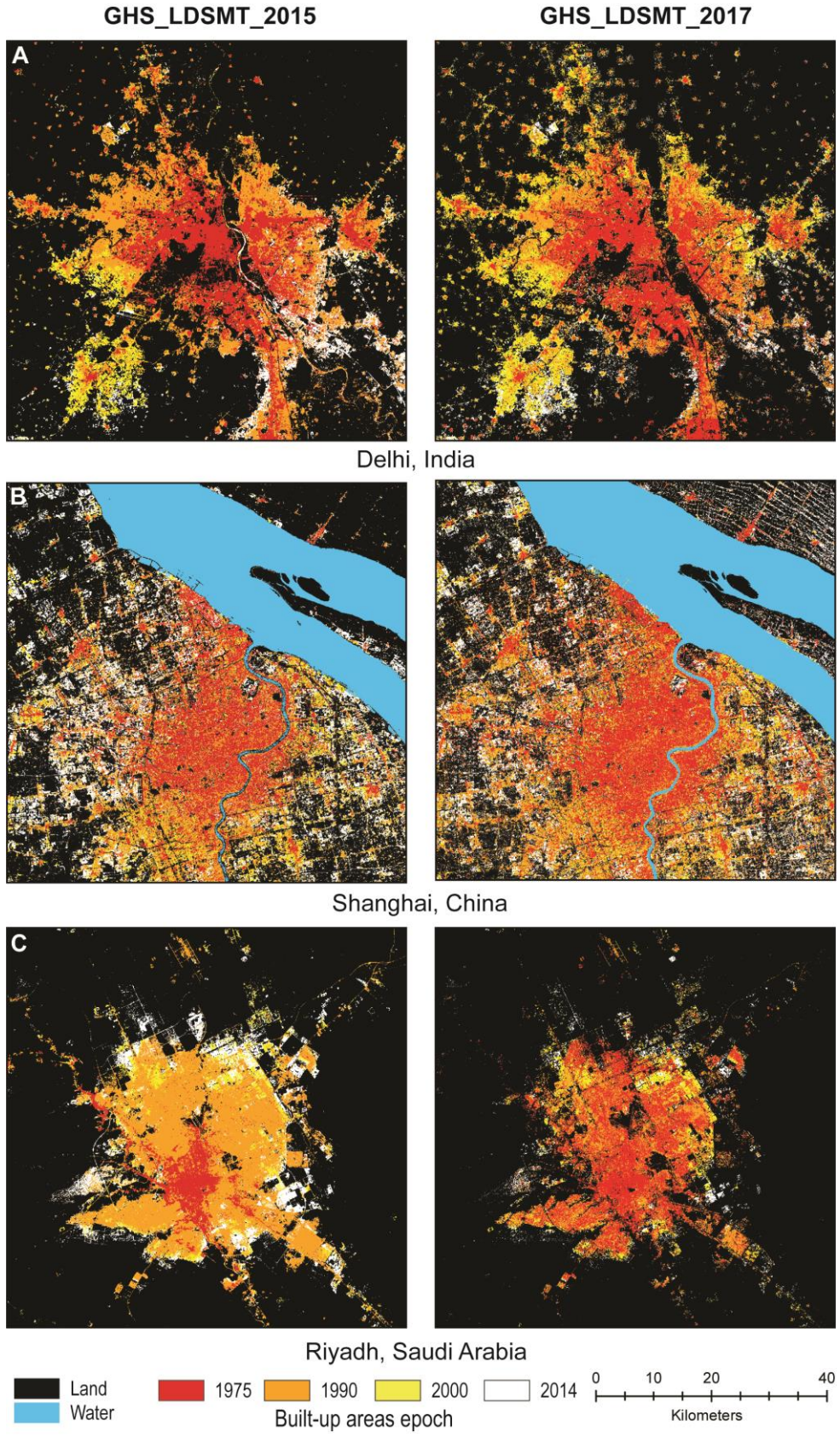

Figure 21. Examples from selected cities showing the reduction of over-detection and under-detection errors in the new multitemporal built-up layer. The results of GHS_LDSMT_2015 are compared against those of GHS_LDSMT_2017 respectively for the cities of New Delhi (India -A), Shanghai (China -B) and Riyadh (Saudi Arabia -C)

Most importantly, we observe a gradual improvement in the accuracy measures starting from the first layer GHS-LDMST_2015 (BA=0.83), the GHS_S1 layer (BA=0.84) and the last GHS-LDMST_2017. The observed trend of increasing BA rates in subsequent generations of GHSL data including the precedent releases as learning set, is an empirical confirmation of the positive impact of the incremental learning approach of the GHSL framework.

4.2 Multi-temporal Population Grids (GHS-POP)

This spatial raster dataset depicts the distribution and density of population, expressed as the number of people per cell. Residential population estimates for target years 1975, 1990, 2000 and 2015 provided by CIESIN Gridded Population of the World, version 4.10 (GPWv4.10) were disaggregated from census or administrative units to grid cells, informed by the distribution and density of built-up as mapped in the Global Human Settlement Layer (GHSL) global layer per corresponding epoch (for disaggregation method see Freire *et al.*, 2016).

The new version of the GHSL population distribution grids aimed at incorporating improvements originating from input datasets, namely population estimates and built-up presence. While the disaggregation relied essentially on the same clear and simple approach, there were significant differences to the input data that had a positive effect on the final quality and accuracy of population grids. For the new GHS-POP, the GHS-BU was used as target for disaggregation of population estimates. Cells declared as "NoData" in built-up layers were treated as zero for population disaggregation. The base source of population estimates (both counts and geometries) for the four epochs was the Gridded Population of the World, version 4.10 (GPWv4.10), from CIESIN/SEDAC. Respect to the previous release of GHSL grids (R2015A), this pre-Release used GPW source data that incorporated boundary or population updates for 67 countries. Due to the previous GHSL population grids being produced in last quarter of 2015, before the final GPWv4 data set was fully assembled, more changes were included in population sources in the current pre-Release than those incorporated in the GPW data between GPWv4 and the current GPWv4.10. For detailed information on what has changed in GPWv4.10, refer to:

http://beta.sedac.ciesin.columbia.edu/data/collection/gpw-v4/whatsnewrev10

Figure 22 © Adobe Stock, 2018

4.3 Urban Centres Delineation

Be *X* a squared grid of cells *x* with uniform surface of 1 km^2 representing the global Earth surface with a Mollweide pseudo cylindrical geographical projection. Be POP_x the estimated amount of resident population in the cell *x* by the GHSL, and be BU_x the estimated share of built-up surface in the cell *x* by the GHSL by observing 30-m-res satellite measurements. Be $LAND_x$ the estimated share of permanent land surface in the cell *x* by a GHSL processing of the JRC Global Surface Water (GSW) input data[22]. $LAND_x$ was estimated as $LAND_x = 1 - w_x^{0.8}$, with $w_x^{0.8}$ the share of surface water occurring for more than 80% of the 30-m-resolution satellite measurements of the past 20 years (15 days interval) in the cell *x.*

Given the above, the densities of population and built-up areas per land surface are calculated as follows:

$$POP'_x = \frac{POP_x}{LAND_x}$$

$$BU'_x = \frac{BU_x}{LAND_x}$$

Consequently, the support set of the HDC spatial domain is determined as follows:

$$HDC_x^{supp} = \{x : POP'_x > 1500 \cup BU'_x > 0.5\}$$

The HDC_x^c spatial clusters are determined by the application of the "*contiguous grid cells of 1km^2*" criteria of the root definition, by assuming 4-connectivity rule on the grid X representing the HDC_x^{supp} set. 4-connected samples are neighbours to every sample that touches one of their edges. These samples are connected horizontally and vertically. The 4-conn rule it is showed in the schema below. Respect to the sample X, the cells in the horizontal and vertical directions and one step of displacement are considered adjacent. The cells in the diagonal along the grid are not considered adjacent.

	not	yes	not	
	yes	**X**	yes	
	not	yes	not	

The population size of each cluster *c* of the HDC_x^c is calculate as

$$POP_x^c = \sum POP_x \cap HDC_x^c$$

Finally, the HDC_x^c clusters are selected so that $POP_x^c > 50000$

$$HDC_x^{50K} = HDC_x^c, c : POP_x^c > 50000$$

Subsequently, the HDC_x^{50K} individual clusters that passed the above test are processed by a spatial generalization procedure *G* including an iterative local union-majority filter (also called "smoothing") until idempotence it is reached followed by a gap filling step. That gap filling step is filling all the holes remaining after the smoothing, and having an area

[22] Jean-Francois Pekel, Andrew Cottam, Noel Gorelick, Alan S. Belward, High-resolution mapping of global surface water and its long-term changes. Nature 540, 418-422 (2016). (doi:10.1038/nature20584) https://global-surface-water.appspot.com/download

less than 15 km^2. The local union-majority filter applied in the generalization *G* has a kernel *K* of 3x3 spatial units in the grid X, corresponding to a surface of 9 km^2.

At each iteration, the union-majority filter Φ it is defined as follows:

$$\Phi_x = \begin{cases} x = true \rightarrow \Phi_x = true \\ x = false \rightarrow \begin{cases} \sum_{x \in K} true_x > \frac{\hat{n}^K}{2} \rightarrow \Phi_x = true \\ \sum_{x \in K} false_x > \frac{\hat{n}^K}{2} \rightarrow \Phi_x = false \end{cases} \end{cases}$$

With $\frac{\hat{n}^K}{2}$ being the half of the number of samples included in the kernel *K* considered in the spatial filtering. In the specific case, $\frac{\hat{n}^K}{2} = \frac{3x3}{2} = 4.5$

The iterative local union-majority filter Φ it is applied individually to each HDC, testing at each iteration that the total number of HDCs determined before the filtering process it is maintained constant. Consequently, avoiding the merging of two distinct HDCs because of the spatial filtering process.

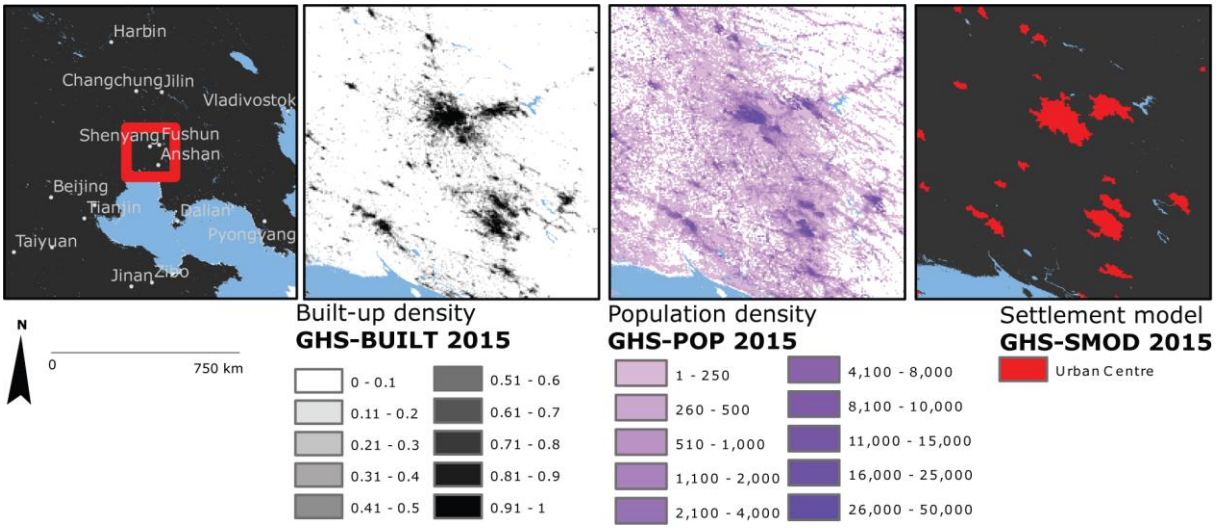

Figure 23 example at 1km resolution of GHSL baseline data (GHS-BU, GHS-POP) for the delineation of urban centres in the Northern Region of China.

4.4 Urban Centres Database Attributes

The new Urban Centres Data Base (GHS-UCDB) builds on the improved GHS-BU and GHS-POP grids. The Urban Centres were spatially delimited by applying the "degree of urbanization" model. The GHS-UCDB (Figure 24) was generated by spatial integration of the urban centres with the GHSL data and with other sources related to five main thematic areas: geography, socio-economic, environment, Disaster Risk Reduction, and Sustainable Development Goals (Table 1). The principal methods used to derive the attributes to characterise urban centres through geospatial processing is displayed in Figure 25. An additional list of attribute complements the one by thematic area. It includes mainly classification and reference attributes (such as name, latitude-longitude, etc.).

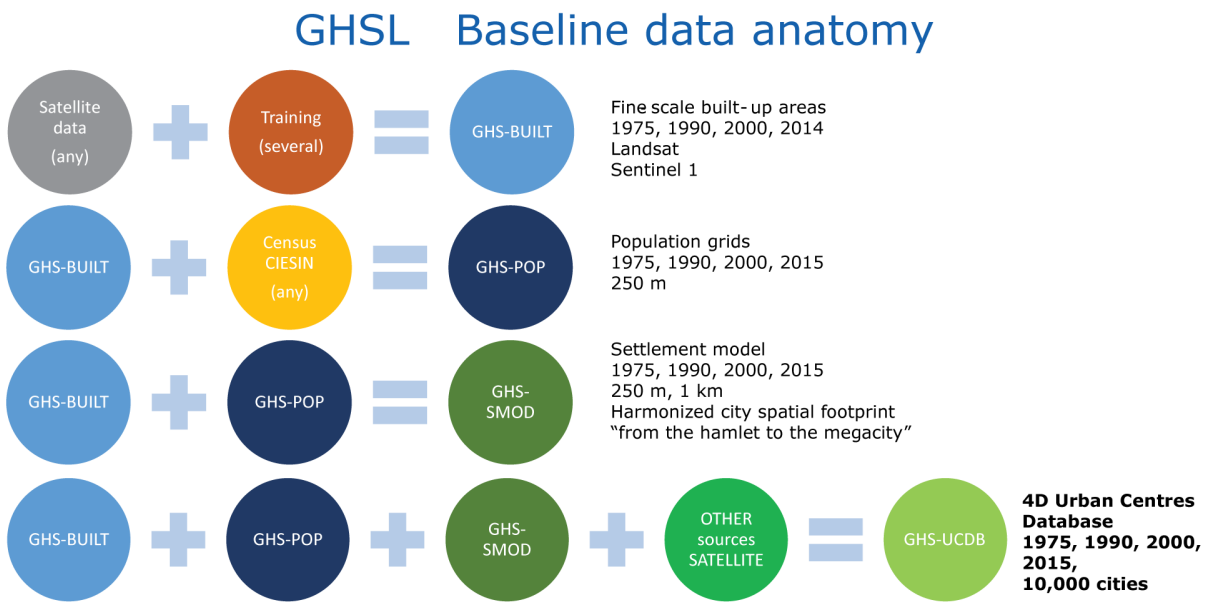

Figure 24 Anatomy of the key information components and data processing/integration used to create the GHS-UCDB

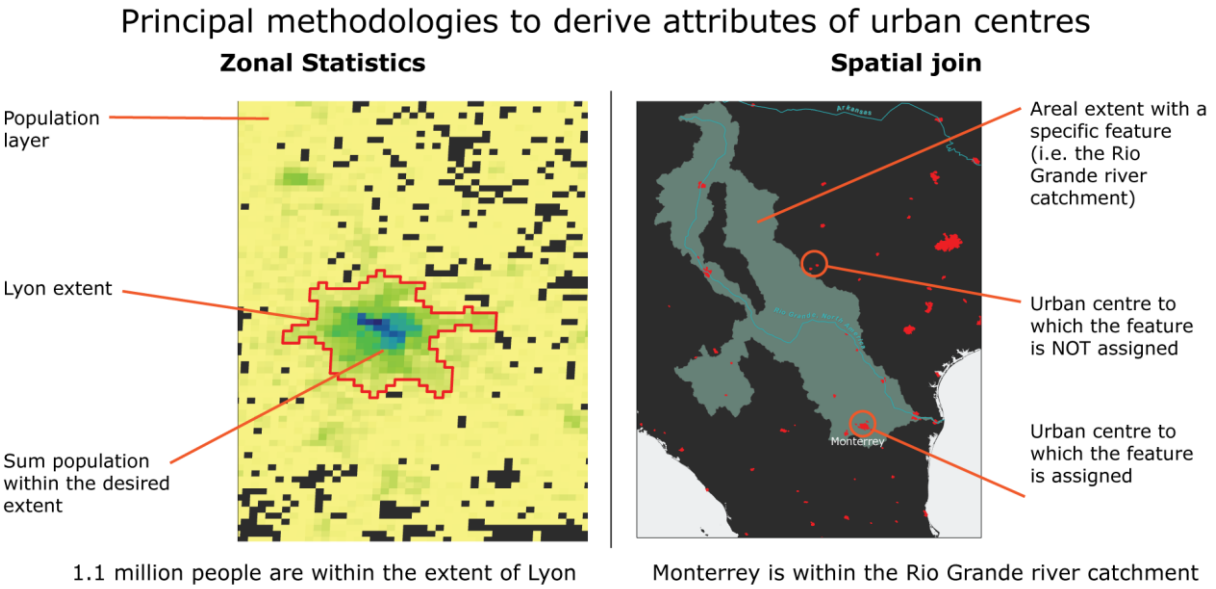

Figure 25 Elements of geospatial operations tasks to derive attributes of urban centres

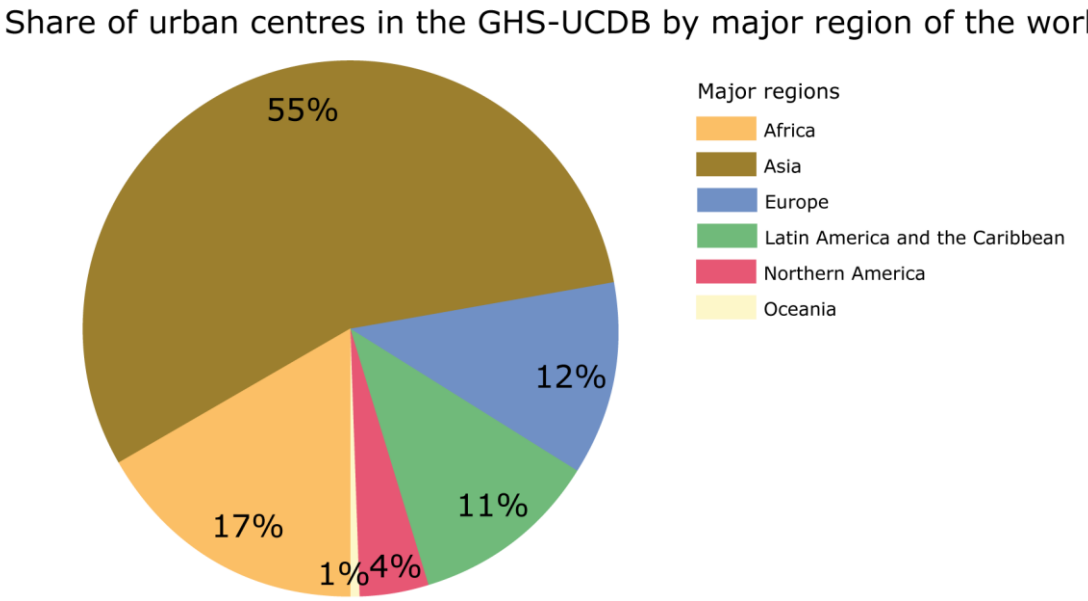

Figure 26 GHS-UCDB regional coverage, share of centres by major region of the world

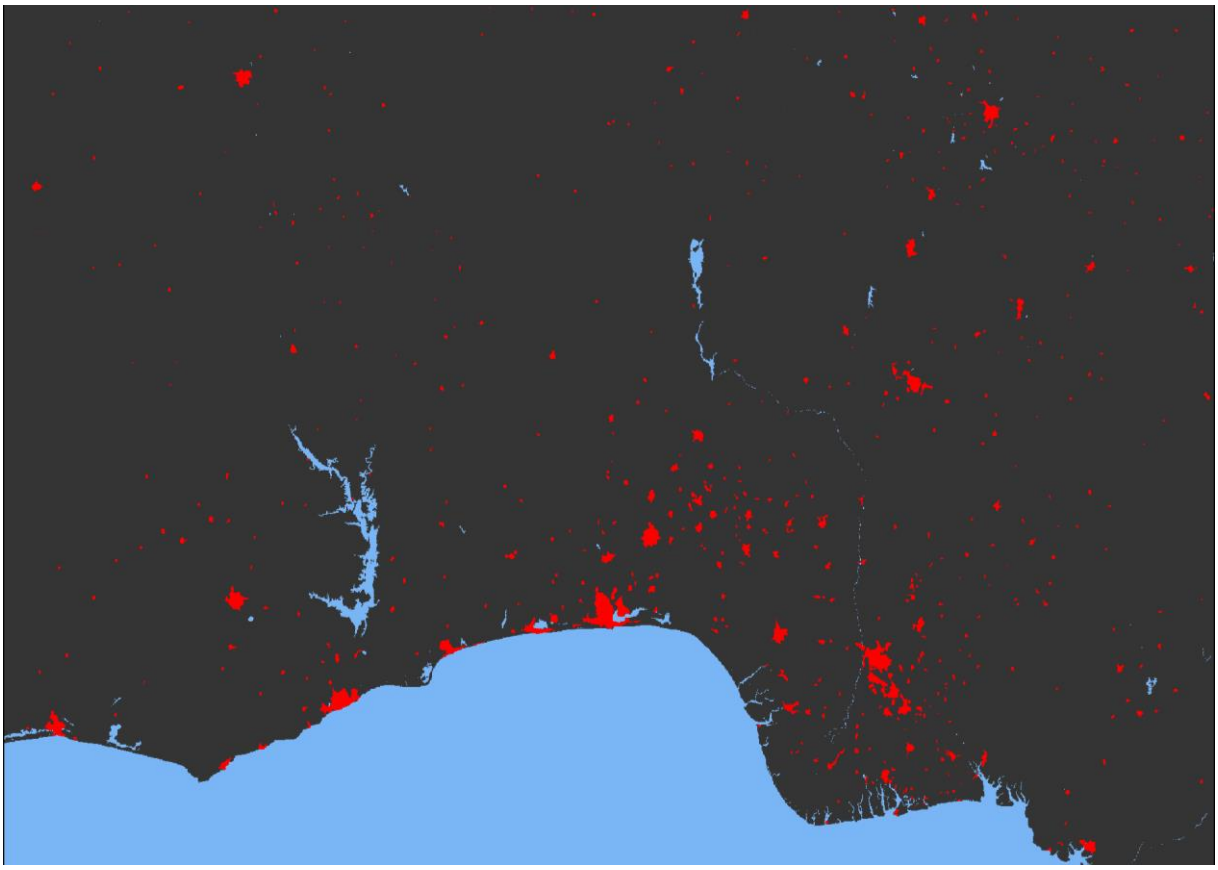

Figure 27 Urban centres in the northern Gulf of Guinea

Table 2 List of UCDB attributes by thematic area and temporality. Some attributes are classification of the urban centres and their temporal coverage (here, 2015) refers to the epoch for which the urban centres were delineated. Land Use Efficiency attribute refers to a temporal span.

Thematic area	Attribute	Temporal coverage			
		1975	1990	2000	2015
Geography	Travel time to capital centre	2015			
	Elevation				
	Biome type				
	Climate class				
	Income group				
	Soil group				
	River basin				
	Temperature		■	■	■
	Precipitation		■	■	■
Socio-economic	Built-up areas	■	■	■	■
	Population	■	■	■	■
	Night-time light				■
	GDP		■	■	■
Environment	Greenness		■	■	■
	CO_2	■	■	■	■
	PM2.5	■	■	■	■
DRR	Exposure to floods	■	■	■	■
	Exposure to earthquake	■	■	■	■
	Exposure to storm surge	■	■	■	■
	Exposure to heatwave	■	■	■	■
SDG	Land Use Efficiency (11.3.1)	1990–2015			
	Open spaces (11.7.1 –proxy)		■	■	■

Table 3 List of additional UCDB attributes. The temporal coverage (here, 2015) refers to the epoch for which the urban centres were delineated

Variable	Attribute	Temporal coverage
Position	Latitude	2015
	Longitude	
Name	Main name	
	List of names of populated places in the urban centre area	
	UN Geographic region level 2	

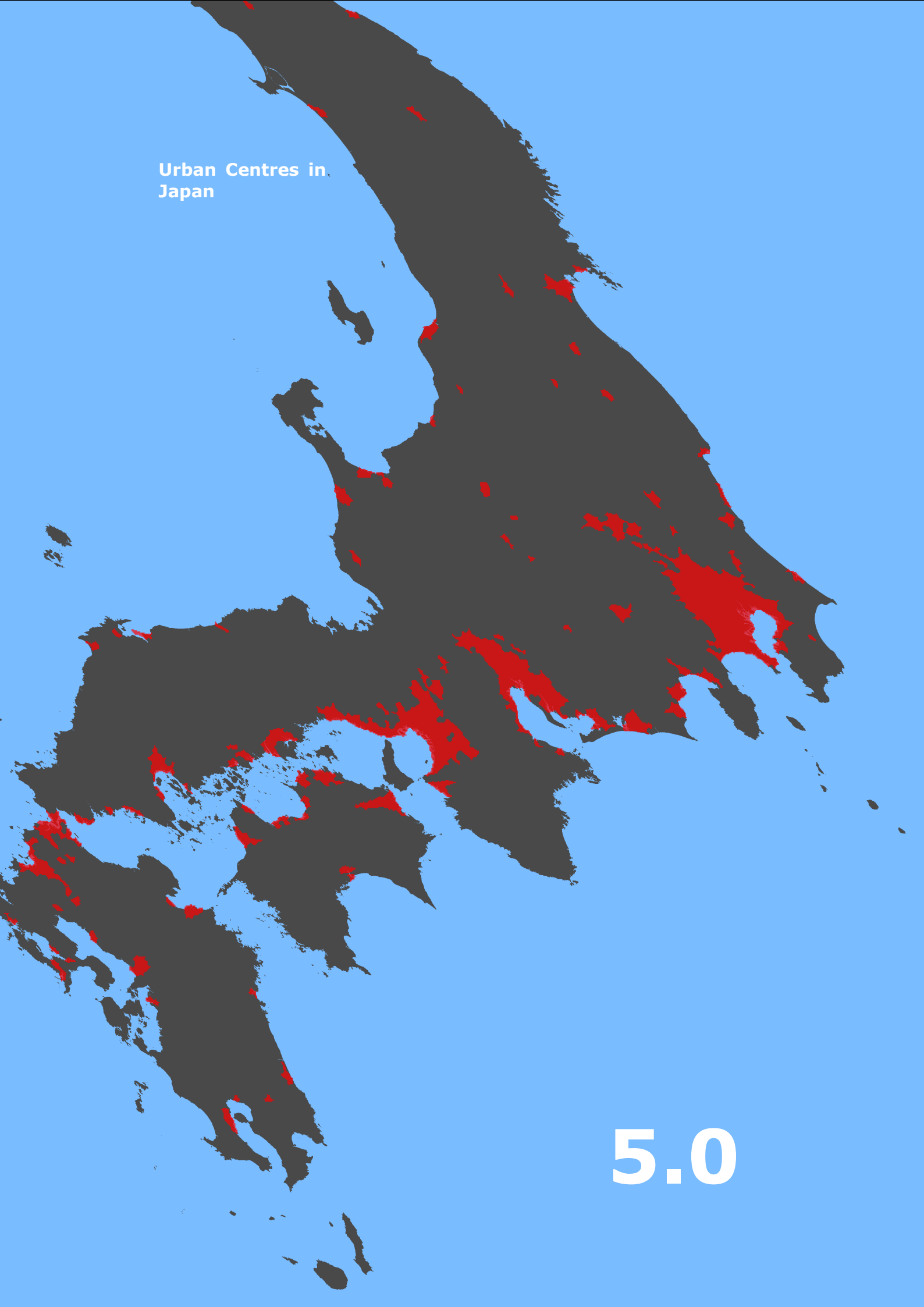
Urban Centres in Japan
5.0

5 Urban Centres Database

The Urban Centres Database derived from the Global Human Settlement data (GHS-UCDB) is the first global, harmonised, consistent 4-D city database worldwide.
It **is a 4-dimensional database,** offering for each city:

- Location (geographic position and names);
- Extent (surface and shape);
- *N* attributes which can be considered and represented as volumes (i.e. population, greenness, night-time light etc.);
- Information over time (for several attributes)

Some established city databases contain some of the above features. For example, the UN World Urbanization Prospects (UNDESA, 2018) contains names of urban agglomerations, their location, their population, and its variation over time. However, the spatial extent is not available to date. Moreover, as compared to the UN World Urbanization Prospects accounting cities greater than 300,000-population size, the GHS-UCDB extends the universe of cities until the 50,000-population size cut-off value, expanding significantly the universe of cities described by the data (Figure 28).

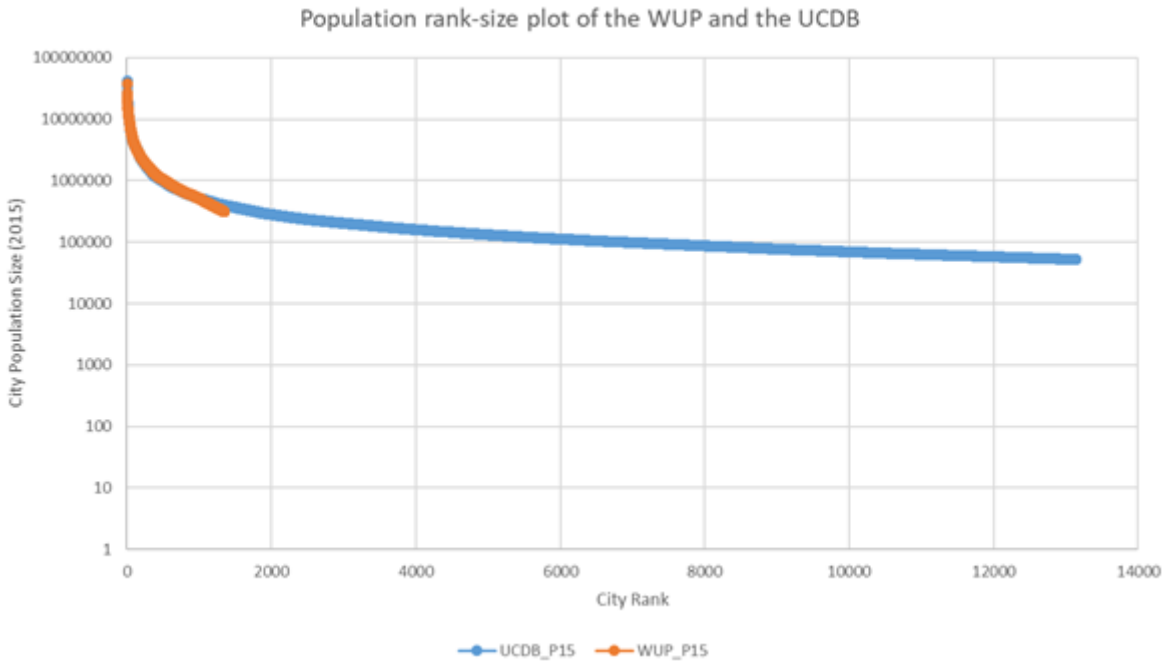

Figure 28 Population (year 2015) rank-size plot of the cities included in the WUP as compared to the GHS-UCDB records

The GHS-UCDB can support diversified needs across several thematic domains, including baseline for SDG indicators, Disaster Risk Reduction exposure estimates, environmental analyses and geographic analyses (Figure 29).

The GHS-UCDB is a key information source when the user is interested in analysing and comparing cities across the world ensuring the consistency of the comparison. In particular, the user can query the database to answer questions such as:

- *Which are the cities with value above X in the attribute Y?*

Be Y the population attribute and X the threshold of 10 million people (the established megacity threshold). The result of the query will be a list of urban centres that are megacity in the selected epoch (i.e. 2015). The user can consequently analyse the GHS-

UCDB attributes for this group of centres (i.e. built-up areas and population in the previous epochs.

- *How many cities are there below the value X in the attribute Y?*

Be Y the Modified Mercalli Intensity class attribute (intensity scale of earthquakes), and X the class V of the scale (moderate shaking). The result of the query will be a list of cities exposed to earthquakes below class V intensity. The user can consequently analyse where these urban centres are and i.e. population and built-up areas over time.

- *How much is the total/average of the attribute Y in cities?*

Be Y the greenness attribute of an urban centre, it is possible to calculate the average NDVI value of the city.

- *How much more is the attribute Y in the city A vs B?*

Be Y the night-time light emission attribute. The result of this query is useful to compare how much light two or more cities emit at night. This comparison is particularly useful when aggregated with other attributes i.e. income groups, region of the world, or population size.

- *How much the attribute Y has changed in city A?*

Be Y_t the temperature attribute for the epoch 1990 and Y_{t+1} the temperature attribute for the epoch 2015. The user can calculate the change in the temperature for any of the urban centres.

The GHS-UCDB is organised in five main thematic areas: geographic, socio-economic, environment, Disaster Risk Reduction, and Sustainable Development Goals – as presented in the data section. This section presents the features of the GHS-UCDB, proposes ways, in which the GHS-UCDB can be used and in dedicated thematic sections presents results and key messages derived from the analysis of the GHS-UCDB.

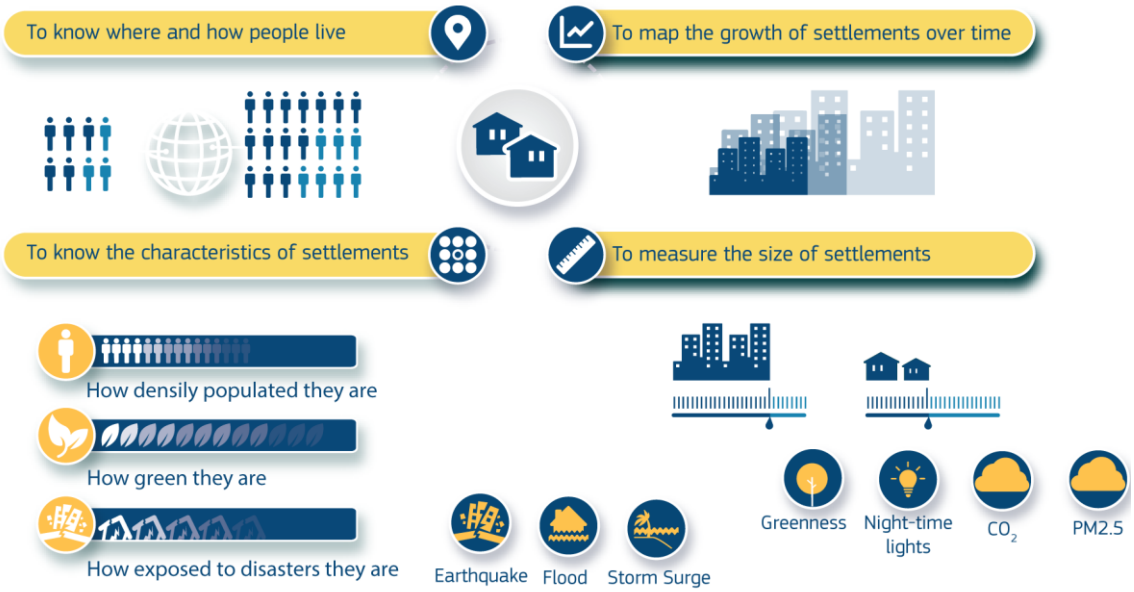

Figure 29 Examples of GHS-UCDB uses

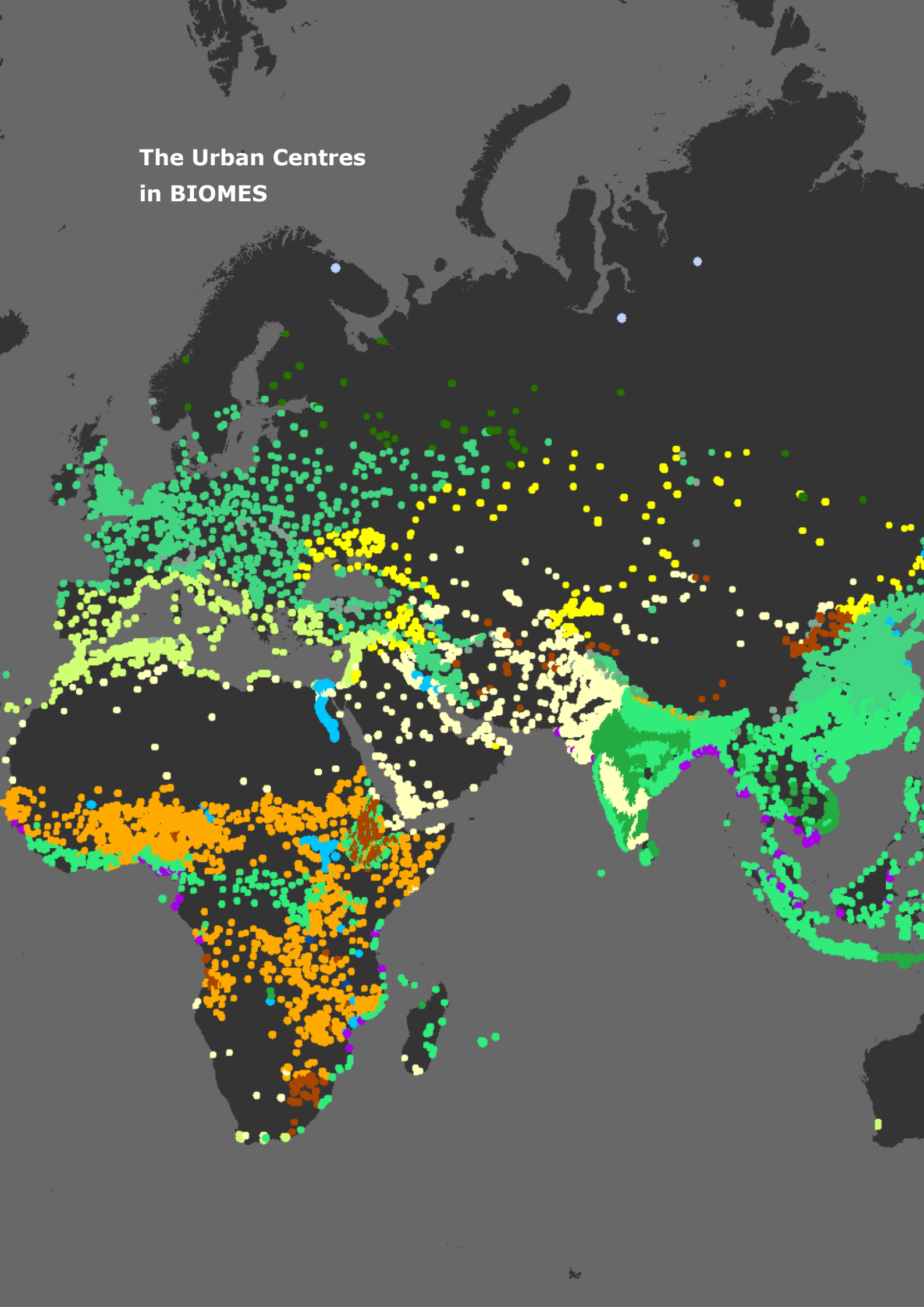
The Urban Centres
in BIOMES

5.1 Geography

Geographic conditions impact cites and urban centres. They have long enabled the emergence and expansion of cites and urban centres, but also affect and constraint their growth and development. The global set of urban centres as mapped by GHSL was intersected with a set of relevant geographic variables for which global geospatial datasets were available, but novel attributes were also computed for the purpose of this Atlas (e.g. travel time to country capital). Enriching the urban centres database with these physiographic attributes enables analysis of the interplay of cities with their geographic setting. The geographic variables discussed in the UCDB report are: *Biome type, Soil type, Elevation, Climate, Temperature, Precipitation, and River Basins.*

Figure 30 © Adobe Stock, 2018

5.1.1 Biome

Urban centres according to biomes.

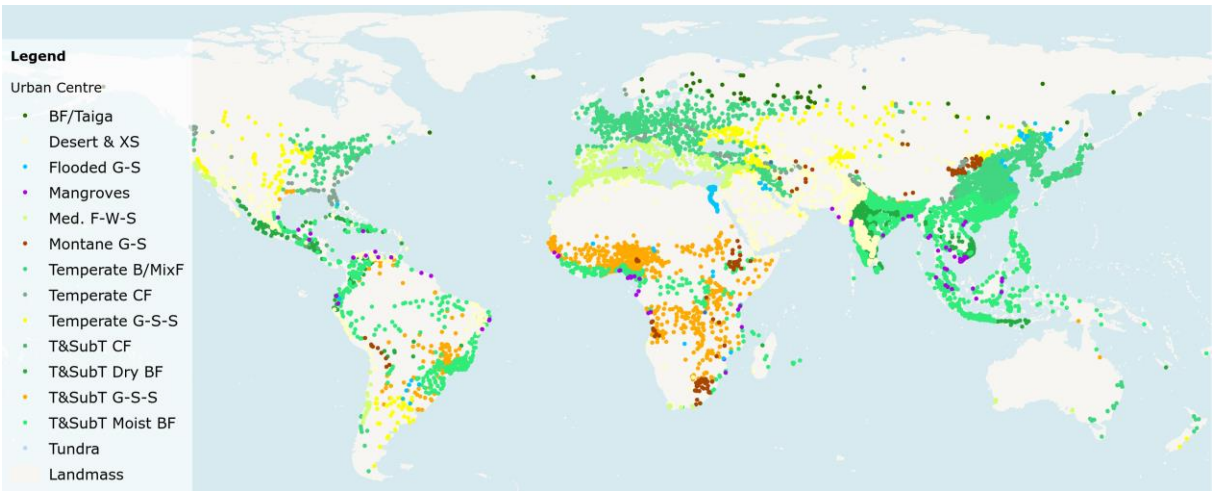

Figure 31 Urban centres according to their location in the biomes of the world.

Note: Tropical and Subtropical Dry Broadleaf Forests (T&SubT Dry BF), Mediterranean Forests, Woodlands, and Scrub (Med. F-W-S), Temperate Grasslands, Savannas, and Shrublands (Temperate G-S-S), Deserts and Xeric Shrublands (Desert & XS), Temperate Coniferous Forests (Temperate CF), Tropical and Subtropical Coniferous Forests (T&SubT CF), Temperate Broadleaf and Mixed Forests (Temperate B/MixF), Boreal Forests/Taiga (BF/Taiga), Tropical and Subtropical Moist Broadleaf Forests (T&SubT Moist BF), Tropical and subtropical grasslands, savannas, and shrublands (T&SubT G-S-S), Flooded Grasslands and Savannas (Flooded G-S), Montane Grasslands and Shrublands (Montane G-S)

Biomes are the most basic units that ecologists use to describe global patterns of ecosystem form, process, and biodiversity. Interestingly, existing descriptions of biome systems mostly ignore human influence or use a limited number of anthropogenic ecosystem classes (Ellis, 2018; Ellis and Ramankutty, 2008). Without entering into the on-going discussions in ecology, this section uses the Terrestrial Ecosystems of the World (TEOW) map, which contains a distinct assemblage of natural communities sharing a large majority of species, dynamics, and environmental conditions, to map each urban centre into one of its biomes (Figure 31). Urbanization is reported as one of the most important threats to biodiversity worldwide as urban areas may threaten ecosystems through direct habitat conversion (Clergeau et al. 1998, Blair 1999, McKinney 2002). Also, high concentrations of human population has various indirect effects, which include freshwater contamination, waste generation, resource use or habitat fragmentation (Mikusinski and Angelstam 1998).

The urban centres are classified according to the biome within which the given urban centre is located (considering its extent). Almost 2/3 of all urban centres are located in three biomes: (1) *Tropical and Subtropical Moist Broadleaf Forests*, (2) *Temperate Broadleaf and Mixed Forests*, and (3) *Deserts and Xeric Shrublands with a share of global* urban centre population in 2015 of 32 %, 26% and 11%, respectively in 2015. Asia has the highest share of urban centre population living in these three biomes. Most of urban centre population of Africa lives in *Tropical and subtropical grasslands, savannas, and shrublands*, while the urban centre population of Latin America and Caribbean region is concentrated *in Tropical and Subtropical Moist Broadleaf Forests* and *Deserts and Xeric Shrublands*.

Between 1990 and 2015 the population of urban centres increased by almost one billion. A large part of the population (about 1/3 of the global increase) live in urban centres of the *Tropical and Subtropical Moist Broadleaf Forests,* resulting in a relative increase of 47% in this class. The urban centres population living in *Boreal Forests/Taiga and Tundra* has declined between 1990 and 2015, while the urban centre population settled in (1) *Montane Grasslands and Shrublands*, (2) *Tropical and subtropical grasslands, savannas,*

and shrublands, and (3) *Lakes* have doubled during this period. Figure 32 shows for each bioe the urban centre population change in absolute numbers and the ratio of change between 1990 and 2015.

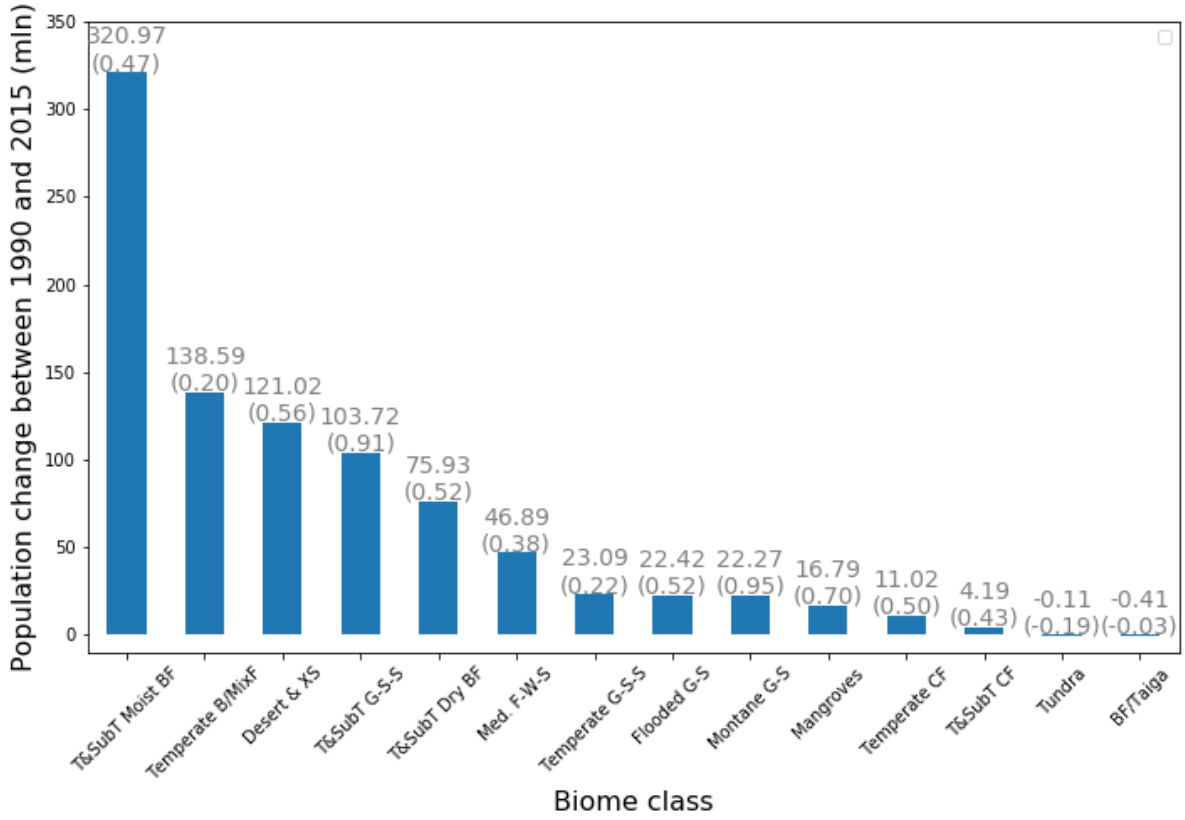

Figure 32 Change of urban centre population between 1990 and 2015 by biome. The total change of population (in millions) is provided per biome, and the ratio of population change is given in brackets.

Key Messages

- In 2015, the biome with the highest share (32%) of city dwellers is the Tropical and Subtropical Moist Broadleaf Forests biome (also known as rainforest). Population in this biome increased by 47% between 1990 and 2015 and puts significant pressure on remaining natural rain forests.
- In the observation period 1990-2015 the urban centre population in the African savannahs (e.g. the Sahel), montane grasslands and shrublands (e.g. Ethiopia) almost doubled. Both biomes are prone to degradation, risking the livelihoods of their population.
- Population in arctic regions (Tundra and Taiga) shrunk by 20%.

5.1.2 Soil

The rapid urbanisation and population growth described by the GHSL data have a strong impact on soils. In the process of urbanisation many soils are permanently sealed or considerably altered due to excavation, mixing and compacting. This changes the capacity of food production and other diverse ecological services. It consequently increases the risk of potential floods and water scarcity, endangers biodiversity, and leads to environmental change on a larger scale. This section analyses, which are the soil types that are mostly affected by urbanisation.
In 2015, 69.7% of the built-up surface in urban centres is concentrated in soil types with a high agricultural suitability, which are accounting for 29.4% of the Earth landmass. Collectively, we are consuming 0.46% of these soils for built-up surface use in urban centres, making home for nearly 2 billion urban dwellers globally (62.4% of the total dwellers in urban centres).

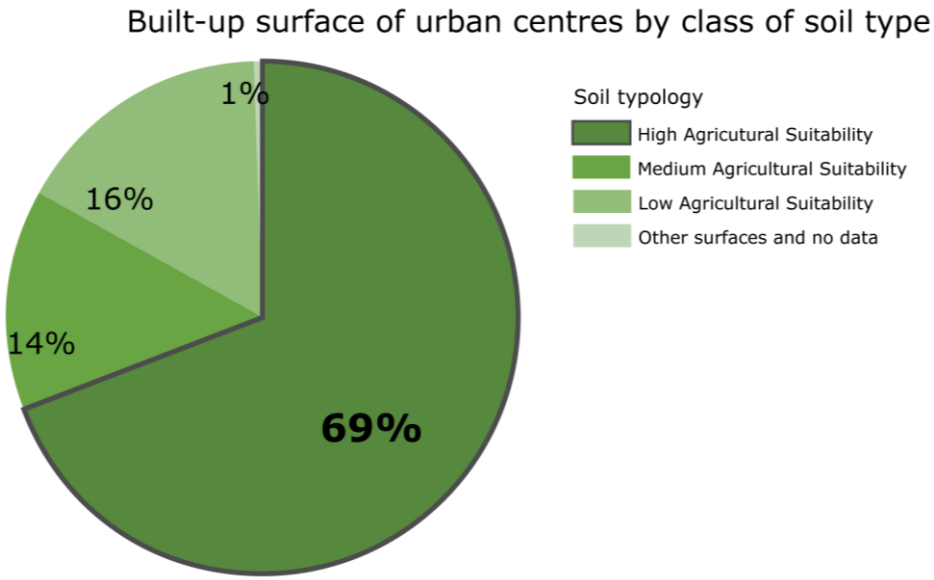

Figure 33 Share of urban centres built-up areas by soil type

Table 4 Aggregation of soil types according to agricultural suitability

High Agricultural Suitability	Medium Agricultural Suitability	Low Agricultural Suitability	Black Soils
Fluvisols Anthrosols Cambisols Luvisols Acrisols Phaeozems Nitisols Andosols Chernozems Planosols Kastanozems	Lixisols Vertisols Ferralsols Arenosols Podzoluvisols Alisols Greyzems	Calcisols Gleysols Leptosols Regosols Solonchaks Podzols Plinthosols Histosols Solonetz Gypsisols	Chernozems Kastanozems Phaeozems

The most frequent location of urban centres in the world is on Fluvisols. In 2015, the 13.6% of the population living in urban centres (more than 423 million) are settling on Fluvisols, which are accounting for 2.7% of the Earth Landmass. This is not surprising,

since Fluvisols typically occur along rivers and lakes, in deltaic areas and in areas of recent marine deposits like coastal lowlands. These are typical areas of large urban agglomerations mostly related to the availability of water and transport opportunities. The good natural fertility of most Fluvisols and attractive dwelling sites on river levees and on higher parts in marine landscapes were recognized in prehistoric times. Later, great civilizations developed in river landscapes and on marine plains. Hence the high percentage of urbanization on these soils.

The second most important class are Anthrosols; 11.5% (more than 358 million) of the urban population in the year 2015 are living in urban centres constructed on Anthrosols, which are accounting for 0.4% of the Earth landmass. Anthrosols comprise soils that have been modified profoundly through human activities, such as addition of organic or mineral material, charcoal or household wastes, or irrigation and cultivation. Not surprisingly, they are very frequent in urban agglomerations, where the anthropic impact has been profoundly modifying the local soil properties, essentially making artificial man-made soils as a result of human activities.

About 10.4% (more than 325 million) of the urban population in the year 2015 living in urban centres are settling on Cambisols, and 1,100 (12.3%) urban centres are located on this soil type. Cambisol is one of the most common soil types, particularly well represented in temperate and boreal regions that were under the influence of glaciations during the Pleistocene, partly because the parent material of the soil is still young, but also because soil formation is slow in cool regions. Cambisols generally make good agricultural land and are used intensively. Cambisols on irrigated alluvial plains in dry zones are used intensively for production of food and oil crops. Cambisols in undulating or hilly terrain are planted with a variety of annual and perennial crops or are used as grazing land.

Figure 34 © Adobe Stock, 2018

Chernozems, Kastanozems and Phaeozems are among the best soils in the world, and they form the so-called "Black Soils" group, that accounts for 6.5% of the Earth landmass. Protecting those soils from urbanization is strategic for maintaining the global

food production and for global food security. 510 (5.8%) Urban centres are located on Black Soils, providing home for more than 164 million (5.3%) of urban dwellers in 2015. In the 25 years from 1990 to 2015, the built-up surface included in the urban centres on Black Soils was growing from 21,178 to 26,336 km^2, causing an estimated Black Soil consumption for urban use of 5,158 km^2.

Table 5 Absolute and relative (in 2015) built-up areas surface, resident population, number of urban centres, and share of global land mass per soil typologies in the High Agricultural Suitability class.

SOILTYPE	Built-up surface (10^6 Km^2)				Resident Population (10^6 people)				Urban Centres		Landmass	
	1990	2000	2015	BU15%	1990	2000	2015	P15%	Number	%	Surface (10^6 Km^2)	%
Fluvisols	29	34	37	13%	308	355	424	14%	1,118	12.5%	4	2.7%
Anthrosols	27	33	37	13%	268	305	359	12%	759	8.5%	1	0.4%
Cambisols	21	24	26	9%	248	281	325	10%	1,100	12.3%	12	7.8%
Luvisols	27	32	35	12%	175	202	242	8%	740	8.3%	8	5.4%
Acrisols	19	22	24	8%	162	188	221	7%	698	7.8%	7	4.5%
Phaeozems	12	14	15	5%	89	99	109	3%	286	3.2%	3	2.0%
Nitisols	4	5	5	2%	68	81	106	3%	233	2.6%	1	0.8%
Andosols	6	7	7	2%	60	68	78	2%	131	1.5%	1	0.7%
Chernozems	6	6	7	2%	35	35	34	1%	133	1.5%	3	1.8%
Planosols	3	4	4	1%	17	20	23	1%	71	0.8%	1	0.6%
Kastanozems	3	4	4	1%	16	19	22	1%	91	1.0%	4	2.7%

Key Messages

- Urban centres are mostly (69%) built on soils with a high agricultural suitability. Rapid, unplanned urbanisation processes may reduce the local capacity for food production. Moreover, the reduced ecological services of soils due to urbanisation may increase the risk of potential floods and water scarcity, and endangers biodiversity, leading to environmental change on a larger scale.
- Fluvizols, Anthrosols and Cambisols are mostly affected by urbanisation (35% of built-up area in urban centres).
- The most valuable soils for food production (Chernozems, Kastanozems and Phaeozems) are strategic for maintaining the global food production and for global food security. Urbanisation processes should be limited and strictly controlled on these soils.

5.1.3 Elevation

Most of the urban centres population is located in elevation from sea level to 500 m but a number of urban centres in Asia, Latin America, and Africa area to be found in all elevations including that of above 2500m.

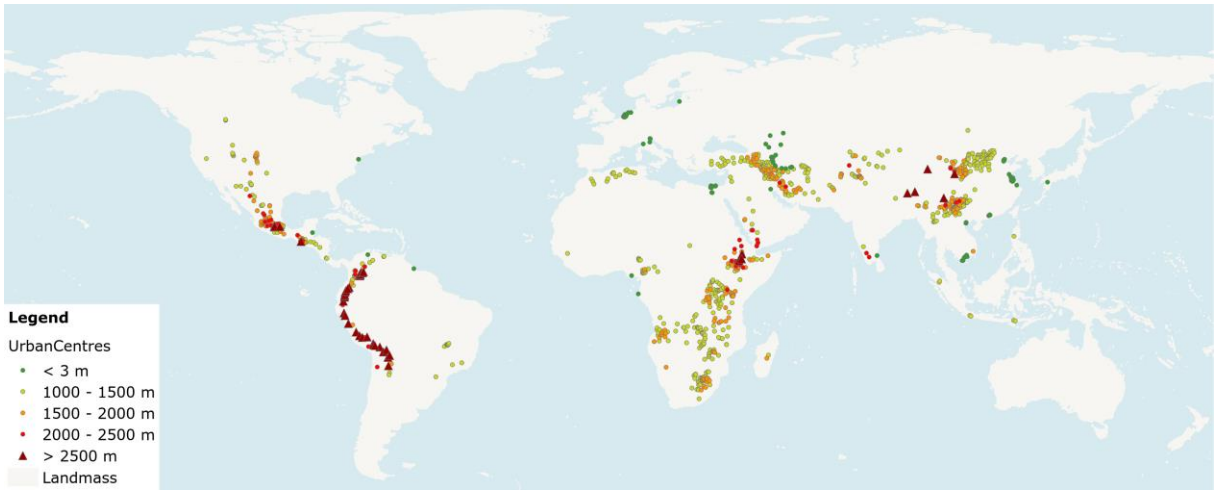

Figure 35 Urban centres located in elevation classes below 3m and above 500m.

Elevation affects humans in direct and indirect way. The direct effect is on human health. In fact, over the 2500 m altitude that the lower oxygen content may be not suited to everybody, in addition, altitude brings harsher climatic conditions. The indirect effect relate to the ruggedness that comes with living in elevated areas that makes , it makes it more prone to natural hazards, especially landslides, flash floods, but also earthquakes. Elevation and ruggedness also hampers accessibility of urban centres that are more difficult to get to and for which goods and transports are more costly to deliver. A direct effect of elevation in low elevated coastal areas is the increase risk to coastal flooding due to sea level surge and also climate induced sea level rise. This analysis only looks at the elevation of urban centres.

The urban centre elevation attribute is computed as the average altitude within the spatial extent of each urban centres expressed in metres above sea level (MASL). We used the ALOS DSM dataset and processed it using uses Google Earth Engine. The analysis groups population in urban centres based on seven elevation classes (Figure 35) with elevation of the urban centres; 1) below 3 m and less, 2) between 3 and 500m, 3) between 500 and 1000m, 4) between 1000 and 1500, 5) between 1500 and 2000m, 6) between 2000 and 2500m, and 7) above 2500m. The first class includes the low lying cities in the centre of continents and in those in low lying coastal areas that may be susceptible to coastal flooding. The 7th class aims to locate the cities at high elevation that may not be suitable for habitation for all people.

Figure 35 shows the population of urban centres from below 3m to those above 2500 m. Of the low elevated urban centres a number cluster at the edge of the Caspian sea, a few in major rivers delta including that in the Netherlands, in the Nile river Delta and Guangzhou in the Pearl River delta. More urban centre are to be found in low lying coastal areas that are not selected is this analysis as we are using an average elevation measured within the urban centres boundaries - not the lowest elevations of the urban centres. Figure 35 also shows the urban centres in all elevation above 500. For example, there are 45 urban centres above 2500 meters elevation a most are clustered in along the Andes in South America, in Central Asia and in the Horn of Africa.

Most urban centres of the world are located at an elevation suitable for human habitation; few are at very high elevation (Figure 36). That, however, varies with continents. In Asia, the mean and the median of the urban centres in the elevation classes overlap. Most of the population (83%) is in the lower class. In Europe and North

America population in the class between sea level and 500 m is above 90%. For Africa and Latin America this is different. Africa shows population also in classes above 500, up to 1500 with three urban centres above 2500m. Latin America shows population between 6 and 8 % in all elevation classes above 500m including that above 2500m.

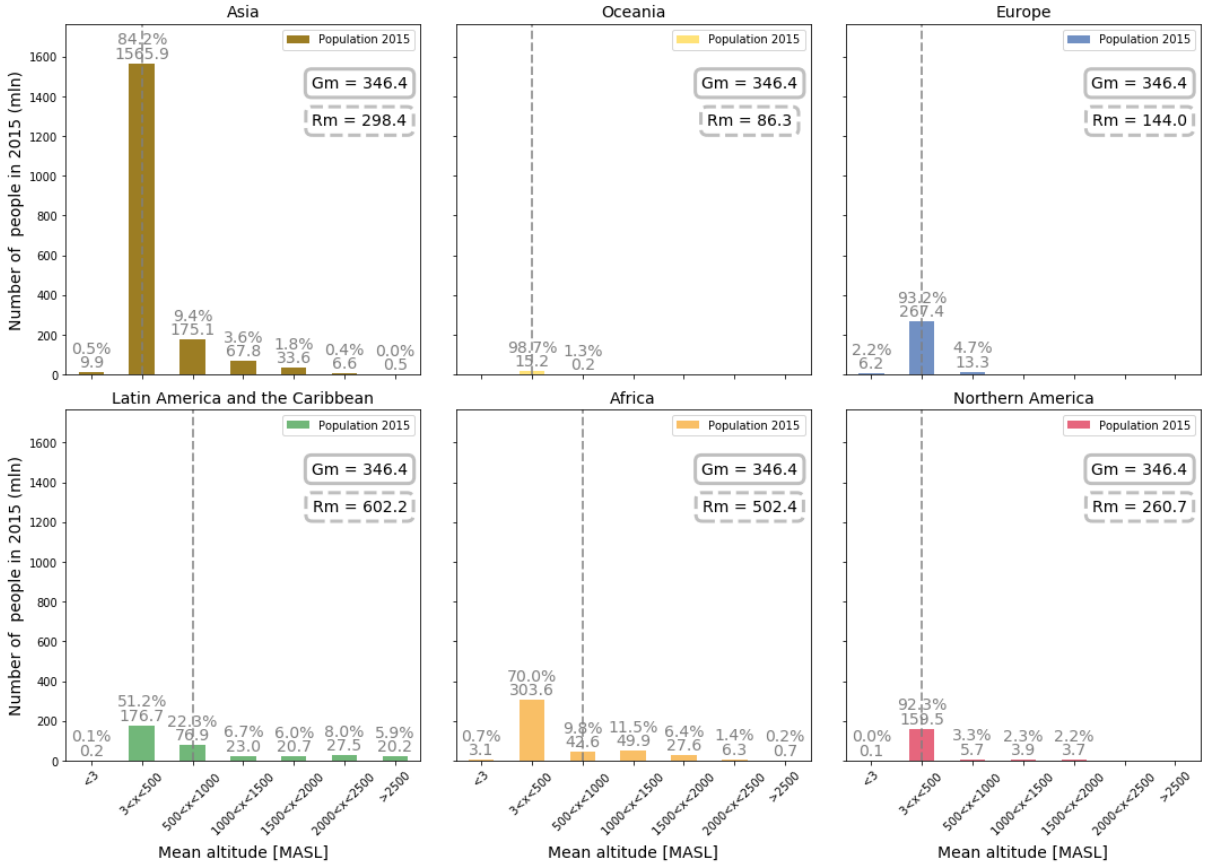

Figure 36. Total urban centre population by elevation class per region (Gm – global mean, Rm – regional mean).

The statistics on the number of urban centres reveals their distribution in all elevation classes (Table 6). Urban centres can be found at elevation above 2500 m in all continents except of Oceania and Europe and Northern America. Europe and Oceania list urban centres in classes bellow 1000 m only while North America also above 2000 meters. Latin America shows 37 urban centres in elevation zone above 2500 m. The urban centres in elevated areas are smaller and account for less population on average than those in lower elevation classes.

Table 6 Number of urban centre by elevation classes

	Elevation classes in metres above sea level						
UN Major Regions	***<3***	***3-500***	***500-1000***	***1000-1500***	***1500 – 2000***	***2000-2500***	***>2500***
Asia	49	3957	528	253	131	20	5
America Latina & Caribbean	3	590	223	54	58	42	37
Africa	14	972	222	192	89	13	3
North America	1	328	19	16	8	0	0
Europe	22	983	45	0	0	0	0
Oceania	0	38	3	0	0	0	0
TOTAL	**89**	**6868**	**1040**	**515**	**286**	**75**	**45**

Key Messages

- Most of the urban centres in the world are located at elevation below 500m
- A number of urban centres are located on low elevated areas. Those in the proximity of low elevated coastal zones are at risk of sea level rise
- South America and Asia host urban centres at higher elevation classes including that of above 2500m.

5.1.4 Climate

Urban centres across climate zones

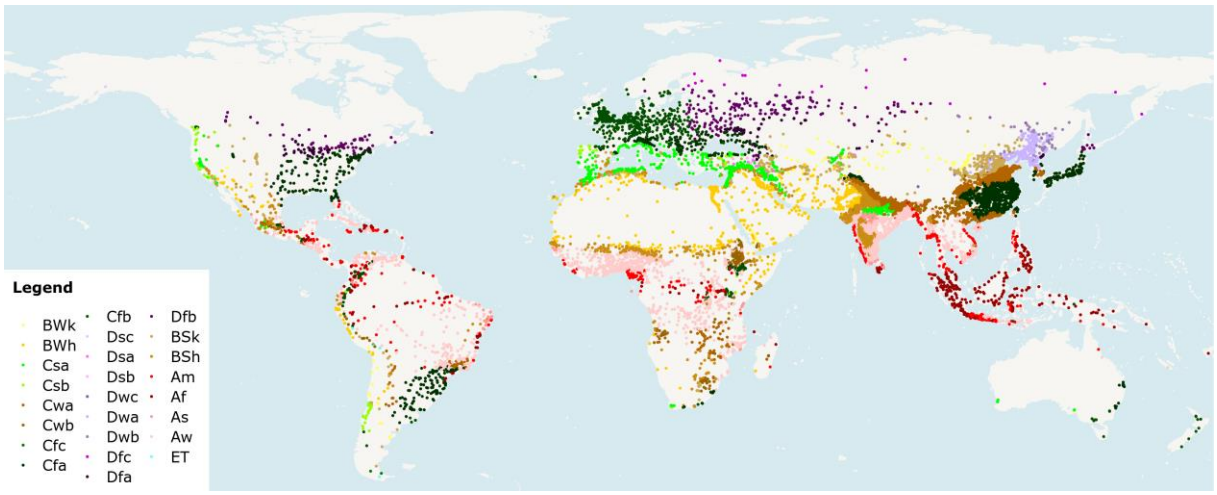

Figure 37 Urban centres classification according to the Köppen-Geiger climate zones map

Human settlements interact with the climate conditions in which they lay (Landsberg 1976). Climate characteristics are principally important for weather related disasters (i.e. floods, cyclones), energy use, for the adoption of specific building construction techniques and materials, and for health (i.e. air pollution). The GHS-UCDB contains a climate typology attribute, derived from (Rubel et al. 2017) on the basis of the Köppen-Geiger climate zones map. Mild temperate zones concentrate the largest share of urban centres (40%) hosting 1.3 billion people in 2015. Urban centres in tropical zones are more than 3,000 and accommodate a population of almost 1 billion people. 16% of the urban centres are located in zones of steppe; their population reaches almost 500 million. About 8% and 7% of the centres lay in desert and snow zones, respectively. Population increased the most between 1990 and 2015 in urban centres in desert areas (+70%), while increasing by half in tropical and steppe zones, by 1/3 in tundra and mild temperate zones, and by about 8% in snow zones (Figure 38).

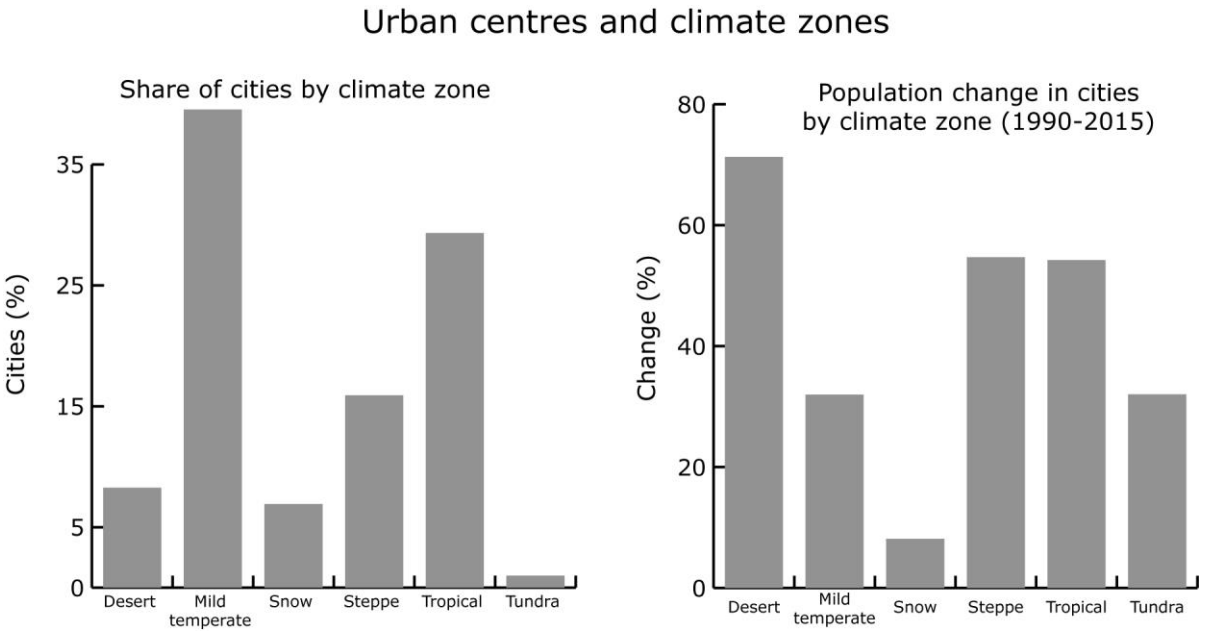

Figure 38 Share of urban centres by climate zone and population changes between 1990 and 2015

5.1.5 Temperature

Changes in temperatures in the period 1990-2015

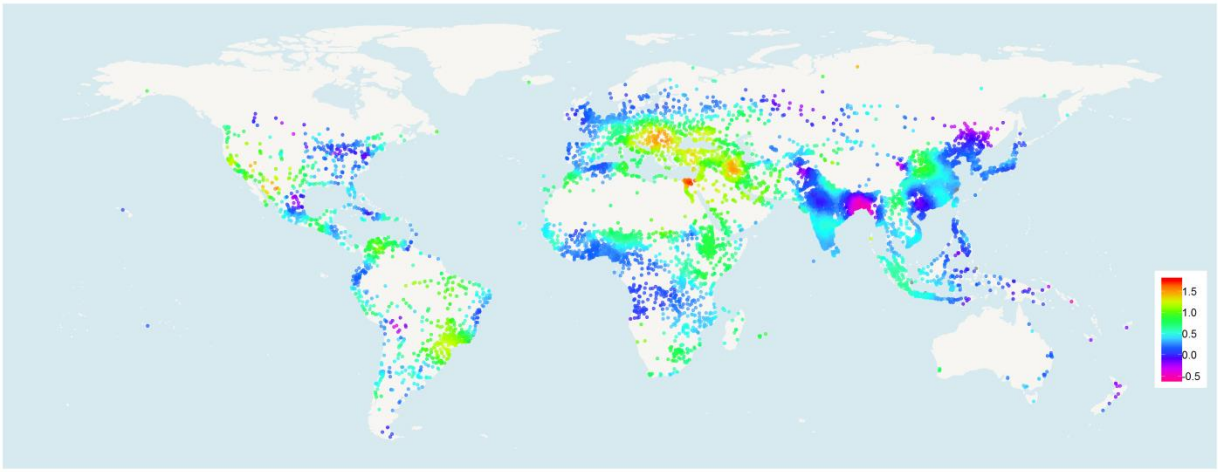

Figure 39 Changes in the temperature (°C) per urban centre in the period 1990-2015

Global temperature is a popular metric for summarizing the state of global climate. The Intergovernmental Panel on Climate Change in its most recent report (AR5) in 2013 stated: *'Warming of the climate system is unequivocal, and since the 1950s, many of the observed changes are unprecedented over decades to millennia. The atmosphere and ocean have warmed, the amounts of snow and ice have diminished, sea level has risen, and the concentrations of greenhouse gases have increased'*. According to Morice et al., 2012, the period 2001-2010 (0.49°C above the 1961-90 average) was 0.21°C warmer than the 1991-2000 decade (0.28°C above the 1961-90 average).

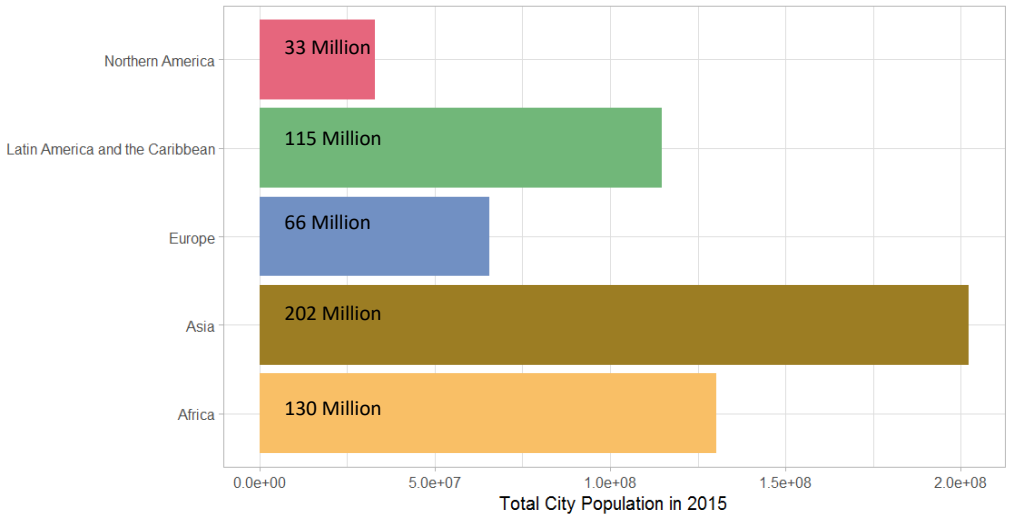

Figure 40 population living in cities where temperature increase was more than 0.8 °C in the period 1990-2015

Data on annual average temperatures obtained from the CRU database (http://www.cru.uea.ac.uk/data) were used in the analysis(Harris et al., 2014). These data are based on observations from ground stations combined with interpolation at a coarse resolution aiming for global coverage. Therefore, they do not (yet) consider

localized city effects such as urban heat island that may modify intra-city observed and perceived temperatures.

Average temperatures per urban centre were calculated for three time intervals centred on the years 1990, 2000 and 2015 as follows: for 1990, the interval spans from 1988 to 1991; for 2000, the interval spans from 1999 to 2002; for 2015, the interval spans from 2012 to 2015. The intervals were chosen in order to match the dates of the Landsat data collections used to derive the multi-temporal built-up areas (GHS-BUILT) and to reduce inter-annual and seasonal variability that may affect the change analysis.

The map in Figure 39 above shows changes in average yearly temperatures. They depict how much areas, in which the cities of the world are located, have warmed or cooled in the period 1990-2015:

- The most significant warming occurred in the cities located in Egypt, followed by the cities in the Balkans and those on the western coast of the Caspian Sea.
- Temperature has also increased on the western coast of United States, in Venezuela and Brazil.
- Despite a general increase in average urban temperatures, in some areas the city temperatures decreased mainly in Bangladesh and North-Eastern China.
- Considering a cut-off value of +0.8°C for the increase in temperatures, we can observe that in Asia around 202 Million people living in cities are affected by the increase in temperatures, 130 Million in Africa and 115 Million in America. At global level, 546 Million people living in cities are affected by an increase in temperatures of more than 0.8°C.

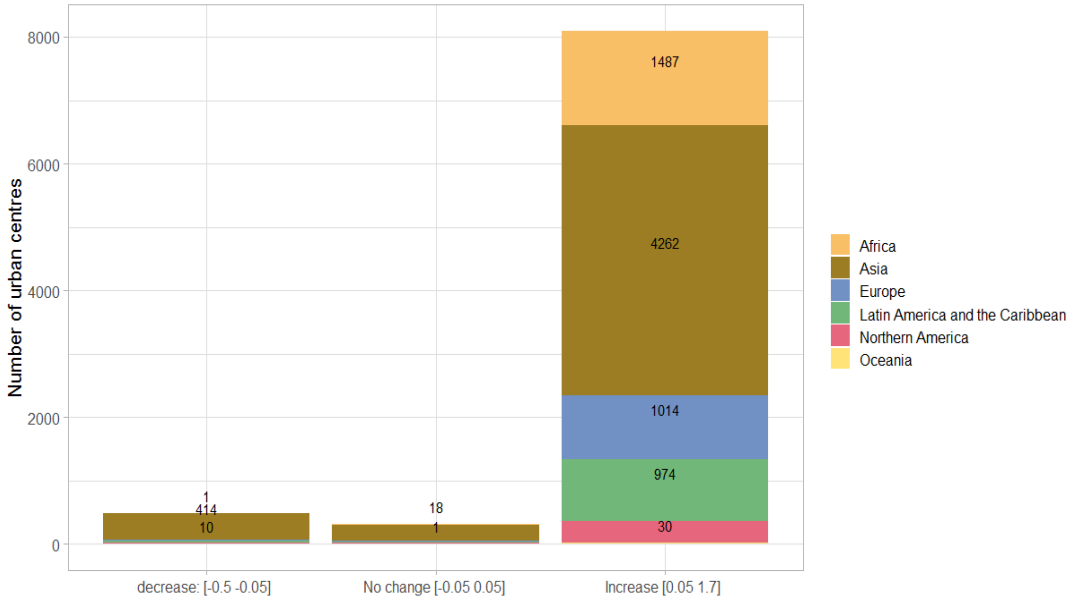

Figure 41 Number of urban centres affected by changes in the temperatures (°C) in the period 1990-2015

Figure 41 classifies cities according the changes in temperatures in the period 1990-2015. It shows the following:

- A total of 486 cities have experienced a decrease of average temperatures between 1990-2015.
- The majority of these cities affected by a decrease in temperatures are located in Asia (414 cities).
- The majority of the cities experienced increase in average temperatures :
    - Asia: 4262 cities out of 4946 (86%),
    - Africa: 1487 cities out of 1506 (98%),
    - Europe: 1014 out of 1051 (96%),
    - Latin America and the Caribbean: 974 out of 1007 (97%),
    - Northern America: 332 out of 372 (0.89%),
    - Oceania: 30 out of 41 (73%).

Key Messages

Though warming has not been uniform across the planet, the upward trend in the globally averaged temperature shows that more cities are warming than cooling. Since 1901, the planet's surface has warmed by 0.7–0.9° Celsius (1.3–1.6° Fahrenheit), but the rate of warming has nearly doubled since 1975 to 1.5–1.8° Celsius (2.7–3.2° Fahrenheit), according to the international State of the Climate in 2017 report (NOAA, 2018). The 10 warmest years on record have all occurred since 1998.

- The most significant warming occurred in cities in Egypt, followed by cities in the Balkans and those on the western coast of the Caspian Sea. Temperature has also increased on the US West Coast, in Venezuela and Brazil.
- Despite a general increase in average urban temperatures, in some areas the city temperatures decreased mainly in Bangladesh and North-Eastern China.
- Considering a cut-off value of +0.8°C for the increase in temperatures, we can observe that in Asia around 202 Million people living in cities are affected by the increase in temperatures, 130 Million in Africa and 115 Million in America. At global level, 546 Million people living in cities are affected by an increase in temperatures of more than 0.8°C.

5.1.6 Precipitation

Changes in precipitation in the period 1990-2015

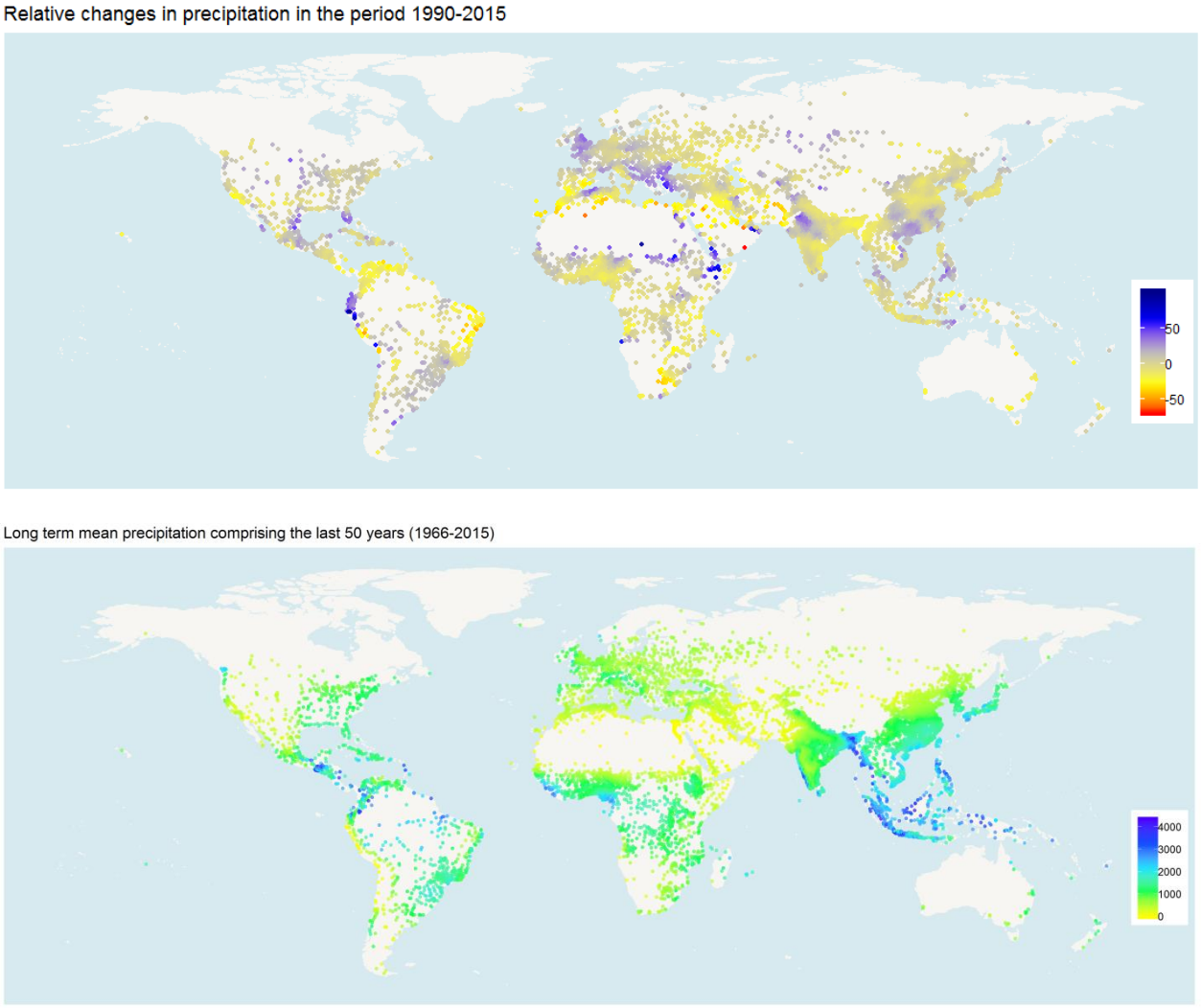

Figure 42 Relative changes in the average precipitation (%) calculated for the urban centres in the period 1990-2015 and long term mean precipitations (mm) in the period 1966 – 2015.

Among the effects of global warming is the increase in atmospheric evaporative demand, which intensifies the hydrological cycle, resulting in more intense and frequent storms, but also contributing to drying over some land areas. Increasing global temperatures are very likely to lead to changes in precipitation pattern, due to changes in atmospheric circulation (see section 5.1.5). Overall, global land precipitation has increased by about 2% since the beginning of the 20th century(Jones and Hulme, 1996). The increase is statistically significant, though neither spatially nor temporally uniform(Doherty et al., 1999).

Using global annual precipitation data, derived from the CRU database (http://www.cru.uea.ac.uk/data, (Harris et al., 2014)), changes in the average precipitations were calculated for the urban centres in the period 1990-2015 and compared to the long term mean precipitations in the period 1966 – 2015.

The results presented in Figure 42 show the following:

- Precipitation increased relatively in European cities, in the Sahel and some of the cities of Western Latin America (e.g. in Ecuador).
- In Asian-Pacific cities, there is a general decrease in precipitations.
- Decreasing precipitations are generally observed around the Mediterranean Sea, in India and Bangladesh, Southern Africa and Latin America despite some regional differences.
- Overall, the majority of the cities have experienced no significant change in precipitations, but 24% have experienced an increase in precipitations in the period 1990-2015 and 19% a decrease in precipitations during the same period.

The results observed in precipitation changes in the period 1990-2015 need to be analysed in parallel with the long term mean precipitations in the last 50 years. It can be seen that:

- Despite a general impression of decreasing precipitations in urban centres, it is important to note that long-trend analysis needs to complement these results. Besides, the exact rates of precipitations changes depend on the method of calculating these changes. Difficulties in the measurement of precipitation remain an area of concern in quantifying the extent to which global and regional scale precipitation has changed.

Figure 43 classifies cities according the relative changes in precipitations in the period 1990-2015. It shows the following:

- A total of 1672 cities have experienced a decrease of average precipitations between 1990-2015. Most of these cities are located in Asia and Africa.
- A total 2091 cities have experienced an increase in precipitations. Most of these cities are located in Asia, Europe and Latin America.

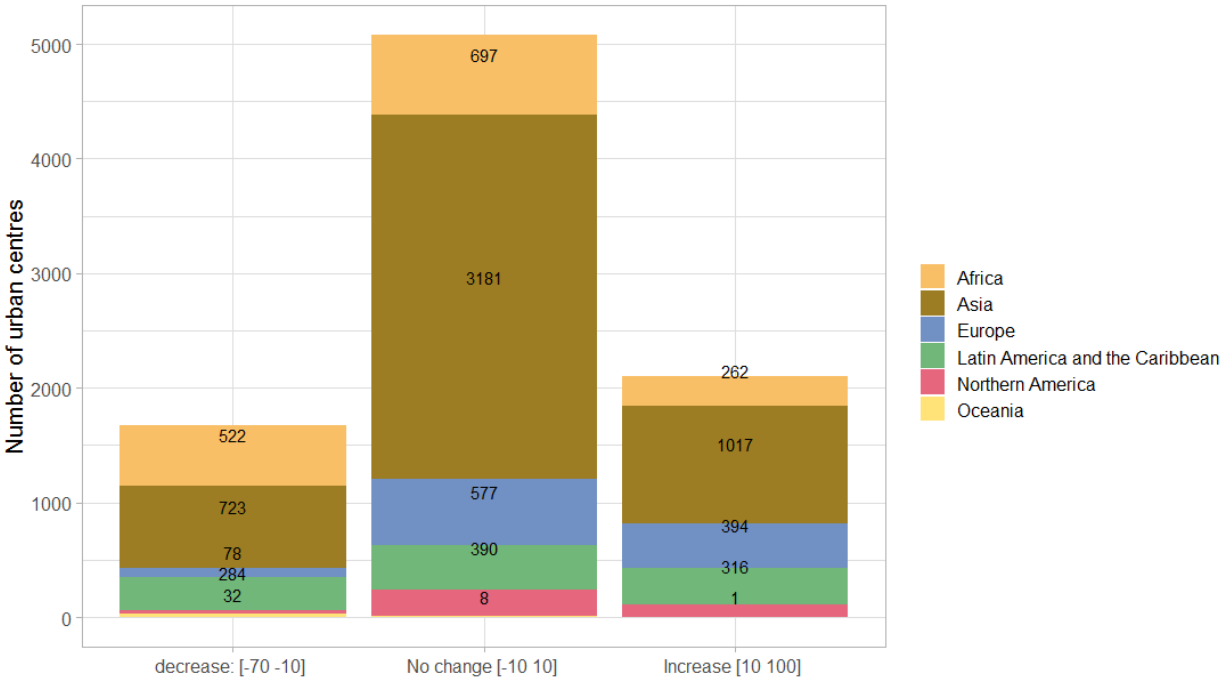

Figure 43. Number of city centres per classes of relative changes in precipitations (in %)

Key Messages

Overall, global land precipitation has increased by about 2% since the beginning of the 20th century. The results of our analysis at city level confirm these observations.

- 24% of the cities in the World experienced an increase in precipitations in the period 1990-2015
- 19% of the cities experienced a decrease in precipitations during the same period.
- While African cities are the most affected by the decrease in precipitations, these same cities have the highest share of population increase with an average increase of 375% between 1990 and 2015.

5.1.7 River Basin

Urban centres located in Major River Basins of the world

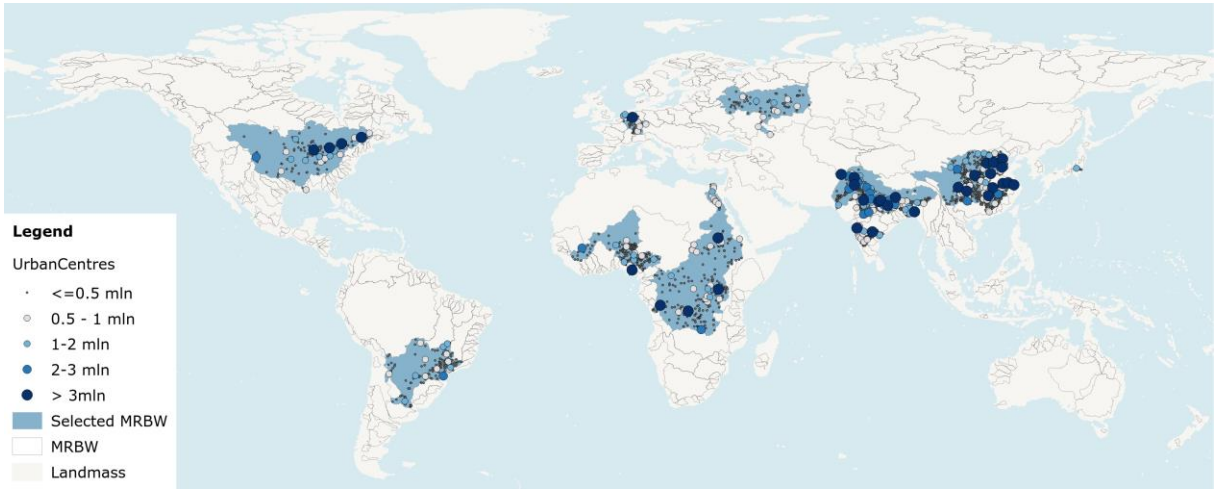

Figure 44 Urban Centres located in the selected Major River Basins of the World (MRBW).

Water is an essential element in the Earth's system. It is critical for socio-economic development, healthy ecosystems and for human survival itself. At the same time, the excess of water (in the form of inundation and flooding, see section 5.4.1 –p. 90) poses a threat to socio-economic development. Water and water management in all its forms is at the core of any sustainable development. However, population growth, agricultural intensification, urbanization and industrial production are putting pressure on fresh water resources. The Sustainable Development Goals have recognized this issue and dedicate Goal 6 to 'Ensure availability and sustainable management of water and sanitation for all'.

This section of the Atlas looks at the urban centres that are located in the major river basins of the world. Not by chance, the first civilisations developed along river systems: the Mesopotamian civilization along Euphrates and Tigris, the Egyptian Empire along the Nile, the Harappa culture along the Indus, and the Chinese Empires along the Huang He (Yellow River). All, except the Euphrates and Tigris, still feature in the top ten list as shown in Table 7. The global dataset of Major River Basins (MRB)[23] used in this study consists in 405 basins across the globe. Out of these basins 158 (approx. 40%) are in scarcely populated areas (Siberia, Alaska, Amazonia, Australia). The remaining 247 MRB's include 5731 urban centres, which are two thirds of all cities around the world. They are home to 63% of the global city population in 2015, and 64% of total urban centre built-up area is falling within these MRB's.

Figure 44 shows the location of the top-ranking MRB's in terms of number of urban centres and amount of population and built area in the urban centres. According to these criteria, the Ganges and Yangtze in India/Bangladesh and China, respectively, are the most important MRB's hosting together 980 cities with more than 360 million inhabitants. Several megacities are located along these rivers (e.g. Kolkata, Dhaka, Shanghai). These long rivers with large populations living along the shores tend to be highly polluted, since the current waste management is not adequate. The Yangtze, for example, deposits 1.5 million metric tonnes (55%) of the total 2.75 million metric tonnes of plastic waste deposited into the ocean by rivers each year (Schmidt et al., 2017).

[23] Global Runoff Data Centre (2007): Major River Basins of the World / Global Runoff Data Centre. Koblenz, Germany: Federal Institute of Hydrology (BfG). https://www.europeandataportal.eu/data/en/dataset/1b19599d-a17e-49f3-9829-d59d1eab43b7

The Ganges and Yangtze are followed by two other Asian river systems, namely the Indus and the Huang He (also known as Yellow River). Overall, seven out of the ten highest-ranking river catchments in terms of population are in Asia. The Asian rivers are exceeded only in the category of amount of built-up area in urban centres by the North American river systems of the Mississippi and the St. Lawrence. It is only in this category, where also the European rivers Rhine and Volga appear. The most important MRB in South America is the Parana catchment that includes the megacity of Sao Paulo. In Africa, the most important MRB is the Nile with almost 60 million urban dwellers along the river, most of them living in Cairo and the Nile Delta.

Table 7 Mayor river basins ranked by the number of urban centres, city population (2015), and built-up area (2015). RB – river basin; MR – Major Region (UN)

Urban Centres			*Population (2015)*			*Built-up area (2015)*		
RB	**MR**		**RB**	**MR**	**millions**	**RB**	**MR**	**km²**
Yangtze	Asia	519	Ganges	Asia	225.2	Mississippi	N.Am.	15226
Ganges	Asia	461	Yangtze	Asia	137.1	St.Lawrence	N.Am.	9223
Indus	Asia	283	Indus	Asia	89.3	Yangtze	Asia	9087
Huang	Asia	259	Huang	Asia	65.6	Huang	Asia	6599
Niger	Africa	202	Nile	Africa	59.5	Ganges	Asia	6147
Parana	Lat.Am.	177	Parana	S.Am.	54.8	Parana	Lat.Am.	5465
Nile	Africa	170	Yongding	Asia	52.1	Yongding	Asia	5254
Yongding	Asia	138	Bei Jiang	Asia	45.0	Rhine	Europe	5050
Krishna	Asia	132	Brahmaputra	Asia	41.6	Tone	Asia	4301
Congo	Africa	118	Niger	Africa	41.5	Volga	Europe	4135

Key Messages

- Rivers have been the lifelines of human civilisations and socio-economic development. However, population growth, and rapid urbanization, agricultural intensification, and industrial production are putting pressure on the rivers systems and threaten their functioning.
- The majority of urban centres (63% of the global city dwellers) is located in 257 Major River Catchments.
- Ganges (India, Bangladesh) and Yangtze (China) are hosting together 980 cities with more than 360 million inhabitants.
- These findings underline the importance of policies to protect the rivers, and water in general, as an essential resource for a sustainable and resilient urban future.

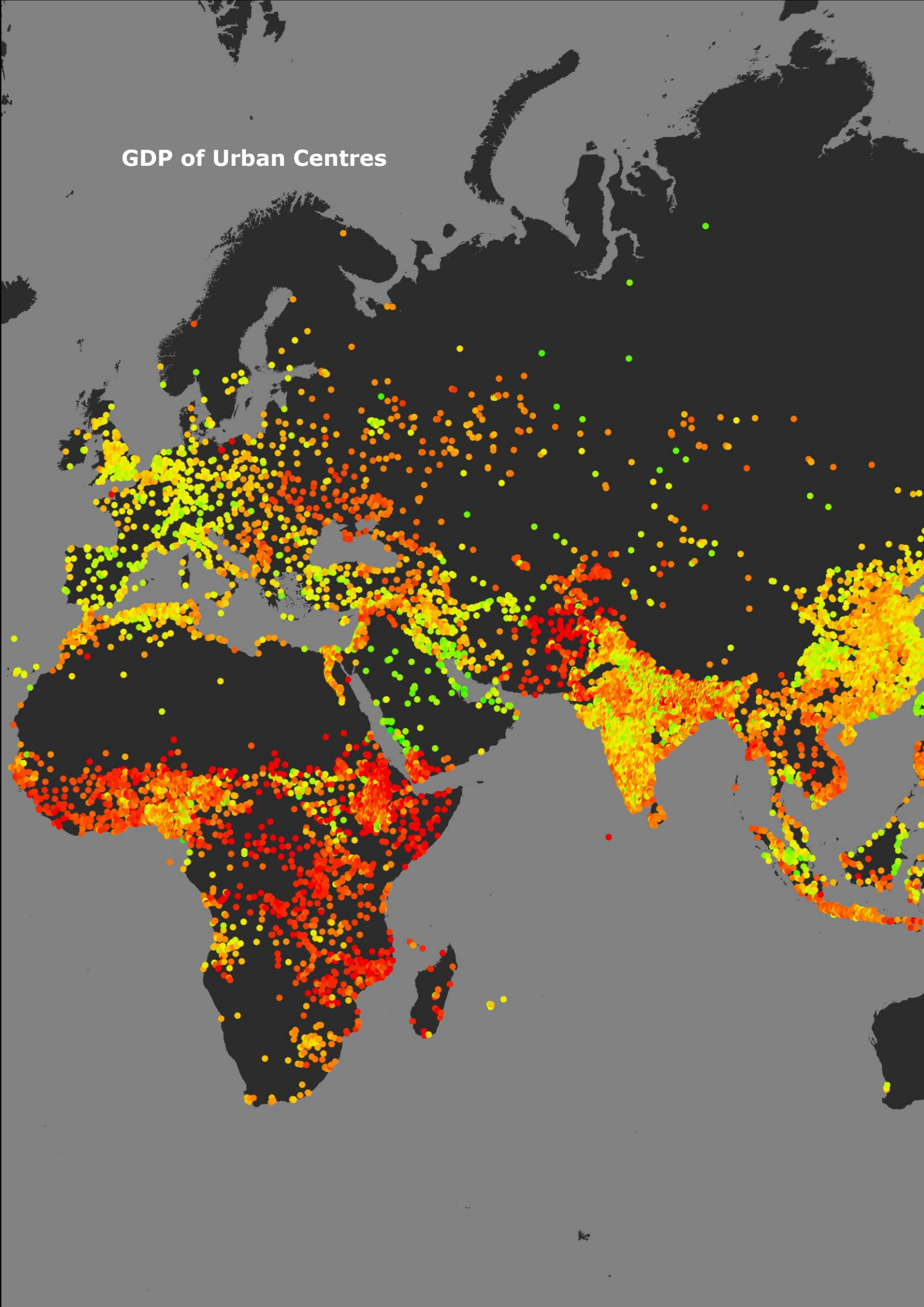
GDP of Urban Centres

5.2 Socio-Economic

The UCDB variables directly linked to the socio-economic development discussed are: i) the resident population 1975-1990-2000-2015, ii) the built-up surface 1975-1990-2000-2015, iii) the nightlight emissions 2015, iv) the income class 2015, v) gross domestic product, and VI) travel time to the capital 2015.

The resident population and the built-up surface data are derived from the GHS-POP and GHS-BU products at the different epochs. The GHS-BU is generated by spatial aggregation (upscaling) of the information collected at various decametric spatial resolution satellite image data records (10-15-30-80 metres) available in the different GHSL epochs and different satellite platform (M. Pesaresi et al., 2016a), (Corbane et al., 2017b) , (Corbane et al., 2018a), to the 250x250 metres resolution grid. The GHS-POP is generated by spatial disaggregation (downscaling) of census spatial data to 250x250 metres resolution grid, using GHS-POP as principal spatial covariate (Freire et al., 2016).

The Night Light Emission (NLE) data recorded by satellite platforms have been introduced in a number of application areas (Elvidge et al., 2007) (Elvidge et al., 2017). In particular, they have been prosed for global urban delineation (Elvidge et al., 2010), for the production of spatially explicit measure of human development (Elvidge et al., 2012), as proxy measure of human well-being (Ghosh et al., 2013), and for post-conflict humanitarian needs assessment (Corbane et al., 2016). The NLE data integrated in the current UCDB are the *Version 1 VIIRS (Visible Infrared Imaging Radiometer Suite) DNB (Day/Night Band) Night-time Lights Composites suite*[24] produced by the Earth Observations Group (EOG) at NOAA/NCEI. These grids span the globe from 75N latitude to 65S and have a resolution of 15 arc-second in WGS84 geographic coordinates (EPSG 4326), which corresponds to roughly 500 m at the equator. The following analysis uses the "vcm-orm-ntl" (VIIRS Cloud Mask - Outlier Removed - Night-time Lights) layer showing the cloud-free average radiance emitted, expressed as nano-watt per steradian per square centimetre (nW cm^{-2} sr^{-1}) with outlier removal process to filter out fires and other ephemeral lights. The year of reference for these data is 2015.

The income class (IC) reported in the UCDB it is derived from the country-level income class structured in four income groups: High Income Countries (HIC), Upper-middle Income Countries (UMIC), Lower-middle Income Countries (LMIC) and Low Income Countries (LIC). The classification schema is according to the World Urbanization Prospects 2018, (UNDESA 2018). The UC entities have been associated to the single Country by a spatial join. In case of cross-Country UCs, the Country showing the majority of resident people in the UC was selected for the join in the UCDB.

The Gross Domestic Product (GDP) is a key indicator of the development status of an area as it is a measure of the monetary value of goods and services produced in a given period of time. The urban centres GDP is calculated using the gridded global annual Gross Domestic Product (Purchasing Power Parity) (Kummu et al., 2018), which is summed within the extent of each urban centre for the epochs 1990, 2000 and 2015.

The travel time to country capital represents the travel distance to reach the country capital urban centre from each urban centre considered, flight connections not taken into account. Travel time to capital city is important measure of accessibility and remoteness of an urban centre and it represents the distance from each person to the central administration of the country.

[24] https://www.ngdc.noaa.gov/eog/viirs/download_dnb_composites.html#NTL_2015

5.2.1 Built-up Areas

Status and evolution of built-up areas in Urban Centres between 1975 and 2014

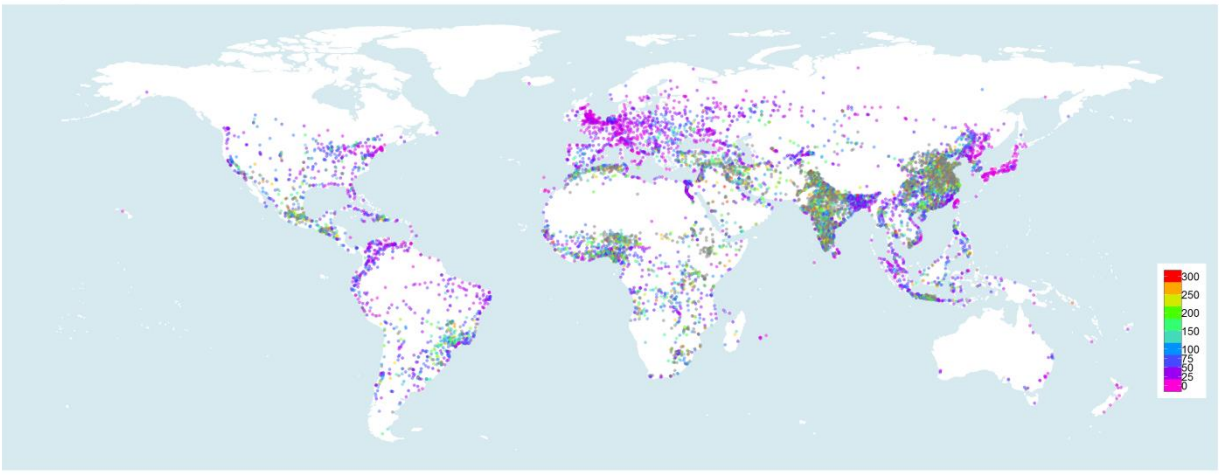

Figure 45. Percentage changes in built-up areas in urban centres between 1975 and 2014

Knowledge of the global spatial distribution and evolution of human settlements is one of the key requirements for monitoring progress toward sustainable development of urban and rural areas. Human settlements and built-up areas feature in several goals and targets of the major international frameworks agreed in 2015 and 2016, namely the United Nations Sustainable Development, Goals (SDGs)[25], the Sendai Framework for Disaster Risk Reduction[26], the Paris Agreement on Climate Change, and New Urban agenda [27].

These agreements articulate a set of indicators that require homogeneous and consistent information on the spatial distribution and the dynamics of human settlements. E.g. the indicators on pressure on natural habitats and biodiversity (SDG Goal 15), resilience to natural hazards (Priority 3 of the Sendai Framework for Disaster Risk Reduction), land use efficiency and access to basic services (SDG Goal 11 Monitoring Framework – UN-Habitat, 2017).

Using Landsat data archives organized in four collections (1975, 1990, 2000 and 2014) and advanced methods in automatic information extraction, global grids reporting about the presence of built-up areas in the past 40 years were produced in the context of the GHSL project(Corbane et al., 2017b). The results reported here are derived from the multi-temporal built-up area grids (GHS-BU) aggregated at 1 km. The built-up areas are assessed within the spatially delineated urban centres.

Figure 45 shows the percentage changes in built-up areas between 1975 and 2014 for all urban centres:

- Built-up areas have overall significantly increased in most of the urban centres
- This trend is less marked in European cities and the cities located on the Eastern coast of United States, North of Latin America, Japan and North of China and Northern Korea.

The percentage change in built-up areas is further disaggregated by each period of the GHS-BU dataset: between 1975 and 1900, between 1990 and 2000, and between 2000 and 2014. Figure 46 shows the probability density function for each of the three periods:

[25] (United Nations, 2015)

[26] Sendai Framework for Disaster Risk Reduction 2015-2030, March 18, 2015, http://www.wcdrr.org/uploads/Sendai_Framework_for_Disaster_Risk_Reduction_2015-2030.pdf.

[27] United Nations Conference on Housing and Sustainable Urban Development.

We can notice that the most significant increase in built-up areas occurred in the first period 1975-1990, followed by the period 1990-2000. In the last period 2000-2014, through built-up areas continued to expand, the rate of increase has significantly dropped in comparison to the first period.

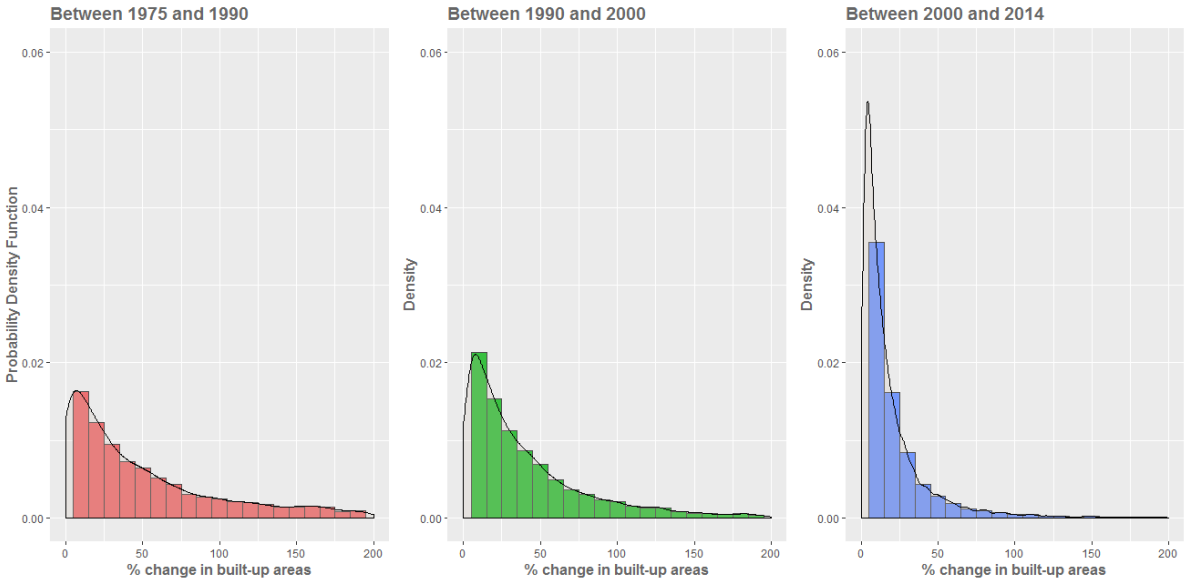

Figure 46. Percentage change in built-up areas per each period of the GHS-BU multi-temporal dataset

In Figure 47, we can see a further breakdown of the percentage changes per continent. The results show that:

- The most significant increase in built-up areas occurred in Asia followed by Africa over the three time periods.
- The cities located in Latin America and the Caribbean witnessed a significant expansion in built-up areas between 1990-2000
- Urban centres in Europe have the lowest rate of increase for all three epochs at just 4.6% in the period 2000-2014.

Continent	%Change_BU_75_90	%Change_BU_90_00	%Change_BU_00_14
Africa	285.29	75.64	39.27
Asia	304.19	93.31	41.43
Europe	23.15	8.79	4.66
Latin America and the Caribbean	69.94	137.48	17.44
Northern America	57.88	23.71	8.41
Oceania	25.16	12.80	12.53

Figure 47. Percentage change in built-up areas per each period of the GHS-BU multi-temporal dataset

5.2.2 Population

Status and evolution of population of urban centres between 1975 and 2015

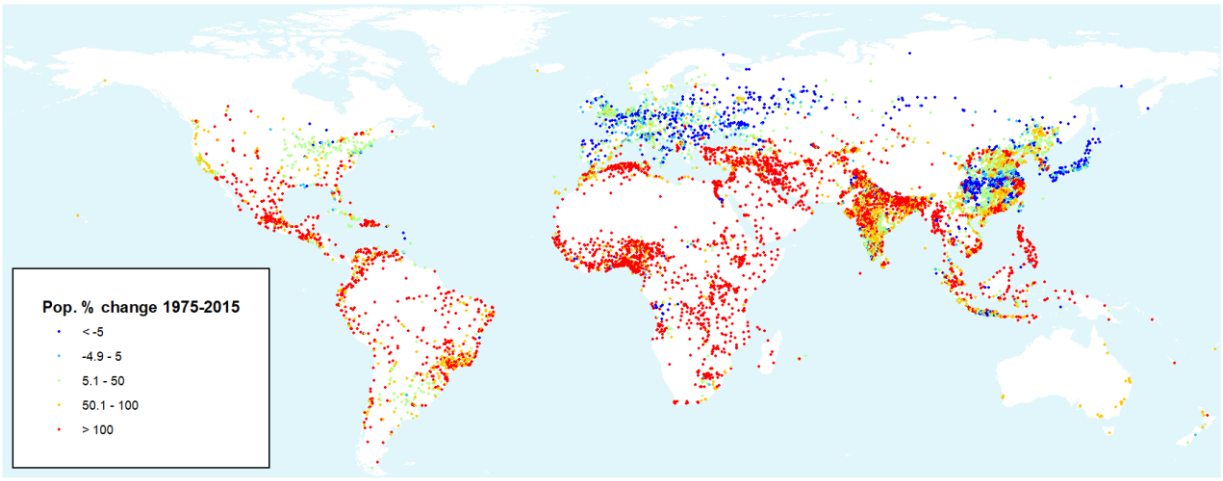

Figure 48. Percentage changes in population in urban centres between 1975 and 2015

Population is one key variable for characterizing cities and urban centres, respect to its size, density, and temporal changes. Population distribution grids for each epoch, as mapped by GHSL (GHS-POP), were aggregated to the current urban centre extent.

Figure 48 shows the percentage changes in population between 1975 and 2015 for all urban centres considered:

- While overall population in urban centres has grown by about 92% in the period, it decreased in about 9% of cities.
- Cities that have decrease in population are mostly concentrated in Europe (including Russia), China, and Japan.
- Population has more than doubled in 46% of cities.

The rate of growth of population in cities is a strong indicator of urban vitality. Growth rates averaged by year help to standardize measure accounting for different length of epochs analysed. Figure 49 shows for each continent the differing average change of population (in percent) per year in the epochs considered:

- Population change rates are positive in all continents and have been generally decreasing from 1975 to 2015.
- Despite a general decrease in growth rates, these have increased slightly between 2000-2015 in Africa, Europe, and Oceania.

Cities in Africa have been displaying the highest growth rates in all epochs (at or above 3%), while Europe displays the lowest, and followed by Northern America.

The concentration of people within cities, measured through their population density, reveals different underlying policies, settlement patterns, and living conditions. Urban centres classified by their overall population density are shown in Figure 50:

- The classification of cities according to their population density reveals some clear regional patterns.
- Cities of Northern America and parts of Oceania have lower population densities, while the highest population densities occur in Africa and in the India sub-continent.
- 141 cities display very high population densities, above 20,000 people/km^2.

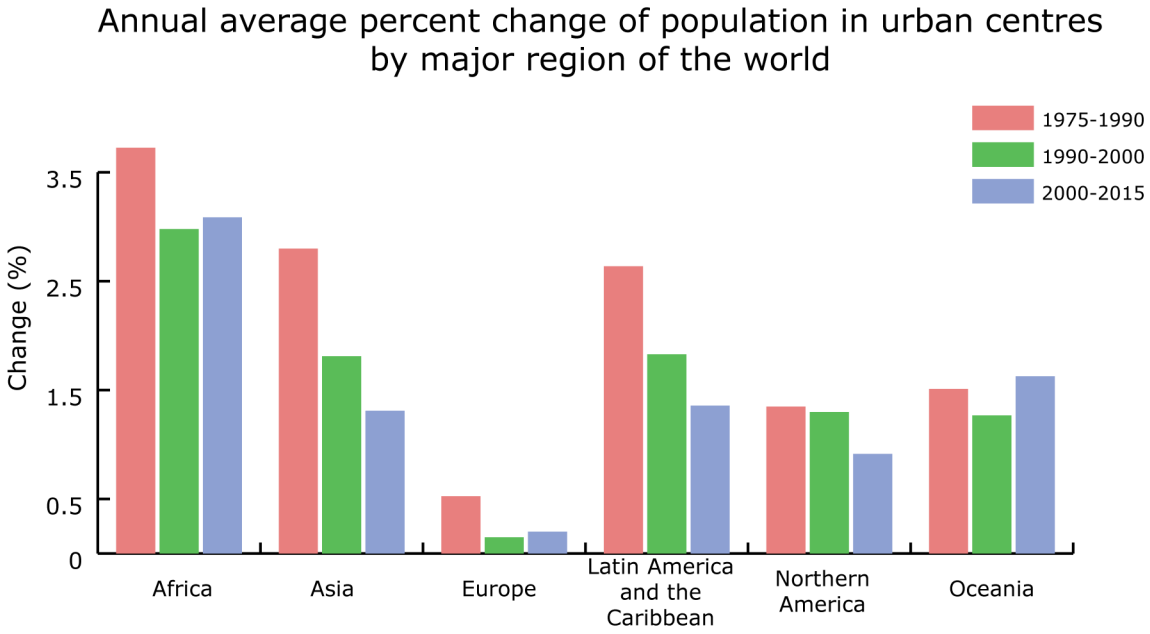

Figure 49. Annual average percent change of population in urban centres, by continent

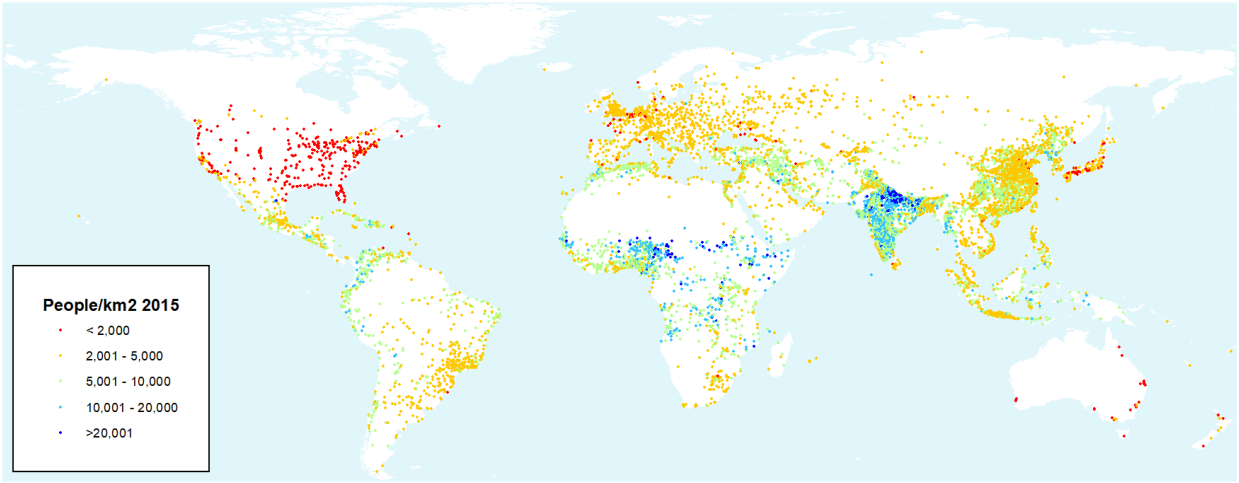

Figure 50. Population density of urban centres in 2015

Figure 51 © Adobe Stock, 2018

5.2.3 Night Time Lights

More than half of people leaving in urban centres have less night-time light than the global average

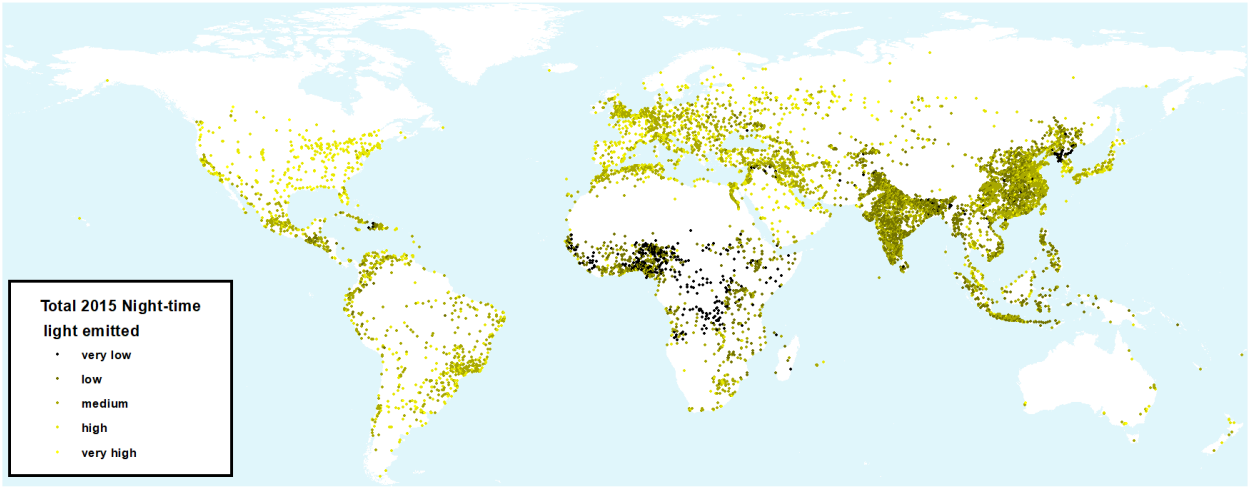

Figure 52 Total 2015 Night-time light emitted in urban centres

Night-time light (NL) represents the average illumination of an area as the emitted cloud-free average radiance (expressed as nW cm^{-2} sr^{-1}) produced by the Earth Observation Group (EOG) at NOAA/NCEI as a global composite from the VIIRS (Visible Infrared Imaging Radiometer Suite) satellite sensor. At present, the global NL is produced for the reference year 2015. In the UCDB, we collected NL data for each urban centre as the total radiation emitted, the average radiation and its standard deviation within each urban centre boundary.

Presence and intensity of NL has been observed and utilized in several studies as an indicator of human economic activity (Sutton et al., 2007; Sutton and Costanza, 2002), associated with human well-being or deprivation(Ghosh et al., 2013), with insight of informal economy (Ghosh et al., 2009) and inequality in human development (Elvidge et al., 2009).

Figure 52 shows the radiation emitted by each urban centre considered. Almost 3000 urban centres are in the very low illuminated class: 52% of those are located in Africa and 46% are located in Asia. In the top 100 most illuminated urban centres 36% are in North America; 34% are in Asia; 14% in Europe and 9% in Latin America and the Caribbean. The top five most illuminated urban centres are located in the United States (Los Angeles; Chicago; New York; Houston; Dallas).

Figure 53 (right) shows for each major region of the globe the local share of urban centres with an average illumination below the global average (grey) and below half of the global average (black). Asia, Africa and Oceania have more than 75% of urban centres with an average illumination below the global average. In Africa and Asia most of them, 69% and 70% of their urban centres respectively, are even below half of the global average. Figure 53 (left) shows how Asia, Africa and Oceania have also more than 75% of their urban population living in low illuminated areas: in Africa 77% (about 330 million people); in Asia 76% (about 1.4 billion people) and in Oceania 96% (about 15 million people). When the threshold is set to half the global average the urban population shares of Europe, Latina America and Caribbean, North America and Oceania fall below 10% with North America even below 1%; Africa has the highest share (58%) with almost 250 million people in such conditions and Asia 47% (about 860 million people).

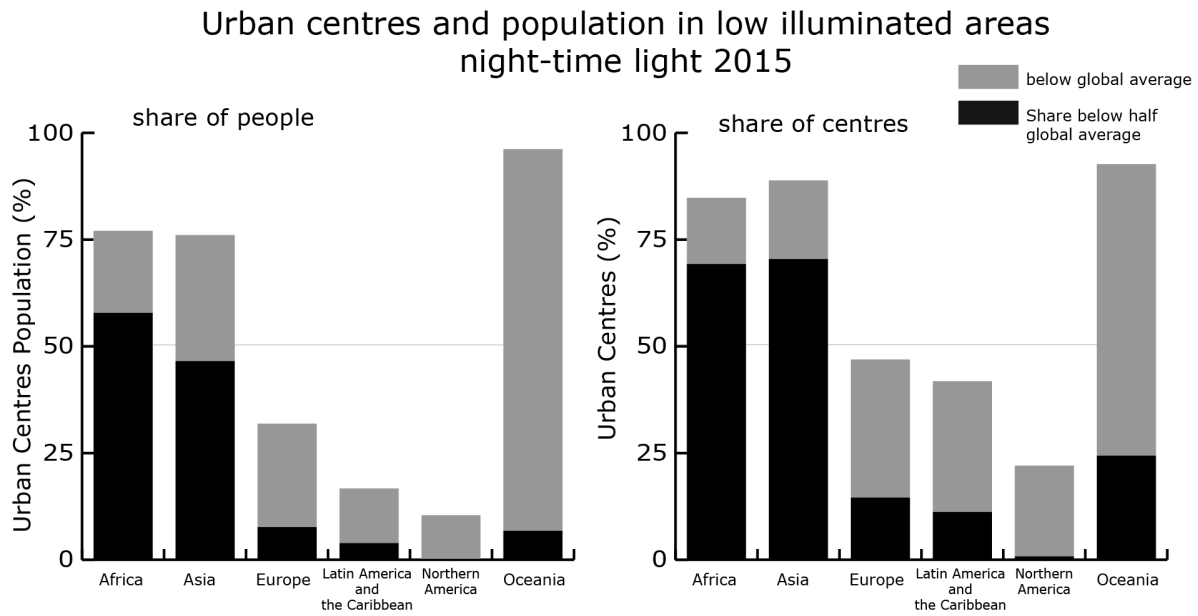

Figure 53 Regional shares of urban centres and population in low illuminated areas

Key Messages

- 52% of urban centres in the very low illuminated class are located in Africa and 46% in Asia;
- In the top 100 most illuminated urban centres 36% are in North America; 34% are in Asia; 14% in Europe and 9% in Latin America and the Caribbean;
- Asia, Africa and Oceania have more than 75% of their urban population living below the global average illumination value;
- In Africa 58% of urban population lives below half the global average illumination value; in Asia this value is 47%.

Figure 54 © Adobe Stock, 2018

5.2.4 Income

Disparities between cities across income groups

This section groups the urban centres according to the income group of the country where the centre is located. Territories are classified in four income groups, High Income Countries (HIC), Upper-middle Income Countries (UMIC), Lower-middle Income Countries (LMIC) and Low Income Countries (LIC), according to the World Urbanization Prospects 2018 (UNDESA 2018).

More than 75% of the global population in urban centres in 2015 lives in LMIC and UMIC (1.5 and 1.1 billion people respectively). The Urban centres in HIC are responsible for 40% of the global built-up areas of urban centres (circa 130 thousand km^2) despite the fact they host only 16% of the global urban centres population (about 580 million people). Urban centres in HIC have in 2015 an average areal extent and population size greater than the one of all other income groups (average size of 150 km^2 and population of 400 thousand people). Urban centres in LIC are on average the smallest in area (20 km^2) and population size (200 thousand inhabitants). While urban centres in HIC tend to be bigger on average in areal extent and population size, urban centres in UMIC and LMIC are more numerous (more than 6300 and 3800 respectively), and their size is quite large (more than 50 km^2 and 60 km^2 respectively). Variable is also the average population density in urban centres. It ranges in 2015 between 2.5 thousand inhabitants per km^2 in HIC, to 10 thousand inhabitants per km^2 in LIC.

Figure 55 © Adobe Stock, 2018

The changes in population and in the extent of built-up areas between 1990 and 2015 are diversified across income groups. Figure 56 highlights this differentiation and shows the built-up areas and population of urban centres in 1975, 1990, 2000 and 2015. It shows that the ratio between new inhabitants and new built-up areas in urban centres increases with the income group tier. While in HIC this ratio corresponds to 195 m^2 of built-up areas per inhabitant, this value is less than half in UMIC (about 90 m^2), it is 1/3 of this latter one in LMC (circa 30 m^2), and it is half of it in LIC (15 m^2). Accordingly, while population of urban centres in LIC more than doubles between 1990 and 2015

(+140 million people), and built-up areas expand by 40% (+2,000 km^2) the chart displays a rather vertical trajectory. Lines tend to be more flat towards higher income group tiers. In HIC, population in 2015 is 21% higher than the one in 1990 (+100 million people) and built-up areas expanded by 18% (+20 thousand km^2). The highest absolute population change and built-up areas expansion of urban centres takes place in LMIC where centres settle 500 million more people in 2015 (+50%), and account 17 thousand km^2 (40%) more built-up area compared to 1990.

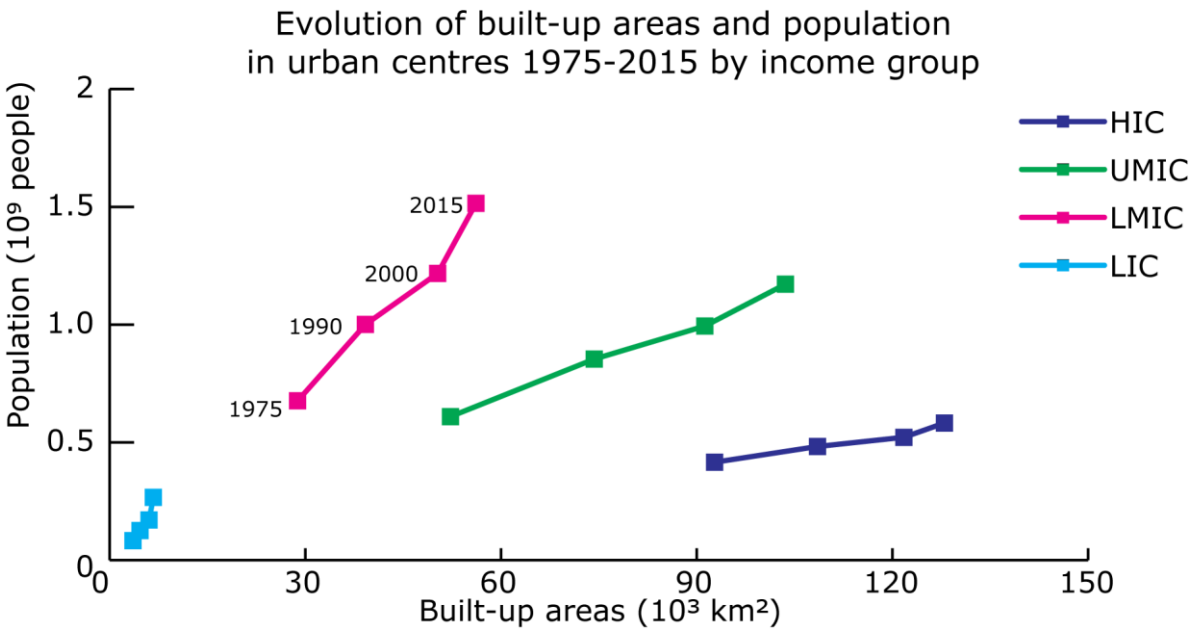

Figure 56 multi-temporal trajectories of built-up areas and population development by income group

Key Messages

- Urban centres in Low Income Countries have doubled in population in 25 years, are on average the smallest (20 km^2), the most densely populated (with 10,000 inhabitants per km^2) and have the lowest built-up areas per person – approximately 15 m^2 per person for each new inhabitant between 1990 and 2015.
- Urban centres in Lower Middle Income Countries are the ones that concentrated the largest share of population growth (+500 million people), while concerning built-up areas this has occurred in Upper Middle Income Countries (+17 thousand km^2).

5.2.5 GDP

Almost half of African urban centres have a very low GDP while most of Northern American urban centres have very high GDP

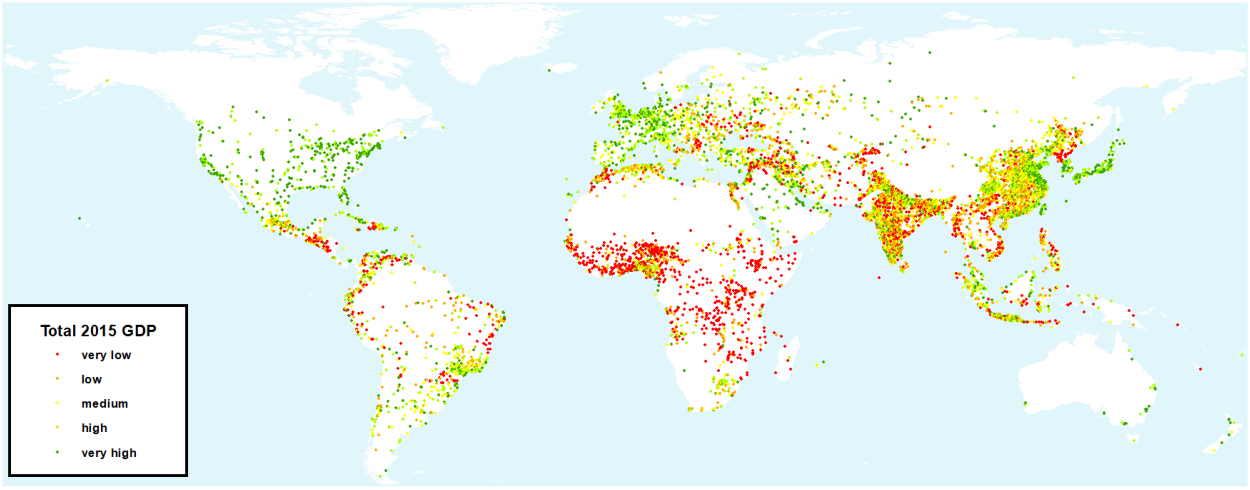

Figure 57 Total Gross Domestic Product of urban centres in 2015

Gross Domestic Product (GDP) is a key indicator of the development status of an area as it is a measure of the monetary value of goods and services produced in a given period of time.

The urban centres GDP is calculated using the gridded global annual Gross Domestic Product (Purchasing Power Parity) (Kummu et al., 2018) summed within the extent of each urban centre for the epochs 1990, 2000 and 2015. Given the input dataset, it represents the constant 2011 international US dollars of the total values produced in an urban centre in each epoch.

Figure 57 shows the 2015 GDP of each urban centre considered, grouped in five classes (quantiles). Most of the urban centres in the very low GDP class are in Asia and Africa: 45% are in Asia (16% of Asian urban centres); 41% are in Africa (48% of all African cities); 10% are in Latin America and the Caribbean (18% of Latin America and the Caribbean) and the rest (less than 5%) is in Europe and Oceania. Half of the urban centres in the very high GDP class are in Asia; 18% in Europe (30% of European urban centres); 14% in Northern America (66% of Northern America); 12% in Latin America and the Caribbean (21% of Latin America and the Caribbean) and the rest in Oceania (almost half of Oceanian urban centres).

The top 10 urban centres with the highest 2015 GDP (ranging between 372 billion dollars and 1008 billion dollars) are, in decreasing order: Tokyo; New York; Los Angeles; Shanghai; Bangkok; Seoul; Jakarta; Singapore; Osaka; Sao Paulo. Most of them are in Asia (70%); two of them in Northern America and one in Latin America and the Caribbean. Figure 58 (left) shows the built-up area, population and 2015 GDP of these 10 urban centres: Los Angeles is the biggest urban centre in terms of built-up area followed by New York, while Jakarta has the largest population. Tokyo, the urban centre with the highest GDP, ranks third in built-up surface and second in population size. Figure 58 (right) shows the relative evolution of population and GDP in the period 1990-2015. The most dynamic urban centres were: Shanghai, with an almost 9-times increase in GDP and 135% increase in population; Bangkok, with the highest increase in population (141%) and similar increase in GDP (176%); Jakarta, with a 3-times increase in GDP and 77% increase in population; and Singapore, 241% increase in GDP and almost doubled population. As predicted in some studies (Bettencourt and West, 2010; Bettencourt, 2013), GDP grows faster than population in these urban centres. In some cases (New York, Osaka, Seoul, and Shanghai), the ratio of GDP increase and population variation is around seven.

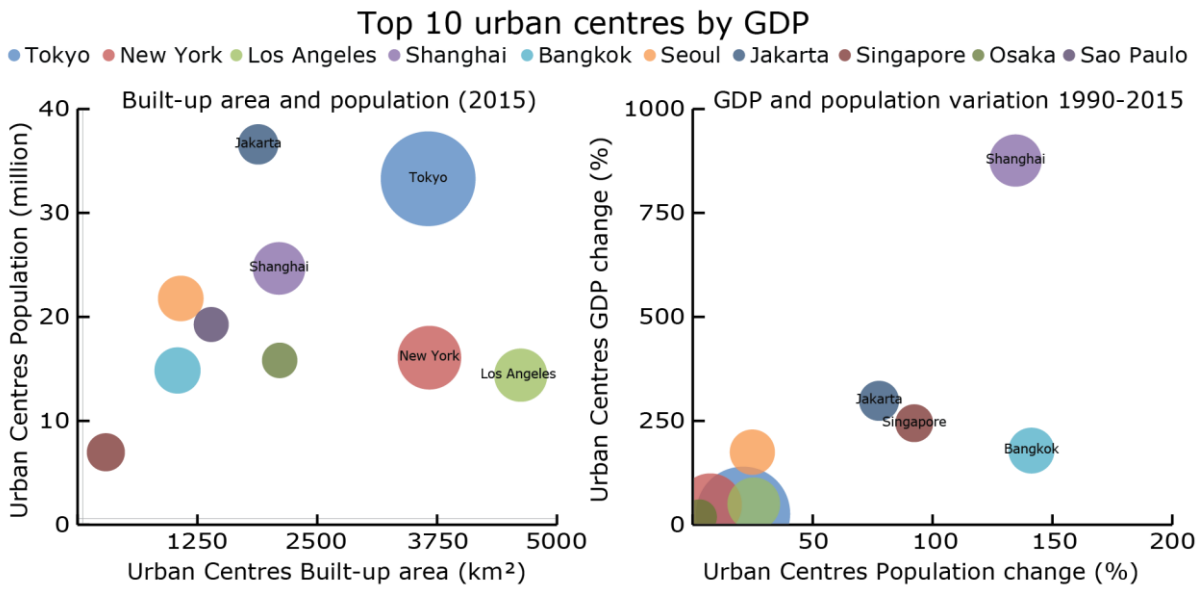

Figure 58 Top 10 urban centres by 2015 GDP. Population, Built-up area and GDP (circle size) of 2015; grey lines represents the average urban centres population and built-up area; percentage population variation and GDP variation between 1990 and 2015 (right).

Key Messages

- In 2015, 45% of African urban centres are in the very low GDP class;
- 66% of Northern American urban centres are in the very high GDP class in 2015;
- The top 10 urban centres with the highest 2015 GDP (372 - 1008 billion USD) are: Tokyo; New York; Los Angeles; Shanghai; Bangkok; Seoul; Jakarta; Singapore; Osaka; Sao Paulo;
- In New York, Osaka, Seoul, and Shanghai GDP has increased seven times more than population in the period 1990-2015.

5.2.6 Travel Time to Capital

Measuring the by-land travel time to reach the country capital urban centre

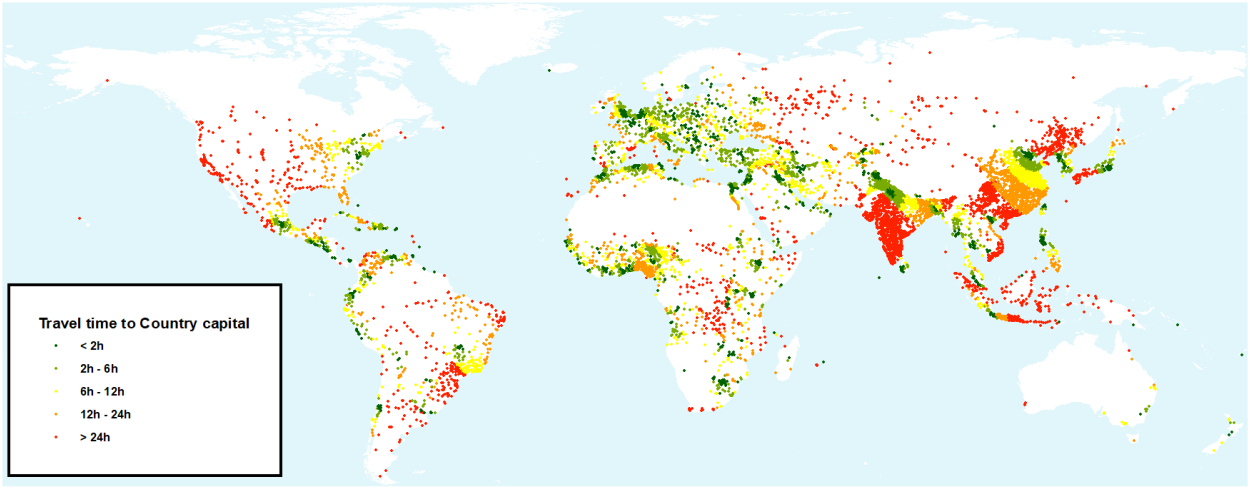

Figure 59 Travel time to country capital for all urban centres

The travel time to country capital represents the travel distance to reach the country capital urban centre from each urban centre considered. It is calculated by looking for the shortest path between each urban centre boundary and the country capital urban centre boundary according to the accessibility of the area between them. The accessibility is evaluated using the impedance layer(Weiss et al., 2018) that allows the calculation of the time needed to cross each areas. Therefore, flight connections are not taken into account. Travel time to capital city is important measure of accessibility and remoteness of a urban centre and it represents the distance from each person to the central administration of the country.

Figure 59 shows the global view of urban centres associated with their travel time to the capital. Many national patterns are easily recognizable as for Japan, United States, China and India. The possible patterns are due to morphological reasons such as in Japan, where the northern area is closer to Tokyo than the more mountainous southern part; or in US and China where the travel time gradually increases from the capital urban centres (Washington and Beijing, respectively) and the surrounding plain area. In India the visible pattern is due to the impedance that is very high all over the country as a consequence of the level of connections among urban centres, with the only exception of the main road between New Delhi and Kolkata. Urban centres close to this road are the only below 2 days of travelling to reach their country capital.

At global level, only 1335 urban centres (15%) are closer than 2 hours to their country capital; and 4492 (52%) are below half day of travel. More than 2000 urban centres (25%) are more than a day of travel away from the country capital. Figure 60 shows the population living in urban centre at given travel time from their country capital. More than 300 million people (12%) are closer than 2 hours to the country capital while 665 million are farer than one day of travel from the country capital. Europe is the region with the highest share of population (68%, about 130 million people) living in less than 12 hours from the country capital followed by Latin America and the Caribbean (64%; 170 million people) and Africa (63%, 190 million people). North America, is the region with the highest share of population (44%, 80 million people) living more than a day far from the country capital, followed by Oceania (40%, 3.4 million people) and Asia (30%, about 450 million people).

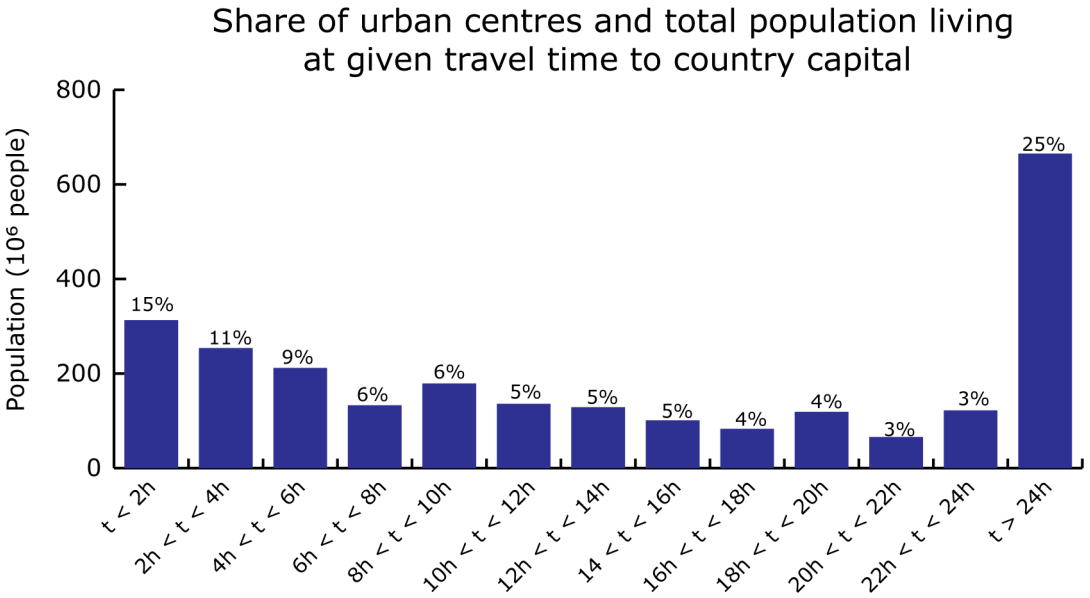

Figure 60 Total population distribution per class of travel time to country capital. Shares represent the abundance of urban centres for each class.

Key Messages

- 1335 urban centres (15%) are closer than 2 hours to their country capital;
- more than 2000 urban centres (25%) are more than a day of travel away from the country capital;
- more than 300 million people (12%) are closer than 2 hours to the country capital;
- 665 million are farer than one day of travel from the country capital.

Figure 61 © Adobe Stock, 2018

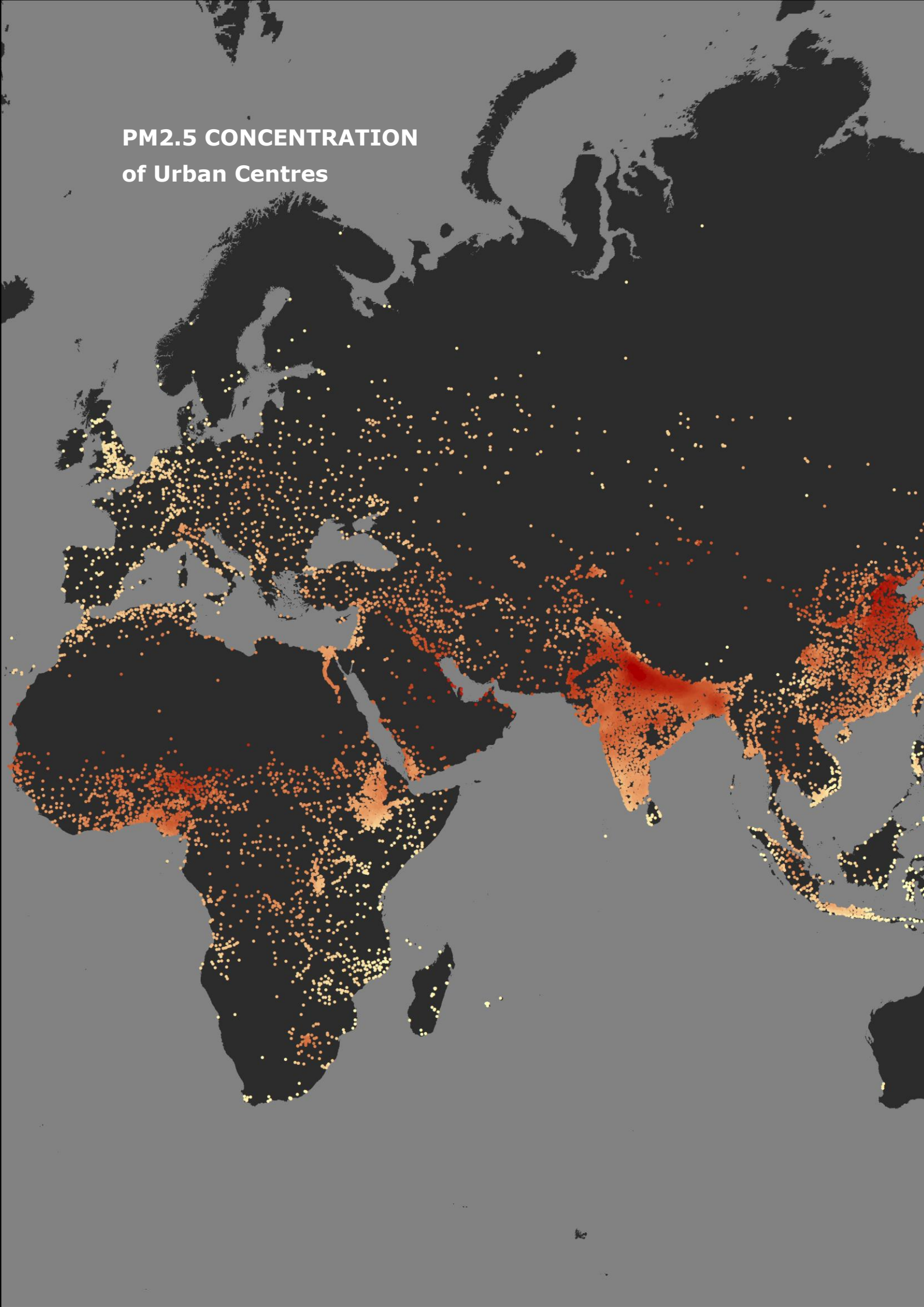
PM2.5 CONCENTRATION
of Urban Centres

5.3 Environment

Urban centres comprise less than 1% of the Earth's surface, but there is an extraordinary concentration of population, industry and energy use, leading often to massive local pollution and environmental degradation. Urban environmental problems are mostly related to pollution of soil, water and air through traffic, industrial production, inadequate wastewater/solid waste management. It leads to loss of green and natural spaces, and urban sprawl. All these problems are particularly serious in developing countries and countries with economic transition, where there is often a conflict between the short-term economic plan and the protection of the environment.
Cities consume much of the world's energy and account significantly to global CO_2 emissions. In particular, in developing countries, cities are faced with the worst urban air pollution in the world, which occurs as a result of rapid industrialization and increased motorized traffic.

This section provides information about the environmental status of the urban centres in the world. Many of the above-mentioned environmental issues are only collected at the local (city) level and are not available in a globally harmonized manner. Therefore, this section focusses on two parameters that can be derived from global data sets, the urban green and the PM2.5 concentration. Both variables are linked to the SDG's (indicator 11.7.1 for the urban green and 11.6.2 for the air pollution).

Figure 62 © Adobe Stock, 2018

5.3.1 Greenness

Multi-temporal analysis of greenness

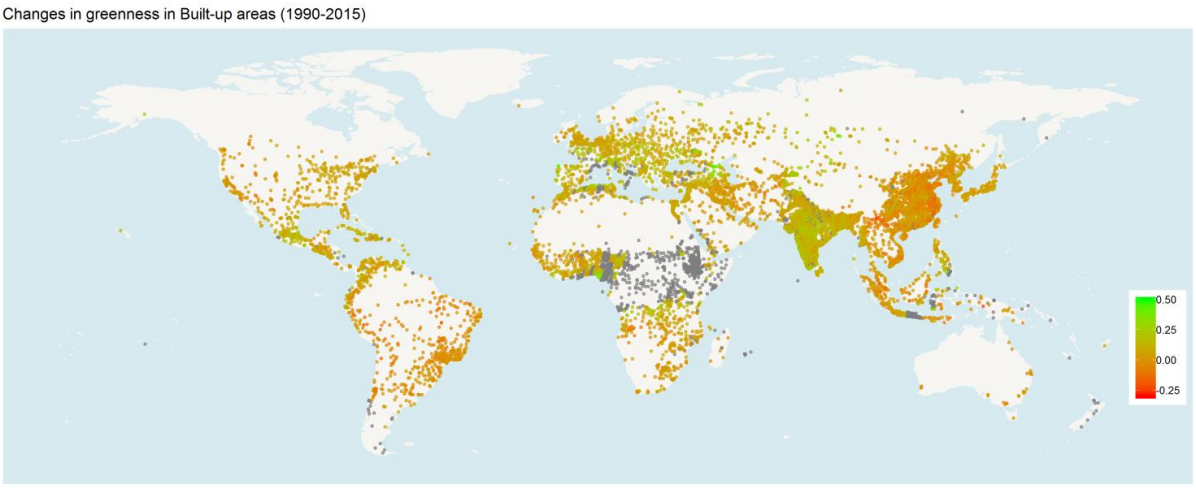

Figure 63 Spatial distribution of changes in greenness values in the built-up areas of the urban centres in the period 1990–2015 (no data is shown in grey)

The presence of green spaces within urban centres has been recognized as an essential component of the urban environment (Lee et al., 2015). Green spaces in cities are mostly composed of semi-natural vegetation cover, e.g. street trees, lawns, parks, gardens, forests, green roofs (Gan et al., 2014). Improving availability of green spaces in cities is considered in the United Nations Sustainable Development Goals (SDG), specifically in target 11.7, which aims to achieve the following: 'By 2030, provide universal access to safe, inclusive and accessible, green and public spaces, in particular for women and children, older persons and persons with disabilities' (United Nations, 2015).

The data on green spaces (also called greenness) within urban centres has been produced by analysing Landsat annual Top-of-Atmosphere (TOA) reflectance composites available as collections in the Google Earth Engine (GEE) platform for the period 1990-2015. These composites are created by considering the highest value of the Normalized Difference Vegetation Index (NDVI) as the composite value (i.e. greenest pixel).
Two types of analysis are presented here:

1) Changes in the amount of greenness within cities are investigated in the periods centred on 1990, 2000 and 2015 by estimating it within the respective built-up areas. Given our interest in analysing changes in greenness in urban centres in relation to urbanization in the period 1990–2015, for each of the 10,323 urban centres, the average of all greenest pixels located within the built-up area of the urban centre was calculated for three time intervals centred on the years 1990, 2000 and 2015 as follows: for 1990, the interval spans from 1988-01-01 to 1991-12-30; for 2000, the interval spans from 1999-01-01 to 2002-12-30; for 2015, the interval spans from 2012-01-01 to 2015-12-30. The intervals were chosen in order to match the dates of the Landsat data collections used to derive the multi-temporal built-up areas (GHS-BU) and to mitigate inter-annual variability and seasonal anomalies that may affect the greenness change analysis. The detailed methodology on multitemporal assessment of greenness with the built-up areas is described in Corbane et al., 2018b.
2) The continuous greenness values per each epoch calculated following the methodology described in point 1, are classified into three classes as follows:

- Low green for greenness < 0.1 : corresponding to barren rock, sand or snow or impervious surfaces (e.g. built-up areas)
- Medium green for 0.2 <Greenness <0.5: corresponding to shrubs or agriculture
- High green for 0.6 <Greenness < 0.9: corresponding to dense vegetation (e.g. forest, private gardens, etc.).

The areas of each of the three classes were estimated for each epoch within the boundaries delimited by the urban centres.

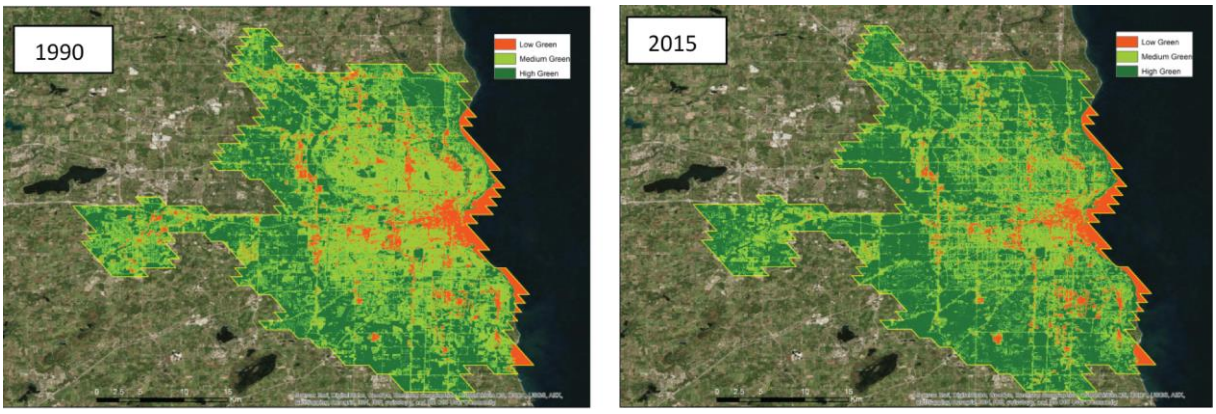

Figure 64 Classified greenness values for the urban centre of Milwaukee (United States) for the period 199 and 2015.

Figure 63 provides an overview of the spatial distribution of greening and 'browning' world urban centres for the period 1990–2014 according to the results of the analysis presented in point 1:

- The map depicts a concentration of decreasing greenness in the urban centres of Europe, India and Nigeria.
- In China, we observe contrasting situations with increasing and decreasing greenness in urban centres with evidence of decreasing green in the coastal cities.

When observed at a global scale, changes in greenness can be eventually explained by changes in CO2 concentrations and climate factors. Human influences are more difficult to assess at this scale. As suggested by Schut et al., 2015 on a global scale, land use change is not expected to affect greenness as strongly as the changes in climate or CO2. Figure 65 shows changes in the average share of green surfaces relative to the areas of the urban centres in the periods 1990, 2000 and 2015. The three classes of green surfaces are shown:

- Between 1990 and 2015, the share of high green surfaces (corresponding to dense vegetation, such as forests) has increased. In 2015, the average share of high green surfaces in urban centres is around 47%.
- The increase in high green surfaces is evidently accompanied with a decrease in the areas of low green and medium green surfaces.

To complement the results presented in Figure 65, we calculated for the period 2015 the number of urban centres where the share of high green surfaces is greater than the share of low green surfaces. The counts per continent are shown in Figure 66 . They confirm that in the majority of the cities, the share of high green surfaces is larger than that of low green surfaces, in particular in Asia and Europe.

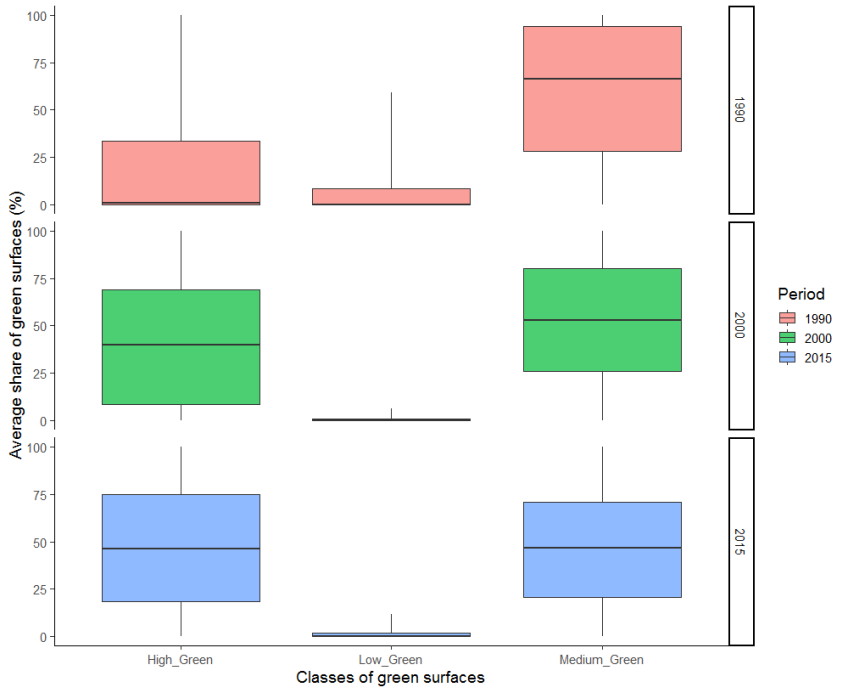

Figure 65. Changes in the average share of green surfaces relative to the areas of the urban centres in the periods 1990, 2000 and 2015

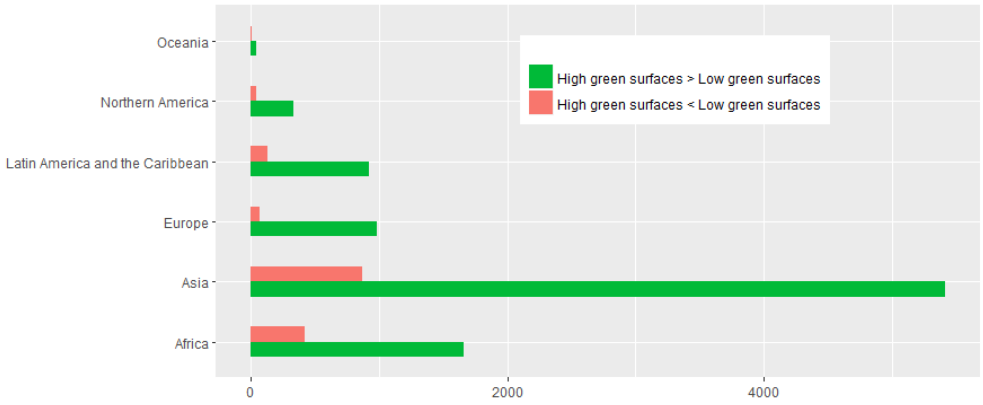

	HighGR_above	HighGR_below
Africa	1664	417
Asia	5417	873
Europe	982	73
Latin America and the Caribbean	925	127
Northern America	330	39
Oceania	46	3

Figure 66. Number of urban centres per continent where the share of high green surfaces is greater than the share of low green surfaces in the period 2015.

Key Messages

- Linked to the increasing global temperatures (as in 5.1.5 –p. 56) and the rapid urbanization, the analysis of greenness in urban centres shows an increase in green urban areas and in the share of green surfaces.
- These results should be analysed in conjunction with land cover or land use transitions to better understand the main drivers for this trend.
- Future works should be directed towards a better understanding of the combined effects of urbanization and climate factors on the dynamics of greenness in urban centres (e.g. relationship between greenness and Gross Domestic Product, influence of physical/topographic factors on greenness, relationship between greenness and air temperature and precipitation, and changes in population and built-up areas). This information may provide a valuable reference for urban planners and decision-makers to mitigate extreme urban heat island phenomena.

Figure 67 © Adobe Stock, 2018

5.3.2 Particulate Matter (PM2.5)

Changes in PM2.5 emissions and concentration across urban centres

"*Fine particulate matter (PM2.5) is responsible for significant negative impacts on human health*[28]" (Directive 2008/50/EC of The European Parliament and Of The Council). PM2.5 is of natural (i.e. sand and dust) or of anthropogenic source (i.e. combustion residuals), and its concentration is of high concern especially in urban agglomerations that concentrate many people and develop fast (Chan and Yao 2008).
The GHS-UCDB contains information on PM2.5 emissions (by sector, and over time 1975-2012), and on PM2.5 concentration (2000-2005-2010-2014).
Half of the PM2.5 emission in cities in 2015 is due to industrial sources, such emissions exceed 3 million ton/year. Emissions from industrial sources have increased by 40% between 2000 and 2012.

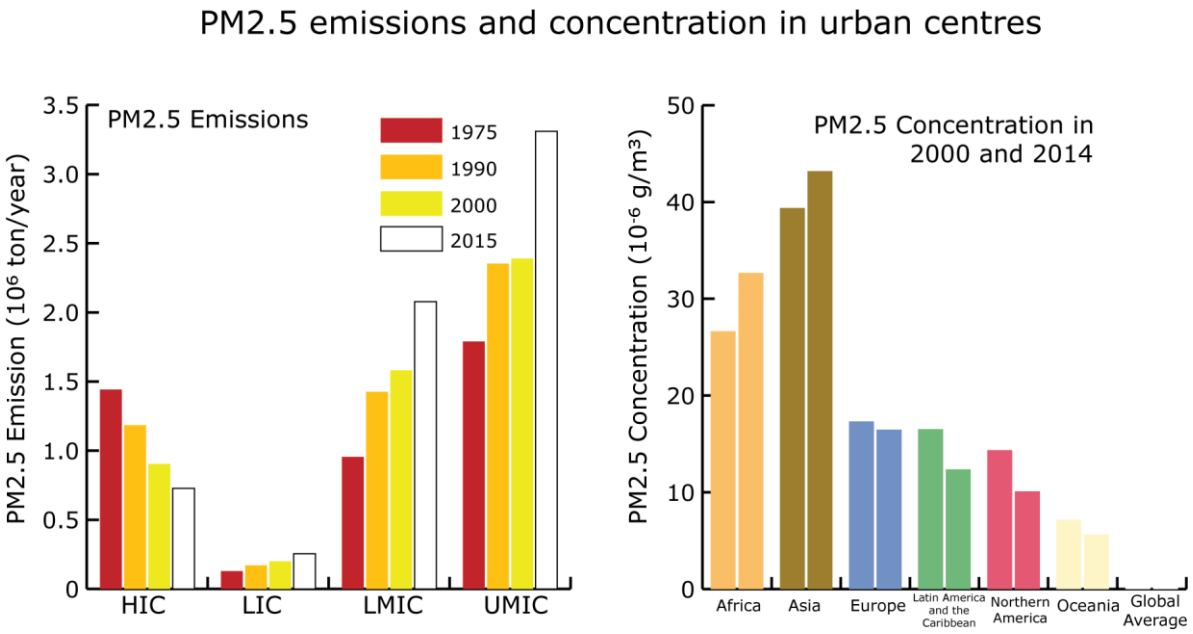

Figure 68 Urban centres multi-temporal PM2.5 emissions per income group, and PM2.5 concentration in 2000 and 2014 per region of the world

These emissions have mostly increased in Asia (+74%), and Africa (+45%) while they have declined substantially in Europe (-40%), and Northern America (-26%). The residential sectors is responsible for 1/3 of the PM2.5 emissions but total emissions have increased by 9% since 2000. Considerable reductions took place in Europe (-60%) and Northern America (-35%). Similar patterns of change are observed about emissions from the transport sector. Considering a classification of urban centres by income groups, it emerges that only HIC have reduced the PM2.5 emissions (by about 40%) in the period 1975-2012. LIC increased total emissions by 50%, led by almost doubling the ones of the transport sector, increasing by ¾ the ones of the residential sector and by 1/3 the ones from industrial sources. LMIC and UMIC more than doubled the emissions of the transport sector, while UMIC have by far increased the most the emissions of their industrial sectors in cities (+80%).
Regarding PM2.5 concentration, globally it has constantly increased across the epochs 2000-2005-2010-2014. Regional changes return a pattern of increase in Africa and Asia, and of decrease in the other major regions of the world. Across income groups, PM2.5 concentration in 2014 has moderately increased in UMIC (+6%), LMIC (+11%) and LIC (+16%) and decreased by 6% in HIC compared to concentrations in 2000.

[28] PM2,5' shall mean particulate matter which passes through a size-selective inlet as defined in the reference method for the sampling and measurement of PM2,5, EN 14907, with a 50 % efficiency cut-off at 2,5 µm aerodynamic diameter;

5.3.3 Carbon Dioxide (CO_2)

CO_2 emissions across urban centres

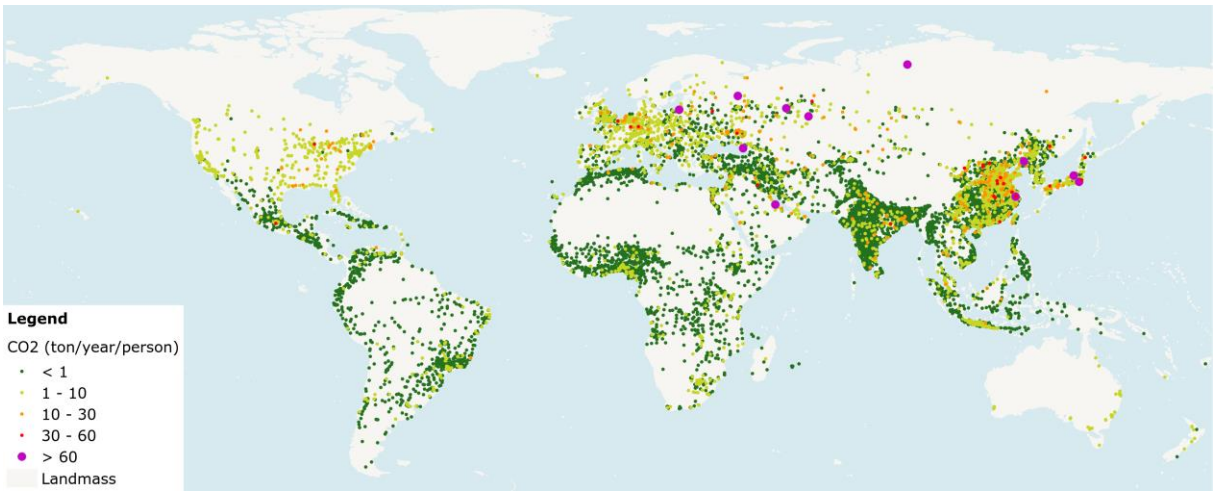

Figure 69 Urban centres classified by annual CO_2 emission per inhabitant (ton/year/person) in 2012.

Carbon dioxide (CO_2) is the primary greenhouse gas contributing to global warming. It is naturally present in the atmosphere as part of the Earth's carbon cycle. However, human activities are adding more CO_2 to the atmosphere. In addition, human activities influence the ability of natural sinks, like forests and soils, to remove CO_2 from the atmosphere. While CO_2 emissions come from a variety of natural sources, human-related emissions are responsible for the increase that has occurred in the atmosphere since the industrial revolution. The industrial activities have raised atmospheric carbon dioxide levels from 280 parts per million to 400 parts per million in the last 150 years (IPCC, 2014).
The data on CO_2 emission for the urban centres have been extracted from the Emissions Database for Global Atmospheric Research (EDGAR v4.3.2) that compiles gaseous and particulate air pollutant emissions for the years 1970 to 2012 (Crippa et al., 2018). The calculation of the emissions includes all human activities, except large scale biomass burning and land use, land-use change, and forestry. The results are comparable between countries thanks to the bottom-up compilation methodology of sector-specific emissions applied consistently for all world countries. The sectors definition uses the following IPCC 1996 codes: *energy* - Power Industry (IPCC 1A1a), *residential*: Energy for buildings (IPCC 1A4), waste (IPCC 6), *industry*: Oil refineries and Transformation industry (IPCC 1A1b, 1A1c), Combustion for manufacturing (IPCC 1A2), Fuel exploitation (IPCC 1B), Industrial Processes (IPCC 2), Solvents and products use (IPCC 3), *transport* - Transport (IPCC 1A3), and *agriculture*: Agriculture (IPCC 4).

The global annual emissions of urban centres have increased steadily since the epoch 1975 with the strongest increase of 33% between 2000 and 2012 (Table 8). Although industrial production is still the biggest global source of CO_2 emissions from urban centres, the energy sector is increasing its share.

The regional contribution of cities and their inhabitants to the global CO_2 emissions is very diverse. Figure 69 Urban centres classified by annual CO_2 emission per inhabitant (ton/year/person) in 2012. Figure 69 maps CO_2 emission per inhabitant of the urban centres (calculated as total emission of urban centre divided by total population of urban centre). In most urban centres of the Global South, the respective population produces less than one ton CO_2 per year in 2012, while the urban centres of more developed countries including China are emitting between one and ten (and often more) tons per inhabitant in a year. In addition, there are large differences in the temporal evolution of the CO_2 emissions in the various regions (Figure 70). For the epoch 1975, the industrial sectors of Europe, North America, and Asia contributed more or less equally to the global emissions of CO_2. However, with the development of the Asian, and in particular Chinese,

industrial production in the following epochs, the emissions from the Asian industrial sector more than doubled between 1975 and 2012. In addition, emissions from the energy sector in Asian urban centres increased even faster matching in 2012 that of the industrial sector. The period 1975 to 2012 is also characterised by the strongest rates of urbanisation in Asia. Therefore, also the emissions from the residential and transport sector in Asian cities increase. In 2012, Asian urban centres are the largest contributors to global CO_2 emissions compared with the urban centres of other regions in the world. The trend in Europe and Northern America is in the opposite direction; CO_2 emissions in urban centres are stable or decreasing with the exception of the transport sector, which slowly but continuously increase, and the energy sector in Europe, which peaked in 1990 and started to increase the emissions again between 2000 and 2012. Since the 1990s also the emissions from the industrial sector in urban centres of Africa, Latin America and the Caribbean increased steadily.

Table 8 Global annual CO_2 emission of urban centres in billion tons per year and relative contribution of human activity sectors for nominal epochs (1975-1990-2000-2012).

CO_2 source	**1975**	**1990**	**2000**	**2012**
Fossil	4,376	5,368	5,932	8,020
Bio fuels	0,684	0,675	1,049	1,300
Total	***5,061***	***6,043***	***6,981***	***9,319***
Sector	***1975***	***1990***	***2000***	***2012***
Agriculture	0.2%	0.3%	0.3%	0.3%
Residential	24.8%	23.0%	21.4%	16.7%
Transport	5.6%	7.4%	8.5%	8.4%
Industry	53.4%	45.9%	44.5%	42.9%
Energy	16.0%	23.9%	25.3%	31.8%

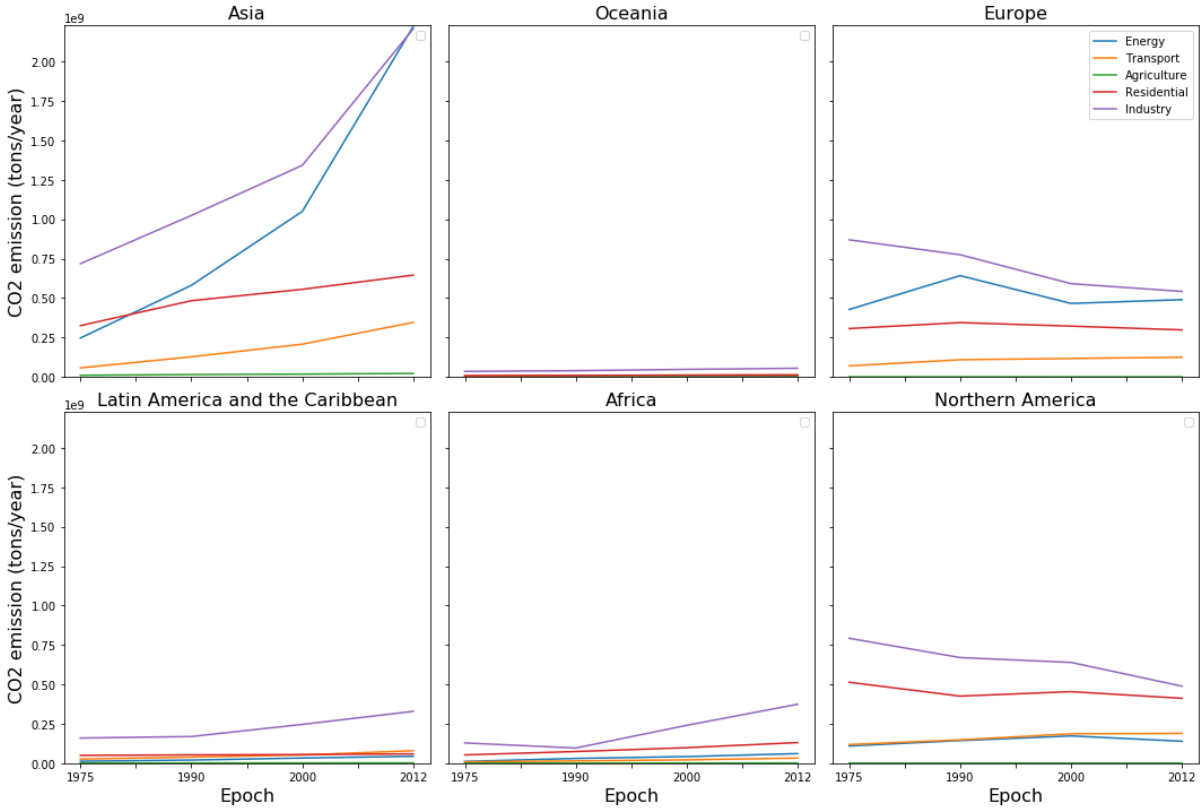

Figure 70 Emission of $C0_2$ of urban centres split by sector for Major Regions in the period 1975-2012.

Key Messages

- The annual emission of CO_2 per person in urban centres in 2012 is much higher in North America, Europe, and NE Asia compared to other regions of the world.
- The overall emission of CO_2 in cities of Europe and North America is decreasing, while in other regions it is growing, with Asia in the first place.
- The CO_2 emission from the energy and industry sectors in Asian urban centres is growing much faster compared to the increase in CO_2 emission by the other sectors.

The Urban Centre's
EXPOSURE TO EARTHQUAKES

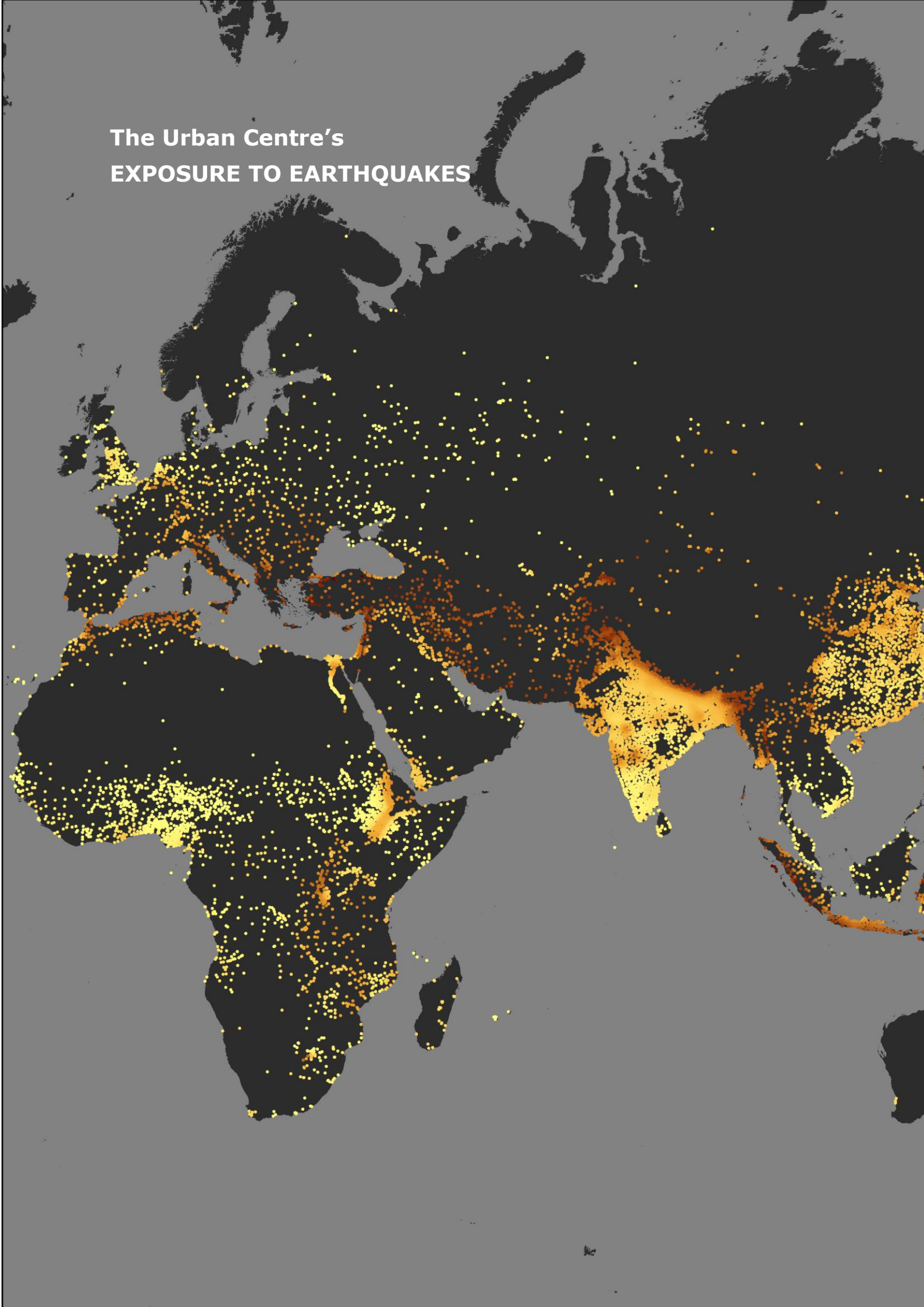

5.4 Disaster Risk Reduction

Natural hazardous events – those that release high energy or that impact human nutrition and health – are part of the Earth system processes of Planet Earth. Atmospheric circulation may generate strong winds and hurricanes and associated storm surges in coastal area. High intensity precipitation may cause flash floods and inundation. Plate tectonics that continuously shape the topography of Planet Earth generate volcanic eruptions and earthquakes; and tsunamis originate when seismic shaking occurs in the proximity of low lying coastal areas. Droughts the impact life supporting system of humanity and in heat waves impacts health condition directly.

When high-energy events are released over or in the proximity of populated areas, disaster unfolds. Over time, these natural events may increase or decrease in magnitude and frequency due to astronomical forces, Planet Earth plate tectonics or as a result of human activities that are altering the biogeochemical cycles and that in turn affect the climate. These events are here to stay and humanity will have to co-exist as it always has. The only option we have is to make sure that we know the frequency and intensity with which these events may affect a given place so that we may have the option to mitigate, avoid – when possible by re-locating – or prepare for. Climate change may have also changed temperature in many cities generating hazardous living conditions.

Cities are most at risk because they concentrate high population and infrastructural assets as built-up areas. In addition, some cities have developed in hazardous prone areas and re-locating them elsewhere is not a viable option. In fact, due to natural population growth and urbanization, many cities are increasing in size and density. Risk of damage to hazardous events can be reduced, but not eliminated. Risk of heat waves may be reduced through adopting cooling technology, a local solution that may not be affordable to everybody. Technology can be used to mitigate mostly through avoiding the hazards, alerting, or preparing.

The pre-condition to reduce risk and create resilient city to natural hazards is to quantify the exposure to hazards. The four sections below succinctly describe the results of the crossing of the spatial information of urban centres with the hazardous information contained in four global hazards maps. The resulting maps of exposure of urban centres to hazard are the best global knowledge for that given hazard at the time of writing that is derived from open source data. It is by far not the ultimate hazard information as hazard information are incrementally improved with the availability of new knowledge and also to take into account the changing nature of the hazard (Ehrlich et al., 2018). The analysis of this Atlas associates city geographical location and extent with information on the exposure to the different hazards.

5.4.1 Flood

Floods occur in urban centres across the globe

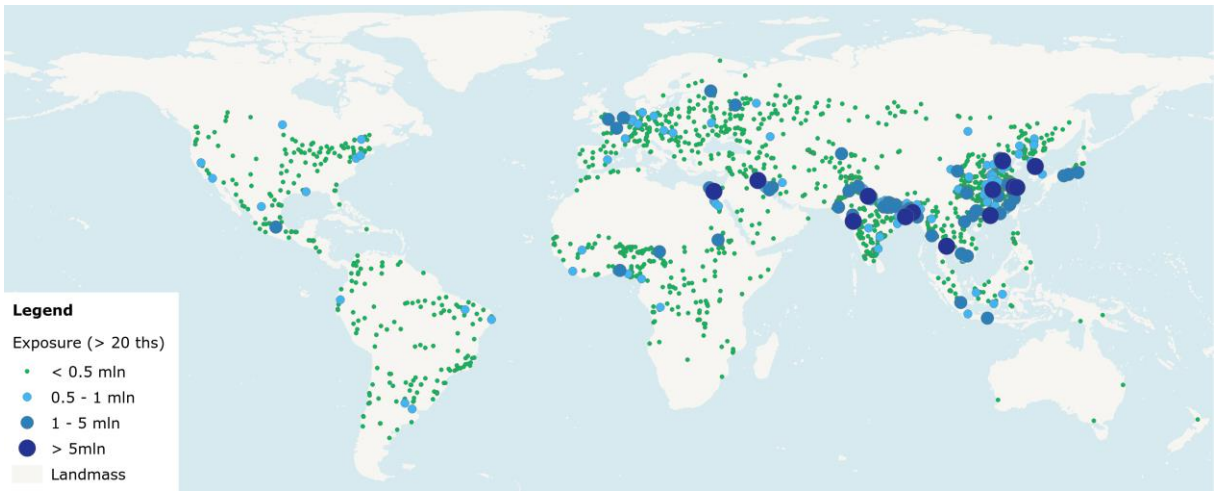

Figure 71 Population of urban centres potentially exposed to floods in 2015 considering a 100-year return period flood hazard map.

Riverine Floods – hereafter referred as floods - affect urban centres across the globe. In fact, human settlements are often located in the proximity of rivers and in the flat fertile low-lying terrain that is the preferred geographical areas for humans to live in. Flooding is the most recurrent and damaging disaster type and most of the countries of the world have experienced damaging floods and will have to respond to floods in the future also due to the increasing population and infrastructure in flood prone areas.

Figure 71 shows the urban centres of the globe exposed to potential flooding when using a hazard flood map with return period of 100 years. That map was produced by selecting urban centres having at least 20000 people within that urban centre potentially exposed. It shows over 4000 urban centres that account to 32% of all the urban centres selected from the GHS-UCDB city database. The size of the circles indicates the size of population exposure in the urban centres grouped in four classes: less than half million, between half million and 1 million, between 1 and 5 million, and over 5 million inhabitants. The map also shows that 11 of the 12 urban centres with more than 5 million inhabitants exposed to floods are located in Asia, and that urban centres in all continents may experience floods.

The analysis conducted using the 2015 GHSL population datasets shows that globally over 590 million people living in urban centres are potentially exposed to floods. That accounts for 19% of the overall population living in urban centres. The share of global population in urban centres exposed to floods has not changed over the 1990-2015 time period.

Figure 72 shows the potential exposure of population per major region in percentage of affected population. It shows two bar charts: the total share of urban centre population per continent for 1990 (a) and for 2015 (b). The population share refers to the total urban centre population potentially affected by flood to the total urban centre population for that region. Nearly three quarters (73.4%) of the total world urban centre population exposed to floods in 2015, lived in Asia. That city population in Asia accounted for 300 million in 1990 and 450 million in 2015. In percentage of the total urban centre population Asia has changed by few decimal points from 22.9% in 1990 to 23.2%. In global terms, the change of the share per major region over time, has slightly increased in Africa and Asia, and decreased in the remaining continents. The total built-up area of all urban centres exposed to floods accounts for 16% of the total area of urban centres. That percentage has remained unchanged when compared to the epochs 1990 and 2000.

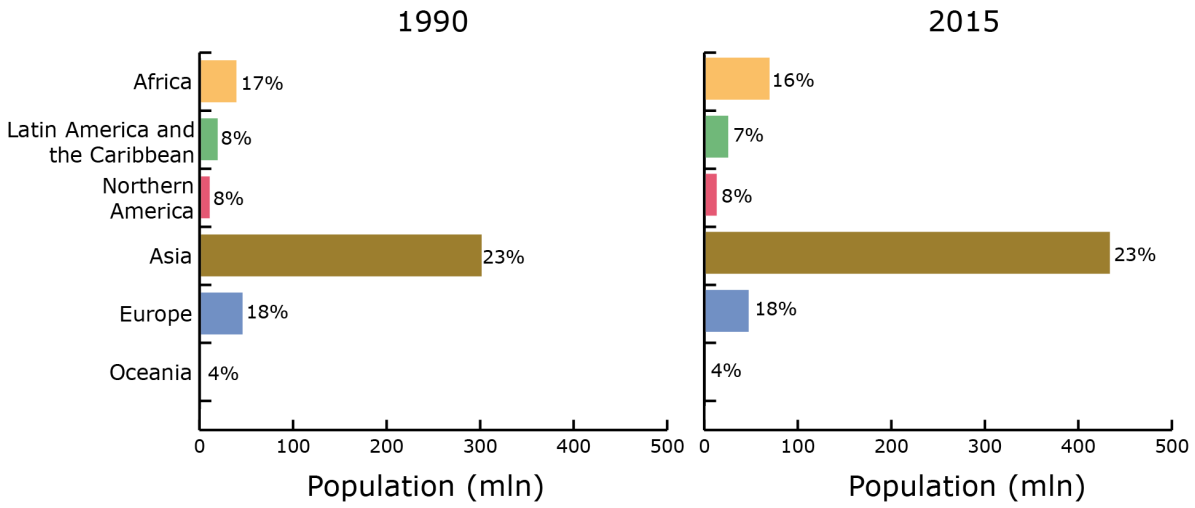

Figure 72 Regional share of the total population living in Urban Centres and exposed to flood hazard in 1990 (a) and in 2015 (b).

Figure 74 shows the number of urban centres (y-axis) grouped based on the rate of change of population in urban centres (x-axis) exposed to flood hazard in the 1990-2015 period per continent. In Latin America, North America and in Europe the rate of changes of population in urban centres exposed to flood has mostly decreased. Asia shows that while population change rates exposed to floods has decreased in a large number of urban centres, still the number, where it has increased, is significant and greater than that of all other continents combined. Africa shows an increase in the number of urban centres exposed to floods where population change rate has significantly increased.

Figure 73 © Adobe Stock, 2018

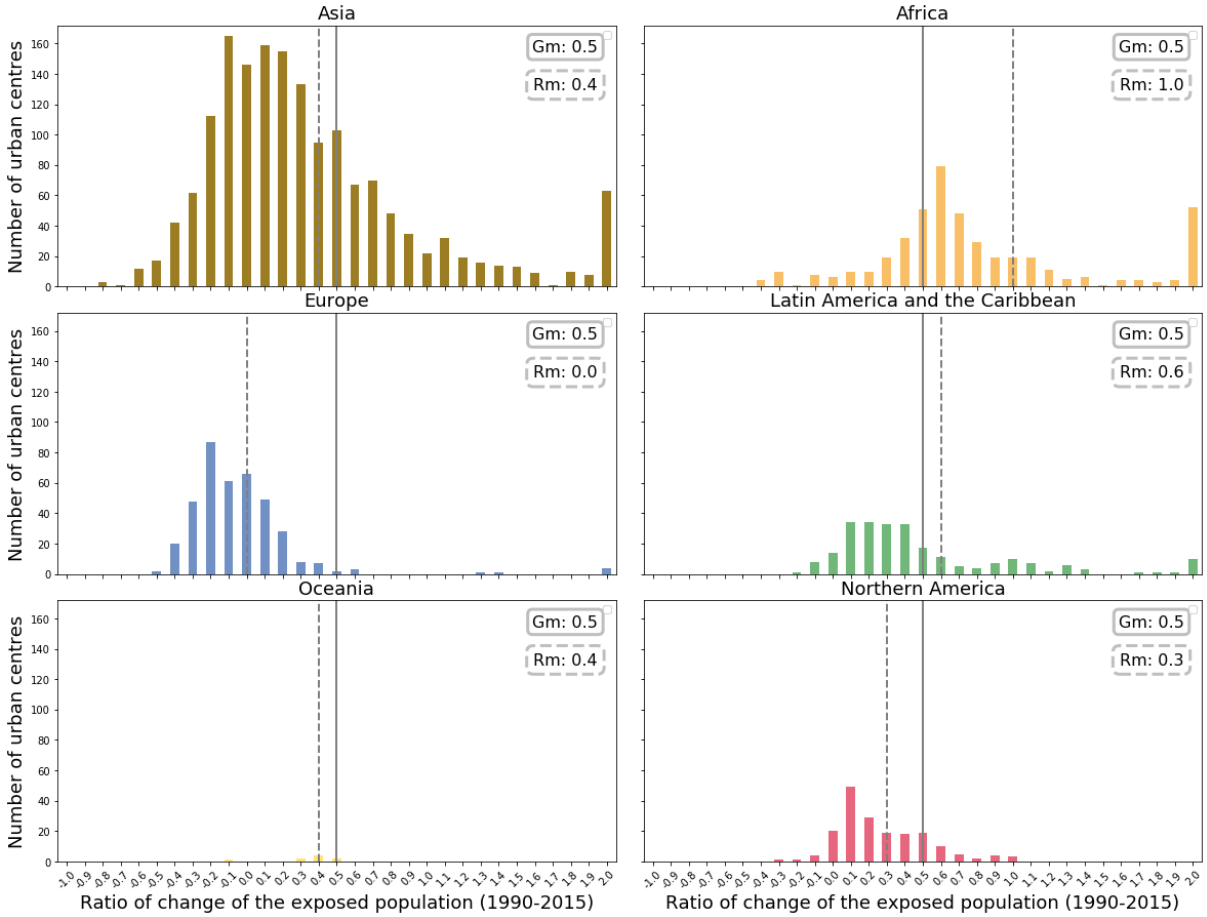

Figure 74 Number of urban centres by ratio of population change (1990-2015) potentially exposed to floods per region (Gm – global mean, Rm – regional mean).

Key Messages

- Most of the people potentially exposed to floods in cities live in Asia, as Asia is also the most populated continent.
- Asia and Africa are the continents, where city population exposed to floods has increased most over the 1990-2015 time period.
- Eleven out of twelve of the urban centres with over 5 million people potentially exposed to floods are located in Asia.
- The increase in exposure to floods in Asia is largely due to the overall increase in population.

5.4.2 Earthquake

One out of 10 urban centres dwellers globally is exposed to damaging earthquakes

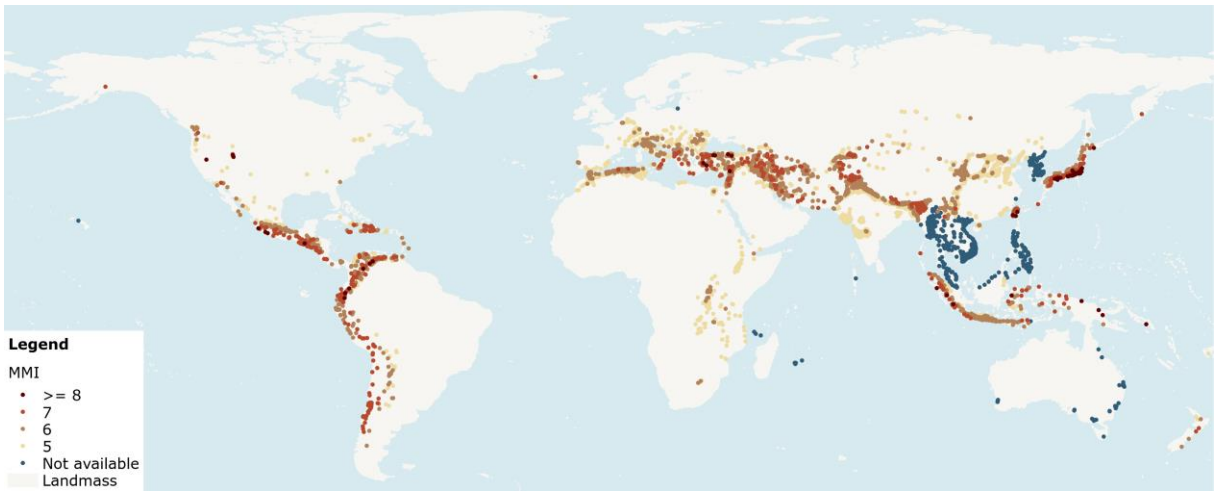

Figure 75 Exposure of urban centres to seismic hazard, considering MMI intensity equal or greater than five (GEM2019, beta version).

Earthquake is a major devastating hazard that strikes unexpectedly and damages urban centres in seismic prone areas of the world (Figure 75). The estimation of exposure in urban centres is related to seismic shaking maps and information layers. Those seismic maps – based on probabilistic assessment of the frequency and magnitude of the shaking intensity - continue to be improved with the accumulation of data and knowledge. The seismic hazard map used to produce the urban centre exposed to hazard maps shown in Figure 75 was made available by the Global Earthquake Model (GEM) initiative. The seismic map is the most up to date global seismic hazard layer available to date and assembled from regional seismic models by GEM. The version used in this Atlas does not contain yet the updates for South East Asia that will be available at the end of 2018.

Figure 75 includes the 3077 the urban centres exposed to intensity of the Mercalli Modified Intensity scale (MMI) of value 5 or greater in 2015. Figure 76 shows the 10 urban centres with highest population exposed. Eight of the most exposed cities are located in Asia, (one, Istanbul, across Europe and Asia and one, Cairo, in Africa). The map shows also the increase in population exposed from 1990 to 2015. The fastest population growth in urban centres occurs in rapidly growing cities of low and medium income countries where fertility is highest. In fact, increase in population exposure is largely due to general population increase.

Figure 78 shows the population in urban centres in the six continents, in the class 5-to 8 of the MMI scale. Earthquake cause increased damages with increased class intensity class on the MMI scale. The figures of exposed urban centres to earthquake are subdivided per continent. Figure 78 reveals the relatively low population in urban centres exposed to earthquakes in Oceania, and the relatively low population in urban centres in Africa. In addition, there are no urban centres in Africa that are likely to experience shakes with seismic intensity 7 or 8. Europe's urban centres are exposed to shaking intensity corresponding to classes 5 and 6 and account for less than 60 million. Asia remains the continent with the highest population exposed.

Figure 78 does not take into account Southeast Asia, for which we have not updated seismic hazards for this Atlas. Despite that, in Asia, the two highest intensity MMI classes that of 7 and 8 – those that always cause devastation – account for over 180 million people that is more than the MMI class 7-8 of Oceania, North America, Africa and Europe combined. Latin America is the continent with highest proportion of population in urban centres exposed to seismic hazard. That population is approximately 180 million, of which 65 million in the most devastating classes 7 and 8.

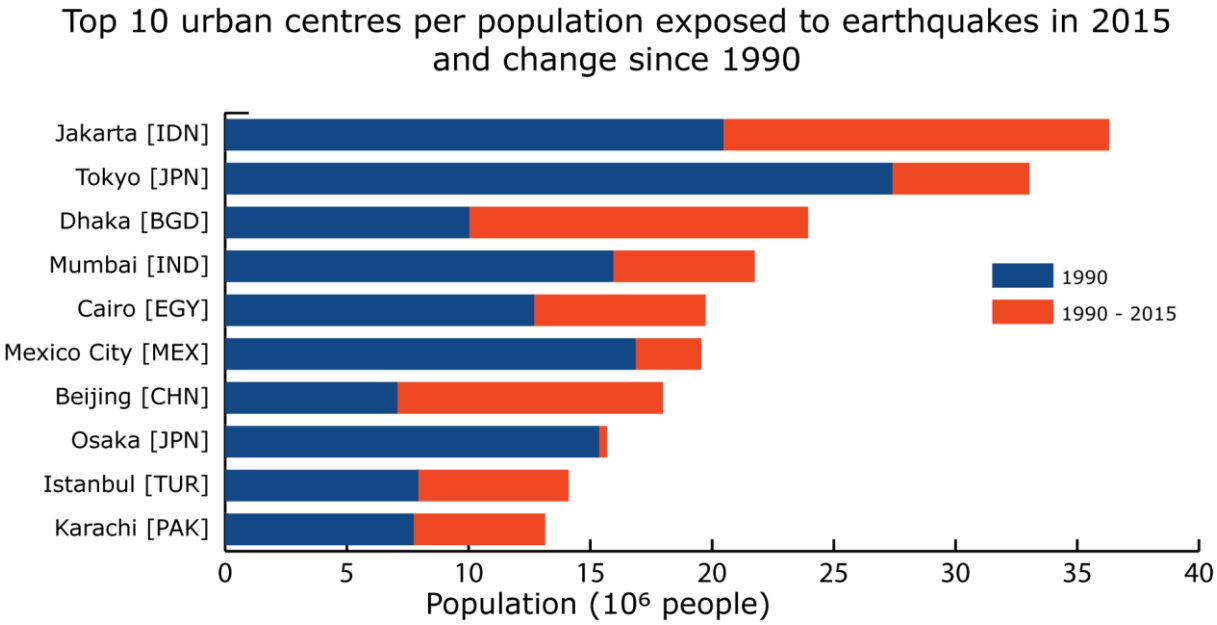

Figure 76 Top ten urban centres population exposed to seismic hazard with magnitude greater than class 5 in MMI scale

Figure 77 © Adobe Stock, 2018

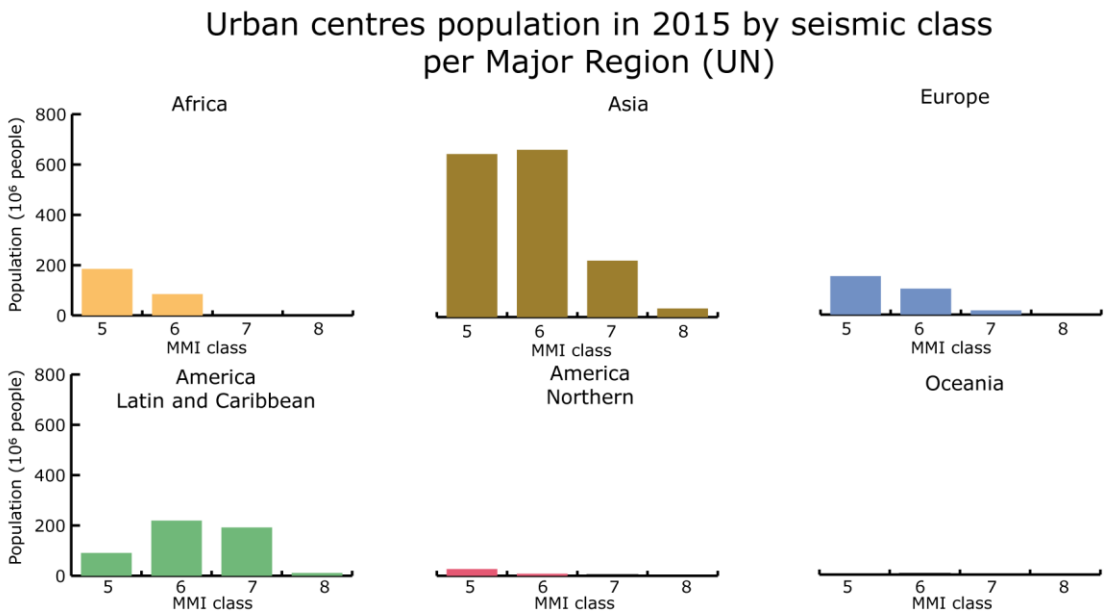

Figure 78 Absolute urban centre population exposed to seismic hazard in 2015 by MMI seismic class and per UN Major Regions.

Key Messages

- Earthquake occurrence is not predicable and over 700 million people living in urban centres are exposed. That is one in every 10 people globally.
- Asia remains the continent with the highest exposed population in cities for its high hazard probability and the large amount of population and built –up exposed.
- Latin America and the Caribbean show also a very high percentage of urban centre population exposed
- The combined urban centre population of ten of the largest cities exposed to earthquakes account for more than 200 million people.
- The large cities of the developing world exposed to earthquakes are growing faster than those in high income countries.

5.4.3 Storm Surge

Most of the people potentially exposed to storm surges live in Asia.

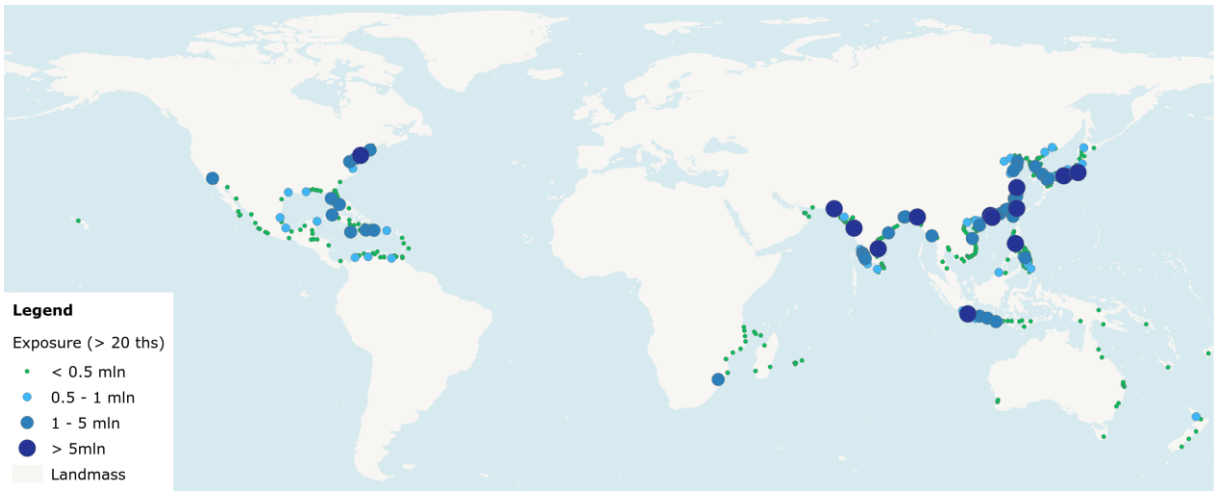

Figure 79 Population of urban centres potentially exposed to storm surges in 2015 calculated with a hazard return period of 250 years.

Storm surges generated by the air pressure of tropical storms and hurricanes on the ocean surfaces can affect a number of cities located in low-lying coastlines. Figure 79 show the exposure of urban centres to storm surge calculated based on a hazard return period of 250 years. The figure is the result of the intersection of the hazard layer and the spatial extent of the urban centres. The figure shows the urban centres that include at least 80% share of built up area in the urban centre and at least 20 thousand people exposed to the hazard in 2015.

In 2015, the total urban centre population of the world potentially affected by storm surges accounted to 330 million; that is 10% of the overall global urban centre population. That percentage has not changed over the decades analysed in this research (1990-2015). In 2015, the cumulated urban built-up area exposed to sea level surge accounted to 16% of the total built up area in urban centres. Also, that percentage did not change over the decades analysed in this research (1990-2015).

The regional analysis by UN Major Region (Figure 80) shows that Asia is by far the continent with the most population in urban centres potentiallyexposed to sea level surge in urban centres. That population accounts to less than 200 million in 1990 and grew to 250 million in 2015. Asia hosts more population in urban centres exposed to sea surge than all the other continents combined. In addition to Asia, also North America and Latin America and Caribbean are significantly exposed. North America has less than 30 million people exposed and Latin America and the Caribbean has over 250 million in 2015.

North America, shows the highest percentage of population in urban centres potentially exposed to sea level surge. Nearly one out of five people in North America living in urban centres is exposed to storm surge and that percentage has slightly decreased from 20% in 1990 to 19.3% in 2015. Also, Oceania shows over 20% of city's population exposed to storm surge – 1 out of 5 – and that percentage slightly increases over the period under scrutiny.

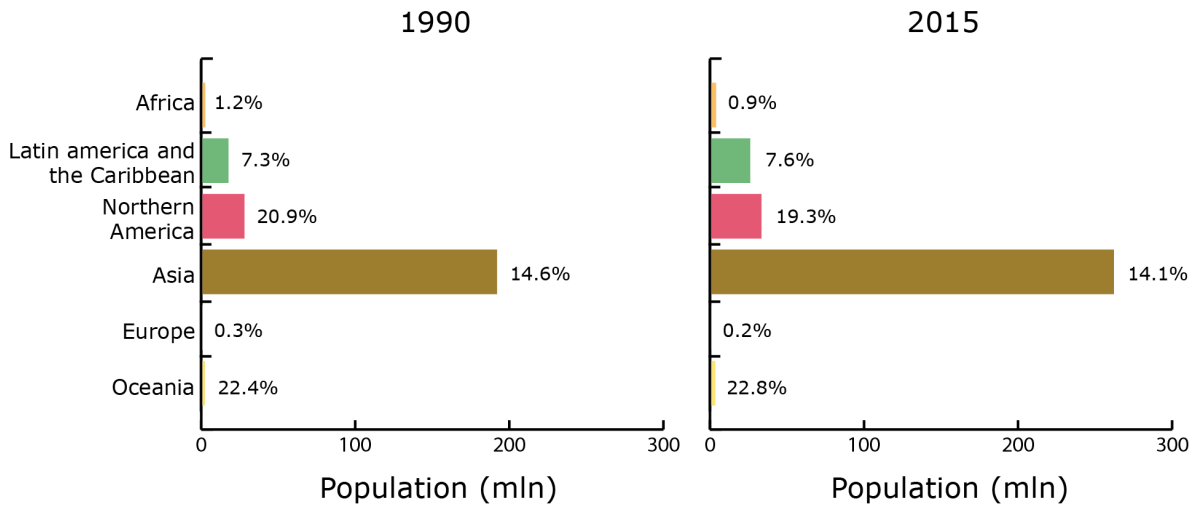

Figure 80. Population of urban centres potentially exposed to storm surge per UN Major Region in 1990 and 2015, as totals and as percentage of overall population in the Region's cities.

Figure 81 shows for each Major Region the number of urban centres (y-axis) grouped based on the rate of change of population in urban centres (x-axis) in the 1990-2015 period. The change classes range between -1 and + 2 changes. The chart shows the total number of urban centres exposed. Asia accounts for the majority of urban centres exposed. That number is larger than the sum of all the urban centre of the other continents combined. The mean change rate of exposure in Asia is slightly below the mean change rate of the global population exposure. Figure 81 also shows that in Latin America and the Caribbean the number of urban centres, in which the exposed population change rate has decreased, is similar to those where exposure has increased over the 1990-2015 period. However, a number of urban centres show rapidly growing population exposed to storm surge. In North America, the average growth rate is below the global average, but the region has a wide spread including some cities with population decrease in cities potentially exposed to storm surge. In Oceania, a number of urban centres show slight decrease in change of exposed population.

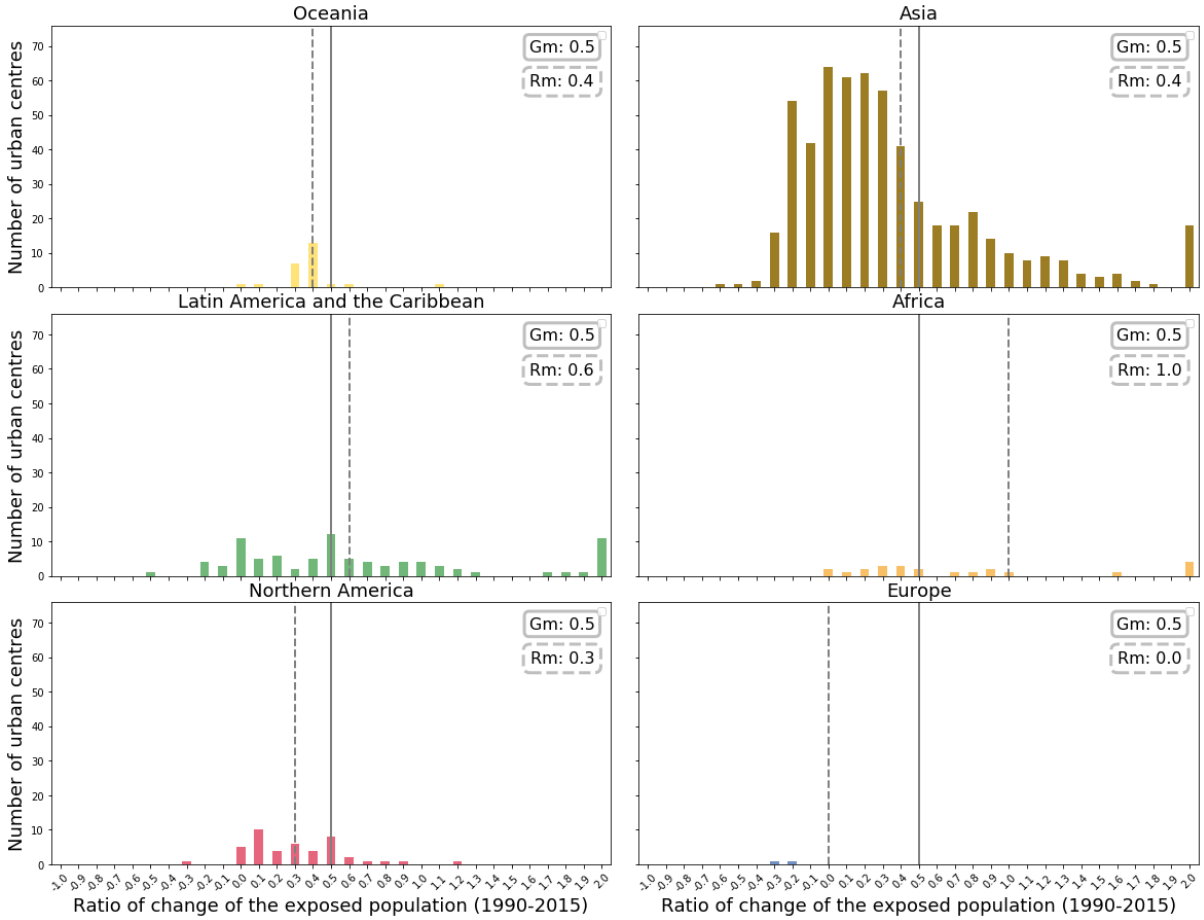

Figure 81 Number of urban centres exposed to storm surge grouped by population change rate between 1990 and 2015 (Gm – global mean, Rm – regional mean).

Key Messages

- Storm surge may especially affect the low lying coastal cities of the tropical belt.
- In Asia, the total urban centre population potentially exposed to storm surge exceeds 250 million.
- There are more urban centres exposed to storm surge in Asia than in all the other continents combined.
- One out of five urban centre dwellers in North America is exposed to storm surge.
- Latin America and the Caribbean show the second highest number of urban centres exposed to storm surge.

5.4.4 Heatwave

The heatwave magnitude index (HWMId) observed during 1982-2010 shows an incidence of heat wave occurrences in urban centres

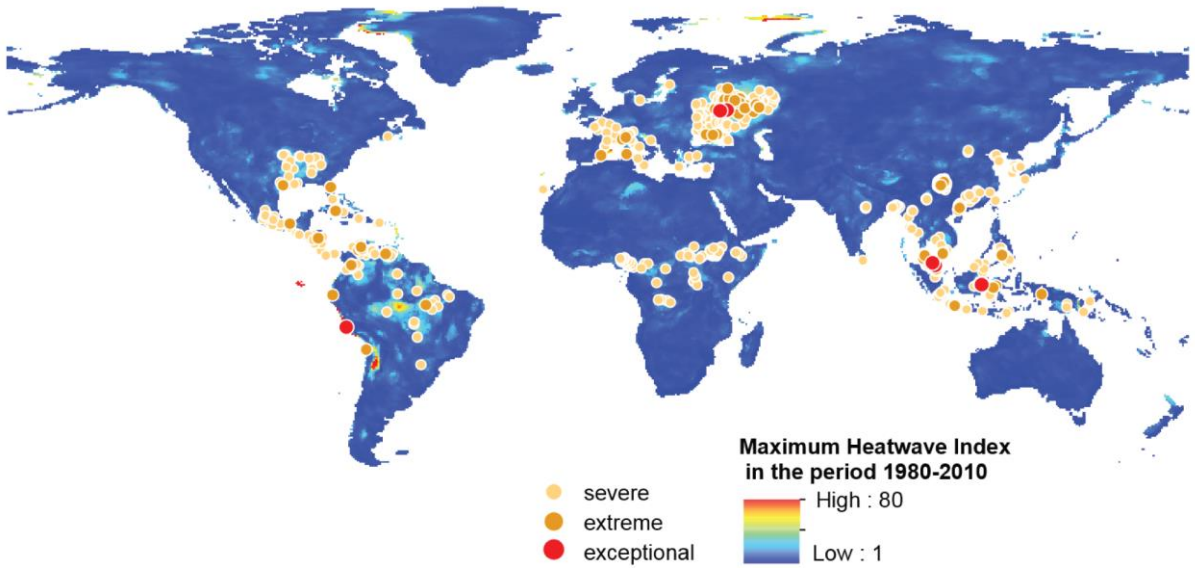

Figure 82 Maximum heatwave magnitude (HWMId) observed during 1980-2010

One of the most severe effects of global warming is the increase in the frequency and intensity of extreme events such as heatwaves[29]. The severe, extreme and exceptional heatwaves that occurred over the Balkans in 2007, France in 2003 or Russia in 2010 are associated with increased mortality and reduced labour productivity[30].

Figure 82 shows a global map of heat waves in urban centres based on the Heatwave Magnitude Index (HWMId). Russo et al. (2015)[31] designed the HWMId to take into account both heatwave duration and intensity. The Heatwave Magnitude Index was successfully applied to classify observed heatwaves that occurred globally in the period 1980-2010[32].

HWMId is defined as the maximum magnitude of the heatwaves occurring in a year, where a heatwave is defined as the periods of at least three consecutive days with maximum temperature above the calendar 90th percentile centreed on a 31 day window reference period. Yearly gridded data Heatwave Magnitude Index on a 0.5 x 0.5 degree grid were used in this analysis and classified as follows: HWMId levels of 20, 40 and 80 are considered as reference levels for severe, extreme and exceptional heatwaves, respectively.

The analysis at city level, allows assessing the number of cities in the world located in areas that suffered from severe (20<HWMId<40), extreme (40<HWMId<80) and exceptional (HWMId >80) heatwaves in the 30 years period and estimate the potentially affected population (Figure 83). A total of 385 cities located in Asia and 206 in Europe have suffered from either severe, extreme or exceptional heatwaves.

---

[29] Sonia I. Seneviratne et al., "Allowable CO2 Emissions Based on Regional and Impact-Related Climate Targets," *Nature* 529 (January 20, 2016): 477, https://doi.org/10.1038/nature16542.

[30] Alessandro Dosio et al., "Extreme Heat Waves under 1.5 °C and 2 °C Global Warming," *Environmental Research Letters* 13, no. 5 (May 1, 2018): 054006, https://doi.org/10.1088/1748-9326/aab827.

[31] Simone Russo, Jana Sillmann, and Erich M Fischer, "Top Ten European Heatwaves since 1950 and Their Occurrence in the Coming Decades," *Environmental Research Letters* 10, no. 12 (December 1, 2015): 124003, https://doi.org/10.1088/1748-9326/10/12/124003.

[32] Matteo Zampieri et al., "Global Assessment of Heat Wave Magnitudes from 1901 to 2010 and Implications for the River Discharge of the Alps," *Science of The Total Environment* 571 (November 2016): 1330–39, https://doi.org/10.1016/j.scitotenv.2016.07.008.

- The population in the cities affected by severe, extreme or exceptional heatwaves is estimated from the 2015 population data.
- Around 23% of the population in Europe and 7.43% of the population in Asian cities live in cities that suffered from heatwaves in the last 30 years.
- Lambayeque in Peru is the city that has experienced the highest number of heatwaves in the 30 years period (1980-2010) with a total of 7 heatwaves (HWMId > 20).
- Kota Bharu in Malaysia registered the second highest number of heatwaves with a total of 6 heatwaves.
- Trujillo also located in Peru has experienced a total of 5 heatwaves in the period 1980-2010

SEVERE	Africa	119
	Asia	348
	Europe	162
	LAC	171
	Northern America	32
	Oceania	4
EXTREME	Asia	33
	Europe	41
	LAC	14
	Northern America	2
EXCEPTIONAL	Asia	4
	Europe	3
	LAC	1

Number of urban centres per class of HWMId

SEVERE	Africa	16,858,147
	Asia	150,940,252
	Europe	42,123,493
	LAC	67,603,276
	Northern America	6,443,808
	Oceania	420,362
EXTREME	Asia	6,824,011
	Europe	22,985,025
	LAC	3738744
	Northern America	5,046,650
EXCEPTIONAL	Asia	1,624,108
	Europe	523,607
	LAC	164,203

Total population (2015) in urban centres per class of HWMId

Figure 83 Urban centres located in areas that suffered from severe (20<HWMId<40), extreme (40<HWMId<80) and exceptional (HWMId >80) heatwaves.

Key Messages

At the 21st Conference of the Parties in Paris (2015) governments committed to keep global warming to below 2°C above the pre-industrial levels, with the aim of limiting it to 1.5°C. Some of the most severe effects of global warming will be related to an increase in the frequency and intensity of heatwaves. The analysis of observed heatwaves during the period 1980-2010 in the cities across the globe shows that:

- Most of the cities that experiences severe, extreme or exceptional heatwaves are located in Asia and Europe.
- Europe (including Russia and Balkans) has the highest share of population living in cities that were affected by one or more heatwaves in the period 1980-2010.
- Peru is the country in that records the highest number of occurrence of heatwaves during the period 1980-2010.

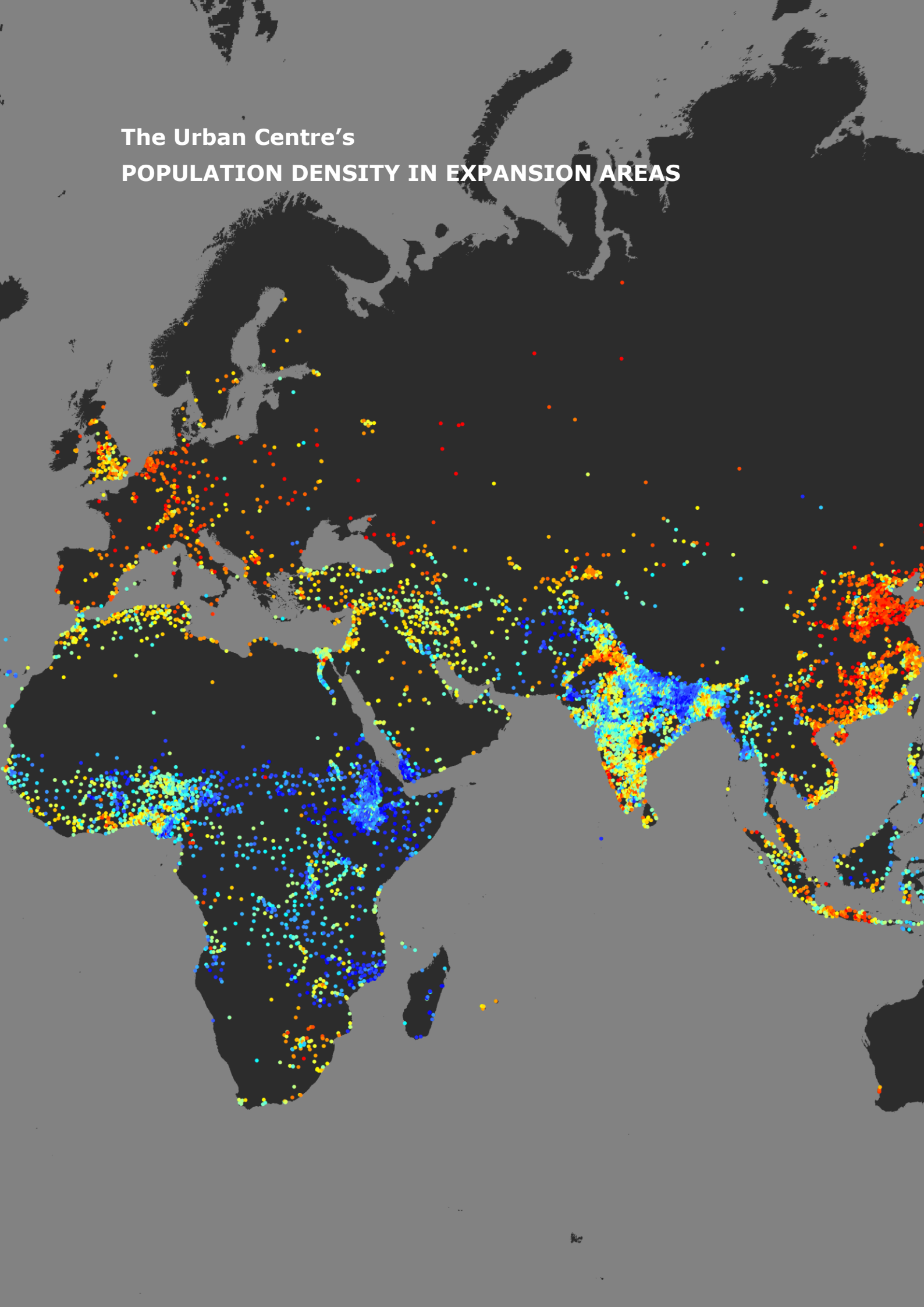
The Urban Centre's
POPULATION DENSITY IN EXPANSION AREAS

5.5 Sustainable Development Goals

With the unanimous adoption of the United Nations (UN) General Assembly resolution 70/1 "Transforming our World: the 2030 Agenda for Sustainable Development" Member States agreed upon a framework of 17 Sustainable Development Goals (SDG) to guide societal development. The action plan, building on the experience of the Millennium Development Goals intertwines aspirational goals with an ambitious monitoring framework composed of 169 targets to monitor progress made in meeting the SDGs. However, the capacity to monitor such progress is entangled by the lack of data and statistical capacity to support the monitoring framework (UN Statistical Commission, 2017). Alternative and innovative sources of data, especially derived Earth Observation (EO) offer significant information, and especially data to support the SDG reporting (Anderson et al., 2017; Paganini and Petiteville, 2018; G. A. United Nations, 2015).

According to the United Nations Department of Economic and Social Affairs, the human society is predominantly urban as more than half of global population lives in cities (UNDESA, 2008). The relevance of urban areas is also recognized in the 2030 Development Agenda, which devoted to urban areas a specific Goal, SDG 11 that aspires to "Make cities and human settlements inclusive, safe, resilient and sustainable". Many SDG 11 indicators require fine scale local data that are to be sourced locally, making it more difficult to reach adequate data availability – especially in countries in transitions and data-poor territories. Against this condition, remote sensing and EO are capable to collect information, at a large scale, at high degree of spatial resolution, repeatedly over time, and over wide geographical areas serving multiple applications (Donaldson and Storeygard, 2016; Zell et al., 2012), especially in the SDG framework ("Earth Observations in supports of the 2030 Agenda for Sustainable Development," 2017; Noort, 2017; Paganini and Petiteville, 2018), or for generic urban development indicators (Chrysoulakis et al., 2014).

The 232 individual indicators of the 2030 Development Agenda monitoring framework require local yet globally consistent, multi-temporal data. The GHSL maps human settlements and produces fine scale built-up areas and population density grids.

The GHS-UCDB integrates core GHSL information on built-up areas and population over time with additional information to characterise urban centres. The database can be applied in support the SDG framework. In the GHS-UCDB there is a specific attribute on the Land Use Efficiency Indicator SDG 11.3.1 of the urban centre between 1990 and 2015, and proxy indicators for SDG 11.7.1 on the share of open spaces available in the urban centre and the share of urban centre population living in areas with high presence of green. SDG 11.3.1 is classified by the Inter-Agency Expert Group on SDG Indicators as a Tier II indicator (meaning an indicator is conceptually clear and with a methodology for its monitoring, but for which data are not regularly produced or available). SDG 11.7.1 is instead classified as Tier III indicator, meaning "No internationally established methodology or standards are yet available for the indicator, but methodology/standards are being (or will be) developed or tested"[33].
For the estimation of the Land Use Efficiency indicator, we adopted the extent of built-up areas as the input data for land consumption, and population as input for demographic change, and applied the internationally agreed methodology[34]. To complement UN-Habitat reporting on SDG 11 at the High Level Political Forum in 2018 (United Nations 2018), the GHS-UCDB offers an analysis of the indicator for the circa 10,000 urban centres in section 5.5.1 and the baseline data in the GHS-UCDB open data. SDG 11.7.1 does not have an established monitoring framework, yet with GHS-UCDB data, it is possible to propose a characterisation of urban centres based on the presence of greenness (NDVI) and of open spaces. Section 5.5.2 presents two proxy indicators to estimate "Average share of the built-up area of cities that is open space"[35]. With remote

[33] https://unstats.un.org/sdgs/iaeg-sdgs/tier-classification/
[34] https://unstats.un.org/sdgs/metadata/files/Metadata-11-03-01.pdf
[35] https://unstats.un.org/sdgs/metadata/files/Metadata-11-07-01.pdf

sensing it is however not possible to fully align with the aspirations of the indicator formulation, that adds a disaggregation "for public use for all, by sex, age and persons with disabilities". Therefore, the proposed estimates may be regarded as proxies to support the ongoing discussion for a viable method to monitor this indicator.

Figure 84 © Adobe Stock, 2018

5.5.1 Land Use Efficiency –SDG 11.3.1

Less than half the urban centres in the globe use land more efficiently than in the past

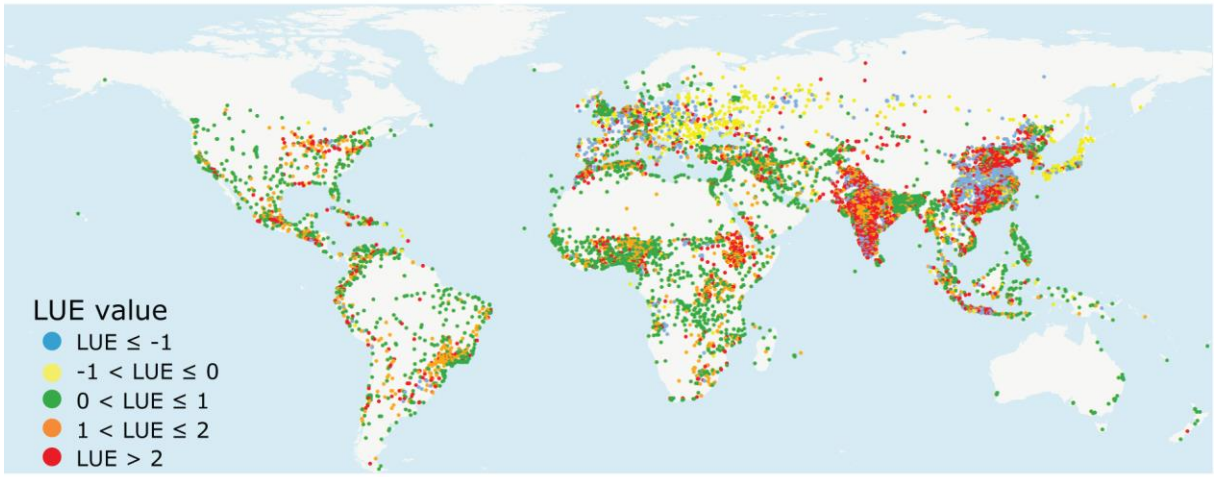

Figure 85 LUE value corresponding to the dynamics of population change and built-up areas expansion in the period 1990-2015 for 10,000 urban centres in the GHSL UCDB

Land Use Efficiency (LUE) is the indicator internationally agreed to monitor the "ratio of land consumption growth rate to population growth rate" in the framework of SDG 11[36]. The indicator estimates the interdependence between spatial expansion of urban centres and demographic change that takes place in them. In the GHS-UCDB the LUE indicator is computed measuring the expansion of the built-up areas in each urban centre between 1990 and 2015, and the changes in population counts in the same period. GHS-UCDB data offers an opportunity to support the SDG 11.3.1 with a baseline information. At present, the indicator is a Tier II one (as a globally agreed methodology to estimate it exists, but data are not regularly produced).

Over the last 25 years, in almost 40% of the centres the rate of demographic growth has been greater than the one of spatial expansion. In these centres, more than half the ones in Africa, Latin and Northern America, the land consumed by each new settled inhabitant has been lower than the built-up areas per capita available to residents in 1990. These urban centres have increased their population density and the areas of expansion and achieved an abstract population density that is higher compared to the city that existed in 1990. The LUE value in these centres is between 0 and 1 (in green in Figure 85). In more than 40% of urban centres the rate of spatial expansion has been greater than that of population, in 20% LUE value has been between 1 and 2 (displayed in orange), and in ¼ of the centres the spatial expansion occurred at rates more than double the one of population growth (in red). In the remaining 18% of the sample, the LUE value is negative corresponding to spatial expansion and demographic decline.

Geographical clusters of LUE can be observed: substantial concentration of negative LUE values (where population declines and built-up areas expand) emerges in central China and central Europe (LUE<-1), Eastern Europe, Russia and Japan (LUE between 0 and 1). In Macedonia and Poland more than half of the urban centres developed with a corresponding LUE<-2, the same LUE value is computed in up to ¼ the centres in countries including: Belgium, France, Bosnia and Herzegovina, Armenia, Puerto Rico, Slovakia, Taiwan, China, Thailand, Italy, Denmark, and Jamaica. In more than 1/3 of the centres in China, India, Sri Lanka, Ethiopia urban centres expanded in space at least twice as fast as they have grown in population (LUE>2).

[36] https://unstats.un.org/sdgs/metadata/files/Metadata-11-03-01.pdf

The land consumed by each new inhabitant in urban centres is very diverse across urban centres. Grouping them by income class, in more than 90% of the centres in LIC and in 70% in LMIC each new inhabitants consumes less than 50 m^2 of land. For each new inhabitant in 1/3 of the urban centres in HIC between 50 and 150 m^2 are consumed. As global average 15,800 people are settled in each km^2 of urban centres expansion. This global value is very diverse across regions. It is almost three times higher in centres in Africa, where with each km^2 of urban expansion more than 40,000 people are accommodated. In centres in Northern America and Europe each km^2 of urban expansion would host less than approx. 3,000 people. Making the example of the two America regions, we report about a development dynamic that the LUE indicator is not capable to capture. The LUE is 0.9 and 0.8 respectively in Latin America and the Caribbean and Northern America. By LUE definition, the value results into higher efficiency in urban centres expansion in Northern America (LUE close above 0 and below 1). However, the abstract population density in areas of expansion, in Northern America is equivalent to 2,870 people settled per each km^2 of land expansion of an urban centre. In Latin America and the Caribbean, for each km^2 of land expansion of an urban centre, 15,000 people were potentially settled. Indeed, the values generated through this metrics is reflected in the total land consumption in the regions, where for the almost 38 million new urban centres inhabitants in Northern America, an overall 13,200 km^2 of land was consumed. In Latin America, urban centres have expanded by 7,000 km^2 to accommodate 105 million people in total.

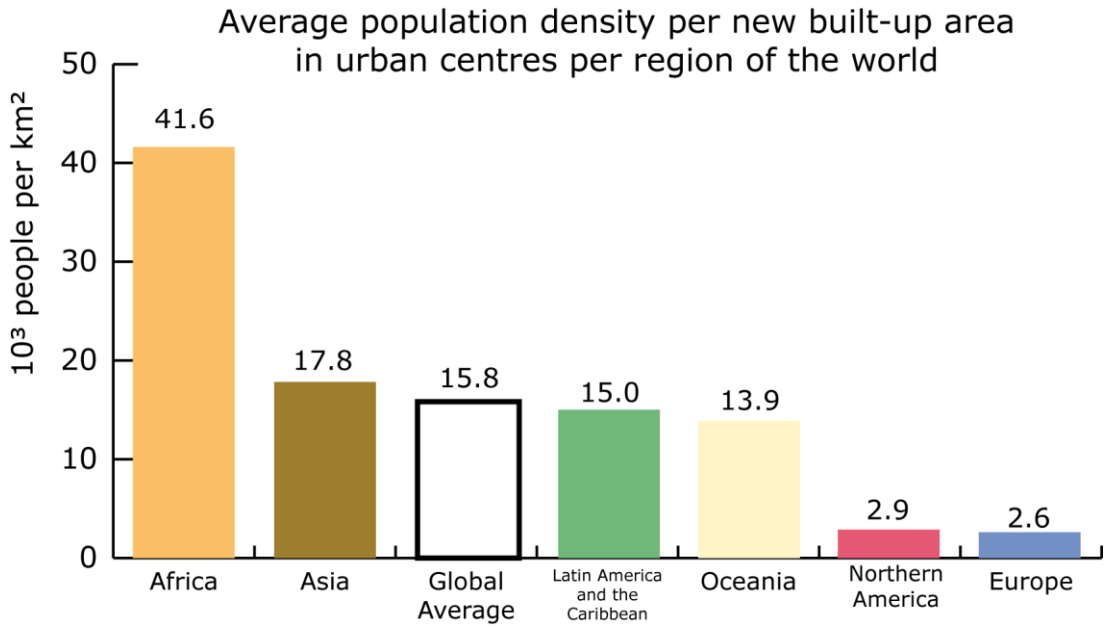

Figure 86 comparison of population density in areas of urban centres expansion between 1990 and 2015 per region of the world

Key Messages

- With GHS-UCDB data it is possible to estimate the Land Use indicator, potentially lifting it from its Tier II classification;
- More than half of the urban centres in the globe use land less efficiently than in the past;
- The present internationally agreed LUE formulation is substantially subject to path dependency in quantifying the efficiency of new development anchoring it to past trajectories;
- The LUE value (dimensionless) can be assisted by proxy measures like the population density per unit of spatial expansion that more closely capture the characteristics of the socio-spatial development.

5.5.2 Access to Green – SDG 11.7.1

Proxies for Tier III indicators

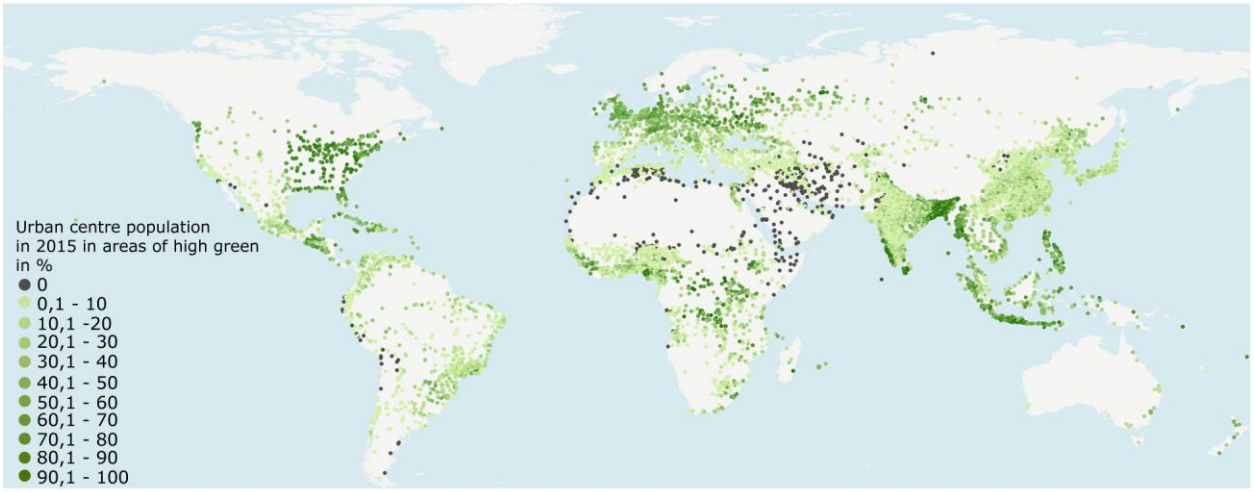

Figure 87 classification of urban centres according to the share of 2015 population with generalized access to green areas

5.5.2.1 Access to green spaces

Green spaces have many functions that can moderate the climate change impact and help prevent disease and thus alleviate public health expenses in a context of aging societies (Ngom et al., 2016). The World Health Organization (WHO) suggests that green spaces with a minimum size of one ha and a maximum distance of 300 m to people's residence should be used as threshold values for accessibility (Annerstedt van den Bosch et al., 2016). The European Environment Agency (Stanners et al., 1995) recommends that people should have access to green spaces within 15 min. walking distance (that is 1.61 km considering an average walking speed). Despite this average, access to urban green spaces is not sufficient, because the spatial distribution may result in a significant bias towards certain locations and hence social groups (Le Texier et al., 2018). Besides, many researchers now argue on the appropriate walking distance to consider for a global scale analysis. Until today, there is still no methodological consensus about how access to conceptualize and measure the provision of urban green spaces and its access.

In this chapter, access to green spaces is measured using a proxy metric, "generalised potential access to green areas", which is based on the calculation of the amount of people living in high green surfaces at the generalisation scale of the spatial data used for the assessment. If this space is actually accessible (i.e. not fenced) for the public cannot be answered. The metric builds on the greenness metric derived from remote sensing Landsat imagery and described in details in section 5.3.1 (p.80) and in (Corbane et al., 2018b). The methodology for calculating access to green spaces in 2015 consists in two main steps:

1) The continuous greenness values extracted form satellite data for period 2015 (with 0 corresponding to low green spaces and 1 corresponding to high green spaces) are further classified into three classes as follows:
    - Low green for greenness < 0.1 : corresponding to barren rock, sand or snow or impervious surfaces (e.g. built-up areas)
    - Medium green for 0.2 <Greenness <0.5: corresponding to shrubs or agriculture
    - High green for 0.6 <Greenness < 0.9: corresponding to dense vegetation (e.g. forest, private gardens, etc.).

2) The share of people living in High Green areas is calculated using the GHS-POP for 2015 per each urban centre of the urban centres database.

Figure 87 shows the estimated share of people in 2015 living in High Green areas (areas where the greenness value is greater than 0.6). The percentages refer to the share of people with generalised access to high greenness value areas with respect to the total number of people living in the urban centre. We can observe the following:

- High concentration of cities with large share of people with access to urban green spaces on the Eastern coast of the United States, Northern Europe, India, Bangladesh as well as Indonesia.
- Cities with very low share of people with access to urban green spaces are mainly located around the Mediterranean sea, in desert areas (e.g. in Africa), western coast of North America, in Latin America and China.
- The patterns of population access to urban green spaces may be related to climate zones, patterns in precipitations and temperatures but also to the characteristics of the urban centres in terms of density of population and total area of the urban centre.

Globally, the presence of green areas drops as the density of built-up surface exceed one fifth of their area. Half of the cities where less than one third of their area is built-up have the majority of their surface characterized by high presence of green.

Figure 88 shows some examples of the continuous greenness values in the built-up areas derived from Landsat NDVI composites. The greenness values are shown here for the time interval centred on 2014 and the six selected cities are displayed here at the same scale and for comparable map extents. The results reflect the variability across cities with each city having varying magnitudes and spatial distribution of greenness. In particular, the assessment of greenness within the built-up areas of Lagos (Nigeria) with a population of 1.7 million people and Minneapolis (United States of America) with about 0.5 million people, highlights strong differences in the structure and patterns of green vegetation in the two cities. In Minneapolis, pixels with high greenness values are abundant and located inside the built-up area of the urban centre. Whereas in Lagos, the high greenness values are observed in the fringes of the built-up area and the centre of the city is mostly dominated by very low greenness values. Not only there are differences in the values of greenness between the two cities, but also the spatial arrangement of the green spaces is quite different. While green spaces are equally spread in the built-up area of Minneapolis city, the pattern is more compact in Lagos.

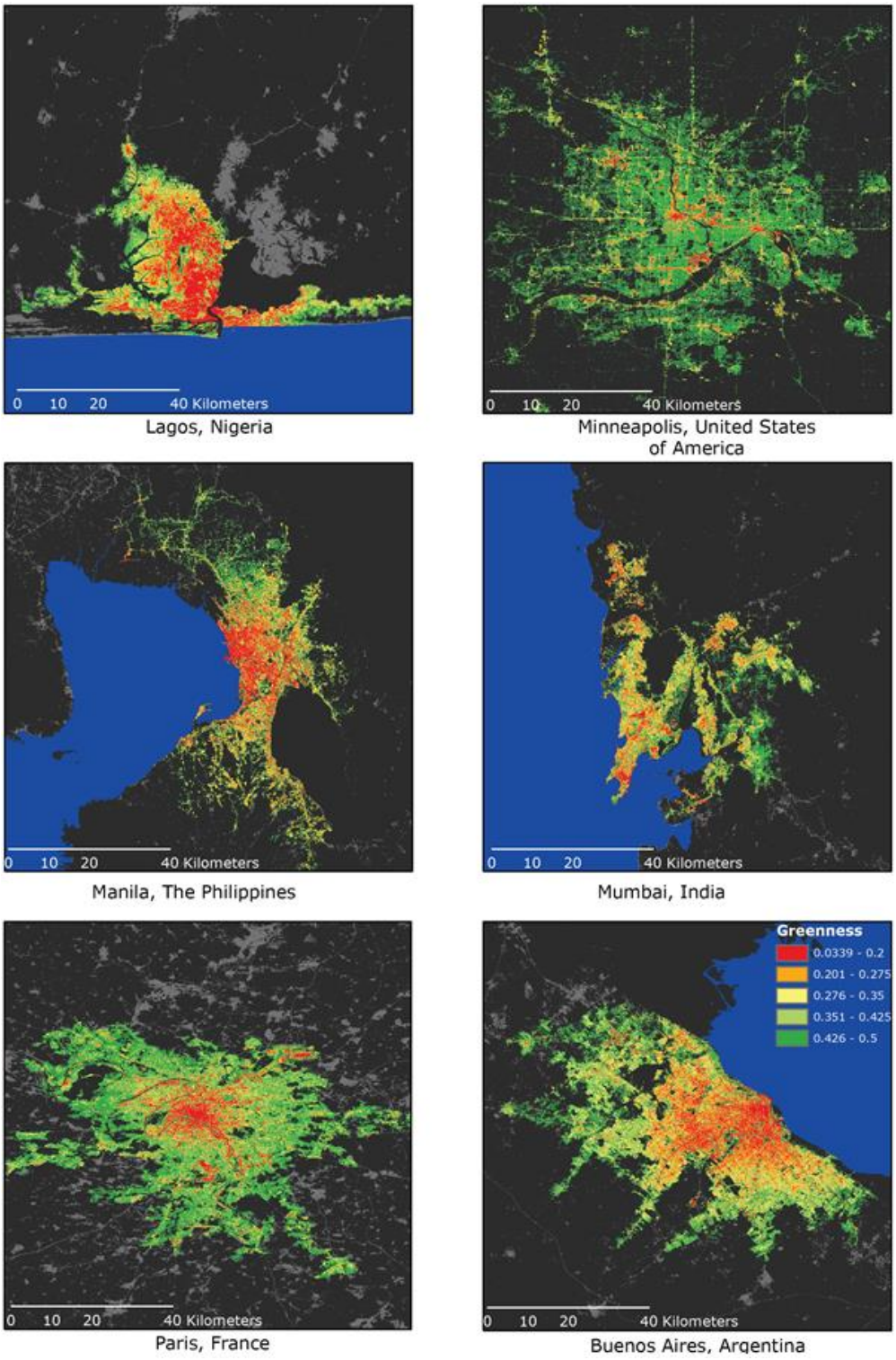

Figure 88. Greeness values in the built-up (period 2015) derived from Landsat NDVI composites in the urban centres of Minneapolis, Lagos, Manila, Mumbai, Paris and Buenos Aires. The maps are shown at the same scale and cover the same extent (from Corbane et al., 2018)

In Figure 89, the average share of population with generalised access to high green surfaces in 2015 is disaggregated per continent. It reflects the differences observed in Figure 88 at the city level:

- With a global generalised access to green spaces of 25.8%, Northern American cities have the highest share of population living in high green areas (50.6%), followed by Europe (36.1%) and Oceania (30.3%).
- Latin America has the lowest average population generalised access to high green areas (17.8%) but also the lowest variability in the values.
- Africa and Asia have close values of average population generalised access to high green areas with 22.2% and 25% respectively.

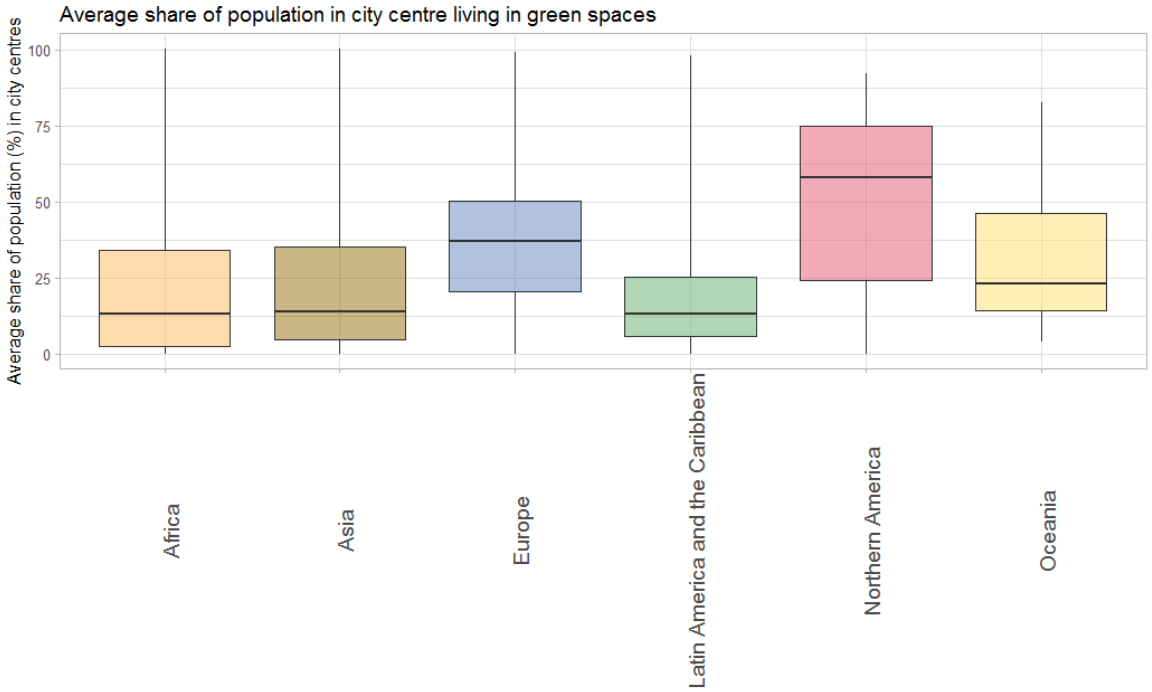

Figure 89. Breakdown of the average share of people exposed to high green spaces by continent

5.5.2.2 Access to open spaces

Open spaces can be of different nature and may include beaches, parks, playing fields and also green spaces. The landscape of urban open spaces can range from playing fields to highly maintained environments to relatively natural landscapes. One definition holds that, "As the counterpart of development, urban open space is a natural and cultural resource, synonymous with neither 'unused land' nor 'park and recreation areas." Another is "Open space is land and/or water area with its surface open to the sky, consciously acquired or publicly regulated to serve conservation and urban shaping function in addition to providing recreational opportunities. (Myers, 1975) " In almost all instances, the space referred to by the term is, in fact, **green space**. However, there are examples of open space which, though not green (e.g. beaches) that are still considered as open spaces.

Owing to the variety of types of open spaces, we measured the surface of open spaces within urban centres as the union of the areas of non-built-up surfaces and high green surfaces. The principle is illustrated in Figure 90 for the city centre of Paris with the area of non-built-up surfaces shown in grey in Figure 90-a, the area of High Green surfaces shown in green in Figure 90-b and the proxy area of open spaces shown in red in Figure 90-c.

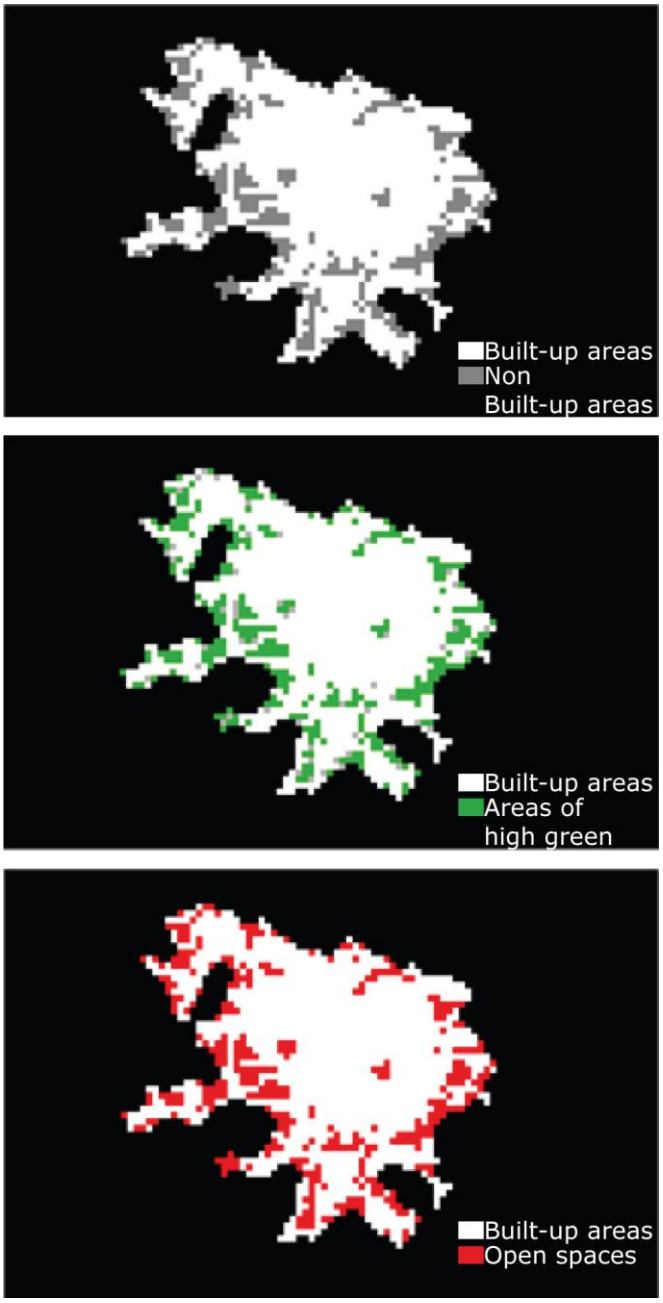

Figure 90. Illustration of the method used to estimate the area of open spaces based on areas of non-built-up surfaces and high green surfaces within the urban centre of Paris.

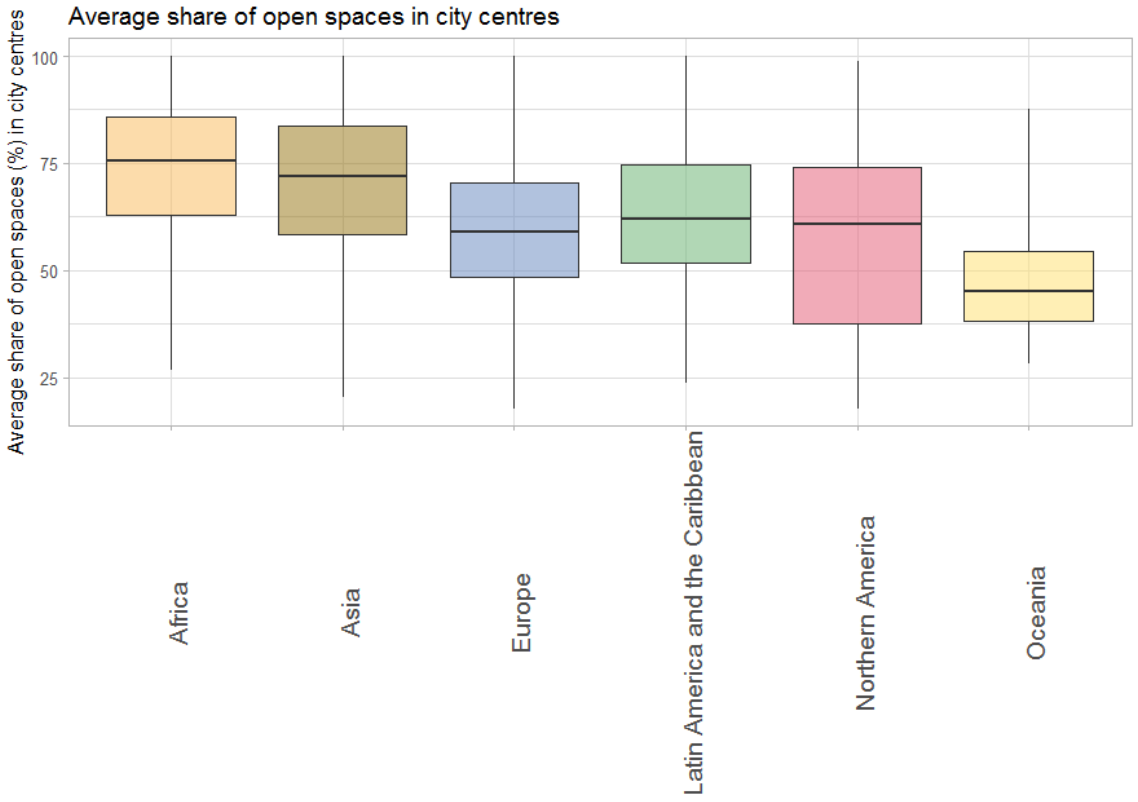

Figure 91. Average share of open spaces in urban centres by continent (reference year 2015).

Figure 91 presents the average share of open spaces in urban centres estimated according to the method illustrated in Figure 90. The highest shares of open spaces (greater than 70%) are observed in African and Asian cities. Latin America, Europe, and Northern America have similar shares of open spaces (around 60%). Cities located in Oceania show the lowest share of open spaces (48%).

Table 9.Summary table on average share of population living in areas of high green (%) and average share of open spaces (%) together with the average land area of the urban centres (km^2)

	Average share of population living in areas of high green (%)	Average share of open spaces (%)	Average urban centre area (km^2)
Africa	22.2	74.4	31.5
Asia	25.1	70.6	52.8
Europe	36.1	60.1	75.1
Latin America and the Caribbean	17.8	63.9	55.8
Northern America	50.6	56.8	272.7
Oceania	30.3	48.5	151.7
Global Average	**25.8**	**68.5**	**59.1**

The summary Table 9 includes the results on the access to green and to open spaces per continent together with the mean areas of urban centres. It highlights the following main findings:

- North American urban centres are the largest in the world in terms of land area; they have the highest shares of population generalised access to green spaces but a low average share of open spaces compared to the global average of 68.5%.
- While African cities are the smallest in terms of land area, they have the highest share of open spaces that does not necessarily correspond to green spaces since the share of people with access to green spaces is among the lowest in the world (below the global average of 25.8%).

Key Messages

Green spaces and in general public open spaces are vital to urban communities and should be prioritized in urban policy. Provision and access to safe and quality green spaces and open spaces are key strategies for achieving sustainable development. While there is no consensus on how to measure and report on the availability and access to open and green spaces, we propose here two metrics derived from remote sensing data namely, the greenness and the built-up layer from GHS-BU. The main findings can be summarized in the following:

- At the measured scale of 1km^2, Northern American cities have the highest share of population living in high green areas (50.6% of urban population) but have paradoxically a low share of open spaces (58.8%) compared to the cities located in other regions of the world.
- African cities have the lowest share of people living in high green areas (22% of urban population) but the highest average share of open spaces (74%) that may not be necessarily maintained or public spaces.
- Different factors play a role in the uneven accessibility to open and green spaces: regional climate conditions, topographic factors and vegetation types. Urban planning policies are likely to have significant influence on urban green spaces as well as morphology of the cities, their population, and their built-up areas. To get a better understanding of the regional disparities in access to green and open spaces, not only the aforementioned factors should be analyzed but also the quality of green spaces and categories of open spaces must be also taken into consideration for more informed decisions and inclusive policies.


The Urban Centres
ACROSS BORDERS

6 GHSL Applications

This section aims at illustrating some applications of GHSL data for research and/or policy, and its usefulness in expanding knowledge in different domains and at different scales.

6.1 Accessibility

A team led by the University of Oxford (Weiss et al., 2018) have used the universe of 13,840 urban centres (i.e. high density clusters, HDC) as mapped by GHS-SMOD released in 2016 to develop a map that quantifies travel time to these cities for 2015 at a spatial resolution of approximately one kilometre. This was done by integrating ten global-scale surfaces that characterize factors affecting human movement rates. The aim was to assess inequalities in accessibility to cities in 2015.

The results show differences in accessibility relative to wealth, as only 51% of the population living in low-income countries (concentrated in sub-Saharan Africa) reside within an hour of a city compared to 91% of people in high-income settings. The Global map of travel time to cities and the friction surface can be used for any application that requires consideration of travel time and is available at:

https://map.ox.ac.uk/research-project/accessibility_to_cities/

Reference: Weiss, D.J., Nelson, A., Gibson, H.S., Temperley, W., Peedell, S., Lieber, A., Hancher, M.,Poyart, E., Belchior, S., Fullman, N. and Mappin, B., 2018. A global map of travel time to cities to assess inequalities in accessibility in 2015. Nature, 553(7688), 333.

6.2 Estimating Carbon Footprints for 13,000 Cities

Moral et al. (2018) have built on GHSL data (settlements and population grid, R2016 and R2015) to estimate carbon footprint for cities and urban areas by creating a Gridded Global Model of City Footprints (GGMCF).

Urban and rural areas from GHS-SMOD were used to distribute the total urban and rural footprint on the basis of the share of aggregate purchasing power in each cell. High density clusters (HDC) were used to estimate the carbon footprints for each of the 13,844 cities mapped by GHSL. Per-city GDP (gross domestic product) was calculated by applying the GHS-SMOD city boundaries to the G-Econ 4.0 global gridded model of GDP. The GHS population grid for 2015 at 250m was used to determine the aggregate purchasing power per grid cell, by multiplying the population in the cell by the mean purchasing power at that location.

Results reveal that a relatively few number of urban areas account for a disproportionate share of the world's carbon footprint. The emissions are concentrated in a small number of cities, with the highest emitting 100 urban areas accounting for 18% of the global carbon footprint (while containing 11% of population).

Reference: Moran, Daniel, Keiichiro Kanemoto, Magnus Jiborn, Richard Wood, Johannes Többen, and Karen C Seto. 2018. "Carbon Footprints of 13 000 Cities." Environmental Research Letters 13 (6): 064041. https://doi.org/10.1088/1748-9326/aac72a.

6.3 Economic Survey of India

The Economic Division of the Ministry of Finance of India has used data from GHSL, within the Economic Survey of India (2017). GHSL is used to look at how built-up areas show the evolution of human settlements across India since 1975.

Both data on High Density Clusters from GHS-SMOD and built-up areas from GHS-BU are considered to map built-up areas in India and to characterize its degree of urbanization. The report acknowledges that GHSL data allows "to go into much greater level of spatial

detail with this data to uncover important insights for promulgating expeditious public policy at centre, state and urban local body level".

Reference: Government of India, Department of Economic Affairs of the Ministry of Finance, 2017. Economic Survey 2016-2017, vol.2, 458pp.

6.4 Functional Urban Area

OECD and JRC have used GHSL data (settlements and population grid, R2016 and CR2018) to map and analyse the extent of urban economic agglomerations – or functional urban areas (FUAs) – globally.

A new model was developed and trained with the previously existing set of FUAs in 31 countries based on commuting/official statistics. Building on the EC-OECD definition of FUAs, which are composed of urban cores with at least 50,000 people surrounded by interconnected commuting zones, FUAs were mapped for all 13,000 urban centres from GHS-SMOD and the GHS population grid for 2015 was used both in the model and to quantify results.

This work allows assessing worldwide basic patterns of suburbanisation, for the first time. Results indicate that around 54% of the world population live in urban agglomerations (FUA), out of which 12% live in their commuting zones, and that both these shares increase with level of development.

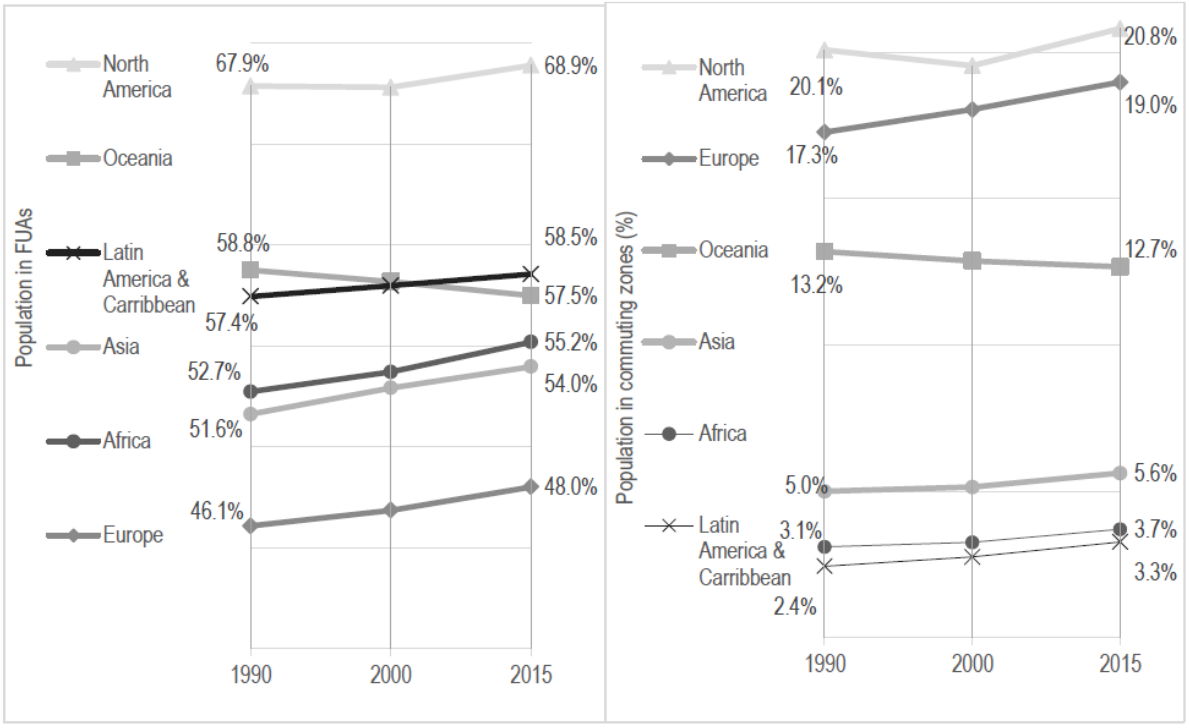

Figure 92 Population in FUAs and Commuting zones by world region, 1990-2015. Source: Moreno-Monroy et al., 2018

The global map of FUAs will soon be made available open and free, and can be used for any application that requires consideration of the extent of functional or economic agglomeration of a city, or of a city and its commuting zone.

Reference: A. Moreno-Monroy, Schiavina M., and Veneri, P., 2018. Urban economic agglomerations and their suburbanization patterns. A global analysis. *Journal of Urban Economics* (submitted).

6.5 Sentinel 1 RGB Mosaic

Copernicus is the European Union's Earth Observation Programme, looking at our planet and its environment for the ultimate benefit of all European citizens[37]. It offers information services based on satellite Earth Observation and in situ (non-space) data. The Programme is coordinated and managed by the European Commission. It is implemented in partnership with the Member States, the European Space Agency (ESA), the European Organisation for the Exploitation of Meteorological Satellites (EUMETSAT), the European Centre for Medium-Range Weather Forecasts (ECMWF), EU Agencies and Mercator Océan. Vast amounts of global data from satellites and from ground-based, airborne and seaborne measurement systems are being used to provide information to help service providers, public authorities and other international organisations improve the quality of life for the citizens of Europe. The information services provided are freely and openly accessible to its users.

Sentinel-1 is the first of the Copernicus Programme satellite constellation conducted by the European Space Agency[38]. This space mission is composed of two satellites, Sentinel-1A and Sentinel-1B, that carry a C-band synthetic-aperture radar instrument which provides a collection of data in all-weather, day or night. The first satellite, Sentinel-1A, was launched on 3 April 2014, and Sentinel-1B was launched on 25 April 2016. Both satellites lifted off from the same location in Kourou, French Guiana, and each on a Soyuz rocket.

The Sentinel-1 imagery data supports the automatic recognition of built-up surfaces in the GHSL baseline data as accounted in the present Atlas (Corbane et al., 2017b).

A *terapixel* global mosaic of Copernicus Sentinel-1 data[39] at about 20m spatial resolution and covering most the land mass has been created on the JRC Earth Observation Data and Processing Platform (JEODPP[40]) in collaboration with the JRC GHSL team. The mosaic it is made by level-1 ground range detected Sentinel-1 (A and B) image products with dual polarisation (VV+VH or HH+HV), covering the entire globe and represented as a false colour RGB composition. The scope of this mosaic is to provide a global base layer for visual assessment of natural and man-made features such as built-up areas (Syrris et al., 2018).

The examples included in this section have been selected from the Sentinel-1 global mosaic produced by the JRC. The purpose of this collection is to display – as seen from the Sentinel-1 sensors - the complex human interactions on the Planet Earth including physical, biological, cultural, economic and socio-political factors contributing to shape the anthroposphere.

[37] https://www.copernicus.eu/
[38] https://sentinel.esa.int/web/sentinel/missions/sentinel-1
[39] http://data.jrc.ec.europa.eu/document/jrc-bigdataeoss-s1-mosaic_2018_11_30_15_33.pdf
[40] https://cidportal.jrc.ec.europa.eu/services/webview/jeodpp/databrowser/?default=jeodppS1Mosaic2016


Singapore
The city state
1°12'54.45"N
103°52'24.18"E

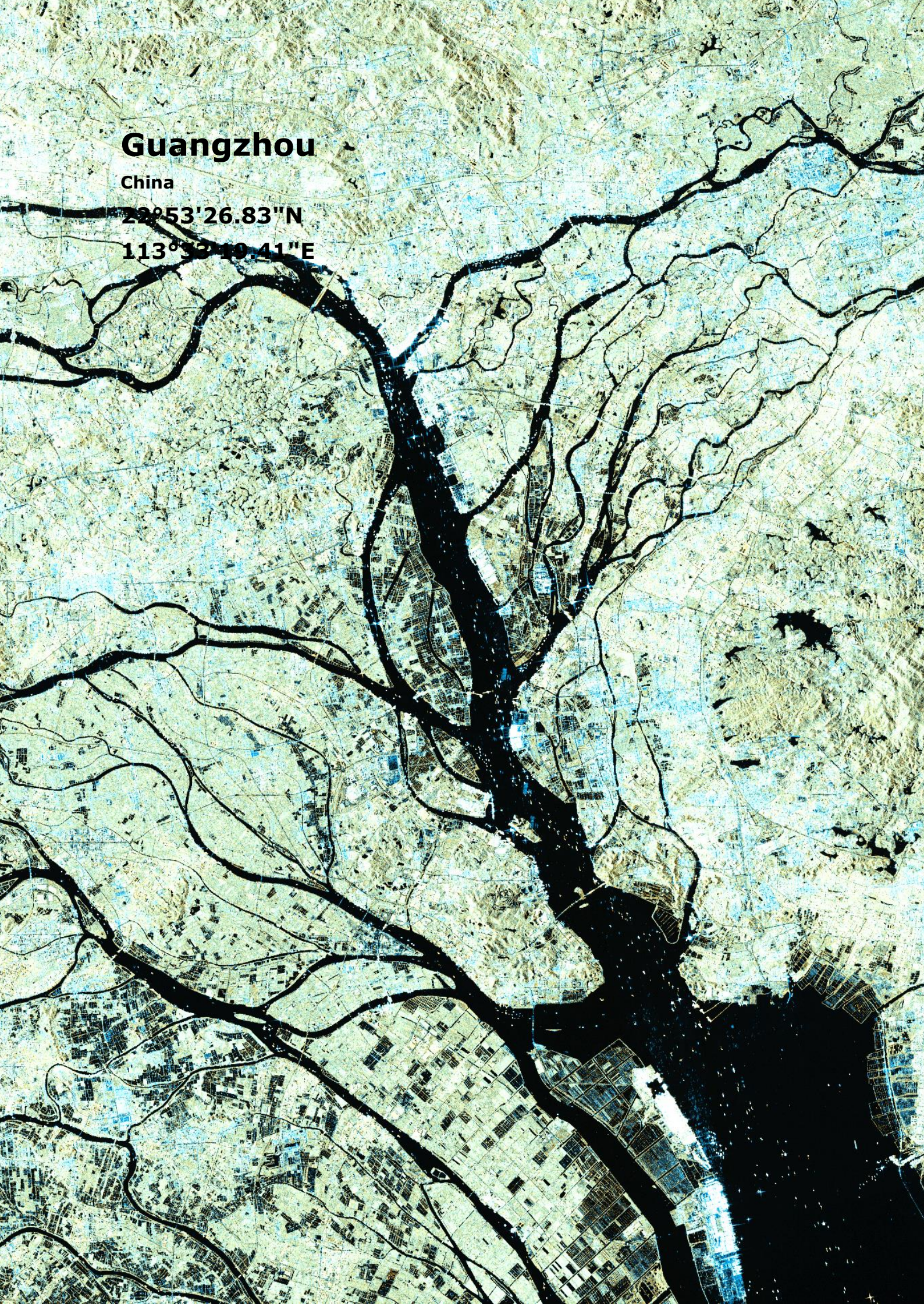
Guangzhou
China
22°53'26.83"N
113°32'10.41"E

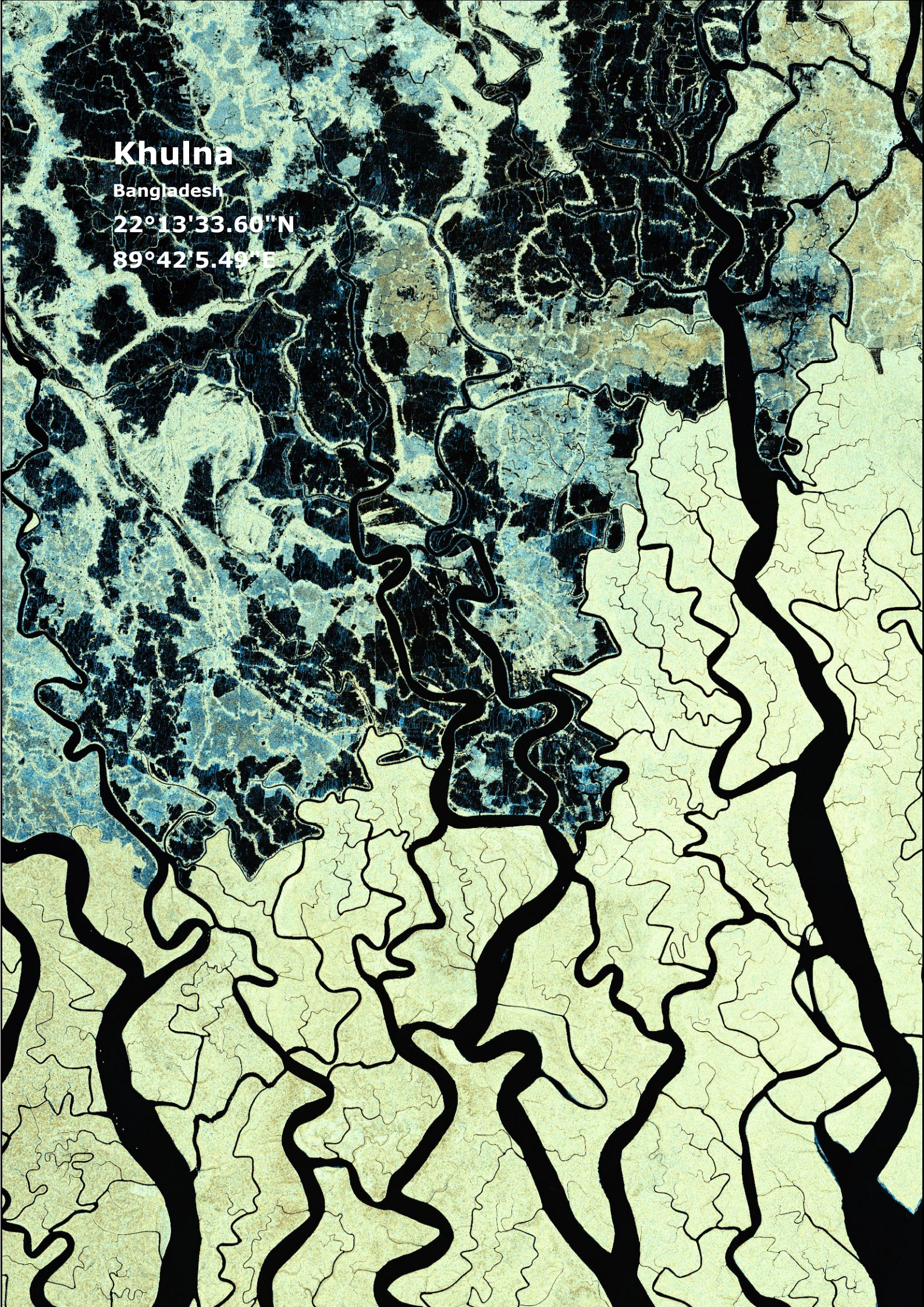
Khulna
Bangladesh
22°13'33.60"N
89°42'5.49" E

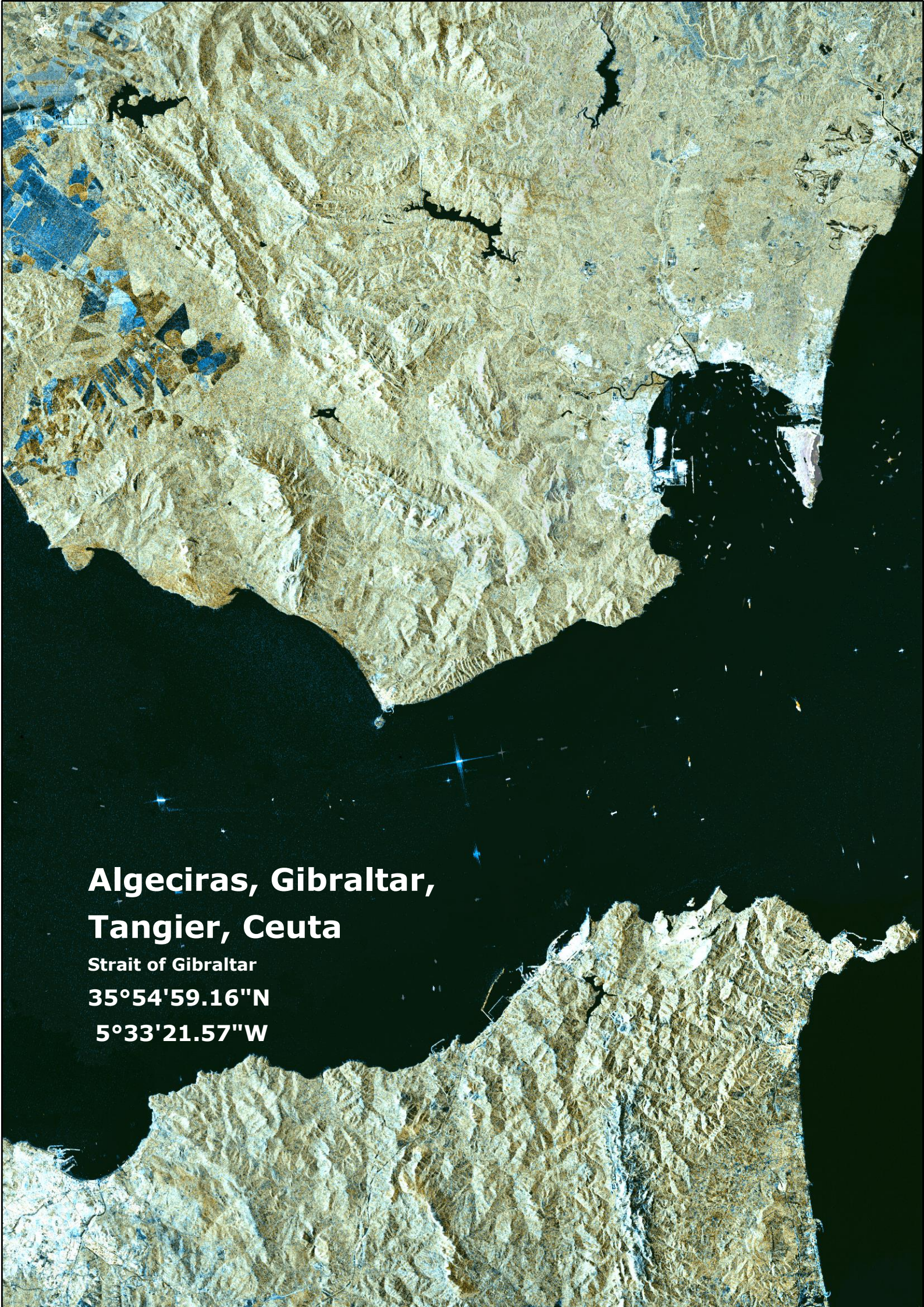
Algeciras, Gibraltar,
Tangier, Ceuta
Strait of Gibraltar
35°54'59.16"N
5°33'21.57"W

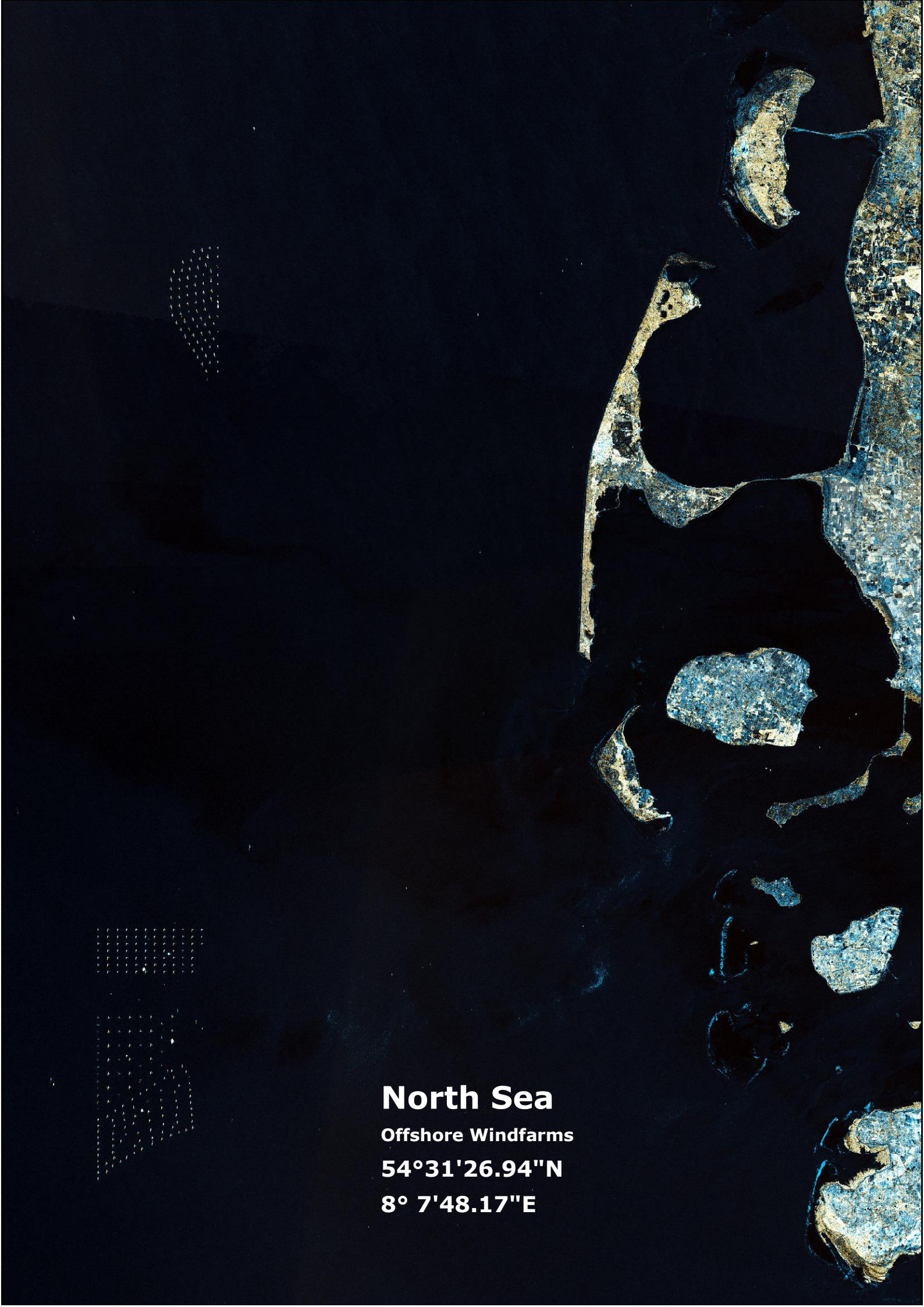
North Sea
Offshore Windfarms
54°31'26.94"N
8° 7'48.17"E


Mississipi
United States
29°17'40.97"N
89°22'0.89"W

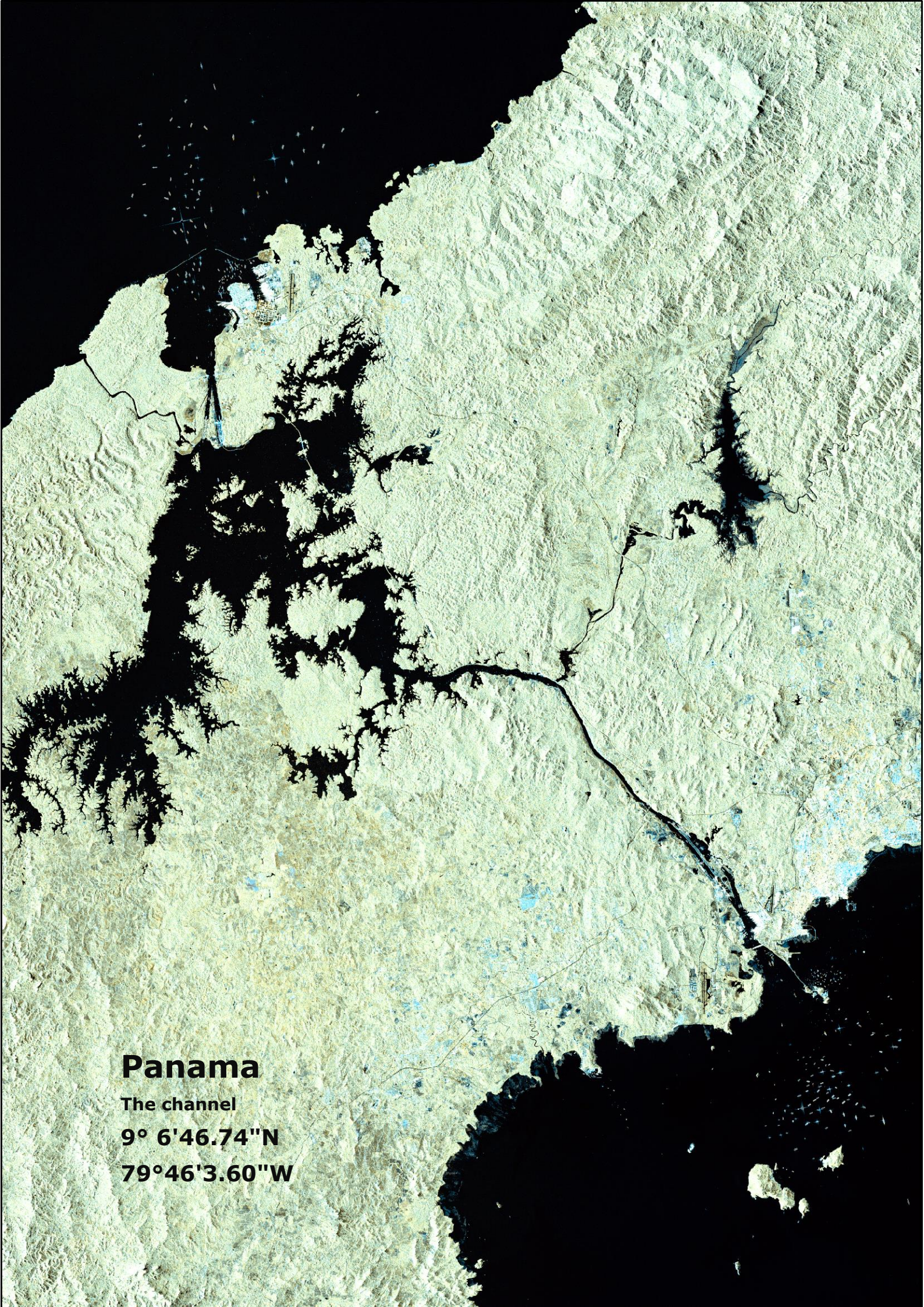
Panama
The channel
9° 6'46.74"N
79°46'3.60"W


Tierra del Fuego
Ushuaia, Argentina
54°49'44.00"S
68°17'28.30"W

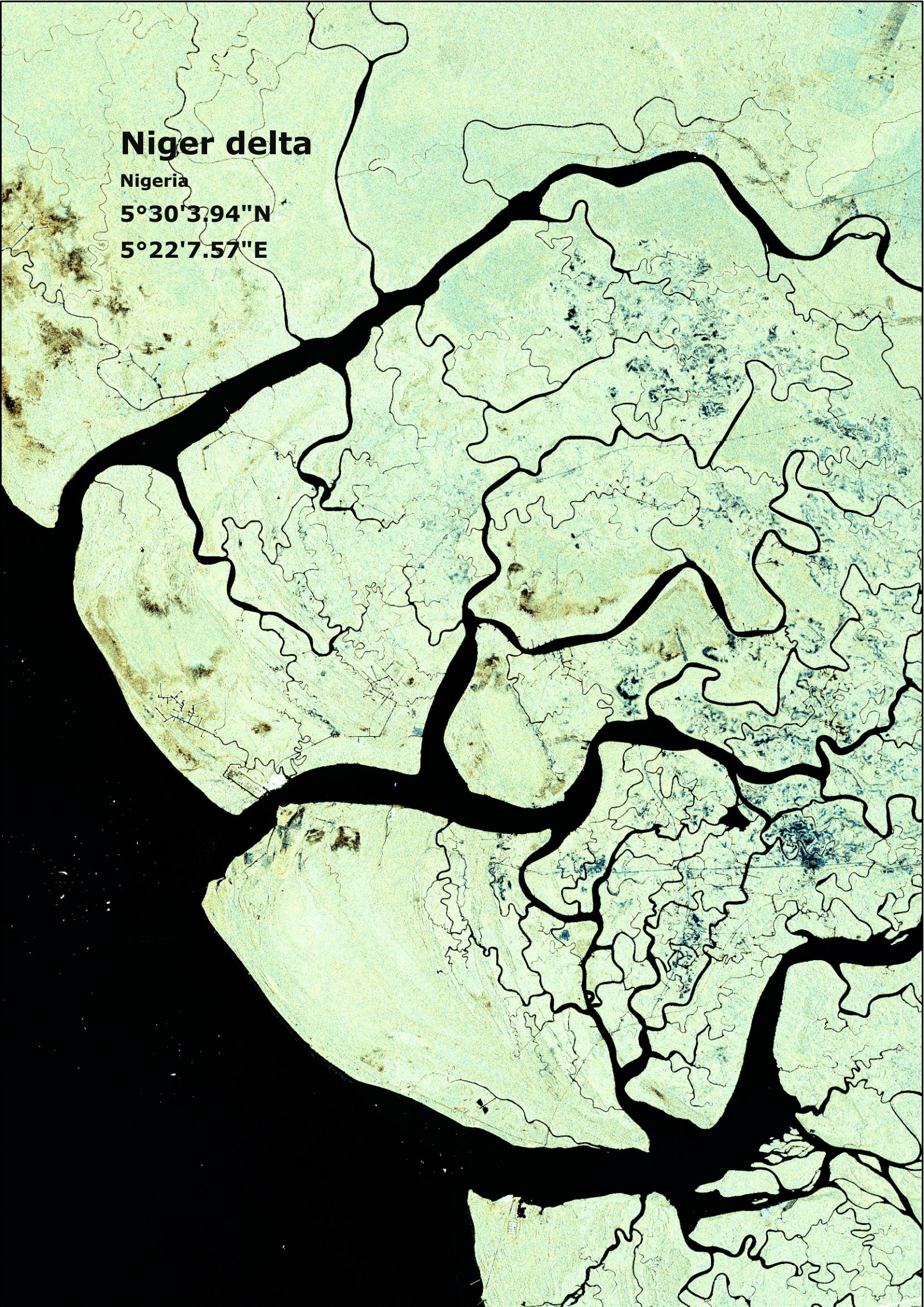
Niger delta
Nigeria
5°30'3.94"N
5°22'7.57"E


Longyarbyen
Svalbard, Norway
78°13'6.03"N
15°39'4.14"E
7.0

7 Conclusion

We live in a world of cities. The urban areas are today home to more than half of the world's seven billion people and their share will increase for years to come. Yet, before this Atlas, it was impossible to assess the whole number of cities existing in the planet Earth in a harmonised, comparable way. Countries use their own definition. These definitions vary from few hundred people in smaller, less urbanised countries, up to 100,000 inhabitants, as in China. The amalgamation of the spatio-temporal GHSL data on population and built-up areas allowed testing and demonstrating the concept of the Degree of Urbanisation developed in the European and the OECD context to the whole Planet. This led to the voluntary commitment at the Habitat III conference in Quito in October 2016 to the develop a global, harmonised definition of cities and settlements that is now supported by mayor international stakeholders, including the European Commission (REGIO, EUROSTAT, JRC), the OECD, the World Bank, the FAO, and UN-Habitat.

The GHSL settlement model (GHS-SMOD), porting the Degree of Urbanization concept in the GHSL data ecosystem, is the baseline for the delineation of the urban centres that are assessed in this Atlas. The Urban Centre Database is the first global dataset on cities derived from an explicit universal definition of "what is a city" that is based on measurable facts, and that is expanding considerably the universe of cities described by open data before today. The database combines basic information as city location and name with the city extent (surface, shape), and describes each city with a set of geographical, socio-economic and environmental attributes, many of them going back 25 or even 40 years in time. It is important to note that the urban centre extent is data-driven and does not take administrative borders into account – neither at the municipal level nor at country borders. In fact, there are a number of cross-border cities that are described as one unit for the purpose of this Atlas (the database denotes clearly the countries sharing these urban centres).

The Atlas of the Human Planet 2018 contributes directly to the joint voluntary commitment (UN Habitat III 2016) to develop a global, people-based definition of cities and settlements. Such a definition is essential for the monitoring of progress in achieving the goals of the 2030 Agenda for sustainable Development; several of the indicators linked to this goal are highly sensitive to where the boundary is drawn around a city. This commitment supports also the implementation the New Urban Agenda. For the Sendai Framework for Disaster Risk Reduction 2015-2030 (DRR), the findings related to the exposure of cities to disasters will be included in the UN Global Assessment Report on Disaster Risk Reduction (GAR), which is the flagship report of the United Nations on worldwide efforts to reduce disaster risk.

The GEO (Group on Earth Observations) Human Planet Initiative supports the Atlas of the Human Planet 2018. The initiative is part of GEO work programme 2017-2019 and is committed to developing a new generation of measurements and information products that provide new scientific evidence and a comprehensive understanding of the human presence on the planet and that can support global policy processes with agreed, actionable and goal-driven metrics. The Urban Centre Database is a prime example of open, coordinated and sustained data sharing, as proposed by the Group on Earth Observations (GEO). The Atlas and the UCDB demonstrate that the combination of open data sets can generate new information and new collective understanding of the processes shaping our planet Earth. The new technology used for generating the GHSL products allows producing globally-consistent, yet locally-precise data for local action at the city level now available for benchmarking and comparison of best practices at all decisional levels from local to global. The uptake of this data for multi-level reporting and decision-making call for a regular update of the information in an operational frame that could integrate the already available products in the portfolio of the European Copernicus Space Programme.

Nowadays, a considerable amount of geo-spatial data is accessible in the public open domain, and can be used to describe the urban centres of the world if they are precisely delineated as in the GHS-UCDB. This includes on the one hand the stable geographic description of biome, soil and climate, river basin, elevation, and travel time to the capital. On the other hand, it includes more dynamic variables like temperature and precipitation, built-up area expansion, population dynamics, night-time lights emissions, income, vegetation, air quality parameters including particulate matter, carbon dioxide emissions as well as disaster risk related variable like exposure to flood, earthquake, storm surge and heatwaves.

Human settlements developed often along rivers, because they provide direct access to water for consumption, but also as a means of transport exchanges. In addition, the fluvial soils provide fertile ground for food production. Today, 69% of all urban centres are built on soils with a high agricultural suitability, and fluvisols are the biggest group therein.

In the recent past the population increase of urban centres significantly shifted to the developing world. Urban centres in Low Income Countries have doubled in population in 25 years. Although these cities are on average the smallest in area (20 km^2), the most densely populated (with 10,000 inhabitants per km^2) and with the lowest amount of built-up areas per person – approximately 15 m^2 per person for each new inhabitant between 1990 and 2015. Many of them are in the tropical areas; one third of the city dwellers (32%) lives in areas that are still or were covered by rainforest. In these areas, the population increased by 47% between 1990 and 2015 and puts significant pressure on remaining natural rain forests.

At the 21st Conference of the Parties in Paris (2015) governments committed to keep global warming below 2°C above the pre-industrial levels, with the aim of limiting it to 1.5°C. However, the climate measurements for cities reveal already significant changes in the precipitation and temperature regime. Precipitation increased relatively in North American and European cities; 73% and 67% of the urban centres in North America and in Europe, respectively, are located in areas with increasing precipitations. In Asia, around 60% of the urban centres are located in areas with decreasing precipitations; most of those urban centres fall in Eastern India and Bangladesh.

Figure 93 Kigali, Rwanda. © Andreas Brink, European Commission 2018

Some of the most severe effects of global warming will be related to an increase in the frequency and intensity of heatwaves. The analysis of observed heatwaves during the period 1980-2010 in the cities across the globe shows that most of the cities that experience severe, extreme or exceptional heatwaves are located in Asia and Europe. European continent (including Russia and Balkans) has the highest share of population living in cities that were affected by one or more heatwaves in the period 1980-2010. However, Peru is the country in that records the highest number of occurrence of heatwaves during the period 1980-2010. Linked to the increasing global temperatures and the rapid urbanization the analysis of greenness in urban centres shows an increase in green urban areas and in the share of green surfaces.

The changing climate increases also the risk of urban centres for be affected by floods and storm surges. Most of the people potentially exposed to floods live in Asian cities, as Asia is also the most populated continent. Asia and Africa are the continents, where urban population exposed to floods has increased most over the 1990-2015 time period. Eleven out of twelve of the biggest urban centres with over 5 million people exposed to floods are located in Asia. However, the increase in exposure to floods in Asia is largely due to the natural increase of population. Sea level surge affects the low-lying coastal cities of the tropical belt. In Asia the total urban centre population exposed to sea level surge exceeds 250 million; that is more than in all the other continents combined. However, in North America one out of 5 urban centre dwellers in is exposed to storm surges.

Generated inside the general GHSL paradigm, the aim of the new Urban Centres Database featured by this Atlas is to provide a first but significant step toward new comprehension of the complex, multi-faceted linkages between Humans and the planet Earth. This Atlas puts the finger in the exact places where those linkages are prominently evident, called "cities".

Coherently with the precedent editions of the Atlas, the perspective of this work is that understanding the spatial dimensions of the human development will be the key to understand the limits and the possibilities of the forthcoming societal advances, in a finite planetary space development paradigm.

8 References

Anderson, K., Ryan, B., Sonntag, W., Kavvada, A., Friedl, L., 2017. Earth observation in service of the 2030 Agenda for Sustainable Development. Geo-spatial Information Science 20, 77–96. https://doi.org/10.1080/10095020.2017.1333230

Annerstedt van den Bosch, M., Mudu, P., Uscila, V., Barrdahl, M., Kulinkina, A., Staatsen, B., Swart, W., Kruize, H., Zurlyte, I., Egorov, A.I., 2016. Development of an urban green space indicator and the public health rationale. Scandinavian Journal of Public Health 44, 159–167. https://doi.org/10.1177/1403494815615444

Bettencourt, L., West, G., 2010. A unified theory of urban living. Nature 467, 912.

Bettencourt, L.M.A., 2013. The Origins of Scaling in Cities. Science 340, 1438–1441. https://doi.org/10.1126/science.1235823

Buettner, T., 2015. Urban Estimates and Projections at the United Nations: The Strengths, Weaknesses, and Underpinnings of the World Urbanization Prospects. Spatial Demography 3, 91–108. https://doi.org/10.1007/s40980-015-0004-2

Chan, C.K., Yao, X., 2008. Air pollution in mega cities in China. Atmospheric Environment 42, 1–42. https://doi.org/10.1016/j.atmosenv.2007.09.003

Chmutina, K., Bosher, L., 2017. Rapid Urbanisation and Security: Holistic Approach to Enhancing Security of Urban Spaces, in: Dover, R., Dylan, H., Goodman, M.S. (Eds.), The Palgrave Handbook of Security, Risk and Intelligence. Palgrave Macmillan UK, London, pp. 27–45. https://doi.org/10.1057/978-1-137-53675-4_2

Chrysoulakis, N., Feigenwinter, C., Triantakonstantis, D., Penyevskiy, I., Tal, A., Parlow, E., Fleishman, G., Düzgün, S., Esch, T., Marconcini, M., 2014. A Conceptual List of Indicators for Urban Planning and Management Based on Earth Observation. ISPRS International Journal of Geo-Information 3, 980–1002. https://doi.org/10.3390/ijgi3030980

Corbane, C., Kemper, T., Freire, S., Louvrier, C., Pesaresi, M., 2016. Monitoring the Syrian Humanitarian Crisis with the JRC's Global Human Settlement Layer and Night-Time Satellite Data. https://doi.org/10.2788/48956 (print),10.2788/297909 (online)

Corbane, C., Lemoine, G., Pesaresi, M., Kemper, T., Sabo, F., Ferri, S., Syrris, V., 2018a. Enhanced automatic detection of human settlements using Sentinel-1 interferometric coherence. International Journal of Remote Sensing 39, 842–853. https://doi.org/10.1080/01431161.2017.1392642

Corbane, C., Martino, P., Panagiotis, P., Aneta, F.J., Michele, M., Sergio, F., Marcello, S., Daniele, E., Gustavo, N., Thomas, K., 2018b. The grey-green divide: multi-temporal analysis of greenness across 10,000 urban centres derived from the Global Human Settlement Layer (GHSL). International Journal of Digital Earth 1–18. https://doi.org/10.1080/17538947.2018.1530311

Corbane, C., Pesaresi, M., Politis, P., Syrris, V., Florczyk, A.J., Soille, P., Maffenini, L., Burger, A., Vasilev, V., Rodriguez, D., Sabo, F., Dijkstra, L., Kemper, T., 2017a. Big earth data analytics on Sentinel-1 and Landsat imagery in support to global human settlements mapping. Big Earth Data 1, 118–144. https://doi.org/10.1080/20964471.2017.1397899

Corbane, C., Pesaresi, M., Politis, P., Syrris, V., Florczyk, A.J., Soille, P., Maffenini, L., Burger, A., Vasilev, V., Rodriguez, D., Sabo, F., Dijkstra, L., Kemper, T., 2017b. Big earth data analytics on Sentinel-1 and Landsat imagery in support to global human settlements mapping. Big Earth Data 1, 118–144. https://doi.org/10.1080/20964471.2017.1397899

Crippa, M., Guizzardi, D., Muntean, M., Schaaf, E., Dentener, F., van Aardenne, J.A., Monni, S., Doering, U., Olivier, J.G.J., Pagliari, V., Janssens-Maenhout, G., 2018.

Gridded emissions of air pollutants for the period 1970–2012 within EDGAR v4.3.2. Earth System Science Data 10, 1987–2013. https://doi.org/10.5194/essd-10-1987-2018

Dijkstra, L., Poelman, H., 2014. A harmonised definition of cities and rural areas: the new degree of urbanisation (Working Papers), Regional Working Paper 2014.

Doherty, R.M., Hulme, M., Jones, C.G., 1999. A gridded reconstruction of land and ocean precipitation for the extended tropics from 1974 to 1994. International Journal of Climatology 19, 119–142. https://doi.org/10.1002/(SICI)1097-0088(199902)19:2<119::AID-JOC358>3.0.CO;2-X

Doldirina, C., 2015. Open Data and Earth Observations: The Case of Opening Up Access to and Use of Earth Observation Data Through the Global Earth Observation System of Systems. J. of Intellectual Property, Inf. Tech. and E-Commerce Law 6, 73–85.

Donaldson, D., Storeygard, A., 2016. The View from Above: Applications of Satellite Data in Economics. Journal of Economic Perspectives 30, 171–198. https://doi.org/10.1257/jep.30.4.171

Dosio, A., Mentaschi, L., Fischer, E.M., Wyser, K., 2018. Extreme heat waves under 1.5 °C and 2 °C global warming. Environmental Research Letters 13, 054006. https://doi.org/10.1088/1748-9326/aab827

Earth Observations in supports of the 2030 Agenda for Sustainable Development, 2017.

Ehrlich, D., Melchiorri, M., Florczyk, A., Pesaresi, M., Kemper, T., Corbane, C., Freire, S., Schiavina, M., Siragusa, A., 2018. Remote Sensing Derived Built-Up Area and Population Density to Quantify Global Exposure to Five Natural Hazards over Time. Remote Sensing 10, 1378. https://doi.org/10.3390/rs10091378

Ellis, E.C., 2018. Anthropocene: A Very Short Introduction. Oxford University Press. https://doi.org/10.1093/actrade/9780198792987.001.0001

Ellis, E.C., Ramankutty, N., 2008. Putting people in the map: anthropogenic biomes of the world. Frontiers in Ecology and the Environment 6, 439–447. https://doi.org/10.1890/070062

Elvidge, C.D., Baugh, K., Zhizhin, M., Hsu, F.C., Ghosh, T., 2017. VIIRS night-time lights. International Journal of Remote Sensing 38, 5860–5879. https://doi.org/10.1080/01431161.2017.1342050

Elvidge, C.D., Baugh, K.E., Anderson, S.J., Sutton, P.C., Ghosh, T., 2012. The Night Light Development Index (NLDI): a spatially explicit measure of human development from satellite data. Social Geography 7, 23–35.

Elvidge, C.D., Safran, J., Tuttle, B., Sutton, P., Cinzano, P., Pettit, D., Arvesen, J., Small, C., 2007. Potential for global mapping of development via a nightsat mission. GeoJournal 69, 45–53. https://doi.org/10.1007/s10708-007-9104-x

Elvidge, C.D., Sutton, P.C., Ghosh, T., Tuttle, B.T., Baugh, K.E., Bhaduri, B., Bright, E., 2009. A global poverty map derived from satellite data. Computers & Geosciences 35, 1652–1660. https://doi.org/10.1016/j.cageo.2009.01.009

Elvidge, C.D., Sutton, P.C., Tuttle, B.T., Ghosh, T., Baugh, K.E., 2010. Global urban mapping based on nighttime lights. Global Mapping of Human Settlements, Taylor and Francis, London 129–144.

Ferri, S., Syrris, V., Florczyk, A., Scavazzon, M., Halkia, M., Pesaresi, M., 2014. A new map of the European settlements by automatic classification of 2.5m resolution SPOT data. Presented at the Geoscience and Remote Sensing Symposium (IGARSS), 2014 IEEE International, pp. 1160–1163.

Florczyk, A., Ehrlich, D., Corbane, C., Freire, S., Kemper, T., Melchiorri, M., Pesaresi, M., Politis, P., Schiavina, M., Zanchetta, L., 2018. Community pre-Release of GHS Data Package (GHS CR2018) in support to the GEO Human Planet Initiative Version 1.0.

Florczyk, A.J., Ferri, S., Syrris, V., Kemper, T., Halkia, M., Soille, P., Pesaresi, M., 2015. A New European Settlement Map From Optical Remotely Sensed Data. IEEE Journal of Selected Topics in Applied Earth Observations and Remote Sensing. https://doi.org/10.1109/JSTARS.2015.2485662

Forstall, R.L., Chan, K.W., 2015. Urban Places: Statistical Definitions, in: International Encyclopedia of the Social & Behavioral Sciences. Elsevier, pp. 854–861. https://doi.org/10.1016/B978-0-08-097086-8.74042-6

Freire, S., Doxsey-Whitfield, E., MacManus, K., Mills, J., Pesaresi, M., 2016. Development of new open and free multi-temporal global population grids at 250 m resolution, in: Proc. of the 19th AGILE Conference on Geographic Information Science. Helsinki, Finland.

Freire, S., Schiavina, M., Florczyk, A., MacManus, K., Pesaresi, M., Corbane, C., Bokovska, O., Mills, J., Pistolesi, L., Squires, J., Sliuzas, R., 2018. Enhanced data and methods for improving open and free global population grids: putting 'leaving no one behind' into practice. International Journal of Digital Earth 11. https://doi.org/10.1080/17538947.2018.1548656

Gan, M., Deng, J., Zheng, X., Hong, Y., Wang, K., 2014. Monitoring Urban Greenness Dynamics Using Multiple Endmember Spectral Mixture Analysis. PLoS ONE 9, e112202. https://doi.org/10.1371/journal.pone.0112202

Gehlke, C.E., Biehl, K., 1934. Certain Effects of Grouping Upon the Size of the Correlation Coefficient in Census Tract Material. Journal of the American Statistical Association 29, 169. https://doi.org/10.2307/2277827

Ghosh, T., Anderson, S., Elvidge, C., Sutton, P., 2013. Using Nighttime Satellite Imagery as a Proxy Measure of Human Well-Being. Sustainability 5, 4988–5019. https://doi.org/10.3390/su5124988

Ghosh, T., Anderson, S., Powell, R., Sutton, P., Elvidge, C., 2009. Estimation of Mexico's Informal Economy and Remittances Using Nighttime Imagery. Remote Sensing 1, 418–444. https://doi.org/10.3390/rs1030418

Halkia, S., Buda, D., European Commission, Joint Research Centre, Institute for the Protection and the Security of the Citizen, 2007. Information support for effective and rapid external action (ISFEREA) support to external security unit. Publications Office, Luxembourg.

Harris, I., Jones, P.D., Osborn, T.J., Lister, D.H., 2014. Updated high-resolution grids of monthly climatic observations - the CRU TS3.10 Dataset: UPDATED HIGH-RESOLUTION GRIDS OF MONTHLY CLIMATIC OBSERVATIONS. International Journal of Climatology 34, 623–642. https://doi.org/10.1002/joc.3711

IPCC, 2014. Climate change 2014: Synthesis Report. Contribution of Working Papers I, II, and III to the Fifth Assessment Report of the Intergovernmantal Panel on Climate Change. IPCC, Geneva.

Jasani, B., Pesaresi, M., Schneiderbauer, S., Zeug, G. (Eds.), 2009. Remote Sensing from Space - Supporting International Peace and Security.

Jones, P.D., Hulme, M., 1996. CALCULATING REGIONAL CLIMATIC TIME SERIES FOR TEMPERATURE AND PRECIPITATION: METHODS AND ILLUSTRATIONS. International Journal of Climatology 16, 361–377. https://doi.org/10.1002/(SICI)1097-0088(199604)16:4<361::AID-JOC53>3.0.CO;2-F

Kummu, M., Taka, M., Guillaume, J.H.A., 2018. Data from: Gridded global datasets for Gross Domestic Product and Human Development Index over 1990-2015. https://doi.org/10.5061/dryad.dk1j0

Landsberg, H.E., 1976. WEATHER, CLIMATE AND HUMAN SETTLEMENTS (No. 448), World Meteorological Organization - SPECIAL ENVIRONMENTAL REPORT 7.

Le Texier, M., Schiel, K., Caruso, G., 2018. The provision of urban green space and its accessibility: Spatial data effects in Brussels. PLOS ONE 13, e0204684. https://doi.org/10.1371/journal.pone.0204684

Lee, A., Jordan, H., Horsley, J., 2015. Value of urban green spaces in promoting healthy living and wellbeing: prospects for planning. Risk Management and Healthcare Policy 131. https://doi.org/10.2147/RMHP.S61654

Lewis Dijkstra, Hugo Poelman, 2014. A harmonised definition of cities and rural areas: the new degree of urbanisation (Regional Working Paper 2014 No. WP 01/2014). European Commission, Regional and Urban Policy, Bruxelles.

Melchiorri, M., Florczyk, A., Freire, S., Schiavina, M., Pesaresi, M., Kemper, T., 2018. Unveiling 25 Years of Planetary Urbanization with Remote Sensing: Perspectives from the Global Human Settlement Layer. Remote Sensing 10, 768. https://doi.org/10.3390/rs10050768

Morice, C.P., Kennedy, J.J., Rayner, N.A., Jones, P.D., 2012. Quantifying uncertainties in global and regional temperature change using an ensemble of observational estimates: The HadCRUT4 data set: THE HADCRUT4 DATASET. Journal of Geophysical Research: Atmospheres 117, n/a-n/a. https://doi.org/10.1029/2011JD017187

Myers, M., 1975. Decision Making in Allocating Metropolitan Open Space: State of the Art. Transactions of the Kansas Academy of Science (1903-) 78, 149. https://doi.org/10.2307/3627339

National Institute for Standards and Technology, 2007. Guidelines for Evaluating and Expressing the Uncertainty of NIST Measurement Results.

Ngom, R., Gosselin, P., Blais, C., 2016. Reduction of disparities in access to green spaces: Their geographic insertion and recreational functions matter. Applied Geography 66, 35–51. https://doi.org/10.1016/j.apgeog.2015.11.008

NOAA National Centers for Environmental Information, 2018. State of the Climate: Global Climate Report for Annual 2017,.

Noort, M., 2017. Earth Observation and Sustainable Development Goals in the Netherlands Towards more synergetic use of Earth Observation: An exploratory study.

Paganini, M., Petiteville, I., 2018. Satellite Earth Observations in Support of the Sustainable Development Goals, The CEOS Earth Observation Handbook. CEOS - ESA.

Pesaresi, M., 2014. Global Fine-Scale Information Layers: the Need of a Paradigm Shift, in: Soille, P., Marchetti, P.G. (Eds.), . Presented at the Conference on Big Data from Space (BiDS'14), JRC.

Pesaresi, M., Ehrlich, D., 2009. A methodology to quantify built-up structures from optical VHR imagery, in: Gamba, P., Herold, M. (Eds.), Global Mapping of Human Settlement Experiences, Datasets, and Prospects. CRC Press, pp. 27–58.

Pesaresi, M., Ehrlich, D., Ferri, S., Florczyk, A., Carneiro Freire Sergio, M., Halkia, S., Julea, A., Kemper, T., Soille, P., Syrris, V., 2016a. Operating procedure for the production of the Global Human Settlement Layer from Landsat data of the epochs 1975, 1990, 2000, and 2014. Publications Office of the European Union.

Pesaresi, M., Ehrlich, D., Ferri, S., Florczyk, A., Freire, S., Haag, F., Halkia, M., Julea, A.M., Kemper, T., Soille, P., 2015a. Global Human Settlement Analysis for Disaster Risk Reduction. ISPRS - International Archives of the Photogrammetry, Remote Sensing and Spatial Information Sciences XL-7/W3, 837–843. https://doi.org/10.5194/isprsarchives-XL-7-W3-837-2015

Pesaresi, Martino, Ehrlich, D., Ferri, S., Florczyk, A., Freire, S., Halkia, M., Julea, A., Kemper, T., Soille, P., Syrris, V., 2016a. Operating procedure for the production of the Global Human Settlement Layer from Landsat data of the epochs 1975, 1990, 2000, and 2014 (JRC Technical Report No. EUR 27741 EN). Publications Office of the European Union, Ispra, Italy.

Pesaresi, M., Ehrlich, D., Kemper, T., Siragusa, A., Florczyk, A., Freire, S., Corbane, C., 2017. Atlas of the Human Planet 2017, Global Exposure to Natural Hazards. Publications Office of the European Union.

Pesaresi, M., Huadong, G., Blaes, X., Ehrlich, D., Ferri, S., Gueguen, L., Halkia, M., Kauffmann, M., Kemper, T., Lu, L., Marin-Herrera, M.A., Ouzounis, G.K., Scavazzon, M., Soille, P., Syrris, V., Zanchetta, L., 2013. A Global Human Settlement Layer From Optical HR/VHR RS Data: Concept and First Results. IEEE Journal of Selected Topics in Applied Earth Observations and Remote Sensing 6, 2102–2131. https://doi.org/10.1109/JSTARS.2013.2271445

Pesaresi, Martino, Melchiorri, M., Siragusa, A., Kemper, T., 2016b. Atlas of the Human Planet 2016. Mapping Human Presence on Earth with the Global Human Settlement Layer (No. EUR 28116 EN). Publications Office of the European Union, Luxembourg.

Pesaresi, M., Syrris, V., Julea, A., 2016b. A New Method for Earth Observation Data Analytics Based on Symbolic Machine Learning. Remote Sensing 8, 399. https://doi.org/10.3390/rs8050399

Pesaresi, M., Syrris, V., Julea, A., 2015b. Benchmarking of the Symbolic Machine Learning classifier with state of the art image classification methods - application to remote sensing imagery, EUR 27518 (JRC Technical Report No. EUR 27518), JRC Technical Report. Publications Office of the European Union.

Pesaresi, M., Vasileios, S., Julea, A., 2016c. Analyzing big remote sensing data via symbolic machine learning., in: Proceedings of the 2016 Conference on Big Data from Space (BiDS'16). Presented at the Big Data from Space (BiDS'16), pp. 156–159. https://doi.org/10.2788/854791

Pesaresi, M.E., 2016. Operating procedure for the production of the Global Human Settlement Layer from Landsat data of the epochs 1975, 1990, 2000, and 2014.

Rubel, F., Brugger, K., Haslinger, K., Auer, I., 2017. The climate of the European Alps: Shift of very high resolution Köppen-Geiger climate zones 1800–2100. Meteorologische Zeitschrift 26, 115–125. https://doi.org/10.1127/metz/2016/0816

Russo, S., Sillmann, J., Fischer, E.M., 2015. Top ten European heatwaves since 1950 and their occurrence in the coming decades. Environmental Research Letters 10, 124003. https://doi.org/10.1088/1748-9326/10/12/124003

Schmidt, C., Krauth, T., Wagner, S., 2017. Export of Plastic Debris by Rivers into the Sea. Environmental Science & Technology 51, 12246–12253. https://doi.org/10.1021/acs.est.7b02368

Schut, A.G.T., Ivits, E., Conijn, J.G., ten Brink, B., Fensholt, R., 2015. Trends in Global Vegetation Activity and Climatic Drivers Indicate a Decoupled Response to Climate Change. PLOS ONE 10, e0138013. https://doi.org/10.1371/journal.pone.0138013

Sendai Framework for Disaster Risk Reduction 2015-2030, 2015.

Seneviratne, S.I., Donat, M.G., Pitman, A.J., Knutti, R., Wilby, R.L., 2016. Allowable CO2 emissions based on regional and impact-related climate targets. Nature 529, 477.

Smith, D.A., 2017. Visualising world population density as an interactive multi-scale map using the global human settlement population layer. Journal of Maps 13, 117–123. https://doi.org/10.1080/17445647.2017.1400476

Soille, P., Burger, A., De Marchi, D., Kempeneers, P., Rodriguez, D., Syrris, V., Vasilev, V., 2017. A versatile data-intensive computing platform for information retrieval from big geospatial data. Futur. Gen. Comput. Syst. https://doi.org/10.1016/j.future.2017.11.007

Stanners, D.A., Bourdeau, P., European Environment Agency Task Force, United Nations (Eds.), 1995. Europe's environment: the Dobříš assessment. European Environment Agency, Copenhagen.

Sutton, P.C., Costanza, R., 2002. Global estimates of market and non-market values derived from nighttime satellite imagery, land cover, and ecosystem service valuation. Ecological Economics 41, 509–527. https://doi.org/10.1016/S0921-8009(02)00097-6

Sutton, P.C., Elvidge, C.D., Ghosh, T., 2007. Estimation of gross domestic product at sub-national scales using nighttime satellite imagery. International Journal of Ecological Economics & Statistics 8, 5–21.

Syrris, V., Corbane, C., Pesaresi, M., Soille, P., 2018. Mosaicking Copernicus Sentinel-1 Data at Global Scale. IEEE Transactions on Big Data 1–1. https://doi.org/10.1109/TBDATA.2018.2846265

UN Statistical Commission, 2017. Work of the Statistical Commission pertaining to the 2030 Agenda for Sustainable Development.

UNDESA, 2018. World Population Prospects The 2018 Revision.

UNDESA, 2008. World Urbanization Prospects The 2007 Revision.

United Nations, 2015. Sustainable development goals - United Nations [WWW Document]. United Nations Sustainable Development. URL http://www.un.org/sustainabledevelopment/sustainable-development-goals/ (accessed 10.17.17).

United Nations Conference on Housing and Sustainable Urban Development, 2016. The New Urban Agenda [WWW Document]. Habitat III. URL http://habitat3.org/the-new-urban-agenda/ (accessed 10.17.17).

United Nations, Department of Economic and Social Affairs, Population Division, 2018. World Urbanization Prospects: The 2018 Revision.

United Nations, G.A., 2015. Transforming Our World: the 2030 Agenda for Sustainable Development.

United Nations, H.S.P., 2018. Tracking Progress Towards Inclusive, Safe, Resilient and Sustainable Cities and Human Settlements SDG 11 SYNTHESIS REPORT HIGH LEVEL POLITICAL FORUM 2018.

Weiss, D.J., Nelson, A., Gibson, H.S., Temperley, W., Peedell, S., Lieber, A., Hancher, M., Poyart, E., Belchior, S., Fullman, N., Mappin, B., Dalrymple, U., Rozier, J., Lucas, T.C.D., Howes, R.E., Tusting, L.S., Kang, S.Y., Cameron, E., Bisanzio, D., Battle, K.E., Bhatt, S., Gething, P.W., 2018. A global map of travel time to cities to assess inequalities in accessibility in 2015. Nature 553, 333–336. https://doi.org/10.1038/nature25181

World Cities Report 2016 Urbanization and Development: Emerging Futures, 2016. . United Nations Human Settlements Programme (UN-Habitat).

Zampieri, M., Russo, S., di Sabatino, S., Michetti, M., Scoccimarro, E., Gualdi, S., 2016. Global assessment of heat wave magnitudes from 1901 to 2010 and implications for the river discharge of the Alps. Science of The Total Environment 571, 1330–1339. https://doi.org/10.1016/j.scitotenv.2016.07.008

Zell, E., Huff, A.K., Carpenter, A.T., Friedl, L.A., 2012. A User-Driven Approach to Determining Critical Earth Observation Priorities for Societal Benefit. IEEE Journal of Selected Topics in Applied Earth Observations and Remote Sensing 5, 1594–1602. https://doi.org/10.1109/JSTARS.2012.2199467

List of abbreviations

AI – Artificial Intelligence

ALOS – Advanced Land Observation Satellite

ASAR – Advanced Synthetic Aperture Radar

BA – Balanced Accuracy

BU – Built-up

CIESIN – Center for International Earth Science Information Network

CO_2 – Carbon dioxide

DESA – Department of Economic and Social Affairs

DG GROW – Directorate General for Internal Market, Industry, Entrepreneurship and SMEs

DG REGIO Directorate General for Regional and Urban Policy

DIAS – Data and Information Access Services

DNA – Deoxyribonucleic acid

DNB – Day/Night Band

DRR – Disaster Risk Reduction

DSM – Digital Surface Model

EC – European Commission

ECMWF – European Centre for Medium-Range Weather Forecasts

EDGAR – Emissions Database for Global Atmospheric Research

EEA – European Environment Agency

ENVISAT – Environmental Satellite

EO – Earth Observation

EOG – Earth Observations Group

EPSG – European Petroleum Survey Group

ESA – European Space Agency

ETM – Enhanced Thematic Mapper

EU – European Union

EUMETSAT – European Organisation for the Exploitation of Meteorological Satellites

EUROSTAT – Statistical Office of the European Union

FAO – Food and Agriculture Organization of the United Nations

FUA – Functional Urban Area

GAR – Global Assessment Report

GDP – Gross Domestic Product

GEE – Google Earth Engine

GEM – Global Earthquake Model

GEO – Group on Earth Observation

GEOSS – Global Earth Observation System of Systems

GHS-S1 – Global Human Settlement data from Sentinel 1 sensor

GHS-BU – Global Human Settlement data on built-up surfaces

GHS-BUILT – Global Human Settlement data on built-up surfaces

GHSL – Global Human Settlement Layer

GHS-POP – Global Human Settlement data on resident population

GHS-SMOD – Global Human Settlement data on rural vs. urban classification

GHS-UCDB – Global Human Settlement data on urban centres

GloFAS – Global Flood Awareness System

GPW – Gridded Population of the World

GSARS – Global Strategy to improve Agricultural and Rural Statistics

HABITAT – United Nations Human Settlements Programme

HDC – High Density Clusters

HIC – High Income Countries

HPI – Human Planet Initiative

HR – High Resolution

HWMId – HeatWave Magnitude Index

HWSD – Harmonized World Soil Database

ISFEREA – Information Support for Effective and Rapid External Action

JEODPP – Earth Observation Data and Processing Platform

JRC – Joint Research Centre

KC – Knowledge Centres

LIC – Low Income Countries

LMIC – Lower-middle Income Countries

LUE – Land Use Efficiency

MASL – Metres Above Sea Level

MMI – Mercalli Modified Intensity scale

MR – Major Region (UN)

MRB – Major River Basins

MRBW – Major River Basins of the World

NCEI – National Centers for Environmental Information

NDVI – Normalized differential vegetation index

NLE – Night Light Emission

NOAA – National Oceanic and Atmospheric Administration

OECD – Organisation for Economic Co-operation and Development

PM2.5 – Fine Particulate Matter

RB – River Basin

SDG – Sustainable Development Goals

SME – Small and Medium Enterprises

SML –Symbolic Machine Learning

SMOD – Settlement MODel

TM – Thematic Mapper

TOA – Top-of-Atmosphere

UC – Urban Centre

UCDB – Urban Centre Database

UMIC – Upper-middle Income Countries

USGS – United States Geological Survey

VHR – Very High Resolution

VIIRS – Visible Infrared Imaging Radiometer Suite

WB – World Bank

WGS84 – World Geodetic System 1984

WHO – World Health Organization

WUP – World Urbanization Prospect

List of definitions

Building – in the GHSL framework, buildings are defined as: *enclosed constructions above ground, which are intended or used for the shelter of humans, animals, things or for the production of economic goods and that refer to any structure constructed or erected on its site* (Pesaresi et al., 2013). This abstraction is contiguous to the standard topographic definition of the "building" class as compiled in the INSPIRE directive, except for the fact that the condition of the permanency of the structure it is not in the GHSL definition. This fact allows including also refugee camps, informal settlements, slums and other temporary settlements and shelters in the notion of built-up area in the GHSL concept.

Built-up area – is the *union of all the remote sensing fine-scale spatial units, where buildings can be found* (Pesaresi, 2016). Assuming an equal-area geographical projection of the spatial units, the sum of the spatial units classified as built-up area are estimating the total built-up surface quantity. The current Atlas is based on remote sensing data spatially harmonized at the scale of 30x30 metres.

Built-up density – the amount of built-up surface over the total surface of the spatial unit considered. In the case of the aggregated GHS-BUILT grids from fine-scale satellite records, the spatial units considered are 250x250metres and 1x1km.

Built-up grids – see GHS-BU

Built-up share – see built-up density

Built-up structure – see Building

Built-up surface – see built-up area

City – see Urban Centre. For the purpose of the present Atlas, the notion of "city" it is reduced to the one of Urban Centre, as ported in the GHSL universe of data

Degree of Urbanization – A harmonised definition of cities and rural areas introduced by the European Commission in 2014 and generated from resident population density criteria, estimated on uniform grids of 1x1km^2 scale, and distinguishing between three classes: "*urban centres*", "*towns or suburbs*", and "*rural areas*"

Earth – A planet in the Solar System, and the third planet from the Sun to the external space.

Earth Observation – the collection of information about the physical, chemical, and biological systems of the planet via remote-sensing technologies

GEO – inter-ministerial Group on Earth Observation. A partnership of more than 100 national governments and in excess of 100 Participating Organizations that envisions a future where decisions and actions for the benefit of humankind are informed by coordinated, comprehensive and sustained Earth observations.

GHS-BU – sometimes referred to as GHS-BUILT – Built-up areas grids produced by the GHSL. They reports about the presence of buildings in every spatial sample of the Earth land mass, with a resolution of 30x30 metres, also aggregated (reporting about built-up surface share) at 250x250metres , and 1x1km2 , in the four GHSL Epochs.

GHSL – Global Human Settlement Layer. A new open and free tool for assessing the human presence on the planet. Produces new global spatial information, evidence-based analytics and knowledge describing the human presence on the planet. Operates in an open and free data and methods access policy (open input, open method, open output). Supported by the DG JRC and the DG REGIO of the European Commission, together with the international partnership GEO Human Planet Initiative.

GHSL Epochs – the nominal years used as temporal reference for the harmonization of the GHSL grids. They are four GHSL epochs, corresponding to 1975, 1990, 2000, and 2015.

GHS-POP – Population grids data produced by the GHSL. They reports about resident population in every spatial sample of the Earth land mass, with a resolution of 250x250metres also aggregated at 1x1km^2 , in the four GHSL Epochs

GHS-SMOD – Settlement Model Grids produced by the GHSL. It is the porting of the Degree of Urbanization model in the GHSL universe of data aggregated at 1x1km^2, in the four GHSL Epochs

GHS-UCDB – Urban Centres Data Base produced by the GHSL. It contains attributes characterising urban centres

Green – The vegetation as observed from remote sensing platforms, by analysis of the reflected energy in wavelengths related to the photosynthesis activity of the plants

NDVI – Normalized differential vegetation index. Index accounting the energy reflected in the red and near-infrared wavelengths as collected from remote sensing sensors, and highly correlated to the presence of living vegetation on the ground.

OECD – Organisation for Economic Co-operation and Development

Planet – see Earth

PM – Particulate matter, defined as the sum of all solid and liquid particles suspended in air, which are hazardous. This complex mixture includes both organic and inorganic particles, such as dust, pollen, soot, smoke, and liquid droplets.

Population Grids – see GHS-POP

Remote Sensing – acquisition of information about an object or phenomenon without making physical contact with the object and thus in contrast to on-site observation. In this Atlas, it is assumed using space borne (artificial orbiting satellites) sensor platforms

Settlement Model Grids – see GHS-SMOD

Symbolic Machine Learning – it is a fully repeatable statistical learning procedure based on data sequencing, data reduction (quantization) and associative analysis. In the GHSL, the automatic recognition of built-up areas from remote sensing data it is based on Symbolic Machine Learning procedures (Pesaresi et al. 2016b).

Urban Centre – In the DEGURBA the Urban Centers are defined as: "*high-density clusters of contiguous grid cells of 1km^2 with a density of at least 1500 inhabitants per km^2 and a minimum population of 50000*" . The Urban Centre abstraction as implemented in the current GHSL settlement model (SMOD) formulation is defined as: "the spatially-generalized high-density clusters of contiguous grid cells of 1 km^2 with a density of at least 1,500 inhabitants per km^2 of land surface or at least 50% built-up surface share per km^2 of land surface, and a minimum population of 50,000."

List of figures

List of tables

GETTING IN TOUCH WITH THE EU

In person

All over the European Union there are hundreds of Europe Direct information centres. You can find the address of the centre nearest you at: https://europa.eu/european-union/contact_en

On the phone or by email

Europe Direct is a service that answers your questions about the European Union. You can contact this service:

- by freephone: 00 800 6 7 8 9 10 11 (certain operators may charge for these calls),

- at the following standard number: +32 22999696, or

- by electronic mail via: https://europa.eu/european-union/contact_en

FINDING INFORMATION ABOUT THE EU

Online

Information about the European Union in all the official languages of the EU is available on the Europa website at: https://europa.eu/european-union/index_en

EU publications
You can download or order free and priced EU publications from EU Bookshop at: https://publications.europa.eu/en/publications. Multiple copies of free publications may be obtained by contacting Europe Direct or your local information centre (see https://europa.eu/european-union/contact_en).

KJ-NA-29497-EN-N

The European Commission's science and knowledge service

Joint Research Centre

JRC Mission

As the science and knowledge service of the European Commission, the Joint Research Centre's mission is to support EU policies with independent evidence throughout the whole policy cycle.

EU Science Hub

ec.europa.eu/jrc

@EU_ScienceHub

EU Science Hub - Joint Research Centre

Joint Research Centre

EU Science Hub

Publications Office

doi:10.2760/124503

ISBN 978-92-79-98185-2